CANCER STEM CELLS IN THE GASTROINTESTINAL TUMOR MICROENVIRONMENT

EDITED BY: Nathaniel Weygant, Dongfeng Qu and Jiannan Yao
PUBLISHED IN: Frontiers in Oncology

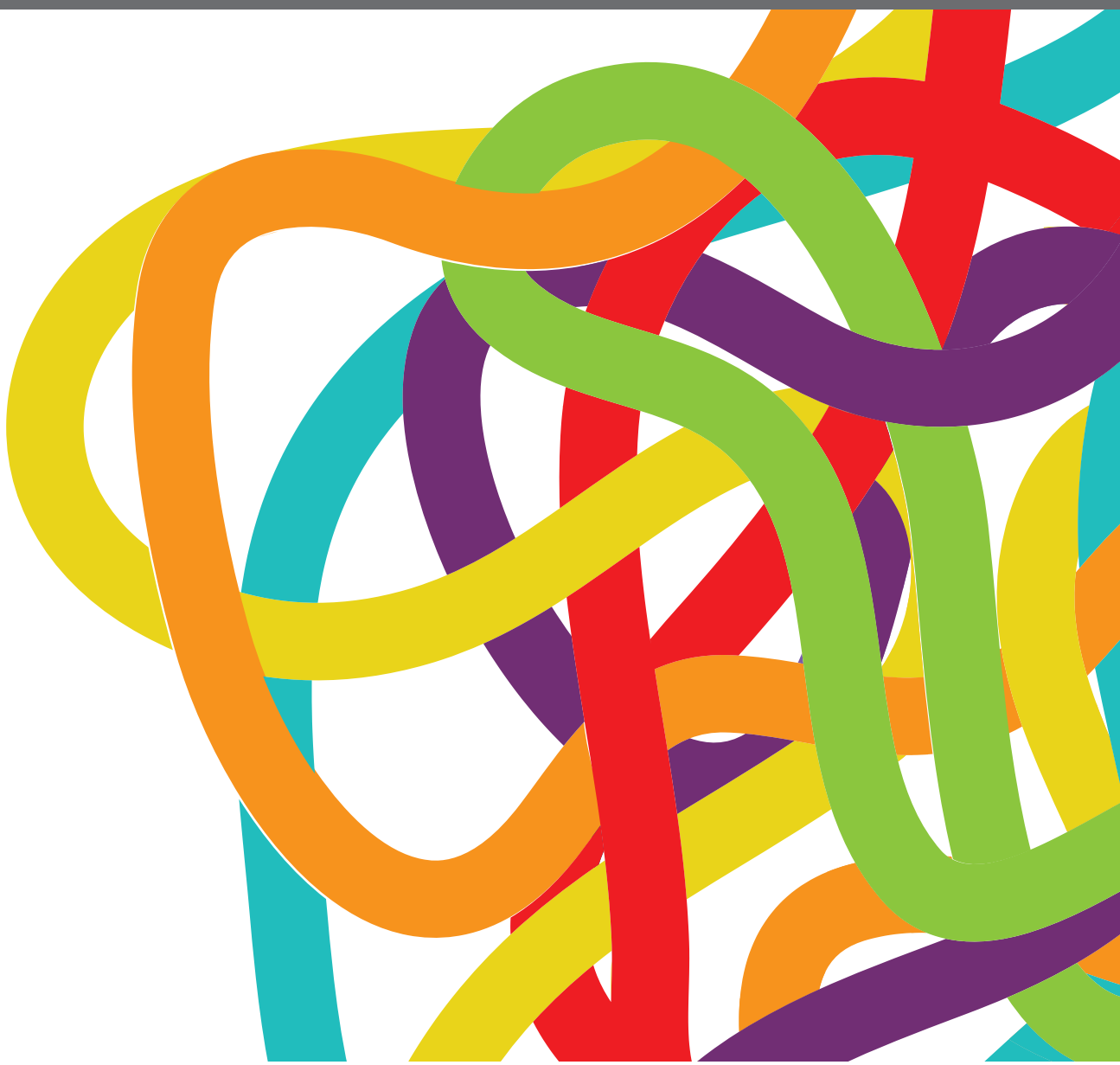

frontiers Research Topics

ISSN 1664-8714
ISBN 978-2-83250-793-3
DOI 10.3389/978-2-83250-793-3

About Frontiers

Frontiers is more than just an open-access publisher of scholarly articles: it is a pioneering approach to the world of academia, radically improving the way scholarly research is managed. The grand vision of Frontiers is a world where all people have an equal opportunity to seek, share and generate knowledge. Frontiers provides immediate and permanent online open access to all its publications, but this alone is not enough to realize our grand goals.

Frontiers Journal Series

The Frontiers Journal Series is a multi-tier and interdisciplinary set of open-access, online journals, promising a paradigm shift from the current review, selection and dissemination processes in academic publishing. All Frontiers journals are driven by researchers for researchers; therefore, they constitute a service to the scholarly community. At the same time, the Frontiers Journal Series operates on a revolutionary invention, the tiered publishing system, initially addressing specific communities of scholars, and gradually climbing up to broader public understanding, thus serving the interests of the lay society, too.

Dedication to Quality

Each Frontiers article is a landmark of the highest quality, thanks to genuinely collaborative interactions between authors and review editors, who include some of the world's best academicians. Research must be certified by peers before entering a stream of knowledge that may eventually reach the public - and shape society; therefore, Frontiers only applies the most rigorous and unbiased reviews.
Frontiers revolutionizes research publishing by freely delivering the most outstanding research, evaluated with no bias from both the academic and social point of view. By applying the most advanced information technologies, Frontiers is catapulting scholarly publishing into a new generation.

What are Frontiers Research Topics?

Frontiers Research Topics are very popular trademarks of the Frontiers Journals Series: they are collections of at least ten articles, all centered on a particular subject. With their unique mix of varied contributions from Original Research to Review Articles, Frontiers Research Topics unify the most influential researchers, the latest key findings and historical advances in a hot research area! Find out more on how to host your own Frontiers Research Topic or contribute to one as an author by contacting the Frontiers Editorial Office: frontiersin.org/about/contact

CANCER STEM CELLS IN THE GASTROINTESTINAL TUMOR MICROENVIRONMENT

Topic Editors:
Nathaniel Weygant, Fujian University of Traditional Chinese Medicine, China
Dongfeng Qu, University of Oklahoma Health Sciences Center, United States
Jiannan Yao, Capital Medical University, China

Citation: Weygant, N., Qu, D., Yao, J., eds. (2022). Cancer Stem Cells in the Gastrointestinal Tumor Microenvironment. Lausanne: Frontiers Media SA.
doi: 10.3389/978-2-83250-793-3

Table of Contents

frontiers in Oncology

ORIGINAL RESEARCH
published: 10 September 2021
doi: 10.3389/fonc.2021.716055

Stromal Galectin-1 Promotes Colorectal Cancer Cancer-Initiating Cell Features and Disease Dissemination Through SOX9 and β-Catenin: Development of Niche-Based Biomarkers

*Kai-Yen Peng[1], Shih-Sheng Jiang[2], Yu-Wei Lee[1], Fang-Yu Tsai[2], Chia-Chi Chang[1,3], Li-Tzong Chen[2,4,5] and B. Linju Yen[1]**

[1] Regenerative Medicine Research Group, Institute of Cellular & System Medicine, National Health Research Institutes (NHRI), Zhunan, Taiwan, [2] National Institute of Cancer Research, NHRI, Zhunan, Taiwan, [3] Graduate Institute of Life Sciences, National Defense Medical Center, Taipei, Taiwan, [4] Department of Oncology, National Cheng Kung University Hospital, College of Medicine, National Cheng Kung University, Tainan, Taiwan, [5] Division of Hematology/Oncology, Department of Internal Medicine, Kaohsiung Medical University Hospital, Kaohsiung, Taiwan

OPEN ACCESS

Edited by:
Nathaniel Weygant,
Fujian University of Traditional Chinese Medicine, China

Reviewed by:
Tae Il Kim,
Yonsei University College of Medicine, South Korea
Shing Yau Tam,
Hong Kong Polytechnic University, Hong Kong, SAR China
Zhiyun Cao,
Fujian University of Traditional Chinese Medicine, China

***Correspondence:**
B. Linju Yen
blyen@nhri.org.tw

Specialty section:
This article was submitted to Gastrointestinal Cancers, a section of the journal Frontiers in Oncology

Received: 28 May 2021
Accepted: 12 August 2021
Published: 10 September 2021

Citation:
Peng K-Y, Jiang S-S, Lee Y-W, Tsai F-Y, Chang C-C, Chen L-T and Yen BL (2021) Stromal Galectin-1 Promotes Colorectal Cancer Cancer-Initiating Cell Features and Disease Dissemination Through SOX9 and β-Catenin: Development of Niche-Based Biomarkers. Front. Oncol. 11:716055. doi: 10.3389/fonc.2021.716055

Over 90% of colorectal cancer (CRC) patients have mutations in the Wnt/β-catenin pathway, making the development of biomarkers difficult based on this critical oncogenic pathway. Recent studies demonstrate that CRC tumor niche-stromal cells can activate β-catenin in cancer-initiating cells (CICs), leading to disease progression. We therefore sought to elucidate the molecular interactions between stromal and CRC cells for the development of prognostically relevant biomarkers. Assessment of CIC induction and β-catenin activation in CRC cells with two human fibroblast cell-conditioned medium (CM) was performed with subsequent mass spectrometry (MS) analysis to identify the potential paracrine factors. *In vitro* assessment with the identified factor and *in vivo* validation using two mouse models of disease dissemination and metastasis was performed. Prediction of additional molecular players with Ingenuity pathway analysis was performed, with subsequent *in vitro* and translational validation using human CRC tissue microarray and multiple transcriptome databases for analysis. We found that fibroblast-CM significantly enhanced multiple CIC properties including sphere formation, β-catenin activation, and drug resistance in CRC cells. MS identified galectin-1 (Gal-1) to be the secreted factor and Gal-1 alone was sufficient to induce multiple CIC properties *in vitro* and disease progression in both mouse models. IPA predicted SOX9 to be involved in the Gal-1/β-catenin interactions, which was validated *in vitro*, with Gal-1 and/or SOX9—particularly Gal-1^{high}/$SOX9^{high}$ samples—significantly correlating with multiple aspects of clinical disease progression. Stromal-secreted Gal-1 promotes CIC-features and disease dissemination in CRC through SOX9 and β-catenin, with Gal-1 and SOX9 having a strong clinical prognostic value.

Keywords: cancer-initiating cells (CICs), tumor stroma, galectin-1, SOX9, biomarkers

INTRODUCTION

Colorectal cancer (CRC) is one of most common cancers worldwide, with its incidence and mortality rising in individuals age 50 and younger (1). While overall decreases in the CRC risk factors of alcohol intake and smoking along with an increased screening has helped reduce its incidence for several decades, alarmingly, in recent years, incidence rates have been on the increase in younger adults 50 years and under (2, 3). Survival rates of CRC strongly correlate with stage, with the 5-year survival for stage I or localized disease (excluding carcinoma-*in-situ*) close to 90%, but decreasing to less than 20% for stage IV or metastatic disease (4, 5). Thus, understanding of the specific molecular factors involved in CRC metastases is important for the control of this globally prevalent cancer.

The Wnt/β-catenin pathway is central to CRC, with the initial step in carcinogenesis determined to be mutations in the *adenomatous polyposis coli* gene, which then results in the activation of β-catenin, a transcription factor critical in the maintenance of the normal intestinal stem cell compartment as well as the cells-of-origin or carcinoma-initiating cells (CICs) for CRC (6–8). Over 90% of patients have mutations in the Wnt/β-catenin pathway, making components of this pathway ironically not useful as prognostic markers (9); rather, the functional triggering of the pathway appears to be a more robust evidence for disease progression (10). Paracrine factors secreted by non-cancerous cells within the tumor microenvironment including stromal cells play important roles in the tumorigenesis of CRC. Fibroblasts, which are key components of the stroma, can promote tumorigenic and metastatic capacity in CRC CICs through the upregulation of β-catenin activity (11–13). Despite such recent key findings, there has not been much effort in using the tumor niche to search for prognostic biomarkers. We therefore became interested in elucidating the molecular interactions between tumor niche stromal cells and CRC metastasis, and to develop prognostically relevant biomarkers based on these interactions.

In this study, we determined the interactions of fibroblast-secreted factors on CRC progression, and found galectin-1 (Gal-1) to be highly secreted by two lines of human fibroblasts as determined by mass spectrometry (MS) analyses of the fibroblast-conditioned medium (CM). Gal-1 is a glycoprotein encoded by the *LGALS1* gene and known to exert immunomodulatory effects including mediating tumor-immune escape (14). We found that the secreted Gal-1 has prominent direct tumor-promoting effects in CRC including enhancing CIC features and β-catenin activity *in vitro*, as well as *in vivo* tumor dissemination and disease progression. Moreover, as predicted by the Ingenuity Pathway Analysis (IPA), we validated the involvement of SOX9 (15)—a newly identified marker for aggressive CRC based on a recent large-scale integrative analysis—in Gal-1/β-catenin interactions. Analyses using human CRC transcriptomic databases and immunohistological staining of tissue array corroborated the strong clinical relevance of Gal-1 and SOX9—particularly Gal-1^{high}/$SOX9^{high}$ samples—as significantly and prognostically correlated with disease presence and progression.

Abbreviations: CRC, Colorectal cancer; CICs, Cancer-initiating cells; CM, Conditioned medium; MS, Mass spectrometry; Gal-1, Galectin-1; IPA, Ingenuity pathway analysis; DMEM/F-12, Dulbecco's Modified Eagle Medium: Nutrient Mixture F-12; FBS, Fetal bovine serum; MEM, Minimum essential medium; qPCR, Quantitative real-time polymerase chain reaction; siRNA, small interference RNA; shRNA, short hairpin RNA; EGF, Epidermal growth factor; bFGF, basic fibroblast growth factor; HRP, Horseradish peroxidase; ELISA, Enzyme linked immunosorbent assay; IF, Immunofluorescence staining; MTT, 3-(4,5-Dimethyl-2-thiazolyl)-2,5-diphenyl-2H-tetrazolium bromide; DiI, 1,1'-Dioctadecyl-3,3,3',3'-Tetramethylindocarbocyanine Perchlorate; DiO, 3,3'-Dioctadecyloxacarbocyanine Perchlorate; IHC, Immunohistochemistry; OCT, Optimal cutting temperature; GEO, Gene expression omnibus; TCGA, The Cancer Genome Atlas; EMT, Epithelial-mesenchymal transition; rhGal-1, Recombinant human Gal-1 protein; siC-WS1, Non-target siRNA control in WS1; siGal-WS1, siRNA specific for Gal-1-knockdown in WS1; shC-WS1, Non-target shRNA control in WS1; shGal-WS1, shRNA specific for Gal-1-knockdown in WS1; KM, KM12C; XAV: XAV939; shC-KM, Non-target shRNA control in KM12C; shSOX9-KM, shRNA specific for SOX9- knockdown in KM12C; DTCs, Disseminated tumor cells.

MATERIALS AND METHODS

Cell Culture

The human CRC cell lines KM12C was obtained from the Korean Cell Line Bank (catalog no.: 80015) (16, 17). The cells were cultured as recommended in a complete medium consisting of Dulbecco's Modified Eagle Medium: Nutrient Mixture F-12 (DMEM/F-12) supplemented with 10% fetal bovine serum (FBS), 2 mM L-glutamine, and 100 U/ml penicillin-streptomycin (all from Invitrogen-Thermo Fisher Scientific, Waltham, MA, USA). The human fibroblast cell lines MRC-5, derived from fetal lung tissue, and WS1, derived from fetal midscapular skin, were obtained from the Bioresource Collection and Research Center (BCRC, Hsinchu, Taiwan) and were cultured as recommended in the Minimum Essential Medium (MEM) with 10% FBS, 2 mM L-glutamine, and 100 U/ml penicillin-streptomycin (all from Invitrogen). Conditioned medium (CM) was collected from the cell culture after 48 hours of culturing. All cell lines were authenticated using a short-tandem repeat profiling.

Invasion Assay

Cells were treated with mitomycin C (10 ug/ml) for 2 hours to inhibit proliferation, and then $1x10^5$ cells were seeded on Matrigel-coated chambers containing 75% Matrigel (Sigma-Aldrich, MO, USA; plates with 8.0-μm pores, BD Bioscience, Franklin Lakes, NJ, USA). After CM or treatment with recombinant protein for 48 hours, detection by light microscopy (Leica Microsystems, Wetzlar, Germany) for quantification of invading cells in polycarbonate membranes was performed. Each chamber was sampled at nine different sites. Images were quantified for the number of invading cells using the Image J software (National Institutes of Health (NIH), USA).

Quantitative Real-Time Polymerase Chain Reaction

qPCR was performed as previously reported (18). Briefly, RNA was extracted from cells with TRIzol (Invitrogen), and converted

to cDNA with the ImProm-ll Reverse Transcriptase system (Promega, Madison, WI, USA) according to the protocol of the manufacturer. qPCR was carried out with Fast SYBR® Green Master Mix containing Thermo-Start DNA polymerase on the ABI 7500 Real-Time PCR System (both from Applied Biosystems-Thermo Fisher Scientific). Relative gene expression levels were analyzed as indicated by the manufacturer. The specific primers used are shown in **Supplementary Table S1**.

Western Blot

Western blot was performed as previously reported (18). Cells were collected from a 10-cm^2 dish (8 x 10^5 cells/dish) and detected for whole cell or nuclear proteins, which was isolated with the nuclear extraction kit (Millipore-Merck, Darmstadt, Germany) according to the recommendations of the manufacturer. Extracted proteins were separated by electrophoresis on a 12.5% SDS-polyacrylamide gel and transferred to a nitrocellulose membrane. The membranes were blotted with antibodies against β-catenin (1:1,000; Cat. No.610153; BD Bioscience), Gal-1 (1:1,000; Cat. No.437400; Invitrogen), Slug (1:1,000; Cat. No. ABE993; Millipore), E-cadherin (1:1,000; Cat. No. MAB3199; Millipore), SOX9 (1:1,000; Cat. No. ab3697; Abcam), GAPDH (1:8,000; Cat. No.14-9523-80; eBioscience, CA, USA), α-Tubulin (1:8,000; Cat. No.14-4502-82; eBioscience), or Histone H1 (1:1,000; Cat. No. ab125027; Abcam). Detection was performed using horseradish peroxidase (HRP)-conjugated secondary antibodies and chemiluminescent HRP substrate (Millipore).

Small-Interfering RNA Knockdown Experiments

Gene knockdown experiments were performed as previously reported (18). Lipofectamine RNAiMAX Reagent (Invitrogen) was used to transfect siRNA specific for galectin-1 (*LGALS1*) or a non-target control (Invitrogen) into cells according to the recommendations of the manufacturer. After 48 hours, RT-PCR and Western blot were used to confirm the expression levels of *LGALS1* in transfected cells. For short hairpin RNA (shRNA) knockdown experiments, MISSION TRC shRNA Lentiviral Particles (Sigma-Aldrich) containing *LGALS1* or *SOX9* shRNA or shLuc were used to infect the cells, which were seeded on 24-wells plates (1 x 10^5 cells/well) for 48 hours. The infected cells were treated with puromycin (2 ug/ml; Invitrogen) for two weeks to select the stably infected cells.

Sphere Formation

For sphere formation, cells were seeded in 6-cm^2 dishes coated with 0.4% agarose gel (6 x 10^5 cells/well), and grown in serum-free DMEM/F-12 containing 20 ng/ml human recombinant epidermal growth factor (EGF) and 10 ng/ml basic fibroblast growth factor (bFGF; both from Peprotech, Rocky Hill, NJ, USA) for 72 hours (10). For each condition, 15 sites were randomly sampled with light microscopy (Leica Microsystems) and then quantified for the number of spheres (>30 μm) using the Image J software.

Mass Spectrometric Analysis

MS analysis on the secretome of fibroblasts was performed by Proteomics Core Lab of Chang Gung University (Taoyuan, Taiwan) as previously reported (19). Briefly, CM (24 ml) was harvested from the fibroblasts cultured in a T175 flask for 48 hours. CM was concentrated by centrifugation in Amicon Ultra-15 tubes (molecular weight cutoff 10 KDa, Millipore) five times at 4,000 g for 30 minutes each time. Proteins were separated by 2D gel electrophoresis and subjected to silver staining. Protein bands were extracted and analyzed for peptide mass by MS with MS/MS used to analyze CM protein profiles.

Enzyme Linked Immunosorbent Assay

ELISA was performed as previously reported (20). Briefly, mouse monoclonal anti-Gal-1 antibody (1:500; Cat. No.437400; Invitrogen) was coated in 96-well plates at 4°C overnight. CM was added into the wells for 2 hours at room temperature. After PBST (PBS with 0.1% Tween 20) wash, wells were incubated in biotinylated rabbit anti-Gal-1 antibody (1:2,000; Cat No.500-P210; Peprotech) for 1 hour. Subsequently, HRP-conjugated streptavidin (1:200; R&D systems, MN, USA) and TMB substrate (Invitrogen) were used to detect biotinylated signaling. Finally, the reaction was stopped by 2N H_2SO_4 and absorbance was measured by optical density at 450 nm. Recombinant human Gal-1 (Peprotech) was used as a positive control. The detection range of the standard curve was from 0 to 20,000 pg/ml.

Luciferase Reporter Assay

The β-catenin-mediated transcriptional activation reporter plasmids of TOPFlash and TOPFlash mutant (contains mutated TCF/LEF binding sites) were obtained from Addgene (Cambridge, MA, USA). Reporter plasmids were transfected with renilla reporter plasmids (for internal control) into cells by using Lipofectamine 2000 reagent (Invitrogen). After 48 hours of transfection, Dual-Luciferase Reporter System (Promega) was used to measure the luciferase activity.

Immunofluorescence Staining

IF was performed as previously reported (21). Briefly, cells were fixed with 4% paraformaldehyde and permeabilized with 0.1% Triton-X 100 (Sigma-Aldrich) for 20 minutes. After blocking, cells were incubated with primary antibodies against E-cadherin (1:100; Cat. No. MAB3199; Millipore) and β-catenin (1:100; Cat. No.610153; BD Biosciences) at room temperature for 2 hours, and then incubated for 1 hour with FITC-conjugated secondary antibodies (1:200; Santa Cruz Biotechnology, Santa Cruz, CA, USA). Nuclei were stained with Hoechst 33342 (Sigma-Aldrich) and cells were visualized by fluorescence microscopy (Olympus, Tokyo, Japan).

Drug Resistance Assay

Cells were seeded in a 24-well plate (4 x 10^4 cells/plate) and pretreated with CM (1:1 mixed with culture medium) or human Gal-1 recombinant protein (rhGal1) for 24 hours. Cisplatin (25 μM; Sigma-Aldrich) was then added to the plates with assessment for cell viability after 48 hours using the 3-(4,5-Dimethyl-2-thiazolyl)-2,5-diphenyl-2H-tetrazolium bromide (MTT) assay (Sigma-Aldrich).

Ingenuity Pathway Analysis (IPA)

IPA (QIAGEN, Redwood, CA, USA) was used to infer the potential pathways in CRC disease progression involving *LGALS1*, *CTNNB1*, and *Twist1*. The pathway explorer of IPA was used to analyze the direct and indirect interactions of these three genes by utilizing Ingenuity Pathways Knowledge Base.

In Vivo Tumor Dissemination and Metastases Experiments

Animal experimentation was performed in accordance with protocols approved by the Institutional Animal Care and Use Committee (approval number: 1080102). All animals were obtained from the National Laboratory Animal Center of Taiwan (Taipei, Taiwan). A rapid metastatic tumor dissemination study was performed (22). WS1 fibroblasts and KM12C CRC cells were labeled respectively with 5 μM of the fluorescent cellular dyes 1,1'-Dioctadecyl-3,3,3',3'-Tetramethylindocarbocyanine Perchlorate (DiI) and 3,3'-Dioctadecyloxacarbocyanine Perchlorate (DiO) (both from Invitrogen) for 5 minutes. WS1 (3×10^5 cells) were co-cultured with KM12C (3×10^5 cells) in a 1:1 ratio for 24 hours and injected into the tail vein of C57BL/6 mice (6–8 weeks old). Mice were then sacrificed 24 hours after injection. The lungs were extracted for sectioning (0.5 mm thickness) with the detection of labeled cells with fluorescence microscopy (Olympus). The fluorescence intensity of images was measured by the Image J software. For *in vivo* metastatic experiments, KM12C (3×10^5 cells) co-cultured with WS1 silenced for short-hairpin RNA (shRNA) of non-target sequences (shC-WS1; 3×10^5 cells) or with WS1silenced with shRNA specific for Gal-1 (shGal-WS1; 3×10^5 cells) for one day, then injected into the tail veins of NOD-SCID mice (6–8 weeks old) and followed for up to 6 weeks with weekly measurement of the body weight. Mice were then sacrificed with lung and spleen tissues collected for histological examination.

Immunohistochemistry of Mouse and Human Tissue

Tissue samples from mice were fixed with 10% formaldehyde and embedded with the optimal cutting temperature (OCT) compound prior to frozen sectioning (Sakura Finetek, Tokyo, Japan). Tissue sections were stained with anti-human histone H1 antibody (1:100; Cat. No. ab125027; Abcam) followed by peroxidase detection (Pierce-Thermo Fisher Scientific) to detect human cells in murine lung and spleen sections. Human CRC tissue arrays were obtained from SUPER BIO CHIPS (Seoul, Korea). The tissue slides were dewaxed with xylene, rehydrated in ethanol, and subsequently stained with antibodies against human Gal-1 (1:100; Cat. No. 437400; Invitrogen) and SOX9 (1:100; Cat. No. AB5535; Millipore).

Public Microarray Gene Expression Dataset Analyses

CRC transcriptome datasets including GSE33113, GSE17536, and GSE9348 were downloaded from Gene Expression Omnibus (GEO) databases of the National Center for Biotechnology Information (https://www.ncbi.nlm.nih.gov/gds/). The Cancer Genome Atlas (TCGA) database was obtained from the NIH (https://cancergenome.nih.gov). Information on the public gene expression datasets used in this study are listed in **Supplementary Table S2**. GSE33113 and GSE17536 were used to analyze the expression of *CTNNB1* and *LGALS1* (23, 24). For comparing the gene expression levels between normal colon tissues and CRC tissue, Oncomine (http://www.oncomine.org) was utilized to analyze for the expression levels of *LGALS1* and *SOX9* in the Kaiser Colon database (25). To analyze the expression levels of *LGALS1* and *SOX9* with respect to early stages of CRC compared to normal colon tissue, GSE9348 and TCGA were used (26, 27), while GSE17536 and TCGA were used to analyze for the stage-specific expression of *LGALS1*, *SOX9*, *and CTNNB1* (24, 27).

Statistical Analyses

All experiments were performed at least in triplicate, with data were represented as mean ± SEM. Statistical analyses were performed using the Student's *t* test for comparisons of two variables and ANOVA for comparisons of more than two variables. For CRC patient transcriptome databases GSE33113, GSE7536, GSE9348, and TCGA, Student's *t* test was used for the analysis of differences in the specific gene expression levels at each stage of CRC. A value of $p < 0.05$ was defined as statistically significant.

RESULTS

Fibroblast-Secreted Factors Significantly Promote Multiple Cancer-Initiating Cell Features in Colorectal Cells

To assess whether fibroblast-derived paracrine factors are involved in CRC progression, the CRC cell line KM12C was cultured in the CM of two human fibroblast cell lines, MRC-5, and WS1, and assessed for a number of CIC properties including invasive capacity, epithelial-mesenchymal transition (EMT), β-catenin translocation, sphere formation, and drug resistance; these functional assays have been shown to be more relevant to disease progression than CIC markers such as CD133 (28). When cultured in MRC-5- and WS1-CM, the invasive capacity of KM12C was significantly increased (**Figure 1A**) and expression of *Twist1*, a critical transcription factor involved in EMT, was increased significantly up to 2-fold (**Figure 1B**). Moreover, we found that after culturing in either MRC-5- or WS1-CM in particular, β-catenin protein levels in KM12C were increased (**Figure 1C**) with the occurrence of nuclear translocation (**Figure 1D**), which has been reported to enhance CRC tumorigenesis and CIC formation (12). In addition, the sphere formation capacity as well as drug resistance were significantly increased in KM12C after culturing in either MRC-5- or WS1-CM (**Figures 1E, F**). We found that KM12C, which was pretreated with MRC-5- or WS1-CM demonstrated a significantly increased resistance to cisplatin-induced cell death, particularly after WS1-CM pretreatment. MRC-5- and WS1-CM also increased CD29 and CD44 expressions, two well-studied

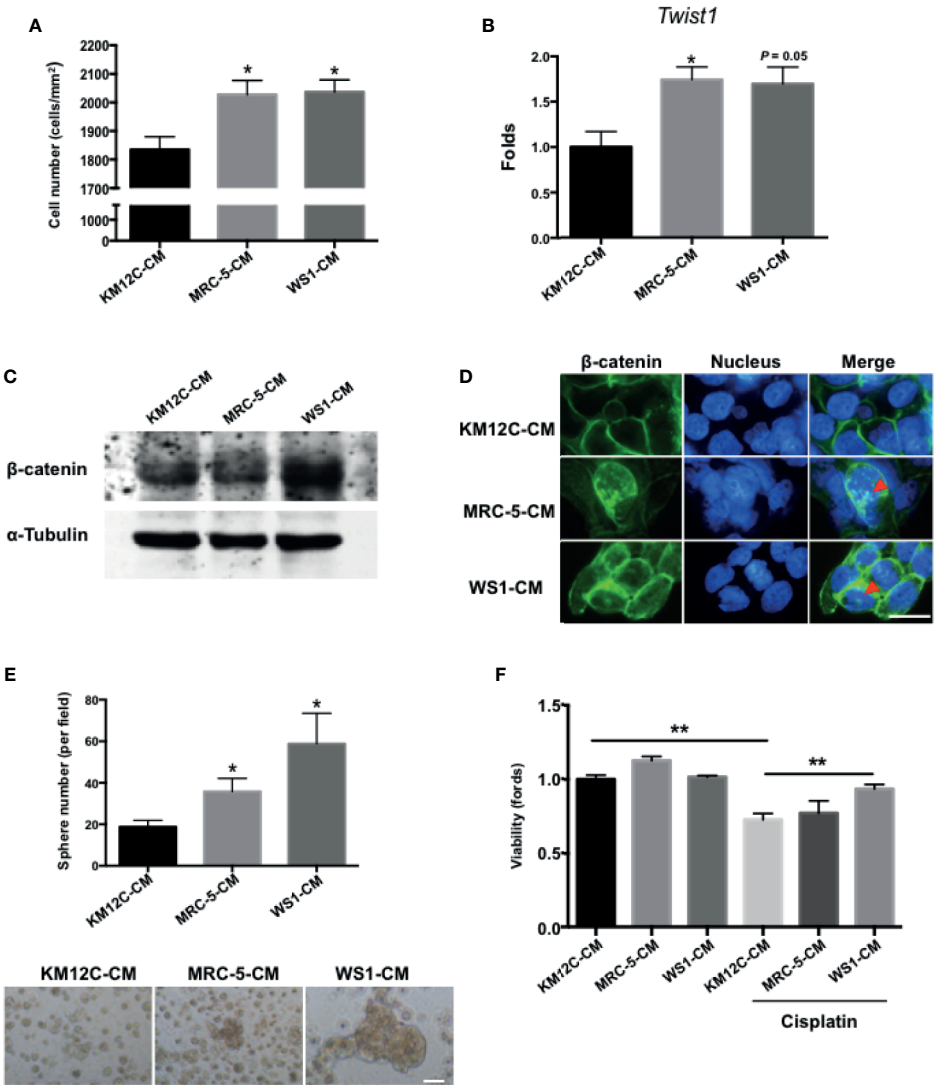

FIGURE 1 | Fibroblast-derived paracrine factors significantly promote multiple cancer-initiating cell (CIC) features in colorectal cancer (CRC) cells. **(A)** Invasion capacity of the CRC cell line KM12C (KM12C) after culturing in conditioned media (CM) of two human fibroblast cell lines MRC-5 and WS1 for 48 hours; control, KM12C-CM. **(B)** Quantitative real-time PCR (qPCR) analysis for the gene expression levels of *Twist1* in KM12C after culturing in MRC-5- or WS1-CM; control, KM12C-CM. **(C)** Western blot for the β-catenin levels in KM12C after culturing in MRC-5- or WS1-CM; control, KM12C-CM. **(D)** Immunofluorescent (IF) staining for β-catenin subcellular localization (green fluorescence) in KM12C after culturing in MRC-5- or WS1-CM; control, KM12C-CM; arrows indicate nuclear β-catenin. Hoechst 33342 was used to detect cell nuclei (blue fluorescence); scale bar, 10 μm. **(E)** Sphere formation capacity of KM12C after culturing in MRC-5- or WS1-CM for 72 hours; control, KM12C-CM. Quantitative results (top panel) and representative images (bottom panel) are shown; scale bar, 30 μm. **(F)** Drug resistance capacity of KM12C to cisplatin (25 μM) after pretreatment with either MRC-5- or WS1-CM (control, KM12C-CM) for 24 hours. Cell viability was assessed 48 hours after drug treatment. All results are shown as mean ± SEM of three independent experiments. *$p < 0.05$ and ** compared to control.

CIC markers, as assessed by flow cytometric analysis (29, 30), in KM12C (**Supplementary Figure S1**). These findings therefore demonstrate that fibroblast-derived paracrine factors significantly promote multiple CIC features in CRC cells.

Fibroblast-Secreted Gal-1 Significantly Promotes Multiple Cancer-Initiating Cell Features in Colorectal Cancer Cells

To identify the specific fibroblast-derived paracrine factor(s) responsible for enhancing multiple CIC features, MS/MS was used to analyze the secretome of MRC-5- and WS1-CM, and Gal-1 was identified as the most highly secreted protein by both fibroblast populations (**Supplementary Figure S2**), which we confirmed with Western blot as well as ELISA (**Figure 2A**). While Gal-1 (*LGALS-1*) is well known to be involved in cancer immune evasion through modulating specific subpopulations of immune cells, there have been no reports of this protein directly targeting the cancer cell itself to promote CIC features. We therefore assessed whether Gal-1 could be the paracrine factor in fibroblast-CM directly responsible for promoting multiple CIC

features in CRC cells. We found that the addition of recombinant human Gal-1 protein (rhGal-1) significantly enhanced the invasive capacity of KM12C (**Figure 2B**). Moreover, the addition of rhGal-1 promoted the EMT of KM12C in a dose-dependent fashion as evidenced by significant increases in the gene expression of *Twist1* with a decreased expression of *E-cadherin* (**Figure 2C**). This was also seen at the protein level with an increased expression of Slug, another transcription factor involved in EMT, along with a concomitant decreased expression of E-cadherin (**Figure 2D**); IF staining also demonstrated a loss of E-cadherin expression at the cell junctions with the addition of rhGal-1 (**Figure 2E**). In addition, the sphere formation capacity (**Figure 2F**) as well as drug resistance (**Figure 2G**) were both significantly enhanced by rhGal-1 in a dose-dependent fashion. Addition of rhGal-1 also increased the expression of CD29 and CD44 in KM12C as well as HCT-116, another well-studied CRC line (**Supplementary Figure S3**). To further verify the role of fibroblast-secreted Gal-1 in promoting CIC features, we generated Gal-1-knockdown WS-1 fibroblasts (siGal-WS1) using gene-specific siRNA (siRNA-I; **Figure 2H**, left panel). We found that KM12C cultured in siGal-WS1-CM demonstrated a significant decreased capacity for invasion, compared to KM12C cultured in control non-target siRNA knockdown WS1-CM (siC; **Figure 2H**, right panel). Correspondingly, KM12C cultured in siGal-WS1-CM compared to siC-WS1-CM also showed a significantly decreased capacity in terms of sphere formation (**Figure 2I**) as well as drug resistance (**Figure 2J**). These results collectively demonstrate that fibroblast-secreted Gal-1 is involved in promoting multiple CIC features of CRC cells.

Fibroblast-Secreted Gal-1 Significantly Increases Metastases and Tumor Dissemination of Colorectal Cancer Cells *In Vivo*

To assess whether the CIC features induced by fibroblast-secreted Gal-1 are involved in CRC disease progression and metastasis, we used two mouse models of metastases to validate our *in vitro* findings: a longer-term metastatic disease model using immunocompromised mice and a rapid lung tumor dissemination model using wild type mice. To assess whether fibroblast-secreted Gal-1 promoted metastatic disease, we generated stable clones of WS1 silenced for Gal-1 expression using short hairpin RNA (shRNA) specific for *LGALS1* (shGal-WS1). We then injected KM12C co-cultured with either shGal-WS1 (KM+shGal-WS1) or with non-target shRNA-silenced WS1 (KM+shC-WS1) into the tail vein of immunocompromised mice for the evaluation of metastatic growths in the lung. As negative and positive controls, we injected mice with WS1 only (shC-WS1; without KM12C) or KM12C only (KM), respectively. After 40 days of follow-up, mice injected with KM+shC-WS1 demonstrated significant decreases in body weight and were nearly moribund when compared to either mice injected with KM+shGal-WS1 or even KM12C only; WS1 only-injected mice, on the other hand, were healthy and demonstrated an increased weight gain over time (**Figure 3A**). Lung and spleen tissue sections from these mice demonstrated a significantly higher number of human cells in the mice injected with KM+shC-WS1 compared to those injected with KM+shGal-WS1 (**Figures 3B, C**; top panel: representative sections, and bottom panel: quantitative results). To ascertain that tumor dissemination was affected by fibroblast-secreted Gal-1, we co-cultured KM12C with either siGal-WS1 (KM+siGal-WS1) or with siC-WS-1 (KM+siC-WS1), and injected cells into the tail vein of C57BL/6 mice which were sacrificed after 24 hours to assess for tumor dissemination within the lungs. Tumor seeding was more significant in the mice injected with KM+siC-WS1 compared with KM+siGal-WS1 (**Figure 3D**). To assess for clinical relevance, we analyzed the human CRC transcriptome databases which contain recurrence information (GSE33113 and GSE17536; **Supplementary Table S2**) and found that high expression levels of *LGALS1*, but not β-catenin (*CTNNB1*), correlate significantly with a high risk of metastasis and/or recurrence within 3 years (**Figure 3E**). Thus, these results demonstrate that fibroblast-secreted Gal-1 significantly promotes metastatic disease progression and tumor dissemination in mouse models, as well as correlate to human CRC disease recurrence.

Gal-1 Promotes β-catenin Expression, Nuclear Accumulation, and Activity in Colorectal Cancer Cells

Wnt/β-catenin signaling is the central pathway involved in CRC pathogenesis, with the activation of the pathway being a feature of CICs and correlating with a more aggressive disease outcome. We therefore assess whether secreted Gal-1 can activate this pathway in CRC cells. We found that treatment of KM12C with exogenous rhGal-1 induced a cytoplasmic to nuclear translocation of β-catenin, as evidenced by IF staining (**Figure 4A**). This was corroborated by the Western blot data, in which both total as well as nuclear β-catenin levels were increased with increasing doses of rhGal-1 (**Figure 4B**). To further ascertain for the activation of β-catenin activity, we performed luciferase reporter assay by transducing either the wild type or mutant TOPFlash reporter into KM12C and then treating with rhGal-1. We found that all doses of rhGal-1 significantly induce reporter activity over baseline in the wild type but not the mutant promoter (**Figure 4C**). β-catenin has also been found to promote EMT (31), and we found that the addition of rhGal-1 strongly induced the expression of the EMT transcription factor *Twist1* in KM12C, which could be suppressed with XAV-939 (XAV), an inhibitor of the β-catenin pathway (**Figure 4D**). XAV also decreased Gal-1-induced CD29 expression in HCT-116 (**Supplementary Figure S4**). These results therefore demonstrate that secreted Gal-1 could activate β-catenin activity in CRC cells.

SOX9 Is a Critical Mediator Involved in Gal-1-Induced Upregulation of β-catenin Activity and Cancer-Initiating Cell Features

Given the inherent complexity of the Wnt/β-Catenin signaling pathway, we were interested in further elucidating the details in

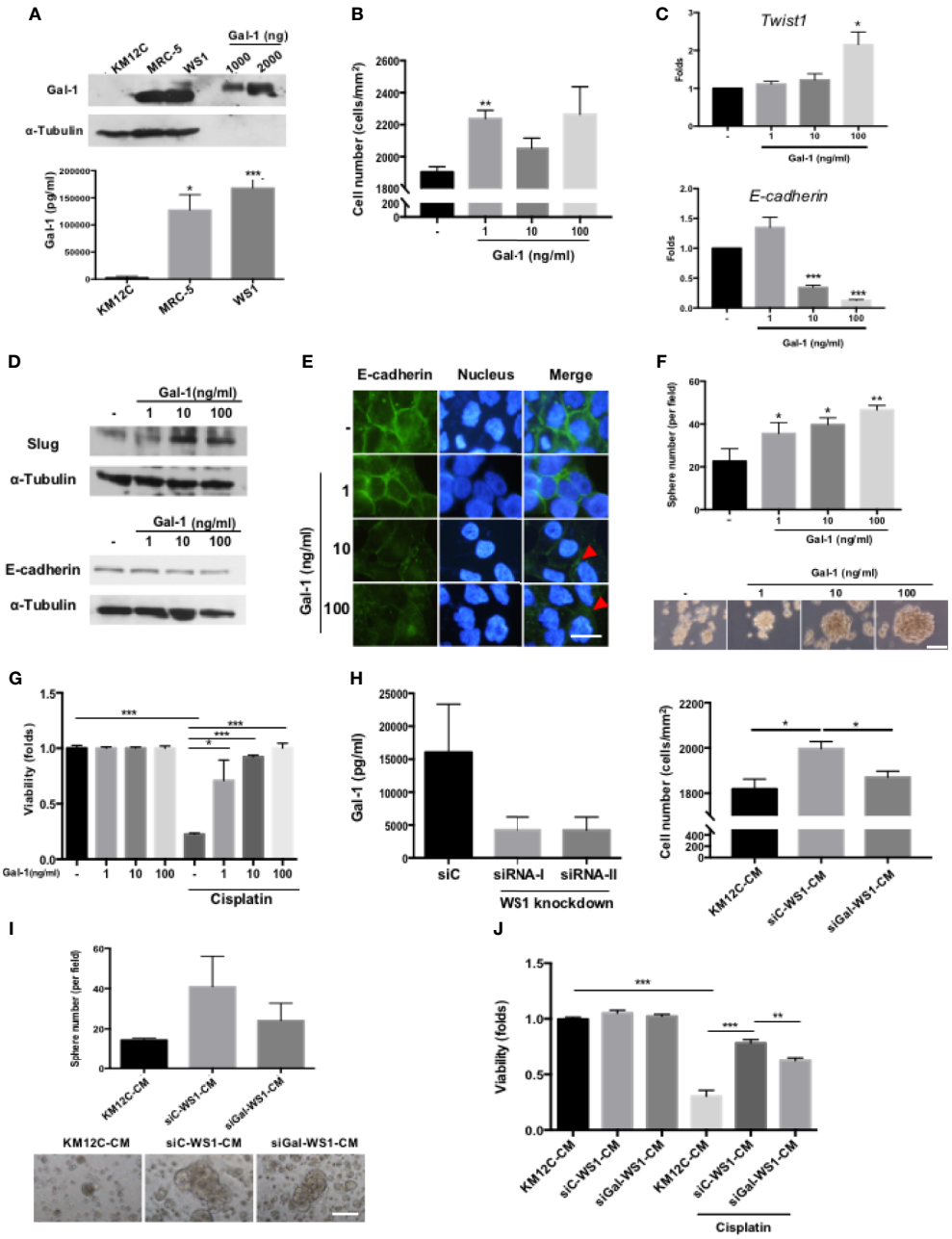

FIGURE 2 | Fibroblast-secreted galectin-1 (Gal-1) significantly promotes multiple CIC features in CRC cells. **(A)** Expression of endogenous Gal-1 in MRC-5 and WS1 fibroblasts as detected through Western blot (top panel; recombinant human Gal-1 protein (rhGal-1) used as positive control) and ELISA (bottom panel). **(B)** Invasion capacity of KM12C with the addition of increasing doses of rhGal-1. **(C)** qPCR analysis for the gene expression of *Twist1* and *E-cadherin* and **(D)** Western blot for protein expression of Slug and E-cadherin in KM12C with the addition of increasing doses of rhGal-1. **(E)** IF staining of E-cadherin (green fluorescence) in KM12C with the addition of increasing doses of rhGal-1 for 48 hours. Nuclei were stained with Hoechst 33342 (blue fluorescence); scale bar, 10 μm. **(F)** Sphere formation capacity of KM12C with the addition of increasing doses of rhGal-1; quantitative results (top panel) and representative images (bottom panel) are shown; scale bar, 30 μm. **(G)** Drug resistance capacity of KM12C to cisplatin (25 μM) after pretreatment with increasing dosages of rhGal-1 for 24 hours. Cell viability was assessed 48 hours after drug treatment. **(H)** Left panel: Validation of Gal-1 knockdown using small interfering RNA (siRNA) specific for Gal-1 (siRNA-I & siRNA-II) in WS1 fibroblasts. Non-target siRNA was used as a negative control. After 48 hours, CM from siRNA-I, siRNA-II, and siC were removed and analyzed by ELISA. Right panel: Invasion capacity of KM12C after culturing in siGal-WS1-CM compared to siC-WS1-CM for 48 hours. **(I)** Sphere formation capacity of KM12C cultured in KM12C-CM, siC-WS1-CM, or siGal-WS1-CM for 72 hours; quantitative results (top panel) and representative images (bottom panel) are shown; scale bar, 30 μm. **(J)** Drug resistance capacity of KM12C to cisplatin (25 μM) after pretreatment with KM12C-CM, siGal-WS1-CM, or siC-WS1-CM for 24 hours. Cell viability was assessed 48 hours after drug treatment; control, KM12C without cisplatin treatment. All results are shown as the mean ± SEM of three independent experiments. $^{*}p < 0.05$; $^{**}p < 0.01$, and $^{***}p < 0.005$ compared to the control.

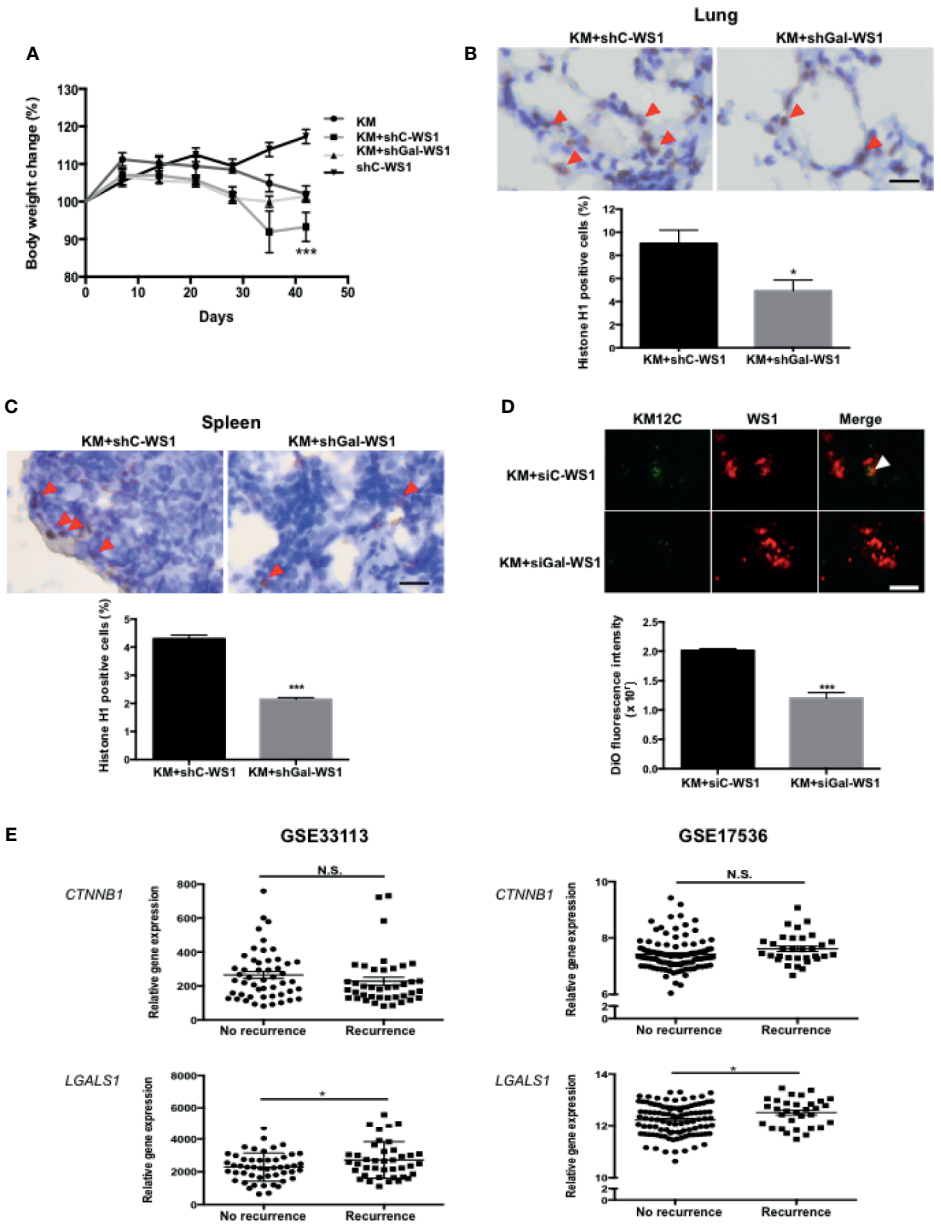

FIGURE 3 | Fibroblast-secreted Gal-1 significantly increases metastasis and tumor dissemination of CRC cells *in vivo*. **(A)** Body weight of NOD-SCID mice 40 days after tail vein injection of KM12C only (3 x 10^5 cells); KM12C (3 x 10^5 cells) admixed with WS1 silenced for with short-hairpin RNA (shRNA) of non-target sequences (shC-WS1; 3 x 10^5 cells); KM12C (3 x 10^5 cells) admixed with WS1 silenced with shRNA specific for Gal-1 (shGal-WS1; 3 x 10^5 cells); or shC-WS1 only (3 x 10^5 cells). Each condition consisted of three mice, with their body weight measured every 7 days. Immunohistochemistry (IHC) staining for human histone H1 (brown nuclei) in **(B)** mouse lung and **(C)** spleen tissue sections; representative sections (top panel) and quantitative results (bottom panel) are shown, with arrows indicating human Histone H1(+) cells; scale bar, 20 μm. **(D)** Visualization of fluorescently labeled co-cultured cells KM12C (3 x 10^5 cells; green fluorescence, labeled with DiO), and siC- or siGal-WS1 (3 x 10^5 cells; red fluorescence, labeled with with DiI) in lung sections 24 hours after injection into the tail vein of C57BL/6 mice. Top panel, representative images; bottom panel; quantitative results. Arrows indicate KM12C; scale bar, 100 μm. All results are shown as the mean ± SEM of three independent experiments. $^*p < 0.05$, and $^{***}p < 0.005$ compared to the control. **(E)** Analyses of Gal-1 (*LGALS1*) and β-catenin (*CTNNB1*) expression with regard to disease recurrence in the public dataset GSE33113 and GSE17536 of gene expression omnibus (GEO); $^*p < 0.05$; N.S., not significant.

the role of Gal-1 within this critical CRC pathway. To identify/search for other mediators involved in *LGALS1/CTNNB1* interactions, we performed IPA with the addition of TWIST1—a downstream target of β-catenin and one of the most important EMT transcription factors—to the analyses. Using this model, SOX9 was predicted as a key candidate gene within this interaction (**Figure 5A**). The role of this transcription factor in CRC remains unclear despite the very recent large-scale

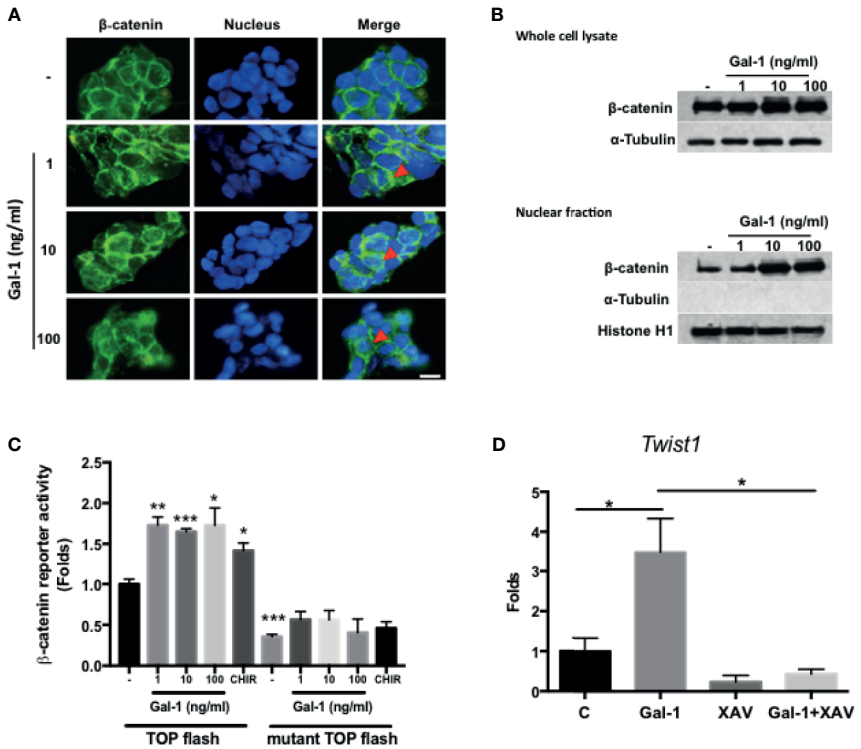

FIGURE 4 | Gal-1 promotes β-catenin expression, nuclear translocation, and activity in CRC cells. **(A)** IF staining for β-catenin (green fluorescence) in KM12C with the addition of increasing doses of rhGal-1 for 48 hours. Nuclei were stained with Hoechst 33342 (blue fluorescence). Arrows show nuclear β-catenin; scale bar, 10 μm. **(B)** Western blot for β-catenin levels in whole cell lysate (top panel) and nuclear fraction (bottom panel) of KM12C with the addition of increasing doses of rhGal-1 for 48 hours; for nuclear fraction, histone H1 is used as the positive control and α-Tubulin as the negative control. **(C)** Luciferase reporter assay for β-catenin activity in KM12C with the addition of increasing doses of rhGal-1. TOPFlash plasmids (β-catenin promoter reporter construct containing TCF/LEF binding sites; please see Materials and Methods) and TOPFlash mutant plasmids (β-catenin promoter reporter construct containing mutated TCF/LEF binding sites; please see Materials and Methods) were transduced into KM12C, with the luciferase activity measured 48 hours later; addition of the Wnt/β-catenin agonist CHIR-99021 (CHIR; 0.3 μM) was used as a positive control. **(D)** qPCR analysis for the gene expression of *Twist1* in KM12C after treatment with rhGal-1 (100 ng/ml) and without or with the Wnt/β-catenin antagonist XAV-939 (XAV; 10 μM) for 24 hours. All results are shown as the mean ± SEM of three independent experiments. $^{*}p < 0.05$; $^{**}p < 0.01$, and $^{***}p < 0.005$ compared to the control.

genomic data identifying this gene to be a significant and novel somatic recurrently mutated gene in this cancer (32). We found that the co-culture of both types of fibroblast-CM increased the protein expression of SOX9 in KM12C (**Figure 5B**). Moreover, the addition of rhGal-1 to KM12C not only enhanced the overall SOX9 protein expression levels, but also increased the nuclear levels of the transcription factor (**Figure 5C**). To investigate the role of SOX9 in CIC formation, we generated *SOX9*-silenced KM12C (shSOX9-KM) and confirmed the efficiency of knockdown by Western blot, which identified the shSOX9-II clone as having a more efficient knockdown. Compared to non-target knockdown KM12C (shC-KM), shSOX9-KM had a significantly decreased capacity for sphere formation; moreover, while the addition of rhGal-1 significantly improved the shSOX9-KM sphere formation capacity, this was still significantly less than the capacity of rhGal-1-treated shC-KM (**Figure 5D**). SOX9 also contributes to Gal-1-mediated drug resistance, since we found that shSOX9-KM was significantly more sensitive to cisplatin compared to shC-KM even with rhGal-1 pretreatment (**Figure 5E**; a decrease of 1.00- to 0.12-fold for cell viability in shSOX9-KM compared with 1.00- to 0.60-fold in shC-KM). To assess whether β-catenin was involved in Gal-1/SOX9 interaction, we analyzed for changes in the expression of *Twist1* as a downstream gene of β-catenin in shSOX9- and shC-KM cells with the addition of rhGal-1 and with or without β-Catenin antagonism (**Figure 5F**). We found that the levels of *Twist1* are significantly increased in shC-KM after the addition of rhGal-1, which could then be significantly suppressed to below baseline levels when the β-catenin antagonist XAV was applied; simultaneous addition of rhGal-1 and XAV in shC-KM restored *Twist1* expression to baseline levels. In shSOX9-KM, however, the baseline expression of *Twist1* was lower than the baseline levels in shC-KM; moreover, neither the addition of rhGal-1 nor XAV to shSOX9-KM increased *Twist1* levels. In terms of invasive capacity, migration capacity was decreased in shSOX9-KM compared to shC-KM (**Figure 5G**), but treatment with rhGal-1 increased the migration capacity significantly in shC-KM and

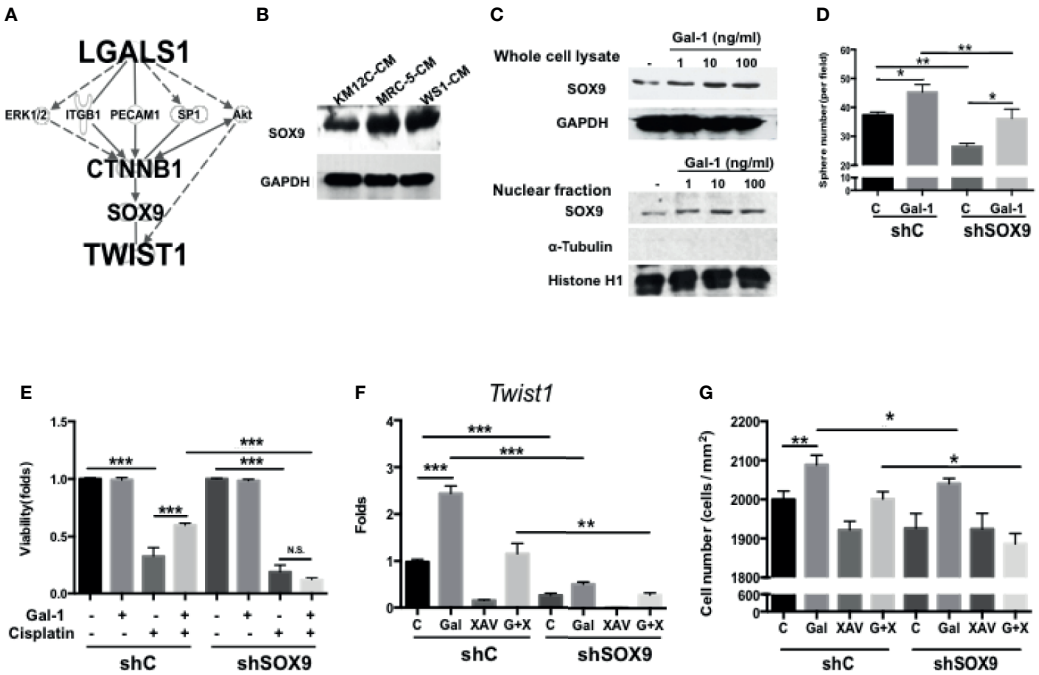

FIGURE 5 | SOX9 is a critical mediator involved in Gal-1-induced upregulation of β-catenin activity and CIC features. **(A)** Ingenuity Pathway Analysis (IPA) for the prediction of candidate mediators within the *LGALS1/CTNNB1/Twist1* axis. IPA database revealed the several major pathways which might be involved in tumor development and metastasis. According to the IPA results and literature review, *SOX9* was selected and confirmed whether it is the downstream gene of Gal-1 by Western blot. **(B)** Western blot for the analysis of SOX9 protein levels in KM12C after culturing in MRC-5- or WS1-CM; KM12C-CM was used as the control. Internal control: GAPDH. **(C)** Western blot for SOX9 levels in whole cell lysate (top panel) and nuclear fraction (bottom panel) of KM12C with addition of increasing doses of rhGal-1 for 48 hours; for nuclear protein blot, histone H1 is used as the positive control and α-Tubulin as the negative control. **(D)** Sphere formation capacity of shC-KM and shSOX9-II-KMC12 (shSOX9-KM) after treating with rhGal-1 (100 ng/ml) for 72 hours. **(E)** Drug resistance capacity of shC- and shSOX9-KM to cisplatin (25 μM) after pretreatment with rhGal-1 (100 ng/ml) for 24 hours. Cell viability was assessed 48 hours after drug treatment. **(F)** qPCR analysis for the gene expression of *Twist1* in shC- and shSOX9-KM after treatment with Gal-1 (100 ng/ml) and XAV (10 μM). **(G)** Invasion capacity of shC- and shSOX9-KM with addition of rhGal-1 (100 ng/ml) and XAV (10 μM). All results are shown as the mean ± SEM of three independent experiments. *$p < 0.05$; **$p < 0.01$, and ***$p < 0.005$ compared to the control. N.S., not significant.

non-significantly in shSOX9-KM. Importantly, rhGal-1-induced migration was abrogated after the treatment with XAV in shSOX9-KM but not shC-KM. Together, these results demonstrate that SOX9 is an important mediator involved in Gal-1-induced upregulation of β-catenin signaling activity as well as the augmentation of CIC features in CRC.

High Expression of Gal-1 and SOX9 Correlate With Clinical Colorectal Cancer (CRC) Outcome

Our results indicate that both Gal-1 and SOX9 promote CIC features, which involve the β-catenin pathway in CRC cells. To assess whether Gal-1 and/or SOX9 expression is clinically relevant for CRC, we analyzed for the expression of either one or both of these genes to various measured clinical parameters in publicly available CRC databases. We first searched the ONCOMINE database of published microarray data with matched normal and cancer specimens, and found, in the Kaiser Colon database, that a higher expression of both *LGALS1* and *SOX9* are seen in CRC samples than in normal colon samples (**Figure 6A**). To further study whether the expression patterns of either or both genes are correlated with more detailed clinical outcomes, we analyzed the gene expression profiles of two datasets from GSE9348 and The Cancer Genome Atlas (TCGA) (**Supplementary Table S2**) which includes early-stage CRC samples and adjacent normal tissue. In both databases, both *LGALS1* and *SOX9* were significantly expressed at higher levels in early-stage CRC tissue compared to adjacent normal tissue, especially *SOX9* (**Figure 6B**). Moreover, in databases with stage-specific gene expression information, such as GSE17536 and TCGA (**Supplementary Table S2**), analyses revealed that the percentage of CRC samples with a high expression of *LGALS1/SOX9* ($LGALS1^{high}/SOX9^{high}$) correlated with an increasing CRC stage (**Figure 6C**): with increasing stage, $LGALS1^{high}/SOX9^{high}$ CRC samples increased from 8.3% to 35.9% and from 8.9% to 20.0% in the GSE17536 and TCGA databases, respectively. On the other hand, neither *CTNNB1/LGALS1* highly expressed ($CTNNB1^{high}/LGALS1^{high}$) nor $CTNNB1^{high}/SOX9^{high}$ highly expressed CRC samples correlate with the CRC stage (**Supplementary Figure S5**). To verify the protein expression, we performed IHC of Gal-1 and SOX9 in a human CRC tissue microarray, which included 40 primary

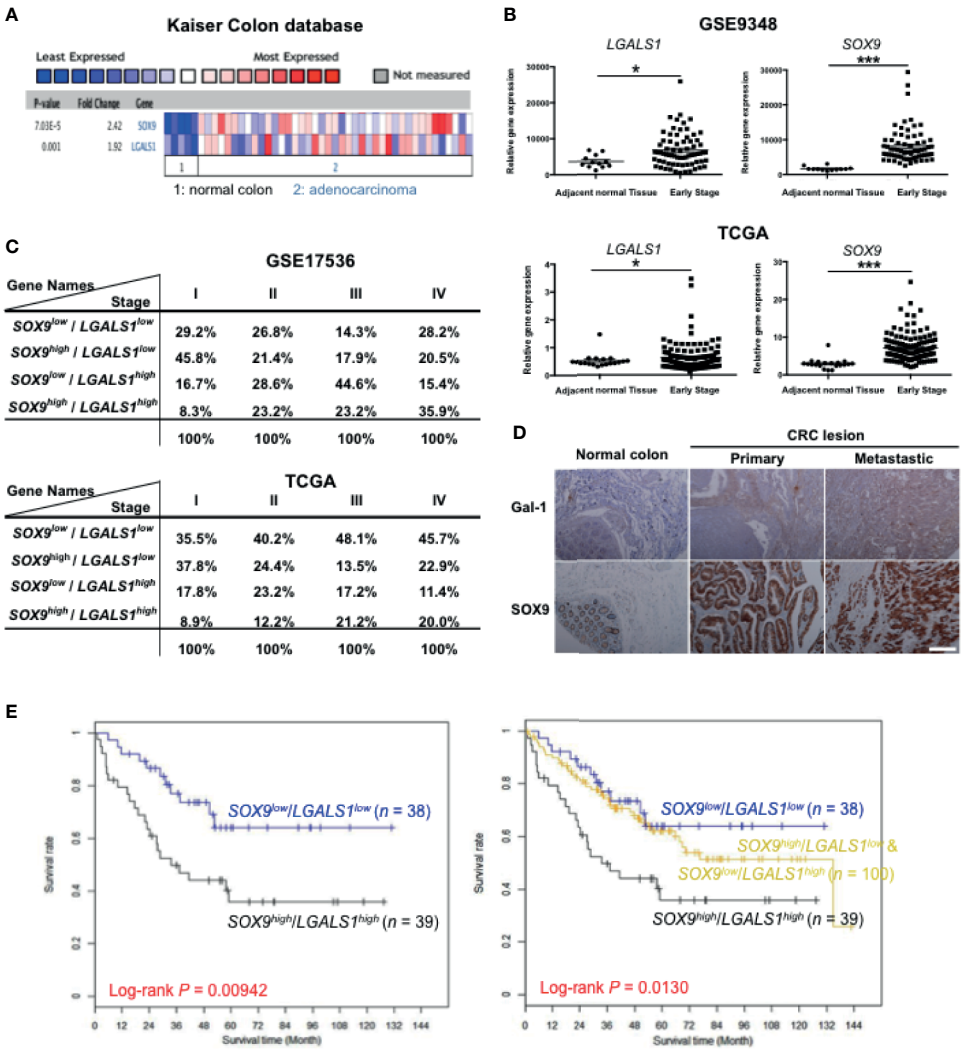

FIGURE 6 | High expression of Gal-1 and SOX9 correlate with clinical CRC outcome. **(A)** ONCOMINE assessment of the expression levels of *LGALS1* and *SOX9* in the Kaiser Colon database. **(B)** Analysis of *LGALS1* or *SOX9* expression levels in tumor tissue compared to adjacent normal tissue using GSE9348 (top panel) and The Cancer Genome Atlas (TCGA) databases (bottom panel). *$p < 0.05$ and ***$p < 0.005$ for early-stage lesions compared to adjacent normal tissue. **(C)** Analysis of *LGALS1* and *SOX9* expression levels to the CRC stage using the GSE17536 and TCGA datasets. **(D)** Immunohistological staining of Gal-1 and SOX9 on CRC tumor samples, which included 40 primary lesions (primary), 10 metastatic lesions (metastatic), and 9 normal colon samples; scale bar, 100 μm. **(E)** Kaplan-Meier survival curves of four groups of CRC patients as stratified by median expression levels of SOX9 and Gal-1 in tumor tissue: SOX9^{low}/Gal-1^{low}, n = 38; SOX9^{low}/Gal-1^{high} & SOX9^{high}/Gal-1^{low}, n = 100; and SOX9^{high}/Gal-1^{high}, n = 39. Survival analyses was performed for two groups: SOX9^{high}/Gal-1^{high} *versus* SOX9^{low}/Gal-1^{low} (left-side graph); or for three groups: SOX9^{high}/Gal-1^{high} *versus* SOX9^{high}/Gal-1^{low} + SOX9^{low}/Gal-1^{high} *versus* SOX9^{low}/Gal-1^{low} (right-side graph).

lesions, 10 metastatic lesions, and 9 normal colon samples (**Figure 6D**). The tissue array staining revealed that both Gal-1 and SOX9 protein expression were more prominent in CRC samples compared to normal tissue. Furthermore, distinct patterns of Gal-1 *vs.* SOX9 expression within CRC samples could be seen: Gal-1 expression appeared to increase with an increasing disease progression, while SOX9 expression appear to more strongly correlate with the presence of any cancerous lesion. Most critically, survival analyses based on expression levels of SOX9 and Gal-1 demonstrate that CRC patients with SOX9^{high}/Gal-1^{high} expression have a significantly shorter survival compared with patients with SOX9^{low}/Gal-1^{low} expression (**Figure 6E** and **Supplementary Figure S5**). Collectively, these analyses of clinical data/samples not only demonstrate that Gal-1 and/or SOX9 overexpression strongly correlate with disease presence, but also with the stage of CRC. Moreover, the presence of both Gal-1 and SOX9 together are strong predictors of a worse outcome in terms of disease survival. Along with our *in vitro* and mouse *in vivo* data, these results therefore demonstrate that stromal cell-derived Gal-1 directly target CRC cells to promote CIC features and disease progression through SOX9 and β-catenin (**Figure 7**).

DISCUSSION

CRC is one of the most common diseases worldwide, and alarmingly in developed nations such as the USA, the incidence and mortality of CRC has begun to increase in younger individuals after decades of decrease for the population at large. While early-stage lesions are amenable to screening and treatment, late and metastatic stage disease still have a dismal 5-year survival of less than 15% (2–5). Thus, there is a critical need for the discovery of biomarkers for early diagnosis as well as relapse. The microenvironment or niche of the solid tumor is increasingly seen to be a crucial partner in mediating disease progression (12, 13, 33–35); we therefore embarked on studying the molecular interactions between tumor niche-stromal fibroblast cells and CRC cells for the discovery of prognostically relevant biomarkers. Our data demonstrate that fibroblast-secreted Gal-1 promotes multiple CIC features in CRC cells including activating β-catenin *in vitro*, promoting metastasis and tumor dissemination *in vivo*, as well as significantly correlating with clinical recurrence and disease progression. These findings strongly suggest that fibroblast-secreted Gal-1 could be involved in promoting the presence of disseminated tumor cells (DTCs), which represent cancer cells that have undergone EMT and can disseminate to distant organ to seed metastatic growths (36, 37). Indeed, we found that fibroblast-secreted Gal-1 enhanced EMT-related gene expression *in vitro* in CRC cells, and increased the number of injected human CRC cells in the lungs in both short-term and long-term *in vivo* mouse models (**Figures 2C, D** and **3C, D**); moreover, high expression of Gal-1 in CRC patients correlated significantly with metastasis and recurrence (**Figure 3E**). Importantly, using transcriptome data and pathway prediction, we found that *SOX9*, a novel CRC driver (32), not only was mechanistically involved in Gal-1/β-catenin interactions but also is a highly relevant biomarker, especially when evaluated in conjunction with Gal-1. These findings collectively demonstrate that tumor niche-derived paracrine factors are not only important in the maintenance of CRC CICs, but can also be prognostically relevant in evaluating clinical disease progression. Our study also outlines the translational utility of niche/non-cancer cell type-based *in vitro* molecular findings to serve as biomarkers, especially given that most patient genomic and transcriptomic databases are derived from bulk tumor specimens that include non-cancer elements of the stroma and immune system.

Gal-1 is a member of the β-galactoside-binding protein family and known to modulate cancer-associated immunosuppression and angiogenesis (14, 20, 38). While the immunomodulatory mechanisms of Gal-1 have been clearly elucidated, its direct role on carcinogenesis has not been studied in much detail even for CRC in which a positive correlation with a worsening disease status has been reported (39, 40). Given the central role of the Wnt/β-catenin pathway in CRC, we postulated that tumor niche-derived paracrine factors might promote disease progression through interactions with this pathway. Our findings on the capacity of Gal-1 to activate β-catenin and induce CRC CIC features not only provide a mechanistic evidence for Gal-1 having direct interactions with CRC cells, but also support previously published clinical correlative findings of Gal-1 to be mainly expressed within the CRC stroma and not the cancer cell itself (38, 39), which we found as well (**Figure 2A**) (16). Critically, our *in vivo* findings strongly support Gal-1 as having an important role in CRC dissemination, which was bore out in analyses of human CRC databases revealing a high Gal-1 expression to be predictive of recurrence. Since Gal-1 is a secreted molecule and released in the circulation, our findings implicate that this marker could be potentially useful as a biomarker in CRC; however, further studies with patient samples are necessary to validate this possibility. Our report therefore provides further molecular understanding on previously reported disease-promoting correlations of Gal-1 in CRC.

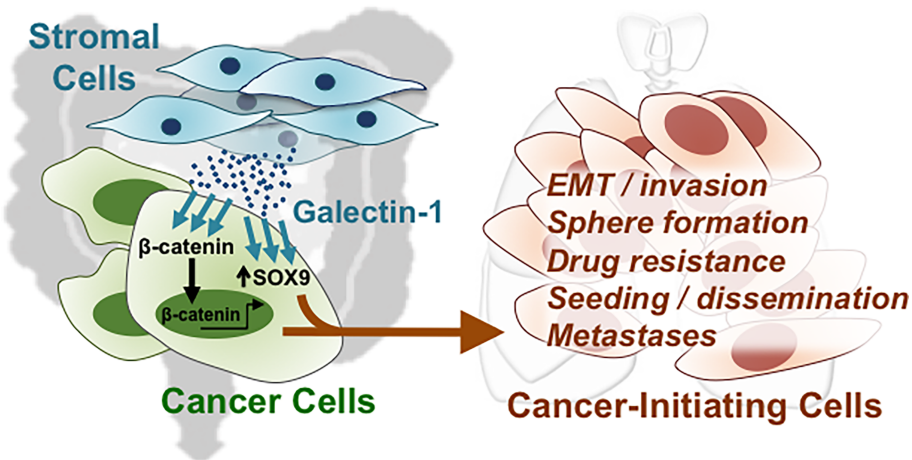

FIGURE 7 | Direct targeting of stromal-secreted Gal-1 on CRC cells promote CIC features and disease progression through SOX9 and β-catenin.

We found SOX9, a transcription factor belonging to the *Sry*-related HMG-box family, to be involved in Gal-1/β-catenin interactions in CRC. An important regulator for numerous developmental processes including in the gastrointestinal epithelium (41, 42), SOX9 has been categorized as belonging in the broader Wnt/β-catenin pathway (32). While SOX9 is known to be transcriptionally repressed by β-catenin in cartilage development (43, 44) and found to contribute to a number of cancer types including CRC (15, 45, 46),, only recently through a comprehensive molecular characterization of CRC has mutations in this transcription factor been implicated in any type of human cancers (32). Previous reports on the role of SOX9 in CRC have yielded mixed results, such as a tumor suppressor (47, 48) and having oncogenic functions (15, 49). These conflicting results have been speculated to be due to a complex relationship of SOX9 dosage on function (50). Intriguingly, these studies rarely take into consideration the fact that SOX9 is a key transcription factor in developmental/non-neoplastic EMT processes, as well as in neoplastic disease (51, 52). We found SOX9 to be involved in a Gal-1/β-catenin-mediated enhancement of a number of *in vitro* CIC features including EMT-related gene expression (**Figure 5**); moreover, analyses of multiple human CRC transcriptome databases as well as tissue microarray immunohistological staining demonstrated a significant correlation of high SOX9 expression to tumor presence, which is highly suggestive of its utility as a CRC biomarker. Critically, the simultaneous use of both Gal-1 and SOX9 is strongly correlated with a worse survival in CRC patients (**Figure 6E**). Our findings therefore not only contribute to a molecular understanding on the roles of Gal-1 and SOX9 in the central CRC pathway of Wnt/β-catenin, but also reveal these molecules as useful prognostic markers in transcriptomic databases.

In summary, we found that fibroblast-secreted Gal-1 significantly enhanced multiple *in vitro* CRC CIC properties including enhancing EMT and activating β-catenin, as well as promoting *in vivo* metastatic disease and tumor dissemination, and clinical recurrence. Bioinformatics pathway analyses predicted SOX9, a recently discovered aggressive CRC marker, as being involved in Gal-1/β-catenin interactions, which was validated *in vitro*. Moreover, Gal-1 or SOX9 but not β-catenin are prognostically correlated with disease presence and progression. Critically, a high expression of both Gal-1 and SOX9 is correlated with a significantly worse disease survival. Our findings highlight the critical role of the tumor niche-stromal component of CRC in disease progression and for discovery of prognostic markers and drug targets.

DATA AVAILABILITY STATEMENT

The datasets presented in this study can be found in online repositories. The names of the repository/repositories and accession number(s) can be found in the article/ **Supplementary Material**.

ETHICS STATEMENT

The studies involving human participants were reviewed and approved by the National Health Research Institutes (human cell line use) and GEO and TCGA (public bioinformatics data). The animal study was reviewed and approved by the Institutional Animal Care and Use Committee, NHRI.

AUTHOR CONTRIBUTIONS

Conception and design: K-YP and BY. Development of methodology: K-YP, S-SJ, and BY. Acquisition of data (provided animals, acquired and managed patients, provided facilities, etc.): Y-WL and F-YT. Analysis and interpretation of data (e.g., statistical analysis, biostatistics, computational analysis): K-YP, S-SJ, F-YT, C-CC, and BY. Writing, review, and/or revision of the manuscript: K-YP, S-SJ, C-CC, L-TC, and BY. All authors contributed to the article and approved the submitted version.

FUNDING

This study was supported in part by grants from the NHRI (10A1-CSPP06), the Ministry of Health & Welfare (MOHW110-TDU-B-212-144026), and the Taiwan Ministry of Science & Technology (MoST108-2314-B-400-035-MY3 and MoST110-2740-B-400-002).

ACKNOWLEDGMENTS

The authors would like to thank the NHRI Microarray Core Facility for the technical support.

SUPPLEMENTARY MATERIAL

The Supplementary Material for this article can be found online at: https://www.frontiersin.org/articles/10.3389/fonc.2021.716055/full#supplementary-material

Supplementary Figure 1 | Flow cytometric analysis for surface marker expression of CD29 (top panel) and CD44 (bottom panel) in KM12C treated with fibroblast-CM (Conditioned Medium).

Supplementary Figure 2 | SDS-PAGE analysis of conditioned media from MRC-5 and WS1.

Supplementary Figure 3 | Flow cytometry analysis for surface marker expression of CD29 and CD44 in KM12C (left panel) and HCT-116 (right panel) after Gal-1(100ng/ml) treatment.

Supplementary Figure 4 | Flow cytometric analysis for surface marker expression of CD29 in HCT-116 after Gal-1(100ng/ml) and XAV(10uM) treatment.

Supplementary Figure 5 | Analyses of the data sets GSE17536 and TCGA for stage-specific expression of *CTNNB1/LGALS1* or *SOX9/CTNNB1*.

Supplementary Table 1 | qPCR primer sequence information.

Supplementary Table 2 | Information on the public microarray gene expression profiles used within this study.

REFERENCES

1. Siegel R, Desantis C, Jemal A. Colorectal Cancer Statistics, 2014. *CA Cancer J Clin* (2014) 64(2):104–17. doi: 10.3322/caac.21220
2. Shin A, Kim KZ, Jung KW, Park S, Won YJ, Kim J, et al. Increasing Trend of Colorectal Cancer Incidence in Korea, 1999-2009. *Cancer Res Treat* (2012) 44 (4):219–26. doi: 10.4143/crt.2012.44.4.219
3. Siegel RL, Fedewa SA, Anderson WF, Miller KD, Ma J, Rosenberg PS, et al. Colorectal Cancer Incidence Patterns in the United States, 1974-2013. *J Natl Cancer Inst* (2017) 109(8):1–6. doi: 10.1093/jnci/djw322
4. Bockelman C, Engelmann BE, Kaprio T, Hansen TF, Glimelius B. Risk of Recurrence in Patients With Colon Cancer Stage II and III: A Systematic Review and Meta-Analysis of Recent Literature. *Acta Oncol* (2015) 54(1):5–16. doi: 10.3109/0284186X.2014.975839
5. Chen PC, Lee JC, Wang JD. Estimation of Life-Year Loss and Lifetime Costs for Different Stages of Colon Adenocarcinoma in Taiwan. *PloS One* (2015) 10 (7):e0133755. doi: 10.1371/journal.pone.0133755
6. Markowitz SD, Bertagnolli MM. Molecular Origins of Cancer: Molecular Basis of Colorectal Cancer. *N Engl J Med* (2009) 361(25):2449–60. doi: 10.1056/NEJMra0804588
7. Fodde R, Smits R, Clevers HAPC. Signal Transduction and Genetic Instability in Colorectal Cancer. *Nat Rev Cancer* (2001) 1(1):55–67. doi: 10.1038/35094067
8. Barker N, Ridgway RA, van Es JH, van de Wetering M, Begthel H, van den Born M, et al. Crypt Stem Cells as the Cells-of-Origin of Intestinal Cancer. *Nature* (2009) 457(7229):608–11. doi: 10.1038/nature07602
9. Walther A, Johnstone E, Swanton C, Midgley R, Tomlinson I, Kerr D. Genetic Prognostic and Predictive Markers in Colorectal Cancer. *Nat Rev Cancer* (2009) 9(7):489–99. doi: 10.1038/nrc2645
10. Ricci-Vitiani L, Lombardi DG, Pilozzi E, Biffoni M, Todaro M, Peschle C, et al. Identification and Expansion of Human Colon-Cancer-Initiating Cells. *Nature* (2007) 445(7123):111–5. doi: 10.1038/nature05384
11. Le NH, Franken P, Fodde R. Tumour-Stroma Interactions in Colorectal Cancer: Converging on Beta-Catenin Activation and Cancer Stemness. *Br J Cancer* (2008) 98(12):1886–93. doi: 10.1038/sj.bjc.6604401
12. Vermeulen L, De Sousa EMF, van der Heijden M, Cameron K, de Jong JH, Borovski T, et al. Wnt Activity Defines Colon Cancer Stem Cells and is Regulated by the Microenvironment. *Nat Cell Biol* (2010) 12(5):468–76. doi: 10.1038/ncb2048
13. Calon A, Espinet E, Palomo-Ponce S, Tauriello DV, Iglesias M, Cespedes MV, et al. Dependency of Colorectal Cancer on a TGF-Beta-Driven Program in Stromal Cells for Metastasis Initiation. *Cancer Cell* (2012) 22(5):571–84. doi: 10.1016/j.ccr.2012.08.013
14. Dalotto-Moreno T, Croci DO, Cerliani JP, Martinez-Allo VC, Dergan-Dylon S, Mendez-Huergo SP, et al. Targeting Galectin-1 Overcomes Breast Cancer-Associated Immunosuppression and Prevents Metastatic Disease. *Cancer Res* (2013) 73(3):1107–17. doi: 10.1158/0008-5472.CAN-12-2418
15. Matheu A, Collado M, Wise C, Manterola L, Cekaite L, Tye AJ, et al. Oncogenicity of the Developmental Transcription Factor Sox9. *Cancer Res* (2012) 72(5):1301–15. doi: 10.1158/0008-5472.CAN-11-3660
16. Morikawa K, Walker SM, Nakajima M, Pathak S, Jessup JM, Fidler IJ. Influence of Organ Environment on the Growth, Selection, and Metastasis of Human Colon Carcinoma Cells in Nude Mice. *Cancer Res* (1988) 48 (23):6863–71.
17. Medico E, Russo M, Picco G, Cancelliere C, Valtorta E, Corti G, et al. The Molecular Landscape of Colorectal Cancer Cell Lines Unveils Clinically Actionable Kinase Targets. *Nat Commun* (2015) 6:7002. doi: 10.1038/ncomms8002
18. Wang CH, Wang TM, Young TH, Lai YK, Yen ML. The Critical Role of ECM Proteins Within the Human MSC Niche in Endothelial Differentiation. *Biomaterials* (2013) 34(17):4223–34. doi: 10.1016/j.biomaterials.2013.02.062
19. Weng LP, Wu CC, Hsu BL, Chi LM, Liang Y, Tseng CP, et al. Secretome-Based Identification of Mac-2 Binding Protein as a Potential Oral Cancer Marker Involved in Cell Growth and Motility. *J Proteome Res* (2008) 7 (9):3765–75. doi: 10.1021/pr800042n
20. Thijssen VL, Barkan B, Shoji H, Aries IM, Mathieu V, Deltour L, et al. Tumor Cells Secrete Galectin-1 to Enhance Endothelial Cell Activity. *Cancer Res* (2010) 70(15):6216–24. doi: 10.1158/0008-5472.CAN-09-4150
21. Peng KY, Lee YW, Hsu PJ, Wang HH, Wang Y, Liou JY, et al. Human Pluripotent Stem Cell (PSC)-Derived Mesenchymal Stem Cells (MSCs) Show Potent Neurogenic Capacity Which Is Enhanced With Cytoskeletal Rearrangement. *Oncotarget* (2016) 7(28):43949–59. doi: 10.18632/oncotarget.9947
22. Chaturvedi A, Hoffman LM, Jensen CC, Lin YC, Grossmann AH, Randall RL, et al. Molecular Dissection of the Mechanism by Which EWS/FLI Expression Compromises Actin Cytoskeletal Integrity and Cell Adhesion in Ewing Sarcoma. *Mol Biol Cell* (2014) 25(18):2695–709. doi: 10.1091/mbc.E14-01-0007
23. de Sousa EMF, Colak S, Buikhuisen J, Koster J, Cameron K, de Jong JH, et al. Methylation of Cancer-Stem-Cell-Associated Wnt Target Genes Predicts Poor Prognosis in Colorectal Cancer Patients. *Cell Stem Cell* (2011) 9(5):476–85. doi: 10.1016/j.stem.2011.10.008
24. Smith JJ, Deane NG, Wu F, Merchant NB, Zhang B, Jiang A, et al. Experimentally Derived Metastasis Gene Expression Profile Predicts Recurrence and Death in Patients With Colon Cancer. *Gastroenterol* (2010) 138(3):958–68. doi: 10.1053/j.gastro.2009.11.005
25. Kaiser S, Park YK, Franklin JL, Halberg RB, Yu M, Jessen WJ, et al. Transcriptional Recapitulation and Subversion of Embryonic Colon Development by Mouse Colon Tumor Models and Human Colon Cancer. *Genome Biol* (2007) 8(7):R131. doi: 10.1186/gb-2007-8-7-r131
26. Hong Y, Downey T, Eu KW, Koh PK. Cheah PY. A 'Metastasis-Prone' Signature for Early-Stage Mismatch-Repair Proficient Sporadic Colorectal Cancer Patients and Its Implications for Possible Therapeutics. *Clin Exp Metastasis* (2010) 27(2):83–90. doi: 10.1007/s10585-010-9305-4
27. Cancer Genome Atlas Research N. Comprehensive Genomic Characterization Defines Human Glioblastoma Genes and Core Pathways. *Nature* (2008) 455 (7216):1061–8. doi: 10.1038/nature07385
28. Shmelkov SV, Butler JM, Hooper AT, Hormigo A, Kushner J, Milde T, et al. CD133 Expression is Not Restricted to Stem Cells, and Both CD133+ and CD133- Metastatic Colon Cancer Cells Initiate Tumors. *J Clin Invest* (2008) 118(6):2111–20. doi: 10.1172/JCI34401
29. Brakebusch C, Fassler R. Beta 1 Integrin Function *In Vivo*: Adhesion, Migration and More. *Cancer Metastasis Rev* (2005) 24(3):403–11. doi: 10.1007/s10555-005-5132-5
30. Chanmee T, Ontong P, Kimata K, Itano N. Key Roles of Hyaluronan and Its CD44 Receptor in the Stemness and Survival of Cancer Stem Cells. *Front Oncol* (2015) 5:180. doi: 10.3389/fonc.2015.00180
31. Song Y, Li ZX, Liu X, Wang R, Li LW, Zhang Q. The Wnt/beta-Catenin and PI3K/Akt Signaling Pathways Promote EMT in Gastric Cancer by Epigenetic Regulation *via* H3 Lysine 27 Acetylation. *Tumour Biol* (2017) 39 (7):1010428317712617. doi: 10.1177/1010428317712617
32. Cancer Genome Atlas N. Comprehensive Molecular Characterization of Human Colon and Rectal Cancer. *Nature* (2012) 487(7407):330–7. doi: 10.1038/nature11252
33. Peddareddigari VG, Wang D, Dubois RN. The Tumor Microenvironment in Colorectal Carcinogenesis. *Cancer Microenviron* (2010) 3(1):149–66. doi: 10.1007/s12307-010-0038-3
34. Guleng B, Tateishi K, Ohta M, Kanai F, Jazag A, Ijichi H, et al. Blockade of the Stromal Cell-Derived Factor-1/CXCR4 Axis Attenuates *In Vivo* Tumor Growth by Inhibiting Angiogenesis in a Vascular Endothelial Growth Factor-Independent Manner. *Cancer Res* (2005) 65(13):5864–71. doi: 10.1158/0008-5472.CAN-04-3833
35. Morris JS, Kopetz S. Tumor Microenvironment in Gene Signatures: Critical Biology or Confounding Noise? *Clin Cancer Res* (2016) 22(16):3989–91. doi: 10.1158/1078-0432.CCR-16-1044
36. Kang Y, Pantel K. Tumor Cell Dissemination: Emerging Biological Insights From Animal Models and Cancer Patients. *Cancer Cell* (2013) 23(5):573–81. doi: 10.1016/j.ccr.2013.04.017
37. Rhim AD, Mirek ET, Aiello NM, Maitra A, Bailey JM, McAllister F, et al. EMT and Dissemination Precede Pancreatic Tumor Formation. *Cell* (2012) 148(1-2):349–61. doi: 10.1016/j.cell.2011.11.025
38. Liu FT, Rabinovich GA. Galectins as Modulators of Tumour Progression. *Nat Rev Cancer* (2005) 5(1):29–41. doi: 10.1038/nrc1527
39. Sanjuan X, Fernandez PL, Castells A, Castronovo V, van den Brule F, Liu FT, et al. Differential Expression of Galectin 3 and Galectin 1 in Colorectal Cancer Progression. *Gastroenterol* (1997) 113(6):1906–15. doi: 10.1016/S0016-5085(97)70010-6

40. Sheng TH, Rong LX, Li ZY, Bo J, Lei S. Tissue and Serum Galectin-1 Expression in Patients With Colorectal Carcinoma. *Hepatogastroenterol* (2012) 59(114):389–94. doi: 10.5754/hge09232
41. Blache P, van de Wetering M, Duluc I, Domon C, Berta P, Freund JN, et al. SOX9 Is an Intestine Crypt Transcription Factor, Is Regulated by the Wnt Pathway, and Represses the CDX2 and MUC2 Genes. *J Cell Biol* (2004) 166 (1):37–47. doi: 10.1083/jcb.200311021
42. Mori-Akiyama Y, van den Born M, van Es JH, Hamilton SR, Adams HP, Zhang J, et al. SOX9 Is Required for the Differentiation of Paneth Cells in the Intestinal Epithelium. *Gastroenterol* (2007) 133(2):539–46. doi: 10.1053/j.gastro.2007.05.020
43. Akiyama H, Kim JE, Nakashima K, Balmes G, Iwai N, Deng JM, et al. Osteo-Chondroprogenitor Cells Are Derived From Sox9 Expressing Precursors. *Proc Natl Acad Sci USA* (2005) 102(41):14665–70. doi: 10.1073/pnas.0504750102
44. Topol L, Chen W, Song H, Day TF, Yang Y. Sox9 Inhibits Wnt Signaling by Promoting Beta-Catenin Phosphorylation in the Nucleus. *J Biol Chem* (2009) 284(5):3323–33. doi: 10.1074/jbc.M808048200
45. Jiang SS, Fang WT, Hou YH, Huang SF, Yen BL, Chang JL, et al. Upregulation of SOX9 in Lung Adenocarcinoma and Its Involvement in the Regulation of Cell Growth and Tumorigenicity. *Clin Cancer Res* (2010) 16(17):4363–73. doi: 10.1158/1078-0432.CCR-10-0138
46. Larsimont JC, Youssef KK, Sanchez-Danes A, Sukumaran V, Defrance M, Delatte B, et al. Sox9 Controls Self-Renewal of Oncogene Targeted Cells and Links Tumor Initiation and Invasion. *Cell Stem Cell* (2015) 17(1):60–73. doi: 10.1016/j.stem.2015.05.008
47. Prevostel C, Rammah-Bouazza C, Trauchessec H, Canterel-Thouennon L, Busson M, Ychou M, et al. SOX9 Is an Atypical Intestinal Tumor Suppressor Controlling the Oncogenic Wnt/ss-Catenin Signaling. *Oncotarget* (2016) 7 (50):82228–43. doi: 10.18632/oncotarget.10573
48. Shi Z, Chiang CI, Mistretta TA, Major A, Mori-Akiyama Y. SOX9 Directly Regulates IGFBP-4 in the Intestinal Epithelium. *Am J Physiol Gastrointest Liver Physiol* (2013) 305(1):G74–83. doi: 10.1152/ajpgi.00086.2013
49. Shi Z, Chiang CI, Labhart P, Zhao Y, Yang J, Mistretta TA, et al. Context-Specific Role of SOX9 in NF-Y Mediated Gene Regulation in Colorectal Cancer Cells. *Nucleic Acids Res* (2015) 43(13):6257–69. doi: 10.1093/nar/gkv568
50. Prevostel C, Blache P. The Dose-Dependent Effect of SOX9 and Its Incidence in Colorectal Cancer. *Eur J Cancer* (2017) 86:150–57. doi: 10.1016/j.ejca.2017.08.037
51. Sakai D, Suzuki T, Osumi N, Wakamatsu Y. Cooperative Action of Sox9, Snail2 and PKA Signaling in Early Neural Crest Development. *Development* (2006) 133(7):1323–33. doi: 10.1242/dev.02297
52. Guo W, Keckesova Z, Donaher JL, Shibue T, Tischler V, Reinhardt F, et al. Slug and Sox9 Cooperatively Determine the Mammary Stem Cell State. *Cell* (2012) 148(5):1015–28. doi: 10.1016/j.cell.2012.02.008

Conflict of Interest: The authors declare that the research was conducted in the absence of any commercial or financial relationships that could be construed as a potential conflict of interest.

Publisher's Note: All claims expressed in this article are solely those of the authors and do not necessarily represent those of their affiliated organizations, or those of the publisher, the editors and the reviewers. Any product that may be evaluated in this article, or claim that may be made by its manufacturer, is not guaranteed or endorsed by the publisher.

frontiers in Oncology

PERSPECTIVE
published: 23 September 2021
doi: 10.3389/fonc.2021.740606

The Microbiome Tumor Axis: How the Microbiome Could Contribute to Clonal Heterogeneity and Disease Outcome in Pancreatic Cancer

Meghna Basu[1,2†], *Lisa-Marie Philipp*[3†], *John F. Baines*[1,2] *and Susanne Sebens*[3*]

[1] Max Planck Institute for Evolutionary Biology, Plön, Germany, [2] Section of Evolutionary Medicine, Institute of Experimental Medicine, Kiel University, Kiel, Germany, [3] Institute for Experimental Cancer Research, University Hospital Schleswig-Holstein (UKSH) Campus Kiel, Kiel University, Kiel, Germany

Pancreatic ductal adenocarcinoma (PDAC) is one of the most malignant cancers. It is characterized by a poor prognosis with a 5-year survival rate of only around 10% and an ongoing increase in death rate. Due to the lack of early and specific symptoms, most patients are diagnosed at an advanced or even metastasized stage, essentially limiting curative treatment options. However, even curative resection of the primary tumor and adjuvant therapy often fails to provide a long-term survival benefit. One reason for this dismal situation can be seen in the evolution of therapy resistances. Furthermore, PDAC is characterized by high intratumor heterogeneity, pointing towards an abundance of cancer stem cells (CSCs), which are regarded as essential for tumor initiation and drug resistance. Additionally, it was shown that the gut microbiome is altered in PDAC patients, promotes Epithelial-Mesenchymal-Transition (EMT), determines responses towards chemotherapy, and affects survival in PDAC patients. Given the established links between CSCs and EMT as well as drug resistance, and the emerging role of the microbiome in PDAC, we postulate that the composition of the microbiome of PDAC patients is a critical determinant for the abundance and plasticity of CSC populations and thus tumor heterogeneity in PDAC. Unravelling this complex interplay might pave the way for novel treatment strategies.

Keywords: PDAC, microbiome, CSC, microbiome-targeted therapy, drug resistance, tumor heterogeneity, cancer stemness

OPEN ACCESS

Edited by:
Dongfeng Qu,
University of Oklahoma Health Sciences Center, United States

Reviewed by:
Ming Cui,
Peking Union Medical College Hospital (CAMS), China
Parthasarathy Chandrakesan,
University of Oklahoma Health Sciences Center, United States

***Correspondence:**
Susanne Sebens
susanne.sebens@email.uni-kiel.de

†These authors have contributed equally to this work and share first authorship

Specialty section:
This article was submitted to Gastrointestinal Cancers: Hepato Pancreatic Biliary Cancers, a section of the journal Frontiers in Oncology

Received: *13 July 2021*
Accepted: *08 September 2021*
Published: *23 September 2021*

Citation:
Basu M, Philipp L-M, Baines JF and Sebens S (2021) The Microbiome Tumor Axis: How the Microbiome Could Contribute to Clonal Heterogeneity and Disease Outcome in Pancreatic Cancer. Front. Oncol. 11:740606. doi: 10.3389/fonc.2021.740606

INTRODUCTION

Pancreatic ductal adenocarcinoma (PDAC) is one of the most common lethal cancer entities with hardly 10% of the patients surviving up to 5 years after diagnosis (1). Owing to the lack of early and specific symptoms, the majority of patients are diagnosed at an advanced- or even metastasized stage (2). This also implies that only 20% of the patients are eligible for resection of the primary tumor combined with adjuvant chemotherapy. However, in most cases even this curative treatment regimen only provides a temporary survival benefit, due to relapse or the development of metastases during or shortly after therapy. One reason for this poor prognosis can be seen in the evolution of resistances towards therapeutic drugs, e.g. through the activation of multidrug resistance and pro-survival pathways (3–5). Furthermore, PDAC is characterized by a pronounced inflammatory tumor stroma, which besides genetic and epigenetic alterations also contributes to the acquisition of a drug resistant phenotype in PDAC cells (6, 7).

The emergence of chemoresistance has been linked to Epithelial-Mesenchymal-Transition (EMT) in diverse cancer entities, including PDAC (8–11). Primarily, EMT is regarded as a key process in metastasis by which epithelial tumor cells acquire the capability to disconnect from the primary context and disseminate to secondary sites. Since EMT can also be seen as a dedifferentiation process, it is not surprising that EMT has been associated with the acquisition of cancer stem cell (CSC) properties. Due to their self-renewal potential and ability to undergo asymmetric cell division, CSCs are undifferentiated cells that are essential for tumor initiation and the emergence of more differentiated cell clones within the tumor. Thus, intratumor heterogeneity of PDAC might be another determinant for the response to therapeutic drugs, as particularly CSCs are highly resistant to cancer therapies (12–16).

As outlined in the review by Zhang et al. recently published in Frontiers in Oncology, the gut and tumor microbiome have emerged as a promising therapeutic target for PDAC (8, 17, 18), due to its impact on tumorigenesis and drug resistance in PDAC (19, 20). Several studies in PDAC patients demonstrated important links between the patient`s tumor microbiome and disease progression, such as correlations between patient survival and tumor microbiome diversity (21) or facilitating immune suppression (19). These findings support a link between the microbiome, disease progression and outcome of PDAC patients. Moreover, chronic inflammation associated with long-term microbial infection promotes EMT, which in turn contributes to drug resistance, cancer progression and metastasis (summarized in 8). Since EMT is linked to the acquisition of CSC properties, we postulate that the abundance and plasticity of CSCs, and thereby intratumor heterogeneity in PDAC, are critically modulated by the patient`s microbiome (of different body compartments). Considering this possible association might provide the basis for innovative therapeutic strategies targeting the microbiome.

Abbreviations: CDD, cytidine deaminase; CSC, cancer stem cell; CTLA-4, cytotoxic T-lymphocyte-associated protein 4; EMT, Epithelial-Mesenchymal-Transition; FMT, fecal microbiota transplant; IPMNs, intraductal papillary mucinous neoplasms; LTS, long-term survivors; MET, Mesenchymal-Epithelial-Transition; PDAC, Pancreatic ductal adenocarcinoma; STS, short-term survivors.

EPITHELIAL-MESENCHYMAL-TRANSITION

EMT is regarded as a prerequisite for epithelial/carcinoma cells to disseminate from the primary tumor to secondary sites. Undergoing this process implies a loss of typical epithelial characteristics and a gain of mesenchymal properties, causing a fundamental functional switch from stationary to a more motile and invasive phenotype. In detail, expression of epithelial proteins like E-cadherin or occludin, both being important for epithelial cell-cell contacts, are diminished, while expression of mesenchymal markers such as N-cadherin, Vimentin, L1CAM or the transcription factor Zeb1 are enhanced (22). Accordingly, EMT is a process by which cells lose their original differentiation and function, which can be regained at secondary sites by reversion of EMT, a process called Mesenchymal-Epithelial-Transition (MET). Thus, it is not surprising that EMT coincides with the acquisition of CSC-characteristics in tumor cells (23–25). Mani et al. demonstrated that breast cancer cells that have undergone EMT acquire a stem cell-like phenotype, and subsequently these stem cell-like cells resemble cells that have undergone EMT (25).

CANCER STEM CELLS

Similar to physiological stem cells, CSCs are characterized by the ability to proliferate indefinitely and to divide asymmetrically, giving rise to both stem cells and differentiated short-lived daughter cells with limited proliferative capability (26–29). Based on these properties, CSCs - although accounting only for a small part of the entire tumor cell population - are regarded as essential for tumor initiation and progression as well as for tumor heterogeneity (27, 30–32). According to the current model, CSCs are not a fixed cell population, but that the aforementioned characteristics can be acquired and lost dependent on environmental stimuli, as CSC are highly dependent on their niche, i.e. oxygen level, surrounding stromal cells and their released factors (24, 29, 33–36). Hence, factors like oxidative, inflammatory and nutritional stress, to which tumor cells are commonly subjected to, determine the differentiation of non-CSCs into CSCs and *vice versa*. From an evolutionary point of view, this model implies that changes in the tissue microenvironment (e.g., inflammation and/or microbiome changes) lead to the selection of subpopulations of CSCs in a Darwinian manner. As a consequence, these CSCs develop strategies that enable them to survive the adverse conditions of the host (37). This might also provide an explanation for the marked resistance of CSCs to different therapies (8). For instance, chemotherapies aim to decrease the total number of rapidly proliferating tumor cells. However, since CSCs rarely divide and exhibit high levels of drug export molecules, this is

only partially successful, as the main tumor cell population might be removed while CSCs survive and can give rise to recurrences or metastases (30, 38–42).

In summary, CSCs contribute to tumorigenicity, tumor progression, metastasis, recurrence as well as therapy resistance in PDAC (26, 42, 43). Given the fact that EMT as well as the interconversion from non-CSC to CSC are both processes defining tumor cell plasticity and heterogeneity, and either process is highly dependent on the inflammatory/stress level of the surrounding microenvironment, it is reasonable to postulate that the microbiome is another important determinant for defining evolution of CSC. Confirming the contribution of the microbiome to tumor cell plasticity might provide additional mechanistic insight into tumorigenesis and the survival of PDAC patients.

THE MICROBIOME - PDAC AXIS

Alterations of the Microbiome in PDAC Patients

The human gut microbiota is comprised of a collection of different bacteria, archaea, fungi, viruses and protozoa. Its composition is unique to each individual and is influenced by a variety of environmental factors such as the mode of birth, age, diet, and, disease (44, 45). The microbiome plays vital roles in immune development, nutrition, energy metabolism and host defense (45). Generally, a higher bacterial diversity is characteristic of a healthy gut microbiome, whereas low diversity accompanies diseases such as inflammatory bowel disease, diabetes mellitus type 2, asthma and various cancers (46–50). An inflammatory environment favors pro-inflammatory bacteria in the diseased gut, thereby establishing a cycle of inflammation (51). In some cases of *Enterococcus faecalis* infection, the bacterium infiltrates the patient´s pancreas and initiates inflammation, resulting in the progression of chronic pancreatitis (52). A state of chronic inflammation as manifested e.g. in chronic pancreatitis or *Helicobacter pylori* infection in the gut is a known risk factor of PDAC development (53–55). Several routes by which bacteria can migrate into the PDAC microenvironment have been proposed, such as through the bile duct, portal circulation system or mesenteric lymph nodes (8). A number of studies support these routes, for example microbiome analysis of the cyst fluid of intraductal papillary mucinous neoplasms (IPMNs) with high-grade dysplasia revealed the presence of *Fusobacterium nucleatum* and *Granulicatella adiacens*, which are commonly found in the oral cavity (56, 57). In line with these findings, Mitsuhashi et al. identified *Fusobacterium* species being enhanced in tumor tissues of PDAC patients and associated with a worse prognosis (58).

The study by Geller et al. revealed that most bacterial species that were identified by 16S rRNA gene sequencing in PDAC tissues belong to Gammaproteobacteria and are predominantly members of the *Enterobacteriaceae* and *Pseudomonadacea* families (17). Furthermore, pancreas, bile, and jejunum samples from patients undergoing pancreaticoduodenectomy showed a distinctly different microbiome than healthy controls (59). Although the process of bacterial translocation from the oral cavity and gut into the pancreatic (tumor) tissue is not fully understood, we can speculate on the factors and mechanisms that favor this migration. For example, the formation of a new niche that offers lower colonization resistance and provides nutrition in the form of increased glycan levels might favor the migration of bacteria into the tumor microenvironment (60). In line with this hypothesis, the tumor microenvironment is enriched with structural proteins, proteoglycans, adapter proteins and enzymes, as well as tumor associated inflammatory cells such as myofibroblasts or macrophages, which are known producers of the aforementioned factors (61). Together, these changes in the microenvironment provide advantageous conditions that may facilitate bacterial migration from the gut into the pancreas on the one hand, and promote tumor development and progression on the other hand.

Impact of an Altered Microbiome on EMT and Therapy Resistance

It was demonstrated that an inflammatory tumor microenvironment and tumor associated microbiome can promote EMT by inducing various signaling pathways that lead to the activation of different EMT transcription factors. Thus, it could be shown that infections by certain pathogens such as *F. nucleatum* are able to induce phosphorylation, and thus internalization of the epithelial marker protein E-cadherin. This in turn mediates the release of bound β-catenin, which translocates into the nucleus and influences the expression of EMT related genes. As a consequence, tumor cells undergo EMT and become capable of leaving the primary tumor and disseminate to secondary sites (8, 54, 55, 62). Given the fact that *Fusobacteria* species are already enriched in premalignant lesions such as IPMN, and their abundance in PDAC tissues is associated with a worse outcome (56, 58), it seems plausible that their abundance contributes to PDAC progression by EMT induction. Importantly, a distinct tumor microbiome was shown to clearly discriminate long-term survivor (LTS) from short-term survivor (STS) PDAC patients. Performing taxonomic profiling of bacterial DNA from 36 LTS and 32 STS PDAC patients revealed a higher species diversity in tumor samples of LTS patients associated with a significantly longer overall survival (median survival: 9.66 years) compared to STS patients with a low diversity (median survival: 1.66 years) (21). Overall, these findings strongly support a tumor promoting role of the microbiome and its suitability as a potential therapeutic target. This view is further supported by recent studies indicating that microbes residing in the tumor microenvironment can contribute to drug resistance, which is a major problem in PDAC treatment. In detail, Geller et al. (17) identified that the tumor microbiome of PDAC patients shows a high abundance of bacterial species belonging to the class Gammaproteobacteria. These bacteria express the enzyme cytidine deaminase (CDD) predominantly in its long form, which enables the metabolization of the chemotherapeutic drug gemcitabine

(2′,2′-difluorodeoxycytidine), which is commonly used for treatment of PDAC patients in the adjuvant and palliative setting, into its inactive form (2′,2′-difluorodeoxyuridine) (17).

Besides demonstrating a novel tumor promoting role of microbiota, these findings suggest a potential mutualistic relationship between tumor cells and bacteria, with both of them exhibiting a form of parasitism towards the host. Furthermore, it can be postulated that the presence of a distinct microbiome provides favorable conditions for selection and survival of those tumor cell clones that have evolved the best survival strategies and exhibit a high degree of plasticity, such as CSCs. Enrichment and survival of CSCs within the tumor essentially add to PDAC development and progression on the one hand, and therapy resistance on the other hand.

First Approaches Towards Microbiome Targeted Therapy

Therapy resistance, e.g. against cytostatic drugs, but also immunotherapies such as cytotoxic T-lymphocyte-associated protein 4 (CTLA-4) inhibitors, is still a major clinical challenge in the treatment of PDAC patients, and has been related to tumor heterogeneity implying the presence of CSCs (12–16). As outlined above, evidence supporting a tumor-promoting role of an altered host microbiome at different sites is accumulating. Pathological microbiome alterations apparently contribute to tumor development and progression in different ways, e.g. by shaping host immunity, impacting differentiation processes such as EMT and determining the efficacy of PDAC therapy (17–19).

Preclinical studies already strongly support the concept of modulating the host`s microbiome to improve treatment responses in PDAC, whereby antibiotic-treated mice displayed a marked anti-tumor response to gemcitabine compared to the control mice, which exhibited rapid tumor progression. Additionally, histological analysis of tumor tissues revealed more apoptosis induction in tumor cells when gemcitabine was applied in combination with antibiotics compared to gemcitabine monotherapy (17).

Furthermore, fecal microbiota transplant (FMT) has gained attention as a promising anti-tumor therapy (21). Thus, an increase in tumor growth was observed in mice after FMT from STS PDAC patients compared to that from LTS PDAC patients (21). These findings correlated with the microbiome composition and overall survival times of these patients, and indicate that the transplanted microbiome from STS patients promotes tumor growth, while that from LTS PDAC patients displays the opposite effect, leading to a slower tumor growth compared to the control group without FMT (21). Furthermore, this study revealed a strong correlation between microbiome diversity and elevated numbers of CD3+, CD8+ and Granzyme B+ T cells in tumor tissues of LTS PDAC patients compared to STS patients. These results support the view that the tumor microbiome modulates immunity in the tumor microenvironment, and thus influences the dynamic interplay between tumor and immune cells during tumorigenesis. In this context, a preclinical study showed that the efficacy of the CTLA-4 inhibitor Ipilimumab is increased in the presence of the gut commensal *Bacteroides* spp., which could in turn be reverted upon administration of antibiotics (18). The presence of these commensals affects interleukin-12 dependent T helper-1 immune responses, which in turn modulates tumor control in mice and humans while preserving intestinal integrity. These findings thus point toward a role of gut commensals in shaping the host immune response and thereby controlling tumor growth. Overall, these findings indicate that the composition of the tumor- as well as the gut microbiome are essential determinants of PDAC evolution and therapeutic responses (17, 18, 20). **Table 1** lists recent studies that have found tangible associations between disease progression and immune regulation with the host microbiome composition. As already mentioned above some of these studies have even singled out distinct groups of bacteria that influenced these changes. Naturally, clinical trials focusing on compiling 16S rRNA profiles of PDAC patient samples are on the rise (based on http://clinicaltrials.gov/). There is mounting evidence that patient microbiome composition can be used as a biomarker for disease progression as well as to increase therapeutic efficacy of PDAC treatment (**Table 1**). Likewise, Leinwand & Miller propose selectively tailoring PDAC therapy with respect to the patients' intratumoral and gut microbiome to enhance therapeutic efficacy (66).

Based on these results it can be envisioned that the above-mentioned microbiome modulating strategies increase therapeutic responses and survival of PDAC patients by lowering the abundance of CSC (properties). Fortunately, there are already ongoing randomized clinical trials that combine 16S rRNA gene analysis, FMT or probiotics along with chemotherapeutics and are listed in the review by Ciernikova et al. (57). The upcoming results may thus further substantiate the interrelationship of the host`s microbiome and tumor cells and provide the basis of novel therapeutic concepts of PDAC therapy.

DISCUSSION AND FUTURE PERSPECTIVES

As summarized above and in the recently published review by Zhang et al. in this journal (8), the microbiome composition (in different body compartments) is considerably altered in PDAC patients compared to healthy individuals. This altered diversity may be a consequence of tumorigenesis, as the evolution of an inflammatory tumor microenvironment might promote bacterial translocation from the gut into the pancreas (8, 17, 21, 57). Besides, there is growing evidence that the microbiome is an important determinant of PDAC development and therapy response (8, 17, 21, 67–69). One mechanism by which the microbiome composition seems to drive PDAC progression and therapy resistance is promoting EMT. Importantly, EMT induction has been linked to the acquisition of CSC properties, and both EMT cells and CSC are characterized by profound drug resistance (30, 38–40). Considering these well-established interrelationships, it is reasonable to speculate that the abundance and plasticity of CSCs, and thereby intratumor heterogeneity in PDAC and patient´s outcome, are essentially influenced by the patient`s microbiome (**Figure 1**). This

TABLE 1 | Compilation of studies on the impact of the microbiome in cancer progression and drug resistance as well as its potential as a biomarker or therapeutic target.

Study system	Targeted Pathway/ Treatment	Specific Microbiome	Biomarker/Target Potential	Reference
MCA205 sarcomas in mice housed in specific pathogen–free (SPF) versus germ-free (GF) conditions	CTLA-4	*Bacteroides thetaiotaomicron* or *Bacteroides fragilis*	Ipilimumab in presence of *Bacteroides* spp. Increases response to CTLA4 blockade. Detection of *Bacteroides* spp. as predictive biomarker CTLA4 inhibition therapy	(18)
Subcutaneous B16.SIY melanoma in C57BL/6 mice with different microbiomes	Programmed cell death protein 1 ligand 1 (PD-L1)	*Bifidobacterium*	(PD-L1)–specific antibody therapy in combination with oral Bifidobacterium administration exerts anti-tumor effect. Detection of oral *Bifidobacterium* as predictive biomarker	(63)
Subcutaneous colon carcinoma (MC-26) in BALB/c mice	Nucleoside analogues-gemcitabine	Bacteria expressing long isoform of bacterial enzyme cytidine deaminase (CDD) e.g.: Gammaproteobacteria, & *M. hyorhinis which expresses the* (short isoform) renders gemcitabine ineffective.	Gemcitabine in combination with ciprofloxacin increases the antitumor response; Detection of CDD and bacteria as a predictive biomarker for gemcitabine treatment	(17)
Formalin-fixed, paraffin-embedded (FFPE) patient tissue specimens of PDAC patients	NA	Fusobacterium species positively correlated with worse prognosis	Detection of Fusobacterium species in PDAC tissue as a prognostic biomarker	(58)
Bacterial DNA from surgically resected (LTS & STS) patient PDAC tumors	NA	LTS patients were enriched in Proteobacteria (Pseudoxanthomonas) and Actinobacteria (Saccharopolyspora and Streptomyces)	Detection of Pseudoxanthomonas, Saccharopolyspora and Streptomyces as a prognostic biomarker	(21)
Orthotopically implanted KPC PDAC cell lines in antibiotic- treated C57BL/6 mice	NA	FMT from LTS patient stool samples inhibited tumor growth	FMT after antibiotic treatment can be used as anti-tumor therapy.	(21)
Cyst fluid and peripheral blood liquid biopsies from patients with suspected pancreatic cystic lesions	NA	Intracystic bacterial DNA quantity positively correlated with the neoplastic grade severity of IPMN, like *G. adiacens, F. nucleatum, P. micra, E. corrodens, H. parahaemolyticus, A. odontolyticus, P. melaninogenica* and *Campylobacter* spp.	Detection and abundance of these bacteria as a diagnostic biomarker	(56)
Pancreatic juice and bile from PDAC and CP patients; caerulein-injected mice model for CP	NA	*Enterobacter* and *Enterococcus spp* were detected in pancreatic tissue and bile from PDAC and CP patients and in CP mice but not in controls suggesting these bacteria may be involved in CP and PDAC development	Detection of *Enterobacter* and *Enterococcus spp may serve* as a diagnostic/prognostic biomarker i	(52)
Antibiotic treated C57Bl/6 mice inoculated with EL4 lymphoma, MC38 colon carcinoma, or B16 melanoma cells	Antitumor immune responses	Antibiotic treated mice showed impaired therapy efficacy and resulted in lower cytokine production and tumor necrosis after CpG-oligonucleotide based immunotherapy.	Ensuring the presence of an intact gut microbiome prior to therapy may boost treatment efficacy	(20)
Germ-free mice transplanted with responder fecal material and later inoculated with B16.SIY melanoma cells	Programmed cell death protein 1 ligand 1 (PD-L1)	*Bifidobacterium longum, Collinsella aerofaciens*, and *Enterococcus faecium were abundantly found in the microbiome of the responders to* anti-PD-1-based immunotherapy	Possible supplementation of probiotic cocktails containing beneficial bacteria may increase anti–PD-1 antibody efficacy	(64)
$KRAS^{G12D}$ $TP53^{R172H}$Pdx-Cre (KPC) mice	NA	Distinct microbial dysbiosis was observed with PDAC tumor growth	Microbiome profiling can serve as a prognostic marker for disease progression	(65)
$KRAS^{G12D}$ $TP53^{R172H}$Pdx-Cre (KPC) mice and fecal samples of PDAC patients	Innate and adaptive immune cell signaling	*Proteobacteria, Actinobacteria, Fusobacteria*, and *Verrucomicrobia* was enriched in the pancreatic microbiome in PDAC patients and repopulation of antibiotic ablated mice with the microbiome of tumor-bearing KPC mice or with *B. pseudolongum* accelerated oncogenesis	Microbial- targeted therapies as part of anti-tumor therapy	(19)

NA, not applicable.

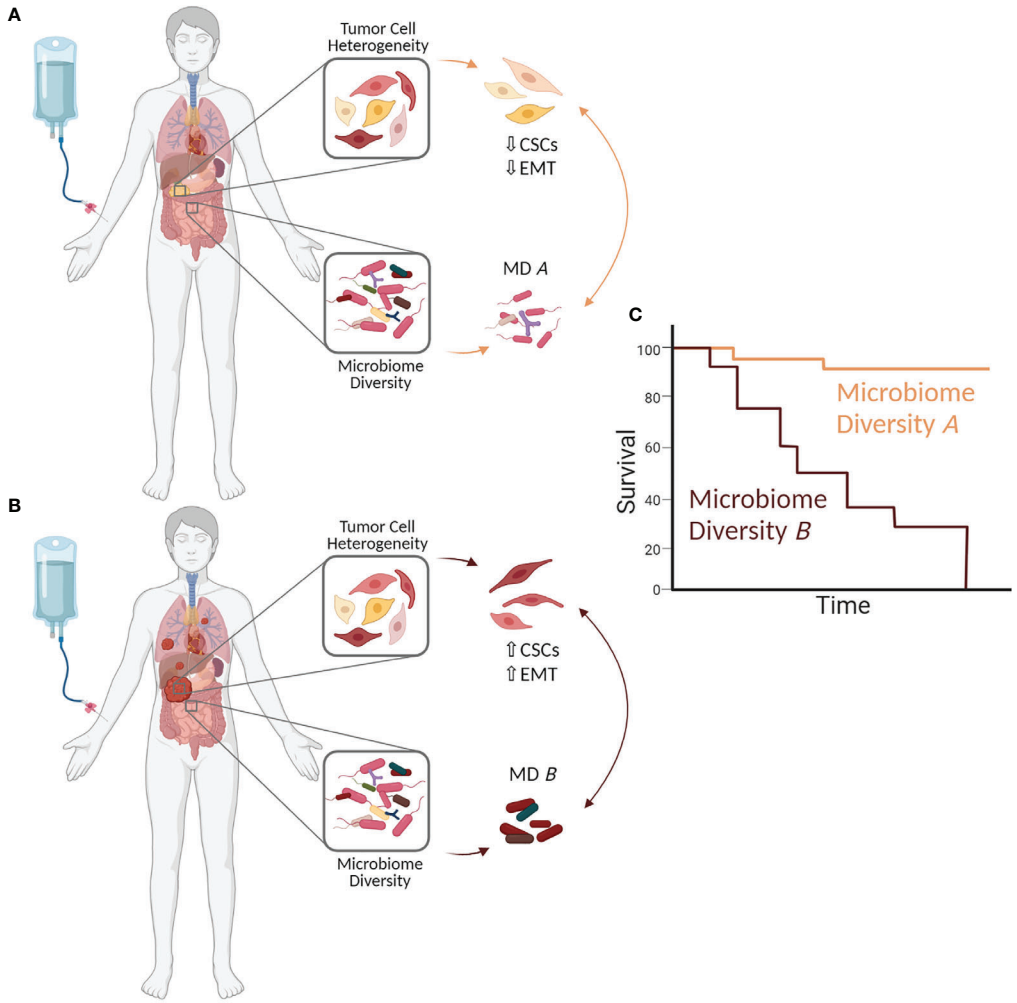

FIGURE 1 | The microbiome impacts clonal heterogeneity of PDAC cells and thereby a patient´s outcome. Changes in the microbiome composition (in the tumor but also other body compartments) may influence Epithelial-Mesenchymal-Transition (EMT) and the abundance and phenotype of cancer stem cells (CSCs) in the tumor by generating optimal niche conditions and impacting their survival and expansion. This in turn impacts PDAC growth and progression as well as therapy responses and outcome of PDAC patients. **(A)** Microbiome diversity A (MD A) may prevent/control EMT induction and the enrichment of CSCs (CSC ↓), thereby inhibiting PDAC progression, drug resistance and **(C)** improving patient´s prognosis. **(B)** In contrast, microbiome diversity B (MD B) may induce EMT and increase the CSC potential within a tumor (CSC↑). As a consequence, a high CSC abundance promotes PDAC progression and drug resistance leading to **(C)** poor patient´s outcome. The figure was created with BioRender.com.

hypothesis is in line with studies supporting the fact that CSC properties can be gained or lost depending on the tumor microenvironment (24, 33–36). Since it is well known that an inflammatory microenvironment impacts the phenotype and genotype of tumor cells, it can be assumed that the altered composition of the gut as well as the tumor microbiome contribute to the inflammatory processes and thereby to the switch from a physiological (tumor suppressive) into an inflammatory (tumor promoting) tumor microenvironment. This in turn may induce EMT and CSC-properties in PDAC cells, e.g. by elevated levels of EMT/CSC inducing factors such as Transforming Growth Factor-beta1 or Tumor Necrosis Factor-alpha. Further, it cannot be ruled out that bacteria and their released factors directly induce EMT, as it could be demonstrated for *F. nucleatum*, and also promote the gain of CSC properties (56, 57, 61). A high abundance of CSCs in PDAC tissues could be related to PDAC dissemination, and with this progression and resistance to therapy (26, 31, 39, 41, 70–72). Hermann et al. (73) demonstrated that different CSC populations exist in PDAC and exhibit distinct functional capabilities. Thus, CD133+CXCR4+ CSCs were found to be particularly responsible for metastasis (73). Adding to the view of CSC heterogeneity in PDAC, own unpublished data indicate that PDAC cells can exhibit different CSC phenotypes that are characterized by distinct CSC marker expression (high Sox2 or high Nestin expressing CSCs) along with different migratory and invasive abilities. As a consequence, different metastasis patterns can be observed in a preclinical PDAC metastasis model (unpublished data). In line with this,

Nestin was found to be upregulated in various human malignancies (74, 75) including PDAC, where it associated with an elevated liver metastatic potential of CSCs (31, 75). Considering this profound knowledge, we postulate that a more diverse microbiome composition, which was detected in LTS PDAC patients (21), might act in favor of a host defense by controlling the number and phenotype of CSCs in PDAC, resulting in a lower metastatic potential and less resistance towards chemotherapy (**Figure 1A**).

Accordingly, future studies are urgently needed to explore whether- and how a certain microbiome composition (e.g., those of LTS patients or *Fusobacteria*) influences intratumor heterogeneity through the gain and loss of CSC phenotypes, and in turn determines disease progression, therapy responses and survival of PDAC patients. Furthermore, since it is known that certain bacteria can increase the efficacy of therapy (18), the potential of microbiome modulation as an integral part of anti-cancer therapy needs to be further investigated. Given the fact that CSCs are mandatory for tumor initiation, novel therapeutic concepts aimed at their complete eradication. However, since the CSC pool can be constantly regenerated by conversion of non-CSC into CSCs, these strategies will likely ultimately fail. Instead, therapeutic strategies aiming to prevent or control CSCs may be more effective. Thus, the therapeutic enrichment of certain bacteria and/or restoring (physiological) microbiome diversity might be a promising strategy to effectively suppress the appearance, heterogeneity and survival of CSCs, thereby controlling disease progression and increasing the efficacy of therapeutics.

DATA AVAILABILITY STATEMENT

Publicly available datasets were analyzed in this study. This data can be found here: https://pubmed.ncbi.nlm.nih.gov.

AUTHOR CONTRIBUTIONS

Conceptualization, MB and L-MP. Supervision, SS and JB. Visualization, L-MP. Writing – original draft, MB, L-MP, and SS. Writing – review and editing, MB, L-MP, JB, and SS. All authors contributed to the article and approved the submitted version.

FUNDING

This project and its publication were supported by the Research and Training Group 2501 on Translational Evolutionary Research (RTG 2501 TransEvo) funded by the Deutsche Forschungsgemeinschaft.

REFERENCES

1. Siegel RL, Miller KD, Fuchs HE, Jemal A. Cancer Statistics, 2021. *CA Cancer J Clin* (2021) 71(1):7–33. doi: 10.3322/caac.21654
2. Rahib L, Smith BD, Aizenberg R, Rosenzweig AB, Fleshman JM, Matrisian LM. Projecting Cancer Incidence and Deaths to 2030: The Unexpected Burden of Thyroid, Liver, and Pancreas Cancers in the United States. *Cancer Res* (2014) 74(11):2913–21. doi: 10.1158/0008-5472.CAN-14-0155
3. König J, Hartel M, Nies AT, Martignoni ME, Guo J, Büchler MW, et al. Expression and Localization of Human Multidrug Resistance Protein (ABCC) Family Members in Pancreatic Carcinoma. *Int J Cancer* (2005) 115(3):359–67. doi: 10.1002/ijc.20831
4. Nath S, Daneshvar K, Roy LD, Grover P, Kidiyoor A, Mosley L, et al. MUC1 Induces Drug Resistance in Pancreatic Cancer Cells via Upregulation of Multidrug Resistance Genes. *Oncogenesis* (2013) 2(6):e51–9. doi: 10.1038/oncsis.2013.16
5. Wang Z, Li Y, Ahmad A, Banerjee S, Azmi AS, Kong D, et al. Pancreatic Cancer: Understanding and Overcoming Chemoresistance. *Nat Rev Gastroenterol Hepatol* (2011) 8(1):27–33. doi: 10.1038/nrgastro.2010.188
6. Müerköster S, Wegehenkel K, Arlt A, Witt M, Sipos B, Kruse ML, et al. Tumor Stroma Interactions Induce Chemoresistance in Pancreatic Ductal Carcinoma Cells Involving Increased Secretion and Paracrine Effects of Nitric Oxide and Interleukin-1β. *Cancer Res* (2004) 64(4):1331–7. doi: 10.1158/0008-5472.CAN-03-1860
7. Müerköster SS, Werbing V, Koch D, Sipos B, Ammerpohl O, Kalthoff H, et al. Role of Myofibroblasts in Innate Chemoresistance of Pancreatic Carcinoma - Epigenetic Downregulation of Caspases. *Int J Cancer* (2008) 123(8):1751–60. doi: 10.1002/ijc.23703
8. Zhang W, Zhang K, Zhang P, Zheng J, Min C, Li X. Research Progress of Pancreas-Related Microorganisms and Pancreatic Cancer. *Front Oncol* (2021) 10:1–12. doi: 10.3389/fonc.2020.604531
9. van Staalduinen J, Baker D, ten Dijke P, van Dam H. Epithelial–mesenchymal-Transition-Inducing Transcription Factors: New Targets for Tackling Chemoresistance in Cancer? *Oncogene* (2018) 37(48):6195–211. doi: 10.2174/1568009613136660097
10. Shang Y, Cai X, Fan D. Roles of Epithelial-Mesenchymal Transition in Cancer Drug Resistance. *Curr Cancer Drug Targets* (2014) 13(9):915–29.
11. Sui H, Zhu L, Deng W, Li Q. Epithelial-Mesenchymal Transition and Drug Resistance: Role, Molecular Mechanisms, and Therapeutic Strategies. *Oncol Res Treat* (2014) 37(10):584–9. doi: 10.1159/000367802
12. Sung PH, Wen J, Bang S, Park S, Si YS. CD44-Positive Cells Are Responsible for Gemcitabine Resistance in Pancreatic Cancer Cells. *Int J Cancer* (2009) 125 (10):2323–31. doi: 10.1002/ijc.24573
13. Ottinger S, Klöppel A, Rausch V, Liu L, Kallifatidis G, Gross W, et al. Targeting of Pancreatic and Prostate Cancer Stem Cell Characteristics by Crambe Crambe Marine Sponge Extract. *Int J Cancer* (2012) 130(7):1671–81. doi: 10.1002/ijc.26168
14. Rajeshkumar NV, Rasheed ZA, García-García E, López-Ríos F, Fujiwara K, Matsui WH, et al. A Combination of DR5 Agonistic Monoclonal Antibody With Gemcitabine Targets Pancreatic Cancer Stem Cells and Results in Long-Term Disease Control in Human Pancreatic Cancer Model. *Mol Cancer Ther* (2010) 9(9):2582–92. doi: 10.1158/1535-7163.MCT-10-0370
15. Xia P, Xu XY. PI3K/Akt/mTOR Signaling Pathway in Cancer Stem Cells: From Basic Research to Clinical Application. *Am J Cancer Res* (2015) 5 (5):1602–9.
16. Sharma N, Nanta R, Sharma J, Gunewardena S, Singh KP, Shankar S, et al. PI3K/AKT/mTOR and Sonic Hedgehog Pathways Cooperate Together to Inhibit Human Pancreatic Cancer Stem Cell Characteristics and Tumor Growth. *Oncotarget* (2015) 6(31):32039–60. doi: 10.18632/oncotarget.5055
17. Geller LT, Barzily-Rokni M, Danino T, Jonas OH, Shental N, Nejman D, et al. Potential Role of Intratumor Bacteria in Mediating Tumor Resistance to the Chemotherapeutic Drug Gemcitabine. *Science* (2017) 357(6356):1156–60. doi: 10.1126/science.aah5043
18. Vétizou M, JM P, Daillère R, Lepage P, Waldschmitt N, Flament C, et al. Anticancer Immunotherapy by CTLA-4 Blockade Relies on the Gut Microbiota. *Science* (2015) 350(6264):1079–84. doi: 10.1126/science.aad1329

19. Pushalkar S, Hundeyin M, Daley D, Zambirinis CP, Kurz E, Mishra A, et al. The Pancreatic Cancer Microbiome Promotes Oncogenesis by Induction of Innate and Adaptive Immune Suppression. *Cancer Discov* (2018) 8(4):403–16. doi: 10.1158/2159-8290.CD-17-1134
20. Iida N, Dzutsev A, Stewart CA, Smith L, Bouladoux N, Weingarten RA, et al. Commensal Bacteria Control Cancer Response to Therapy by Modulating the Tumor Microenvironment. *Science* (2013) 342(6161):967–70. doi: 10.1126/science.1240527
21. Riquelme E, Zhang Y, Zhang L, Montiel M, Zoltan M, Dong W, et al. Tumor Microbiome Diversity and Composition Influence Pancreatic Cancer Outcomes. *Cell* (2019) 178(4):795–806.e12. doi: 10.1016/j.cell.2019.07.008
22. Nieto MA, Huang RYYJ, Jackson RAA, Thiery JPP. Emt: 2016. *Cell* (2016) 166 (1):21–45. doi: 10.1016/j.cell.2016.06.028
23. Andriani F, Bertolini G, Facchinetti F, Baldoli E, Moro M, Casalini P, et al. Conversion to Stem-Cell State in Response to Microenvironmental Cues Is Regulated by Balance Between Epithelial and Mesenchymal Features in Lung Cancer Cells. *Mol Oncol* (2016) 10(2):253–71. doi: 10.1016/j.molonc.2015.10.002
24. Schwitalla S, Fingerle AA, Cammareri P, Nebelsiek T, Göktuna SI, Ziegler PK, et al. Intestinal Tumorigenesis Initiated by Dedifferentiation and Acquisition of Stem-Cell-Like Properties. *Cell* (2013) 152(1–2):25–38. doi: 10.1016/j.cell.2012.12.012
25. Mani SA, Guo W, Liao M, Eaton EN, Zhou AY, Brooks M, et al. EMT Creates Cells With the Properties of Stem Cells. *Cell* (2008) 133(4):704–15. doi: 10.1016/j.cell.2008.03.027
26. Batlle E, Clevers H. Cancer Stem Cells Revisited. *Nat Med* (2017) 23 (10):1124–34. doi: 10.1038/nm.4409
27. Kreso A, Dick JE. Evolution of the Cancer Stem Cell Model. *Cell Stem Cell* (2014) 14(3):275–91. doi: 10.1016/j.stem.2014.02.006
28. Greaves M. Cancer Stem Cells as "Units of Selection". *Evol Appl* (2013) 6 (1):102–8. doi: 10.1111/eva.12017
29. Quail D F, Taylor M J, Postovit L-M. Microenvironmental Regulation of Cancer Stem Cell Phenotypes. *Curr Stem Cell Res Ther* (2012) 7(3):197–216. doi: 10.2174/157488812799859838
30. Lambert AW, Pattabiraman DR, Weinberg RA. Emerging Biological Principles of Metastasis. *Cell* (2017) 168(4):670–91. doi: 10.1016/j.cell.2016.11.037
31. Knaack H, Lenk L, Philipp L-M, Miarka L, Rahn S, Viol F, et al. Liver Metastasis of Pancreatic Cancer: The Hepatic Microenvironment Impacts Differentiation and Self-Renewal Capacity of Pancreatic Ductal Epithelial Cells. *Oncotarget* (2018) 9(60):31771–86. doi: 10.18632/oncotarget.25884
32. Fulawka L, Donizy P, Halon A. Cancer Stem Cells–the Current Status of an Old Concept: Literature Review and Clinical Approaches. *Biol Res* (2014) 47:66. doi: 10.1186/0717-6287-47-66
33. Nallasamy P, Nimmakayala RK, Karmakar S, Leon F, Seshacharyulu P, Lakshmanan I, et al. Pancreatic Tumor Microenvironment Factor Promotes Cancer Stemness *via* SPP1-CD44 Axis. *Gastroenterology* (2021) S0016–5085 (21)03402-8. doi: 10.1053/j.gastro.2021.08.023.
34. O'Leary DP, O'Leary E, Foley N, Cotter TG, Wang JH, Redmond HP. Effects of Surgery on the Cancer Stem Cell Niche. *Eur J Surg Oncol* (2016) 42(3):319–25. doi: 10.1016/j.ejso.2015.12.008
35. Pozza ED, Dando I, Biondani G, Brandi J, Costanzo C, Zoratti E, et al. Pancreatic Ductal Adenocarcinoma Cell Lines Display a Plastic Ability to Bi-Directionally Convert Into Cancer Stem Cells. *Int J Oncol* (2015) 46(3):1099–108. doi: 10.3892/ijo.2014.2796
36. Chaffer CL, Brueckmann I, Scheel C, Kaestli AJ, Wiggins PA, Rodrigues LO, et al. Normal and Neoplastic Nonstem Cells can Spontaneously Convert to a Stem-Like State. *Proc Natl Acad Sci USA* (2011) 108(19):7950–5. doi: 10.1073/pnas.1102454108
37. Crawford HC, Pasca di Magliano M, Banerjee S. Signaling Networks That Control Cellular Plasticity in Pancreatic Tumorigenesis, Progression, and Metastasis. *Gastroenterology* (2019) 156(7):2073–84. doi: 10.1053/j.gastro.2018.12.042
38. Najafi M, Mortezaee K, Majidpoor J. Cancer Stem Cell (CSC) Resistance Drivers. *Life Sci* (2019) 234:116781. doi: 10.1016/j.lfs.2019.116781
39. Valle S, Martin-Hijano L, Alcalá S, Alonso-Nocelo M, Sainz B. The Ever-Evolving Concept of the Cancer Stem Cell in Pancreatic Cancer. *Cancers (Basel)* (2018) 10(2):33. doi: 10.3390/cancers10020033
40. Steinbichler TB, Dudás J, Skvortsov S, Ganswindt U, Riechelmann H, Skvortsova II. Therapy Resistance Mediated by Cancer Stem Cells. *Semin Cancer Biol* (2018) 53:156–67. doi: 10.1016/j.semcancer.2018.11.006
41. Aponte PM, Caicedo A. Stemness in Cancer: Stem Cells, Cancer Stem Cells, and Their Microenvironment. *Stem Cells Int* (2017) 2017:5619472. doi: 10.1155/2017/5619472
42. Heiler S, Wang Z, Zöller M. Pancreatic Cancer Stem Cell Markers and Exosomes - The Incentive Push. *World J Gastroenterol* (2016) 22(26):5971–6007. doi: 10.3748/wjg.v22.i26.5971
43. Patil K, Khan FB, Akhtar S, Ahmad A, Uddin S. The Plasticity of Pancreatic Cancer Stem Cells: Implications in Therapeutic Resistance. *Cancer Metastasis Rev* (2021). doi: 10.1007/s10555-021-09979-x. Online ahead of print
44. Eckburg PB, Bik EM, Bernstein CN, Purdom E, Dethlefsen L, Sargent M, et al. Microbiology: Diversity of the Human Intestinal Microbial Flora. *Science* (2005) 308(5728):1635–8. doi: 10.1126/science.1110591
45. Ley RE, Peterson DA, Gordon JI. Ecological and Evolutionary Forces Shaping Microbial Diversity in the Human Intestine. *Cell* (2006) 124(4):837–48. doi: 10.1016/j.cell.2006.02.017
46. Arrieta MC, Arévalo A, Stiemsma L, Dimitriu P, Chico ME, Loor S, et al. Associations Between Infant Fungal and Bacterial Dysbiosis and Childhood Atopic Wheeze in a Nonindustrialized Setting. *J Allergy Clin Immunol* (2018) 142(2):424–34.e10. doi: 10.1016/j.jaci.2017.08.041
47. Gevers D, Kugathasan S, Denson LA, Vázquez-Baeza Y, Van Treuren W, Ren B, et al. The Treatment-Naive Microbiome in New-Onset Crohn's Disease. *Cell Host Microbe* (2014) 15(3):382–92. doi: 10.1016/j.chom.2014.02.005
48. Harsch I, Konturek P. The Role of Gut Microbiota in Obesity and Type 2 and Type 1 Diabetes Mellitus: New Insights Into "Old" Diseases. *Med Sci* (2018) 6 (2):32. doi: 10.3390/medsci6020032
49. Tang WHW, Li DY, Hazen SL. Dietary Metabolism, the Gut Microbiome, and Heart Failure. *Nat Rev Cardiol* (2019) 16:137–54. Nature Publishing Group. doi: 10.1038/s41569-018-0108-7
50. Dzutsev A, Goldszmid RS, Viaud S, Zitvogel L, Trinchieri G. The Role of the Microbiota in Inflammation, Carcinogenesis, and Cancer Therapy. *Eur J Immunol* (2015) 45(1):17–31. doi: 10.1002/eji.201444972
51. Nishida A, Inoue R, Inatomi O, Bamba S, Naito Y, Andoh A. Gut Microbiota in the Pathogenesis of Inflammatory Bowel Disease. *Clin J Gastroenterol* (2018) 11(1):1–10. doi: 10.1007/s12328-017-0813-5
52. Maekawa T, Fukaya R, Takamatsu S, Itoyama S, Fukuoka T, Yamada M, et al. Possible Involvement of Enterococcus Infection in the Pathogenesis of Chronic Pancreatitis and Cancer. *Biochem Biophys Res Commun* (2018) 506 (4):962–9. doi: 10.1016/j.bbrc.2018.10.169
53. Guo Y, Liu W, Wu J. Helicobacter Pylori Infection and Pancreatic Cancer Risk: A Meta-Analysis. *J Cancer Res Ther* (2016) 12(8):C229–32. doi: 10.4103/0973-1482.200744
54. Padoan A, Plebani M, Basso D. Inflammation and Pancreatic Cancer: Focus on Metabolism, Cytokines, and Immunity. *Int J Mol Sci* (2019) 20(3):676. doi: 10.3390/ijms20030676
55. Hofman P, Vouret-Craviari V. Microbes-Induced EMT at the Crossroad of Inflammation and Cancer. *Gut Microbes* (2012) 3(3):176–85. doi: 10.4161/gmic.20288
56. Gaiser RA, Halimi A, Alkharaan H, Lu L, Davanian H, Healy K, et al. Enrichment of Oral Microbiota in Early Cystic Precursors to Invasive Pancreatic Cancer. *Gut* (2019) 68(12):2186–94. doi: 10.1136/gutjnl-2018-317458
57. Ciernikova S, Mego M, Novisedlakova M, Cholujova D, Stevurkova V. The Emerging Role of Microbiota and Microbiome in Pancreatic Ductal Adenocarcinoma. *Biomedicines* (2020) 8(12):1–21. doi: 10.3390/biomedicines8120565
58. Mitsuhashi K, Nosho K, Sukawa Y, Matsunaga Y, Ito M, Kurihara H, et al. Association of Fusobacterium Species in Pancreatic Cancer Tissues With Molecular Features and Prognosis. *Oncotarget* (2015) 6(9):7209–20. doi: 10.18632/oncotarget.3109
59. Rogers MB, Aveson V, Firek B, Yeh A, Brooks B, Brower-Sinning R, et al. Disturbances of the Perioperative Microbiome Across Multiple Body Sites in Patients Undergoing Pancreaticoduodenectomy. *Pancreas* (2017) 46(2):260–7. doi: 10.1097/MPA.0000000000000726
60. Tada K, Ohta M, Hidano S, Watanabe K, Hirashita T, Oshima Y, et al. Fucosyltransferase 8 Plays a Crucial Role in the Invasion and Metastasis of

Pancreatic Ductal Adenocarcinoma. *Surg Today* (2020) 50(7):767–77. doi: 10.1007/s00595-019-01953-z
61. Hosein AN, Brekken RA, Maitra A. Pancreatic Cancer Stroma: An Update on Therapeutic Targeting Strategies. *Nat Rev Gastroenterol Hepatol* (2020) 17 (8):487–505. doi: 10.1038/s41575-020-0300-1
62. Vergara D, Simeone P, Damato M, Maffia M, Lanuti P, Trerotola M. The Cancer Microbiota: EMT and Inflammation as Shared Molecular Mechanisms Associated With Plasticity and Progression. *J Oncol* (2019) 2019:1253727. doi: 10.1155/2019/1253727
63. Sivan A, Corrales L, Hubert N, Williams JB, Aquino-Michaels K, Earley ZM, et al. Commensal Bifidobacterium Promotes Antitumor Immunity and Facilitates Anti-PD-L1 Efficacy. *Science* (2015) 350(6264):1084–9. doi: 10.1126/science.aac4255
64. Matson V, Fessler J, Bao R, Chongsuwat T, Zha Y, Alegre ML, et al. The Commensal Microbiome Is Associated With Anti-PD-1 Efficacy in Metastatic Melanoma Patients. *Science* (2018) 359(6371):104–8. doi: 10.1126/science.aao3290
65. Mendez R, Kesh K, Arora N, Di ML, McAllister F, Merchant N, et al. Microbial Dysbiosis and Polyamine Metabolism as Predictive Markers for Early Detection of Pancreatic Cancer. *Carcinogenesis* (2020) 41(5):561–70. doi: 10.1093/carcin/bgz116
66. Leinwand JC, Miller G. Microbes as Biomarkers and Targets in Pancreatic Cancer. *Nat Rev Clin Oncol* (2019) 16(11):665–6. doi: 10.1038/s41571-019-0276-3
67. Huang J, Jiang Z, Wang Y, Fan X, Cai J, Yao X, et al. Modulation of Gut Microbiota to Overcome Resistance to Immune Checkpoint Blockade in Cancer Immunotherapy. *Curr Opin Pharmacol* (2020) 54:1–10. doi: 10.1016/j.coph.2020.06.004
68. Thomas RM, Jobin C. Microbiota in Pancreatic Health and Disease: The Next Frontier in Microbiome Research. *Nat Rev Gastroenterol Hepatol* (2020) 17 (1):53–64. doi: 10.1038/s41575-019-0242-7
69. Wei MY, Shi S, Liang C, Meng QC, Hua J, Zhang YY, et al. The Microbiota and Microbiome in Pancreatic Cancer: More Influential Than Expected. *Mol Cancer* (2019) 18(1):1–15. doi: 10.1186/s12943-019-1008-0
70. Fabian A, Stegner S, Miarka L, Zimmermann J, Lenk L, Rahn S, et al. Metastasis of Pancreatic Cancer: An Uninflamed Liver Micromilieu Controls Cell Growth and Cancer Stem Cell Properties by Oxidative Phosphorylation in Pancreatic Ductal Epithelial Cells. *Cancer Lett* (2019) 453:95–106. doi: 10.1016/j.canlet.2019.03.039
71. Dando I, Dalla Pozza E, Biondani G, Cordani M, Palmieri M, Donadelli M. The Metabolic Landscape of Cancer Stem Cells. *IUBMB Life* (2015) 67 (9):687–93. doi: 10.1002/iub.1426
72. Hanahan D, Weinberg RA. Hallmarks of Cancer: The Next Generation. *Cell* (2011) 144(5):646–74. doi: 10.1016/j.cell.2011.02.013
73. Hermann PC, Huber SL, Herrler T, Aicher A, Ellwart JW, Guba M, et al. Distinct Populations of Cancer Stem Cells Determine Tumor Growth and Metastatic Activity in Human Pancreatic Cancer. *Cell Stem Cell* (2007) 1 (3):313–23. doi: 10.1016/j.stem.2007.06.002
74. Neradil J, Veselska R. Nestin as a Marker of Cancer Stem Cells. *Cancer Sci* (2015) 106(7):803–11. doi: 10.1111/cas.12691
75. Matsuda Y, Naito Z, Kawahara K, Nakazawa N, Korc M, Ishiwata T. Nestin Is a Novel Target for Suppressing Pancreatic Cancer Cell Migration, Invasion and Metastasis. *Cancer Biol Ther* (2011) 11(5):512–23. doi: 10.4161/cbt.11.5.14673

Conflict of Interest: The authors declare that the research was conducted in the absence of any commercial or financial relationships that could be construed as a potential conflict of interest.

Publisher's Note: All claims expressed in this article are solely those of the authors and do not necessarily represent those of their affiliated organizations, or those of the publisher, the editors and the reviewers. Any product that may be evaluated in this article, or claim that may be made by its manufacturer, is not guaranteed or endorsed by the publisher.

frontiers in Oncology

ORIGINAL RESEARCH
published: 03 December 2021
doi: 10.3389/fonc.2021.769727

Development and Validation of a Prognostic Gene Signature Correlated With M2 Macrophage Infiltration in Esophageal Squamous Cell Carcinoma

Jiannan Yao[1†], Ling Duan[1†], Xuying Huang[1], Jian Liu[1,2], Xiaona Fan[1], Zeru Xiao[1], Rui Yan[1], Heshu Liu[1], Guangyu An[1], Bin Hu[3] and Yang Ge[1*]*

[1] Department of Oncology, Beijing Chao-Yang Hospital, Capital Medical University, Beijing, China, [2] Medical Research Center, Beijing Chao-Yang Hospital, Capital Medical University, Beijing, China, [3] Department of Thoracic Surgery, Beijing Chao-Yang Hospital, Capital Medical University, Beijing, China

OPEN ACCESS

Edited by:
Jia Wei,
Nanjing Drum Tower Hospital, China

Reviewed by:
Zhuolun Sun,
Third Affiliated Hospital of Sun Yat-sen University, China
Jinhui Liu,
Nanjing Medical University, China

***Correspondence:**
Yang Ge
interna-1@163.com
Bin Hu
hubin705@aliyun.com

[†]These authors have contributed equally to this work and share first authorship

Specialty section:
This article was submitted to Gastrointestinal Cancers: Gastric & Esophageal Cancers, a section of the journal Frontiers in Oncology

Received: *02 September 2021*
Accepted: *16 November 2021*
Published: *03 December 2021*

Citation:
Yao J, Duan L, Huang X, Liu J, Fan X, Xiao Z, Yan R, Liu H, An G, Hu B and Ge Y (2021) Development and Validation of a Prognostic Gene Signature Correlated With M2 Macrophage Infiltration in Esophageal Squamous Cell Carcinoma. Front. Oncol. 11:769727. doi: 10.3389/fonc.2021.769727

Background: Esophageal squamous cell carcinoma (ESCC) is the most common type of esophageal cancer and the seventh most prevalent cause of cancer-related death worldwide. Tumor microenvironment (TME) has been confirmed to play an crucial role in ESCC progression, prognosis, and the response to immunotherapy. There is a need for predictive biomarkers of TME-related processes to better prognosticate ESCC outcomes.

Aim: To identify a novel gene signature linked with the TME to predict the prognosis of ESCC.

Methods: We calculated the immune/stromal scores of 95 ESCC samples from The Cancer Genome Atlas (TCGA) using the ESTIMATE algorithm, and identified differentially expressed genes (DEGs) between high and low immune/stromal score patients. The key prognostic genes were further analyzed by the intersection of protein–protein interaction (PPI) networks and univariate Cox regression analysis. Finally, a risk score model was constructed using multivariate Cox regression analysis. We evaluated the associations between the risk score model and immune infiltration *via* the CIBERSORT algorithm. Moreover, we validated the signature using the Gene Expression Omnibus (GEO) database. Within the ten gene signature, five rarely reported genes were further validated with quantitative real time polymerase chain reaction (qRT-PCR) using an ESCC tissue cDNA microarray.

Results: A total of 133 up-regulated genes were identified as DEGs. Ten prognostic genes were selected based on intersection analysis of univariate COX regression analysis and PPI, and consisted of C1QA, C1QB, C1QC, CD86, C3AR1, CSF1R, ITGB2, LCP2, SPI1, and TYROBP (HR>1, $p<0.05$). The expression of 9 of these genes in the tumor samples were significantly higher compared to matched adjacent normal tissue based on the GEO database ($p<0.05$). Next, we assessed the ability of the ten-gene signature to predict the overall survival of ESCC patients, and found that the high-risk group had

significantly poorer outcomes compared to the low-risk group using univariate and multivariate analyses in the TCGA and GEO cohorts (HR=2.104, 95% confidence interval:1.343-3.295, p=0.001; HR=1.6915, 95% confidence interval:1.053-2.717, p=0.0297). Additionally, receiver operating characteristic (ROC) curve analysis demonstrated a relatively sensitive and specific profile for the signature (1-, 2-, 3-year AUC=0.672, 0.854, 0.81). To identify the basis for these differences in the TME, we performed correlation analyses and found a significant positive correlation with M1 and M2 macrophages and CD8+ T cells, as well as a strong correlation to M2 macrophage surface markers. A nomogram based on the risk score and select clinicopathologic characteristics was constructed to predict overall survival of ESCC patients. For validation, qRT-PCR of an ESCC patient cDNA microarray was performed, and demonstrated that C1QA, C3AR1, LCP2, SPI1, and TYROBP were up-regulated in tumor samples and predict poor prognosis.

Conclusion: This study established and validated a novel 10-gene signature linked with M2 macrophages and poor prognosis in ESCC patients. Importantly, we identified C1QA, C3AR1, LCP2, SPI1, and TYROBP as novel M2 macrophage-correlated survival biomarkers. These findings may identify potential targets for therapy in ESCC patients.

Keywords: Esophageal squamous cell carcinoma, tumor microenvironment, prognostic biomarker, immunotherapy, M2 macrophage

INTRODUCTION

Esophageal cancer (EC) is the seventh leading cause of cancer-related death worldwide due to its high malignancy and poor prognosis, with an estimated 5-year survival rate of approximately 10-15% (1–3). It is estimated that approximately 572034 new cases of esophageal cancer and 508585 deaths due to EC in 2018 worldwide (4). Esophageal Squamous cell carcinoma (ESCC) is the predominant histology of EC, constituting 90% of cases worldwide, and approximately half of the world's 500,000 new cases occur in China each year (5). More than half of ESCC patients are at an advanced stage when diagnosed (6). Despite recent advances in multidisciplinary therapeutic approaches, its prognosis remains unfavorable due to the high rates of recurrence, metastasis and the resistance to systematic therapy (7). Immunotherapy is a revolutionary treatment approach which has led to marked therapeutic responses among advanced melanoma, non–small cell lung cancer and renal cell carcinoma. There is an increasing interest in the potential of immunotherapy against ESCC to improve the prognosis of patients. Currently, a variety of clinical trials are ongoing to evaluate immunotherapy as a first line treatment for ESCC. However, the evidence to date suggests that only a minority of patients can benefit from it. Therefore, an urgent need remains to identify innovative biomarkers to accurately predict the prognosis of ESCC patients receiving immunotherapy.

The tumor microenvironment (TME) is the environment in which tumor cells live, and is comprised of innate immune cells, including macrophages, dendritic cells, neutrophils, natural killer (NK) cells, myeloid derived suppressor cells (MDSCs), T and B cells, and stromal cells including fibroblasts, endothelial cells and extracellular matrix (ECM) (8). Studies have revealed that the TME is heterogeneous, and that various tumor-infiltrating immune cells play a pro- or anti-tumorigenic role within it (9, 10). It is thought to contribute to inhibiting apoptosis, enabling immune evasion, and promoting proliferation, angiogenesis, invasion and metastasis (11). Notably, the TME is a key target for immunotherapy in cancer patients (12, 13). Tumors with high CD8+ T cell infiltration ("hot" tumors) show the best response to immune checkpoint inhibitors (ICIs). In contrast, patients with "cold" tumors—also called immune deserts, do not benefit from ICIs due to lack of infiltration with CD8+ T cells (14). A previous study reported that several immune-suppressive cell populations were enriched in TME of ESCC, including regulatory T cell (Tregs), exhausted $CD8^+$ T, $CD4^+$ T and NK cells, M2 macrophages (15). Moreover, the population densities of NK cells and macrophages has been found to significantly related with postoperative prognosis for stage II-III esophageal cancer patients (16). Further research suggested that Tregs infiltration had an association with the pathological response and showed a potential value in predicting cancer-specific survival (17). Macrophages have been confirmed to impact angiogenesis, tumor cell migration, and invasion and are expected to be attractive targets for cancer immunotherapy. Within the TME, macrophages may polarize into anti-tumorigenic M1 or pro-tumorigenic M2 phenotypes (7, 11). Tumor-associated macrophages (TAM) can promote genetic stability, nurture cancer stem cells, and contribute to tumor progression and metastasis. TAM infiltration is associated with poor responses to chemotherapy and overall poor prognosis (2). Yamamoto et al. confirmed that pre–therapeutic M2 macrophage infiltration would be a useful biomarker for

predicting the response to neoadjuvant chemotherapy (NAC) compared with other immune cells in EC patients (18). Moreover, it has been reported that FOXO1 upregulation in tumor tissues drive the polarization of M0 macrophages and infiltration of M2 macrophages into the TME, resulting in worse prognosis in ESCC patients (19). More recently, CSF-1/CSF-1R blockade has gained widespread attention as a TAM-targeted treatment in cancer research (20, 21). Overall, a better understanding of the status of TME in ESCC patient tumors can help to characterize their immunogenomic profile and improve outcomes.

ESTIMATE (Estimation of STromal and Immune cells in MAlignant Tumor tissues using Expression data) is an algorithm designed to analyze cell purity by calculating the ratio of immune and stromal components based on gene expression (22). In our current study, we utilized ESTIMATE and the CIBERSORT algorithm to quantify the level of tumor immune infiltration of 95 ESCC samples from the TCGA database and identified a predictive 10-gene signature associated with poor prognosis of patients. We further verified its prognostic value in the GEO dataset and confirmed its independent prognostic effect. This work, for the first time, establishes a novel M2 macrophage-related gene signature in ESCC and may be used to predict patient outcomes. Moreover, we validated five of the ten genes (C1QA, C3AR1, LCP2, SPI1 and TYROBP) as independently associated with poor survival and tightly related with macrophage M2 surface biomarkers by qPCR, which may provide new therapeutic avenue for ESCC.

MATERIALS AND METHODS

Data Download and Preparation

The level 3 gene expression profile and corresponding clinical information of ESCC patients were downloaded from UCSC Xena (dataset ID: TCGA-ESCA-sampleMap/HiSeqV2, https://xenabrowser.net/datapages/). The gene expression profile was measured experimentally using the Illumina HiSeq 2000 RNA Sequencing platform by the University of North Carolina TCGA genome characterization center. Gene expression was provided as gene-level transcription estimates with units as log2(x+1) transformed RSEM normalized count. Low-expression genes with mean expression values below 1 RSEM in all samples were filtered out using the "limma" package in R version 4.0.2 software. The original data included 185 tumor tissues and 11 adjacent tissues. Among these, 96 samples were histologically diagnosed as squamous cell carcinoma, including 1 paired metastasis tissue. The clinical information of the patients is shown in **Supplemental Table 1**. The risk score model was further validated using the GSE53624 dataset from the Gene Expression Omnibus (GEO, http://www.ncbi. nlm.nih.gov/geo/). The screening process of the validation dataset is provided in **Supplemental Figure 1**. The GSE53624 dataset included 119 paired tumor and normal ESCC tissues based on GPL18109 platform (Agilent-038314 CBC Homo sapiens lncRNA + mRNA microarray V2.0).

Estimation of Stromal and Immune Components of TME

Immune, stromal, and ESTIMATE scores of the samples were calculated using the estimate R package. We determined the optimal cutpoint based on the function "surv_cutpoint" from the survminer R package. Kaplan–Meier analyses were performed using the survival and survminer packages in R to illustrate the correlation of immune/stromal scores and patient overall survival (OS). The log-rank test was applied to verify the results.

Identification of Differentially Expressed Genes (DEGs)

According the optimal cutpoint, immune and stromal scores were divided into high/low groups, respectively. DEGs were identified using the R package, limma. The threshold set for up- and down-regulated genes was a $|\log 2 \text{ foldchange (FC)}| > 1$ and false discovery rate (FDR) < 0.05. Heatmaps were plotted with the package pheatmap.

Enrichment Analyses and Protein-Protein Interaction (PPI) Network

Functional enrichment analyses of the DEGs with the Kyoto Encyclopedia of Genes and Genomes (KEGG) and gene ontology (GO) were performed with the R package "clusterProfiler", "org.Hs.eg.db", "enrichplot" and "ggplot2". GO enrichment includes biological processes (BP), cellular component (CC) and molecular function (MF). Categories with a p- and q-value of <0.05 were considered significantly enriched. All of the DEGs were uploaded into the STRING (https://string-db.org/) database (v 11.0) to obtain PPI networks, with a combined score > 0.4 considered statistically significant. Cytoscape (version 3.7.1) was used to reconstruct the network. Network nodes represent proteins and edges represent protein-protein associations.

Construction and Validation of 10-Gene Risk Score Model

Univariate cox regression analysis was performed to examine the prognostic value among ESCC patients. 36 genes with $p < 0.05$ were identified as prognostic DEGs and were visualized using the forest diagram. Multivariate analyses were performed to develop the 10-gene risk score model. The model was based on expression data multiplied by Cox regression coefficients. The final risk score model formula was as followed: Risk score = [Expression level of C1QA * (0.32596)] +[Expression level of C1QB * (1.40234)]+[Expression level of C1QC* (-1.36687)+ [Expression level of CD86 * (0.35249)] +[Expression level of C3AR1* (-0.07155)+ [Expression level of CSF1R * (0.28413)]+[Expression level of ITGB2 * (-0.52918)] +[Expression level of LCP2* (-0.22934)+ [Expression level of SPI1 * (1.05328)]+[Expression level of TYROBP* (-0.87910)]. Patients were divided into low-risk and high-risk groups according to the optimal cutpoint. The K-M survival curves for the groups with low or high risk were performed. The predictive ability of the model was assessed by the survival receiver operating characteristic (ROC) package in R software and was used to compare the area under the curve (AUC) of our gene signature and those derived in two other published studies. To confirm the risk model's independent

prognostic value, univariate and multivariate Cox survival analyses were performed with select clinical factors. Finally, external data from GSE53624 was applied to verify the reliability of the gene signature's impact on the prognosis of the patients. The differential expression analysis was performed based on 119 paired tumor and normal samples.

Estimation of Immune Infiltration

CIBERSORT in combination with the LM22 method was carried out to quantify the abundances of immune cell types in the TME. The 22 types of infiltrating immune cells inferred by CIBERSORT include B cells, T cells, natural killer cells, macrophages, dendritic cells, eosinophils and neutrophils. The CIBERSORT p-value reflects the statistical significance of the results, only tumor samples with $p<0.05$ were used for further analysis.

Construction and Validation of the Nomogram

A nomogram was established based on the risk score and select clinicopathologic characteristics including age, gender and stage to predict the survival probability of 1-, 2-, and 3-year OS of ESCC patients. The nomogram and calibration plots were generated based on the rms R package. The calibration curve of the nomogram was plotted to evaluate the prediction possibilities against the observed rates.

Gene Set Enrichment Analysis (GSEA)

GSEA was carried out to evaluate associations between immune pathways and 10-gene signature using the software GSEA-4.1.0. Hallmark (h.all.v7.4.symbols.gmt) and C7 gene sets (c7.all.v7.4.symbols.gmt, Immunologic Signatures) were downloaded from Molecular Signatures Database (MSigDB) as the target sets. Only gene sets with NOM $p < 0.05$ and FDR $q < 0.25$ were considered significant.

cDNA Microarray Chip and Real-Time PCR

Tissue cDNA chips including cDNA from 67 cases of esophageal squamous cell carcinoma tissue and 28 peri-carcinoma tissues with complete clinical and survival information were purchased. A cDNA microarray chip (cDNA-HEsoS095Su01,Outdo Biotech Company, Beijing, China) was used for the tumor or peritumor tissue samples in this study. The mRNA expression levels of hub genes and immune cell surface biomarkers were detected by Hieff qPCR SYBR Green Master Mix (Low Rox Plus) (YEASEN Biotech Co., Ltd). The qPCR protocol was 95°C for 5min, 40 cycles at 95°C for 10 s, and 60°C for 60 s. Primers used in this study are presented in **Supplemental Table 2**. The relative expression levels of hub genes were determined by the $2^{-\Delta\Delta CT}$ method.

Statistical Analysis

The correlation analysis was performed using the Spearman method. Survival curves were compared using the Kaplan-Meier method and the log-rank test. R version 4.0.2 and GraphPad 5.0 were used to perform statistical analysis. The results are presented as mean ± standard deviation (mean ± SD). Differences between groups were evaluated by the Wilcoxon rank-sum test. All tests were two-sided and $p < 0.05$ indicates statistical significance.

RESULTS

Immune and Stromal Scores Are Significantly Correlated With ESCC Survival

The analysis process for this study is presented in **Figure 1**. We estimated the immune/stromal/ESTIMATE scores of 95 ESCC tumors using the ESTIMATE algorithm. The immune scores varied from -1389.05 to 3395.19, the stromal scores ranged from -1859.96 to 1301.57, the ESTIMATE scores ranged from -2672.1 to 3970.4. All samples were categorized to high/low groups with the optimal cutpoint. Using Kaplan-Meier analysis, we found that patients with higher immune scores experienced poorer overall survival (OS) compared to those with low scores ($p=0.015$, **Figure 2A**). In agreement, stromal scores were inversely correlated with OS ($p=0.012$, **Figure 2B**). The high ESTIMATE score group also showed poorer OS in comparison to the low score group ($p=0.057$, **Figure 2C**). These findings demonstrate that the immune/stromal components in TME are significant in predicting the prognosis of ESCC patients. We further explored the potential relationship between the clinicopathological characteristics and the immune/stromal scores, but found no significant associations.

Differential Expression and Functional Enrichment Analysis

To investigate the potential relationship between gene expression profiles and immune/stromal scores, we performed differential expression analysis of high- and low-score groups. According to the analysis (high immune score vs low immune score), a total of 747 DEGs were selected, which contained 674 up-regulated and 73 down-regulated DEGs. Similarly, 1027 DEGs were obtained based on differential analysis of stromal scores, consisting of 855 up-regulated and 172 down-regulated DEGs. Hierarchical clustering (**Figures 3A, B**) showed that DEGs were significantly dysregulated between the two groups. Furthermore, after intersection of the two lists of genes (**Figures 3C, D**), we obtained 133 up-regulated DEGs shared by immune and stromal groups. These DEGs can be regarded as candidate TME-related genes.

Furthermore, functional enrichment analysis was performed to find the potential mechanism of 133 DEGs in the TME. The top 10 significant results of the enrichment analysis for BP, CC and MF are displayed in **Figure 3E**. For BP, DEGs were mainly enriched in immune effector processes, negative regulation of immune system processes, and positive regulation of cell activation. In the CC group, DEGs were mainly enriched in the external side of plasma membrane, protein complex involved in cell adhesion, and secretory granule membrane. In the MF classification, the top terms included immunoglobulin binding, immune receptor activity, chemokine activity, cytokine receptor activity, and chemokine receptor binding. For the KEGG analysis (**Figure 3F**), DEGs were mainly enriched in the Natural killer cell

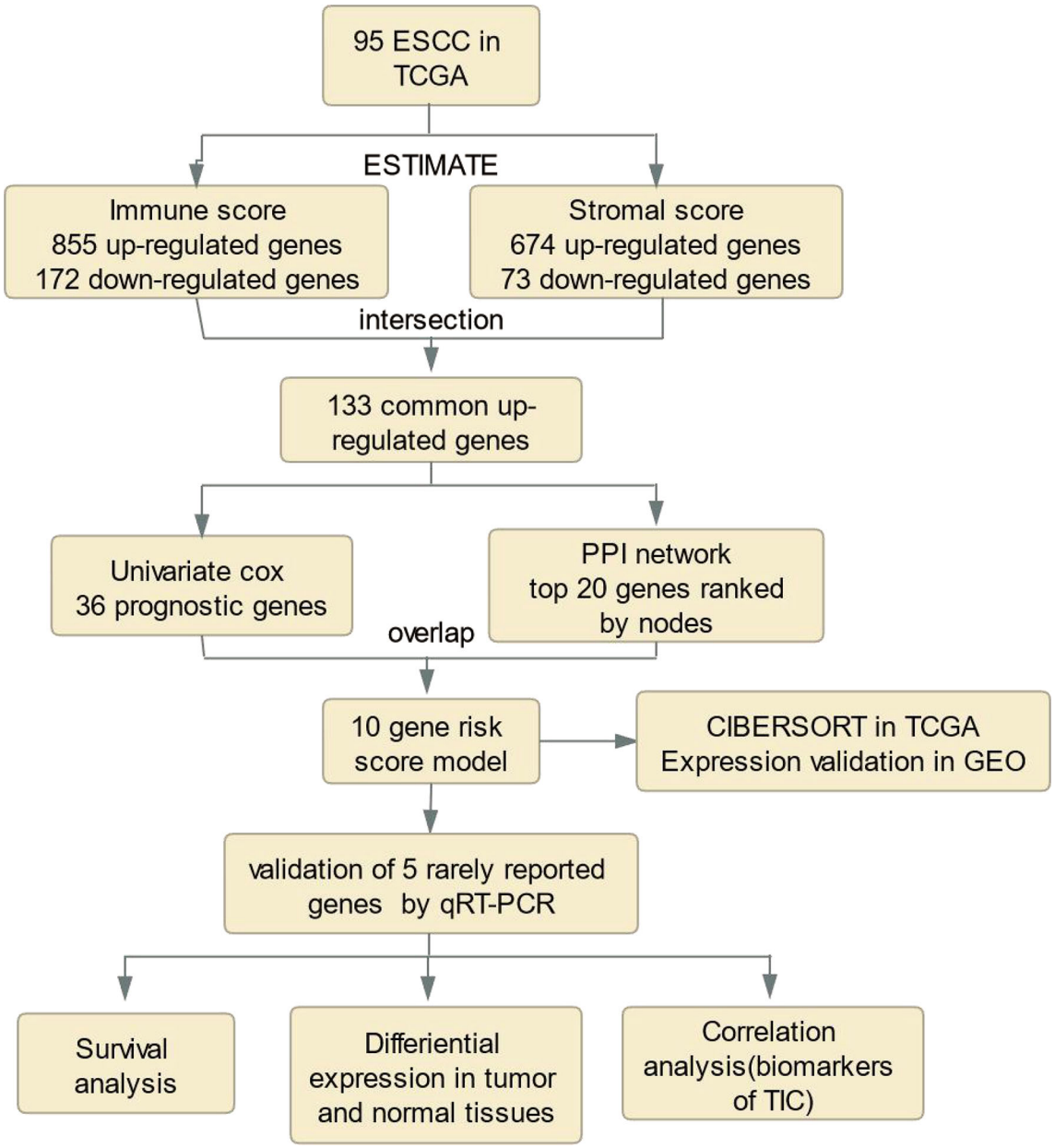

FIGURE 1 | Analysis workflow of this study.

mediated cytotoxicity, Toll–like receptor signaling pathway, viral protein interaction with cytokine and cytokine receptor, cell adhesion molecules, Th17 cell differentiation, and chemokine signaling pathways. Collectively, these findings suggest that the functions of these genes are immune-related.

Intersection of PPI Network and Univariate Cox Regression Analysis

To better illustrate the interrelationship among these DEGs, we used the STRING database and the Cytoscape software to construct a PPI network. As depicted in **Figure 4A**, the color from light to dark represents the ascending logFC value. The barplot (**Figure 4B**) shows the top 20 hub genes ranked by the number of nodes. Next, we carried out univariate cox regression analysis and identified 36 genes significantly associated with the poor OS of ESCC patients ($HR>1$, $p<0.05$). Finally, the 10 independent prognostic genes in the PPI and univariate cox regression analysis were overlapped to identify the common hub genes, including C1QA, C1QB, C1QC, CD86, C3AR1, CSF1R, ITGB2, LCP2, SPI1 and TYROBP (**Figure 4C**). The forest diagram (**Figure 4D**) illustrates the relationships between these 10 genes and prognosis. The Kaplan-Meier curve confirmed that high expression of 9 of the genes

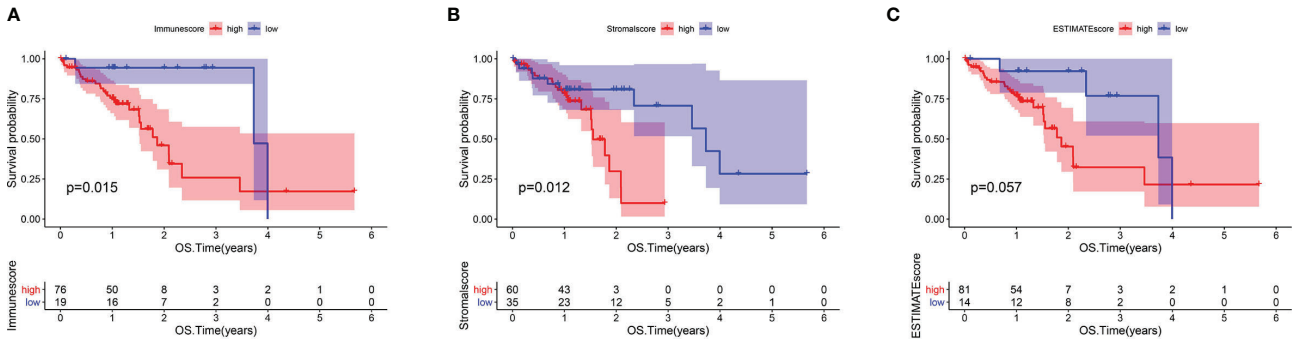

FIGURE 2 | Immune and Stromal scores were correlated with overall survival of ESCC. **(A)** Kaplan–Meier survival analysis for ESCC patients grouped into high or low score in Immunescore determined by the optimal cutoff. p = 0.015 by log-rank test. **(B)** Kaplan–Meier survival curve for Stromalscore with p = 0.012 by log-rank test. **(C)** Survival analysis with Kaplan–Meier method for ESCC patients grouped by ESTIMATEScore (p = 0.057 by log-rank test).

(C1QA, C1QB, CSF1R, C3AR1, ITGB2, LCP2, SPI1, TYROBP) were significantly related to poor OS (**Supplemental Figures 2A–I**, p<0.05). Moreover, for those variables in which survival curves intersected, we carried out landmark analysis discriminating between events occurring before and after 3 years of follow-up to eliminate immortal time bias, which confirmed that all genes are significantly related to overall survival before 3 years (**Supplemental Figure 3B**, p-value<0.05).

Correlations Between Immune Infiltration and Prognostic Genes

The CIBERSORT algorithm was then used to quantify the proportion of tumor-infiltrating immune subsets and further understand the correlation of hub genes with the immune TME. **Figure 5A** shows the relative proportions of immune cells in each ESCC sample. Positive and negative correlations between immune cells were obtained, as displayed in **Figure 5B**. There was a moderate correlation between macrophage M0 and macrophage M2 (r=-0.49) in ESCC. CD8 T cells were moderately and positively correlated with activated CD4 memory T cells (r=0.27), while negatively correlated with resting CD4 memory T cells (r=-0.62). M1 macrophages were positively associated with Tregs (r=0.23) and M2 macrophages (r=0.24), and negatively associated with activated dendritic cells (r=-0.44). These results reveal that different kinds of immune cells interfere with each other in TME. Pearson correlation analysis was further performed to compare the expression of ten genes and the results of ESTIMATE. All ten genes were strongly positively correlated with ImmuneScore but negatively correlated with TumorPurity (**Figure 5C**, p <0.05), demonstrating lower the purity of the tumor and increased immune cells in the TME. Moreover, we searched the CCLE (Cancer Cell Line Encyclopedia) database to help clarify whether these genes are overexpressed in immune cells or tumor cells. The expression values for the ten genes and classic epithelial markers in esophageal cancer cell lines was downloaded. All ten genes showed extremely low expression in esophageal cancer cell lines (**Supplemental Figure 4**), with average expression values (RPKM) of: C1QA 0.0005, C1QB 0.0002, C1QC 0, C3AR1 0.0385, CD86 0.2466, CSF1R 0.1609, ITGB2 1.0324, LCP2 0.0123, SPI1 0.0255, TYROBP 0.0086. Comparably, the epithelial markers selected as controlled genes showed relatively high expression CDH1 57.414, CLDN4 60.703, CLDN7 50.385, MUC1 13.366, TJP3 4.5215. Therefore, these combined evidences lead us to believe that these genes are likely to be specifically expressed in immune cells. To investigate this further, we performed a single-gene immune infiltration analysis for each gene to illustrate its relationships with various immune cells. Most of the genes were related to certain types of immune cells. As depicted in **Figure 5D**, three kinds of tumor infiltrating immune cells (TICs) were positively correlated with all genes, including M1 macrophages, M2 macrophages, and regulatory T cells (Tregs). M2 macrophages had a higher correlation with C1QA (r=0.54), C1QB (r=0.55), C1QC (r=0.53), C3AR1 (r=0.48), CSF1R (r=0.46) and TYROBP (r=0.44). M1 macrophages were moderately linked with LCP2 (r=0.46), ITGB2 (r=0.43), CSF1R (r=0.44), C1QA (r=0.43), C1QB (r=0.44), C1QC (r=0.42) and C3AR1 (r=0.41). All genes were positively associated with M2 macrophages (**Supplemental Figures 5 A–J**, p<0.05). These findings further confirm that these prognostic genes are related to the immune activity of the TME, especially M2 macrophages.

Construction of a Risk Score Model and Validation of Its Predictive Value

Utilizing the multivariate Cox regression analysis, we established a 10-gene risk score model. The risk model met the proportional hazard assumption based on the Schoenfeld Individual Test results which showed that each covariate is not statistically significant (**Supplemental Figure 2A**, p>0.05). We then calculated the risk score for each sample and divided patients into high- or low-risk group according to the optimal cutpoint by maximally selected rank statistics. Kaplan-Meier analysis suggested that patients in the high-risk group have significantly shorter OS than those in the low-risk group (**Figure 6A**, p<0.001). The distribution of risk scores, survival status, and ten-gene expression levels among patients in the high- and low-risk group are given in **Figure 6C**. To evaluate the independent

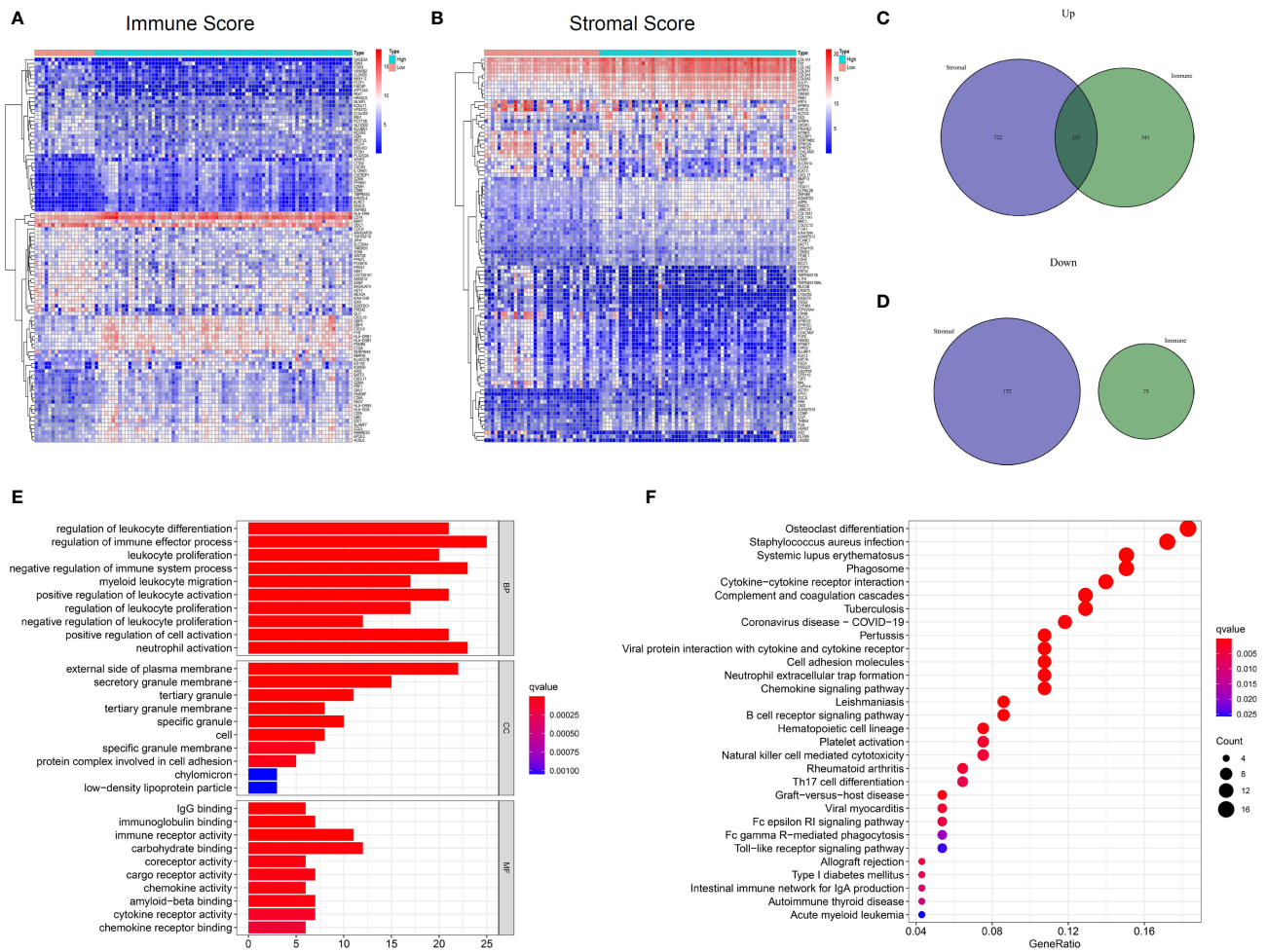

FIGURE 3 | Differential expressed genes identification and enrichment analysis of GO and KEGG. **(A)** Heatmap for DEGs between high and low Immuneacore groups. Row name of heatmap is the gene name, and column name is the ID of samples which not shown in plot. **(B)** Heatmap for DEGs in Stromalscore, similar with **(A)**. **(C, D)** Venn plots for common up-regulated and down-regulated DEGs shared by Immunescore and Stromalscore. **(E)** The top ten biological processes (BP) cellular components (CC) and molecular functions (MF) for GO analysis, respectively. **(F)**The top 30 KEGG enrichment signaling pathways for 133 DEGs, terms with p and q < 0.05 were determined to be enriched significantly.

predictive value of our risk model, univariate and multivariate analyses were performed. The results showed gender, stage, N-stage and risk score were significantly associated with OS in univariate analysis (p<0.05). In the multivariate analysis, only risk score was associated with OS (HR=2.104, 95% CI=1.343-3.295; p=0.001) (**Table 1**). To verify the prognostic value and reliability of our results, the risk score model was further validated using the GEO dataset, which includes 119 ESCC patients. All patients were divided into high- and low-risk group according to the previous formula. In agreement with the training cohort, patients in the high-risk group had significantly worse OS than the low-risk group (**Figure 6B**, p-value=0.008). The univariate and multivariate analyses of risk score and other clinical characteristics confirmed that the risk score model was an independent prognostic indicator (HR=1.6915, 95% CI:1.053-2.717; p=0.0297, **Table 2**). We also carried out differential expression analysis of the complete ten-gene signature in the validation dataset, The Wilcoxon rank sum test revealed that the expression of 9 genes (C1QA, C1QB, C1QC, C3AR1, ITGB2, LCP2, SPI1, TYROBP) in the tumor samples were significantly higher than that in matched normal adjacent tissue (**Supplemental Figures 6A–J**, p<0.05). Time-dependent ROC curve analysis demonstrated that during 1-, 2-, and 3-year follow-up, the area under the curve (AUC) values were 0.672, 0.854, and 0.81 respectively (**Figures 6E–G**) Recently, Sun et al. identified a prognostic gene signature among patients with ESCC (23). Zhang et al. constructed a prognostic model based on immune-related genes to predict prognosis of esophageal cancer (24). We calculated C-indexes to compare the prognostic values of our model and theirs. As shown in **Figures 6E–G**, the concordance index of the risk score model for the 1-, 2-, and 3-year OS was higher than the

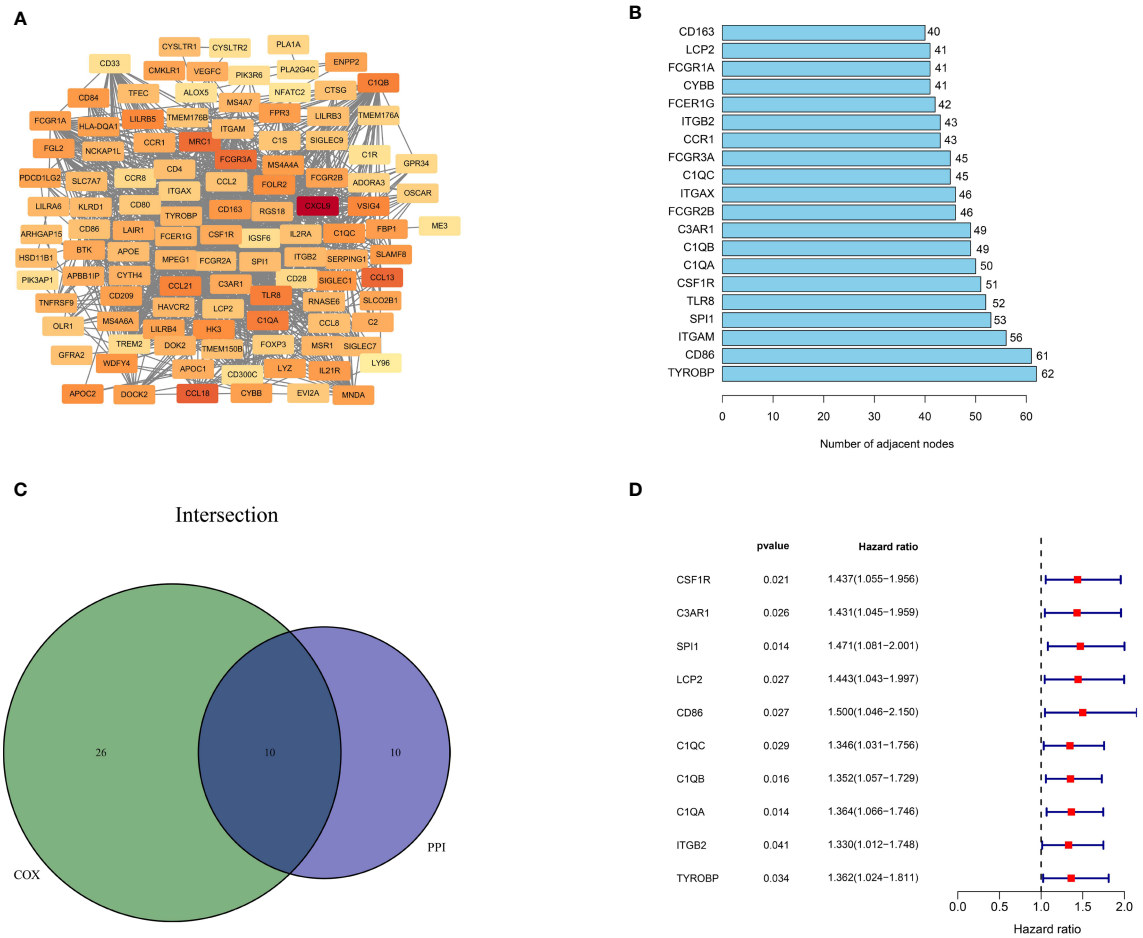

FIGURE 4 | Protein-protein interaction network and univariate COX analysis. **(A)** PPI network constructed with the nodes with interaction confidence value > 0.4. **(B)** The top 20 genes according to the number of nodes. **(C)** Venn plot for 10 hub prognostic DEGs. **(D)** The 10 hub prognostic genes with p < 0.005 in univariate COX regression analysis.

other two studies, indicating that our risk score model may have better performance in predicting prognosis. Taken together, the results confirm that the risk score model is an reliable and independent prognostic factor for ESCC patients.

The Different Immune Infiltration Between High- and Low-Risk Group

We estimated the difference of immune infiltration between high- and low-risk ESCC patients in 22 subpopulations of immune cells using the CIBERSORT algorithm. Levels of M1 macrophages ($p < 0.001$) and M2 macrophages ($p < 0.001$) were markedly higher in the high-risk compared to the low-risk group. Additionally, the proportion of M2 macrophages were significantly higher than M1 macrophages (**Figure 7A**). In contrast, a high fraction of resting CD4 memory T cells, activated dendritic cells, and M0 macrophages mainly infiltrated low-risk ESCC patients. The correlation analysis further confirmed the risk score was moderately correlated with M1 macrophages ($r = 0.43$, $p<0.0001$) and M2 macrophages ($r = 0.47$, $p <0.0001$). Moreover, there were weak associations between risk score and CD8 T cells ($r=0.21$, $p=0.046$), and a negative correlation between risk score and M0 macrophages ($r=-0.36$, $p<0.001$, **Figure 7B**). These results indicate that differences in immune infiltration in high- and low-risk patients with ESCC might be used as a prognostic indicator and target for immunotherapy.

Establishment and Validation of a Nomogram

To establish a more convenient and applicable clinical prognostic approach, we developed a nomogram based on our risk score and other clinical characteristics including age, gender and pathologic stage (**Figure 8A**). The concordance index of the nomogram was 0.734. The calibration plot for the possibility of 1-, 2- and 3-year survival showed good agreement between the prediction and actual observations (**Figure 8B**). These findings illustrate that the nomogram may be a more effective method to predict prognosis of ESCC patients for clinicians.

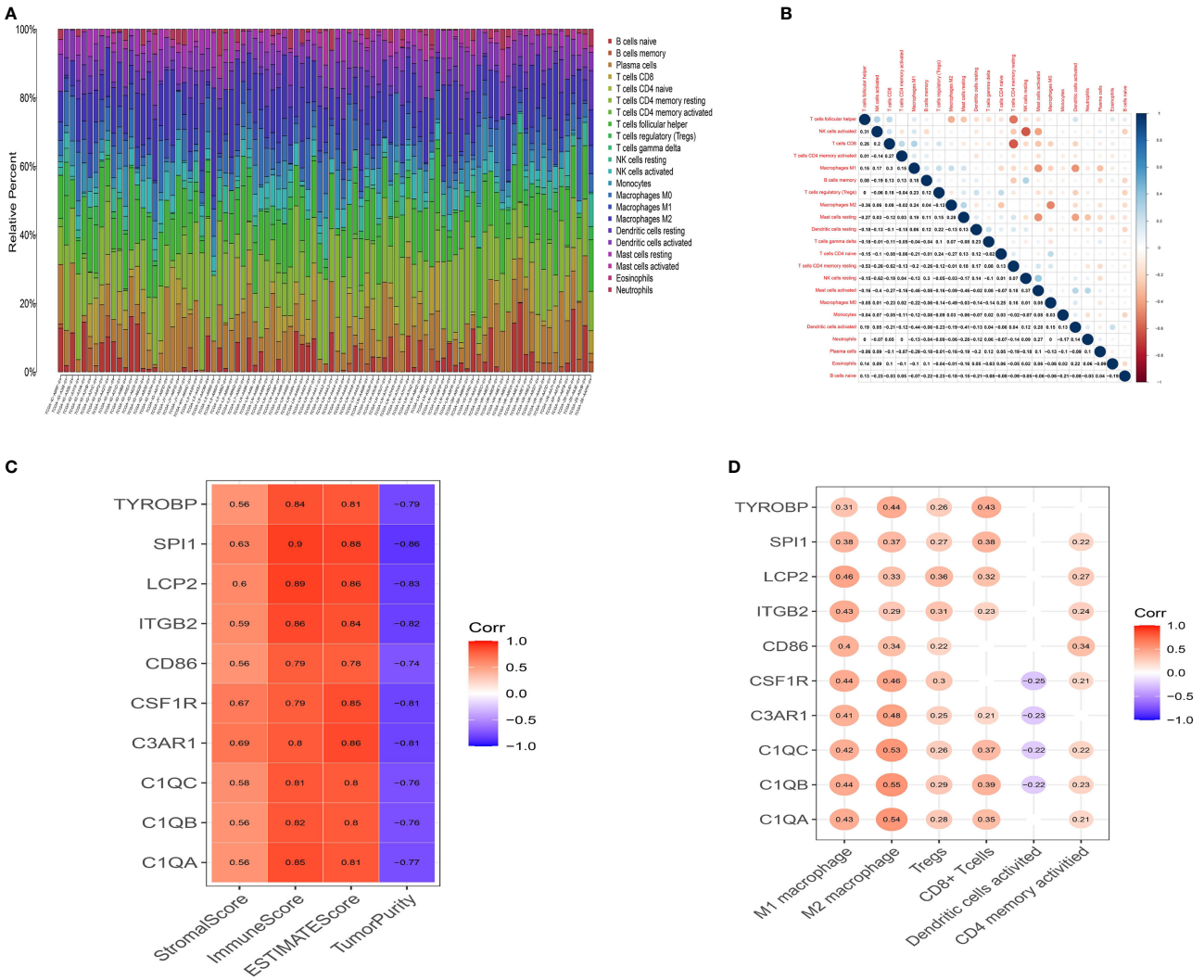

FIGURE 5 | Landscape of tumor infiltration cells in ESCC. **(A)** Barplot for the proportion of 22 types of immune cells in ESCC tissues. Column names are sample ID. **(B)** Heatmap for the correlations between the levels of immune cells among ESCC samples. **(C)** Heatmap for correlation between 10 genes and StromalScore, ImmuneScore, ESTIMATEScore and TumorPurity (p<0.05). **(D)** Heatmap for correlation between 10 genes and six immune cells. The blank means that the p-value is nonsignificant.

Differences in Immune-Related Pathways Between High- and Low-Risk Groups

To help illustrate the underlying mechanism of how these genes impact patient outcomes, GSEA was utilized to evaluate different expression profiles among the two groups. Results showed that genes in the high-risk group were mainly enriched in several immune-related pathways, such as allograft rejection, IL2_STAT 5_SIGNALING, IL6_JAK_STAT6_ SIGNALING, KRAS_ SIGNALING_UP and PI3K_AKT_MTOR_SIGNALING (**Figure 9A**). However, no significant gene sets were enriched in the low-risk group. For the C7 immunologic gene sets defined by MSigDB, multiple immune functional gene sets were enriched in high-risk group (**Figure 9B**) while only three gene sets were enriched in the low-risk group (**Figure 9C**). These results suggest that these genes might affect tumor immune status through these pathways.

qRT-PCR Validation

Finally, we validated five rarely reported genes among these ten genes using an ESCC cDNA microarray by qRT-PCR. As demonstrated in **Figures 10A–E**, the relative expression level of C1QA, C3AR1, LCP2 and TYROBP in ESCC samples were significantly higher relative to normal samples ($p < 0.05$). The expression of SPI1 was also up-regulated although not statistically significant. The survival curve showed that they were all significantly associated with the overall survival of ESCC (log-rank $p < 0.05$; **Figures 10F–J**). In addition, based on the CIBERSORT results, we further examined the correlation

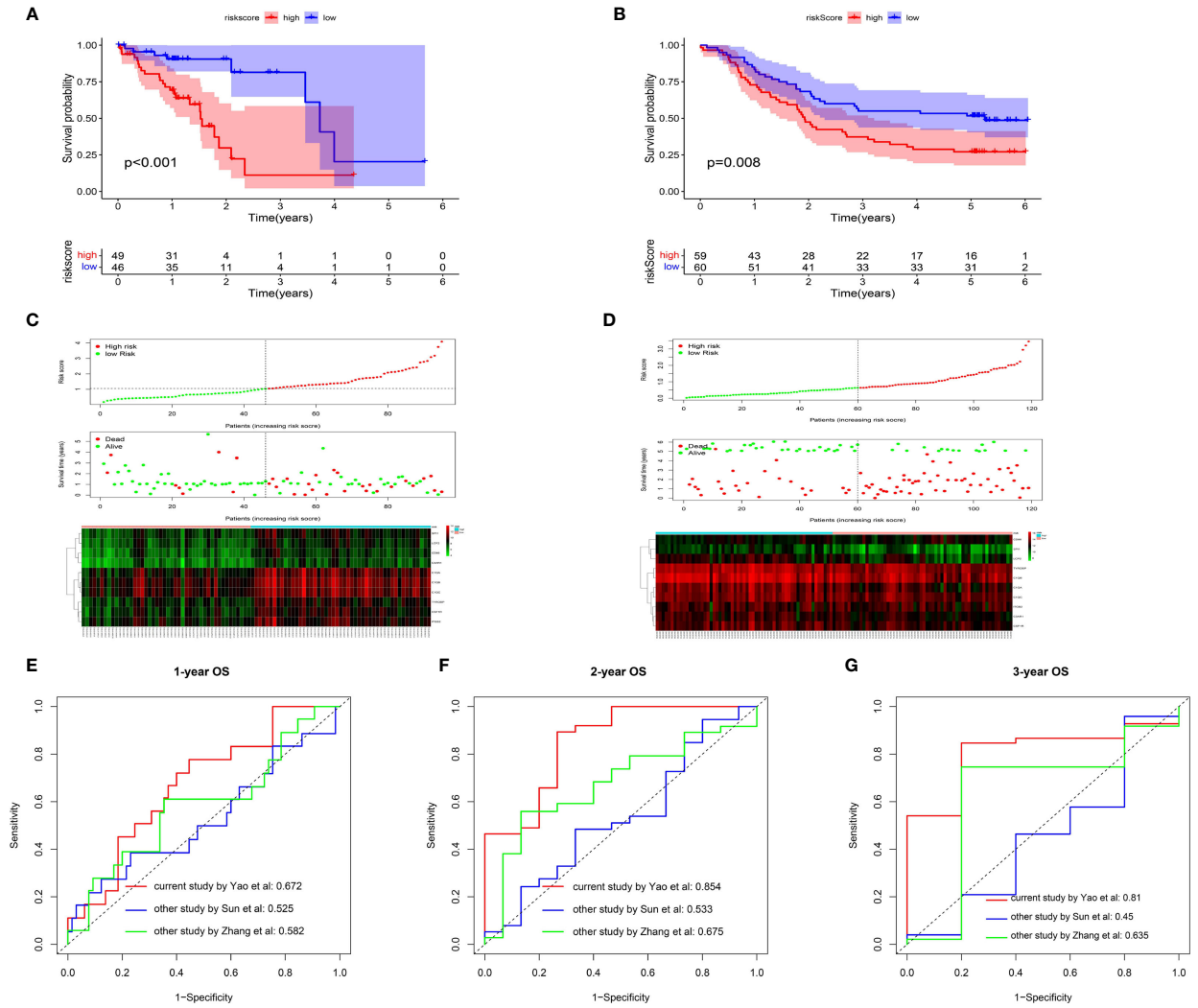

FIGURE 6 | Prognostic analysis of the risk score model. **(A, B)** Kaplan-Meier survival curve of risk score model among ESCC patients in TCGA cohort **(A)** and GEO cohort **(B)**.The high-risk group show the poorly prognosis (p<0.05). **(C, D)** Relationship between the risk score (upper) and the expression of ten prognostic genes (lower) in TCGA cohort **(C)** and GEO cohort **(D)**. **(E, F)** Time-dependent ROC analysis was performed to compare the three models in predicting 1-year **(E)**, 2-year **(F)** and 3-year **(G)** OS.

TABLE 1 | Univariate and Multivariate cox regression analysis-TCGA cohort.

Variables	Univariate analysis		Multivariate analysis	
	HR (95%CI)	P value	HR (95%CI)	P value
Risk score	2.113 (1.388-3.215)	<0.001	2.104 (1.343-3.295)	0.001
Stage (III+IV/I+II)	2.390 (1.165-4.903)	0.017	1.632 (0.771-3.453)	0.200
Grade (2 + 3/1)	1.616 (0.557-4.684)	0.377		
pT (3 + 4/1+2)	1.279 (0.615-2.662)	0.510		
pN (1 + 2+3/0)	1.988 (0.962-4.108)	0.063		
pM (1/0)	2.265 (0.671-7.644)	0.188		
Gender (Male/Female)	5.266 (1.221-22.71)	0.026	3.277 (0.745-14.405)	0.116
Age (≥65/65)	1.838 (0.822-4.112)	0.138		
Smoke (yes/no)	1.564 (0.671-3.647)	0.301		

TABLE 2 | Univariate and Multivariate cox regression analysis-GEO cohort.

Variables	Univariate analysis		Multivariate analysis	
	HR (95%CI)	P value	HR (95%CI)	P value
Risk score (high/low)	1.8663 (1.1557-2.9832)	0.0091	1.6915 (1.053-2.717)	0.0297
Stage (III/I+II)	2.1895 (1.339-3.582)	0.0018	1.4969 (0.753-2.974)	0.2495
Grade (2 + 3/1)	1.0040 (0.56-1.8)	0.989		
pT (3 + 4/1+2)	0.9634 (0.5656-1.641)	0.891		
pN (1 + 2+3/0)	2.1594 (1.319-3.535)	0.0022	1.5383 (0.776-3.050)	0.2175
Gender (Male/Female)	0.8269 (0.4681-1.461)	0.513		
Age (≥65/65)	1.535 (0.941-2.503)	0.0861		
Smoke (yes/no)	1.1634 (0.7203-1.879)	0.536		

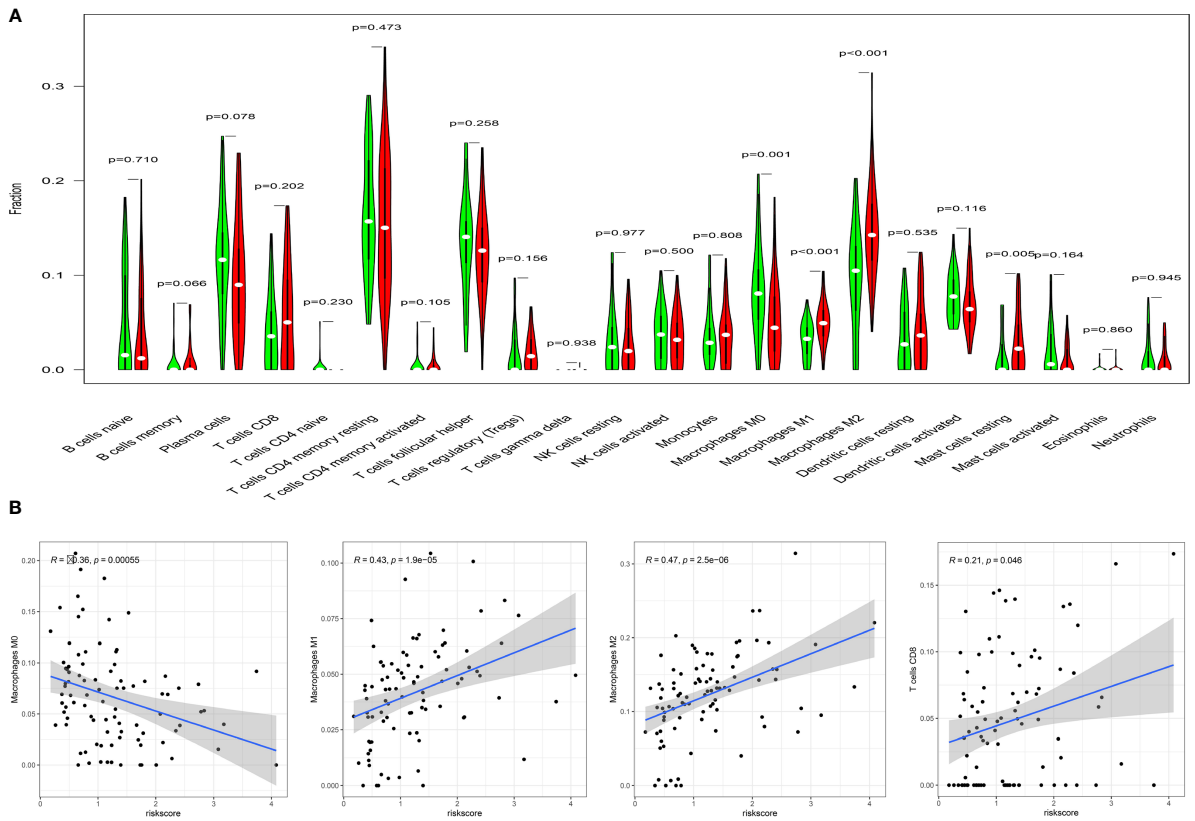

FIGURE 7 | Correlation of TICs with risk score model. **(A)** Violin diagram for the levels of immune cells between high-risk group(red) and low-risk group (green). **(B)** There were significant correlations between risk score model and macrophage M0,M1,M2 and T cells CD8. Pearson test was used for the correlation test (p<0.05).

between 5 genes and macrophage M1 and M2 surface markers. As depicted in **Figure 11**, compared with CD8 and CD86, they had stronger correlation with CD206 and CD4, which further verified they may be involved in the activity of M2 macrophages and play an immunosuppressive role in TME.

DISCUSSION

Esophageal squamous-cell carcinoma (ESCC) is the most common type of esophageal cancer and approximately half of the world's 500,000 new cases occur in China each year (5). Despite advancements in the treatment of ESCC, it continues to be a major challenge for public health worldwide (25). The role of immunotherapy in esophageal cancer is still poorly defined, largely due to high heterogeneity of tumor cells and the microenvironment (26–28). Previous studies have demonstrated that the TME has an important role in tumor progression and prognosis (29, 30).Thus, it is critical to unravel the immune infiltration of ESCC and identify potential predictive markers. In the present study, we identified 133 DEGs related to the TME, and 10 candidate genes were selected according to the intersection of PPI network and univariate cox

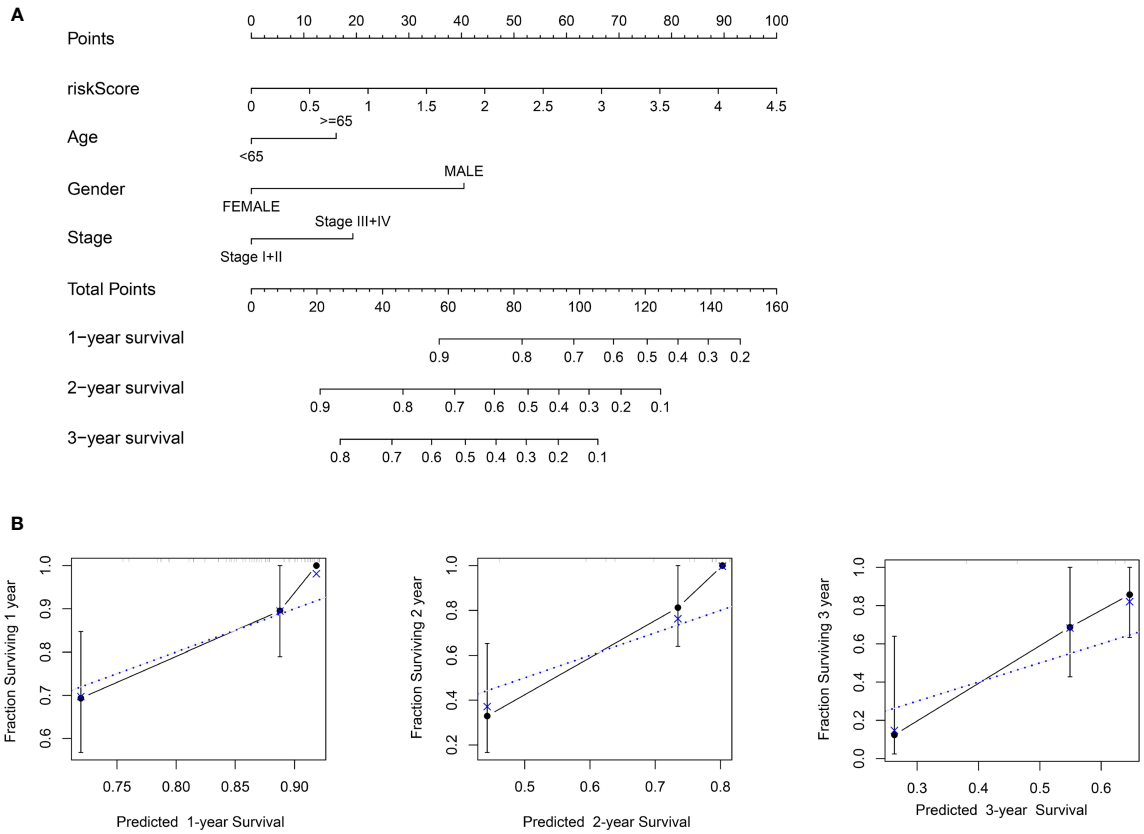

FIGURE 8 | Construction of the nomogram. **(A)** Nomogram predicting 1-, 2-, and 3- year survival based on risk score and other clinical parameters. **(B)** The calibration curves of nomogram between predicted and actual 1-, 2- and 3-year OS in the training cohort. The blue dotted line represents perfect prediction of the nomogram.

analysis. Moreover, we constructed a 10-gene signature correlated with poor overall survival of ESCC patients. The immune infiltration demonstrated the signature had a close relationship with M2 macrophages. Finally, we validated five of the ten genes (C1QA, C3AR1, LCP2, SPI1 and TYROBP) as independently associated with poor survival and tightly related with M2 macrophage surface biomarkers, which may provide new therapeutic avenue for ESCC.

In our research, the ESTIMATE algorithm was utilized to estimate the immune/stromal components of the TME. Our results showed that the immune/stromal scores were both significantly associated with the OS of patients, indicating that TME composition affects the outcomes of ESCC patients. Furthermore, through differential analysis, 133 up-regulated immune and stromal genes were identified. Following functional enrichment analysis of DEGs, they were mainly involved in several immune activities such as the Natural killer cell mediated cytotoxicity, Toll–like receptor signaling pathway, Th17 cell differentiation and so on. These results may give further clues about ESCC etiology and progression. For instance, it has been shown that lipopolysaccharide (LPS)-induced TLR4 signaling promotes cancer cell proliferation and contributes to cancer development and progression in ESCC (31). Next, we constructed a PPI network and univariate cox analysis based on these genes, 10 hub genes were extracted. The above genes were verified using data from the GEO database, and the expression of 9 genes (excluding CSF1R) were significantly up-regulated in the tumor tissues compared with the paired normal tissues. Moreover, they were lowly-expressed in esophageal cancer cell lines compared with classic epithelial markers, and significantly positively associated with ImmuneScore while negatively linked with TumorPurity, suggesting that these genes may be specifically expressed in immune cells. Next, we established a 10-gene signature based on the multivariate cox analysis. The AUC for the 10-gene signature for predicting the 1-, 2-, and 3-year survival were 0.672, 0.854 and 0.81, respectively. The signature was further validated in the GEO dataset. The results suggested that the ten-gene signature was an independent prognostic factor and had a good performance for survival prediction.

In addition, a nomogram was established including the 10-gene signature and age, gender, amd pathologic stage to more accurately predict survival probability. The calibration plot showed good agreement between the prediction by risk score and actual observation. GSEA results showed that several immune-related pathways were enriched in the high-risk group, indicating these ten genes may influence patients' prognosis through these immune response processes. For instance, IL-2 signaling is an essential and multi-functional regulator of many immune cell populations,

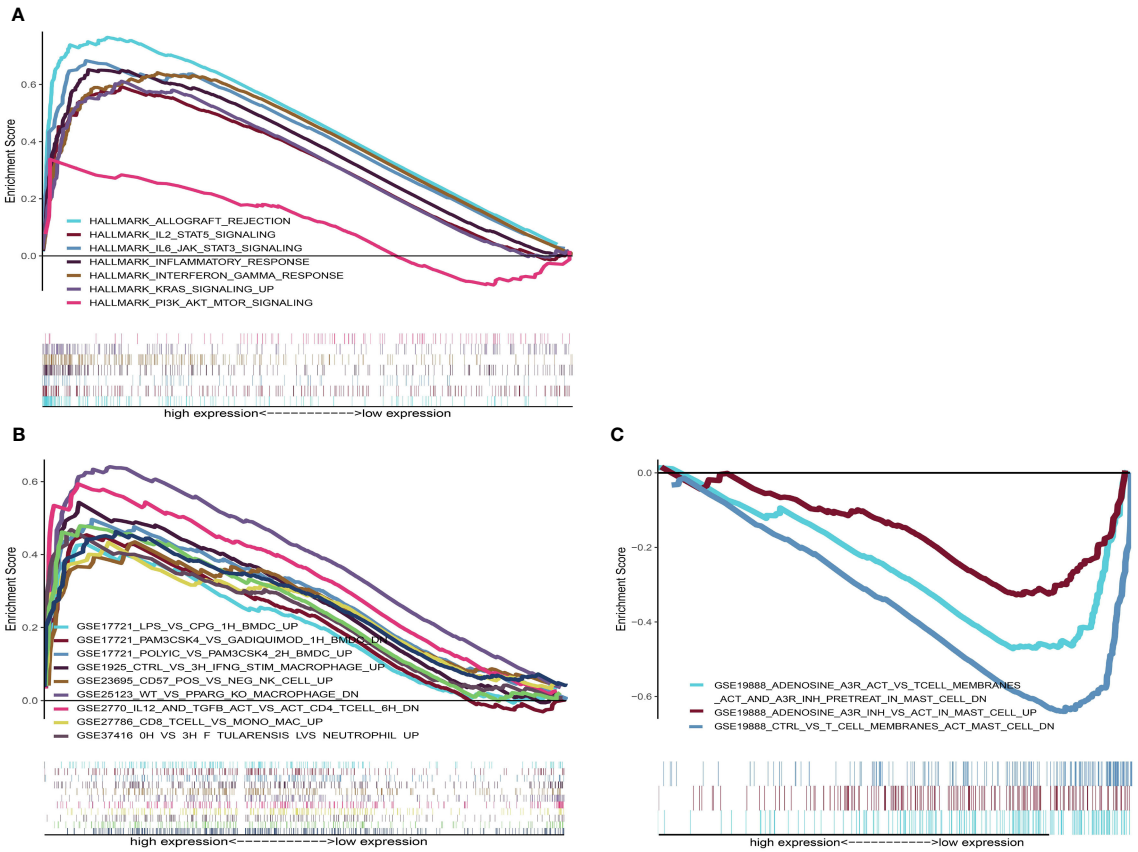

FIGURE 9 | GSEA analysis for patients with high-risk and low-risk. **(A)** The enriched gene sets in HALLMARK collection in high-risk group. Each line representing one particular gene set with unique color. Only gene sets with NOM p < 0.05 and FDR q < 0.25 were considered significant. Only several leading gene sets were displayed in the plot. **(B)** The enriched gene sets in C7 collection (the immunologic gene sets) in high-risk group. **(C)** Enriched gene sets in low-risk group of C7 collection.

including effector and regulatory CD4+ T cell subsets *via* activation of Signal Transducer and Activator of Transcription 5 (STAT5). It's also required for differentiation and functional maturation in early Treg stages. This pathway has long been the target of therapeutic strategies to treat diseases ranging from cancer to autoimmunity (32). JAK-STAT signaling is activated by a number of cytokines including IL-6, TNF-α, and IFN-γ and has been found to be involved in regulation of cell proliferation, differentiation and apoptosis (33). A previous study reported that it is associated with the progression of colorectal cancer (34). KRAS is one of the most frequently mutated oncogenes in cancer, being a potent initiator of tumorigenesis, and a predictive target of response to therapy (35). Importantly, Lastwika et al. showed that the activation of KRAS-downstream pathway PI3K/AKT/mTOR is tightly linked with the regulation of PD-L1 expression both *in vitro* and *in vivo* for human LACs and squamous cell carcinomas, indicating that KRAS may cause immune escape by AKT/mTOR pathway *via* PD-L1 (36).Our findings demonstrated that the 10-gene signature have a close relationship with macrophage M2, which indicates that macrophage M2 might be involved in progression and poor survival outcomes in ESCC. Tumor-associated macrophages (TAMs) have been reported to play an important role in modulating the tumor-microenvironment to an immune suppressive mode, promoting tumor growth, angiogenesis, invasion, and metastasis as well as resistance to therapy (37). Colony-stimulating factor 1 receptor (CSF1R), included in our gene signature, a class III receptor tyrosine kinase, is confirmed to promote TAM transition to a pro-tumorigenic M2-phenotype through binding macrophage colony stimulating factor 1 (MCSF) cytokines (38). As the presence of CSF1R+ macrophages correlates with poor survival in various tumor types (39), a variety of small molecules and monoclonal antibodies (mAbs) directed at CSF1R are in clinical development, which represents an attractive strategy in tumor therapy (40).

We further carried out some experiments to validate five rarely reported genes, which could be used as potential biomarkers for future treatment of ESCC. According to the survival analysis from a cDNA microarray, five genes were up-regulated in tumor samples and predict poor prognosis in ESCC patients. TYROBP, also known as KARAP/DAP12 (killer cell activating receptor-associated protein/DNAX activating protein of 12 kDa), has been found to be linked with the poor prognosis and skeletal metastasis of breast cancer (41). It was also proved that a DAP12-dependent NK cell receptor NKG2D is involved in

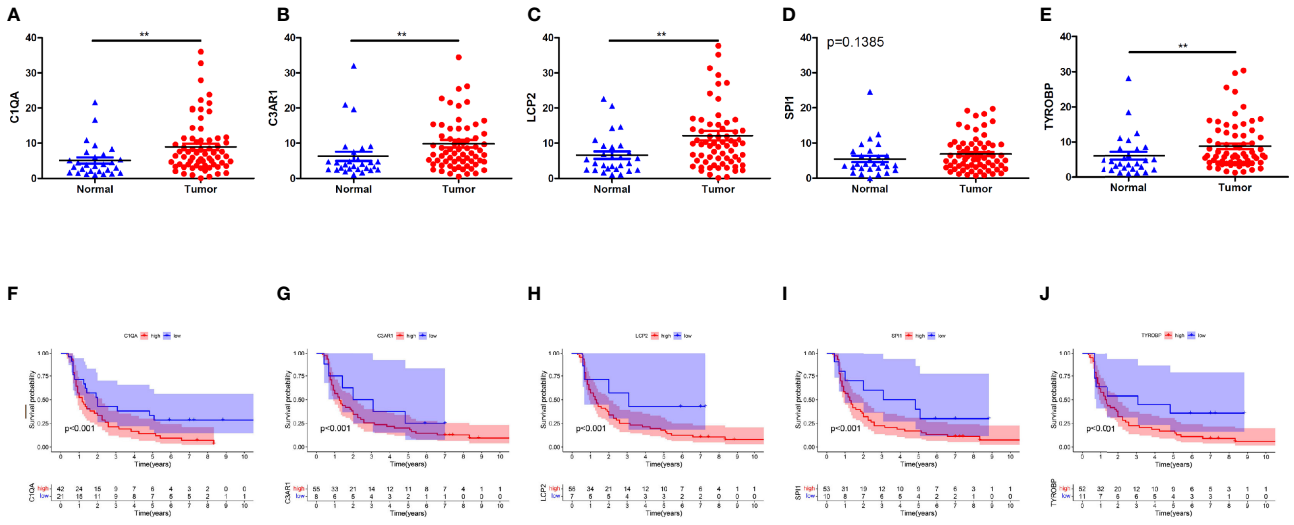

FIGURE 10 | Five genes validation using qRT-PCR for ESCC cDNA microarray chip. **(A–E)** Expression levels of C1QA, C3AR1, LCP2, SPI1, TYROBP were up-regulated in tumor tissues. **(F–J)** The expression of C1QA, C3AR1, LCP2, SPI1, TYROBP were correlated with poor outcomes of ESCC patients. ($p<0.001$). $^{**}p < 0.01$.

antitumoral activity and regulates NK cell function according to experiments with TYROBP knockout mice (42). Consistently, our findings revealed that TYROBP and related genes are mainly enriched in immune-related activities, such as NK cell-mediated cytotoxicity. In the present study, TYROBP had a remarkable positive correlation with M2 macrophages in ESCC. This is consistent with a previous studies indicating that TYROBP is positively linked with M2 macrophages, and may play an important role in immunosuppression and differentiation of TAMs into M2 macrophages in the tumor microenvironment (43). C1q, the first recognition subcomponent of the complement classical pathway, includes three chains (C1qA, C1qB, and C1qC) and has been proved to highly expressed in multiple tumors, including prostate (44), and mesothelioma (45) as well as gliomas (46).In our study, the expression of C1QA were significantly correlated with ESCC patients' survival and upregulated in tumor samples. Our results suggested that C1QA may participate in the regulation of CD8+ T cells, Tregs and M2 macrophages in the immune infiltration of ESCC. Consistently, C1QA and C1QB were confirmed to be drivers of alternatively activated macrophage polarization in a LPS-induced inflammation model (47). Samantha et al. (48) reported that macrophages express high levels of C1QA and C1QB in both primary tumor and metastases. C3AR1 as a receptor of the complement effector C3a, is important in mediating the downstream signal transduction of the complement activation. A previous study had demonstrated that a high concentration of C3a in the serum of esophageal cancer patients was associated with a poor prognosis (49). Meanwhile, there were moderate associations between C3AR1 expression and M1 macrophages, M2 macrophages, CD8 T-cells, and Tregs. A previous indicated that Toll-like receptor(TLR)-initiated DC autocrine C3AR1 signaling causes expansion of effector T cells and instability of regulatory T cells (50). It has been found that C3AR1 can promote the polarization of M2 macrophages and T cell exhaustion, leading to the immune escape of STAD (51). Lawal et al. reported that C3AR1 was associated with tumor immune evasion, prognosis, and immunotherapy in melanoma, colorectal, brain, breast, stomach, and renal cancer (52). We speculated that C3AR1 may play a similar role in tumor immunity and promoting the development of ESCC. SPI1 (PU.1) is a TF crucial for normal T-cell maturation. It is reported that SPI1 is a potent inducer of granulocytic/monocytic differentiation and is often expressed at a low level in AML (53). Gongwei et al. confirmed that overexpression of SPI1 effectively suppresses the growth of MYC-deregulated B-cell lymphomas (54). Alterations in SPI1 lead to oncogenic subversion by cellular proliferation and differentiation arrest in Waldenström macroglobulinemia (55). SPI1 has previously been demonstrated to be associated with the development of different types of immune lineage cells, consisting T-cells, B-cells, monocytes and dendritic cells (56–58). There are a few reports about its role in solid tumors. For instance, Gao et al. proved that SPI1-induced upregulation of SNHG6 promoted the cellular processes in NSCLC *via* miR-485-3p/VPS45 axis (59). In our present study, the expression of SPI1 were significantly up-regulated in tumor tissues and correlated with M2 macrophages, CD8 T cells, Tregs, and predicts poor survival of ESCC patients, suggesting that SPI1 may be a potential biomarker of ESCC and play an equally crucial role in solid tumors. LCP2 is known to participate in T cell progression and it was previously reported that a splice variant of LCP2 resulted in severe immune dysregulation (60). High expression levels of LCP2 contributed to poor outcomes in ESCC patients in our study. Moreover, a previous study confirmed that lncRNA ITGB2-AS1 can promote the migration and invasion of breast cancer cells by up-regulating ITGB2 (61). Zhang et al. uncovered the higher ITGB2 expression in CAFs promote tumor proliferation

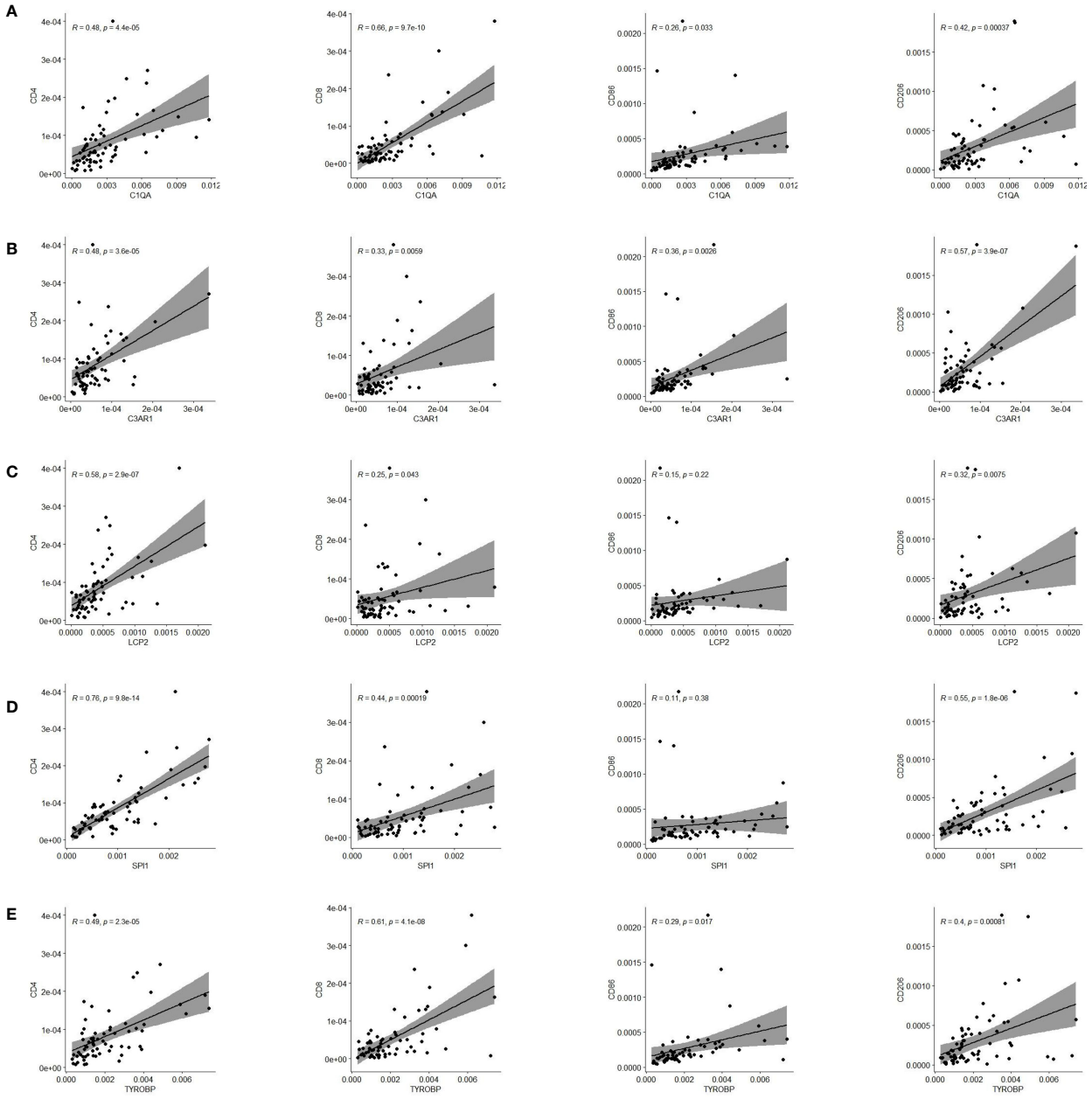

FIGURE 11 | Pearson correlation of five genes expression and immune cells surface biomarkers. **(A)** C1QA is tightly related to CD4, CD8 and CD206. **(B)** C3AR1 is significantly correlated with CD4 and CD206. **(C)** LCP2 has close relationship with CD4 and CD206. **(D)** SPI1 is significantly linked with CD4 and CD206. **(E)** TYROBP is tightly related to CD4, CD8 and CD206.

in OSCC by activating the PI3K/AKT/mTOR pathways and NADH oxidation in the mitochondrial oxidative phosphorylation system (62), and ITGB2 was found to be involved in the proliferation, migration, and invasion of CRC cells (63).

In this study, using the ESTIMATE algorithm, we developed a 10-gene signature to predict the prognosis of ESCC patients. Our TME-related ten-gene prognostic signature was confirmed to have good predictive performance and to represent an independent prognostic factor. We also validated five genes (C1QA, C3AR1, LCP2, TYROBP, SPI1) using cDNA microarray, which could be potential biomarkers for future treatment of ESCC. To our knowledge, this is the first time report of an M2 macrophage-related prognostic gene signature in ESCC. However, there are several limitations. To be useful, this prognostic signature needs to be further validated in some large cohorts and multicenter clinical trials in the future. Additionally, further experiments are required to clarify the potential mechanism and the specific roles of these

TME-related genes in the development, migration, and invasion of ESCC.

CONCLUSION

In summary, we established and validated a novel gene signature that is based on ten immune-related genes to predict the OS of ESCC. This signature is significantly correlated with M2 macrophages in the tumor microenvironment. Notably, C1QA, C3AR1, LCP2, TYROBP and SPI1 were further validated as up-regulated in tumors and independently predict poor outcomes in ESCC. Hence, they may be underlying therapeutic targets for ESCC and are expected to be further applied in future clinical practice.

DATA AVAILABILITY STATEMENT

The datasets presented in this study can be found in online repositories. The names of the repository/repositories and accession number(s) can be found in the article/**Supplementary Material**.

AUTHOR CONTRIBUTIONS

JY and LD contributed equally to this work. JY, LD, YG, and BH designed the research; XH, XF, JL, RY, ZX, and HL performed the experiments; JY, LD, and GA analyzed the data. All authors wrote the paper; YG and BH revised the paper. All authors contributed to the article and approved the submitted version.

FUNDING

This work was supported by National Natural Science Foundation of China (82003057) to Jiannan Yao), and National Natural Science Foundation of China (81802738) to YG.

SUPPLEMENTARY MATERIAL

The Supplementary Material for this article can be found online at: https://www.frontiersin.org/articles/10.3389/fonc.2021.769727/full#supplementary-material

REFERENCES

1. Schizas D, Charalampakis N, Kole C, Mylonas KS, Katsaros I, Zhao M, et al. Immunotherapy for Esophageal Cancer: A 2019 Update. *Immunotherapy* (2020) 12(3):203–18. doi: 10.2217/imt-2019-0153
2. Lin EW, Karakasheva TA, Hicks PD, Bass AJ, Rustgi AK. The Tumor Microenvironment in Esophageal Cancer. *Oncogene* (2016) 35(41):5337–49. doi: 10.1038/onc.2016.34
3. Siegel RL, Miller KD, Fuchs HE, Jemal A. Cancer Statistics, 2021. *CA Cancer J Clin* (2021) 71(1):7–33. doi: 10.3322/caac.21654
4. Bray F, Ferlay J, Soerjomataram I, Siegel RL, Torre LA, Jemal A. Global Cancer Statistics 2018: GLOBOCAN Estimates of Incidence and Mortality Worldwide for 36 Cancers in 185 Countries. *CA Cancer J Clin* (2018) 68 (6):394–424. doi: 10.3322/caac.21492
5. Chen W, Zheng R, Baade PD, Zhang S, Zeng H, Bray F, et al. Cancer Statistics in China, 2015. *CA Cancer J Clin* (2016) 66(2):115–32. doi: 10.3322/caac.21338
6. Lin D-C, Wang M-R, Koeffler HP. Genomic and Epigenomic Aberrations in Esophageal Squamous Cell Carcinoma and Implications for Patients. *Gastroenterology* (2018) 154(2):374–89. doi: 10.1053/j.gastro.2017.06.066
7. Baba Y, Nomoto D, Okadome K, Ishimoto T, Iwatsuki M, Miyamoto Y, et al. Tumor Immune Microenvironment and Immune Checkpoint Inhibitors in Esophageal Squamous Cell Carcinoma. *Cancer Sci* (2020) 111(9):3132–41. doi: 10.1111/cas.14541
8. Hinshaw DC, Shevde LA. The Tumor Microenvironment Innately Modulates Cancer Progression. *Cancer Res* (2019) 79(18):4557–66. doi: 10.1158/0008-5472.CAN-18-3962
9. Chen W, Dai X, Chen Y, Tian F, Zhang Y, Zhang Q, et al. Significance of STAT3 in Immune Infiltration and Drug Response in Cancer. *Biomolecules* (2020) 10(6):834. doi: 10.3390/biom10060834
10. Kuczek DE, Larsen AMH, Thorseth M-L, Carretta M, Kalvisa A, Siersbæk MS, et al. Collagen Density Regulates the Activity of Tumor-Infiltrating T Cells. *J Immunother Cancer* (2019) 7(1):68. doi: 10.1186/s40425-019-0556-6
11. Hirata E, Sahai E. Tumor Microenvironment and Differential Responses to Therapy. *Cold Spring Harb Perspect Med* (2017) 7(7):a026781. doi: 10.1101/cshperspect.a026781
12. Butturini E, Carcereri de Prati A, Boriero D, Mariotto S. Tumor Dormancy and Interplay With Hypoxic Tumor Microenvironment. *Int J Mol Sci* (2019) 20(17):4305. doi: 10.3390/ijms20174305
13. Frankel T, Lanfranca MP, Zou W. The Role of Tumor Microenvironment in Cancer Immunotherapy. *Adv Exp Med Biol* (2017) 1036:51–64. doi: 10.1007/978-3-319-67577-0_4
14. Galon J, Bruni D. Approaches to Treat Immune Hot, Altered and Cold Tumours With Combination Immunotherapies. *Nat Rev Drug Discov* (2019) 18(3):197–218. doi: 10.1038/s41573-018-0007-y
15. Zheng Y, Chen Z, Han Y, Han L, Zou X, Zhou B, et al. Immune Suppressive Landscape in the Human Esophageal Squamous Cell Carcinoma Microenvironment. *Nat Commun* (2020) 11(1):6268. doi: 10.1038/s41467-020-20019-0
16. Xu B, Chen L, Li J, Zheng X, Shi L, Wu C, et al. Prognostic Value of Tumor Infiltrating NK Cells and Macrophages in Stage II+III Esophageal Cancer Patients. *Oncotarget* (2016) 7(46):74904–16. doi: 10.18632/oncotarget.12484
17. Izawa S, Mimura K, Watanabe M, Maruyama T, Kawaguchi Y, Fujii H, et al. Increased Prevalence of Tumor-Infiltrating Regulatory T Cells is Closely Related to Their Lower Sensitivity to H2O2-Induced Apoptosis in Gastric and Esophageal Cancer. *Cancer Immunol Immunother* (2013) 62(1):161–70. doi: 10.1007/s00262-012-1327-0
18. Yamamoto K, Makino T, Sato E, Noma T, Urakawa S, Takeoka T, et al. Tumor-Infiltrating M2 Macrophage in Pretreatment Biopsy Sample Predicts Response to Chemotherapy and Survival in Esophageal Cancer. *Cancer Sci* (2020) 111(4):1103–12. doi: 10.1111/cas.14328
19. Wang Y, Lyu Z, Qin Y, Wang X, Sun L, Zhang Y, et al. FOXO1 Promotes Tumor Progression by Increased M2 Macrophage Infiltration in Esophageal Squamous Cell Carcinoma. *Theranostics* (2020) 10(25):11535–48. doi: 10.7150/thno.45261
20. Cassetta L, Pollard JW. Targeting Macrophages: Therapeutic Approaches in Cancer. *Nat Rev Drug Discovery* (2018) 17(12):887–904. doi: 10.1038/nrd.2018.169
21. Mantovani A, Marchesi F, Malesci A, Laghi L, Allavena P. Tumour-Associated Macrophages as Treatment Targets in Oncology. *Nat Rev Clin Oncol* (2017) 14(7):399–416. doi: 10.1038/nrclinonc.2016.217
22. Yoshihara K, Shahmoradgoli M, Martínez E, Vegesna R, Kim H, Torres-Garcia W, et al. Inferring Tumour Purity and Stromal and Immune Cell Admixture From Expression Data. *Nat Commun* (2013) 4:2612. doi: 10.1038/ncomms3612
23. Sun L-L, Wu J-Y, Wu Z-Y, Shen J-H, Xu X-E, Chen B, et al. A Three-Gene Signature and Clinical Outcome in Esophageal Squamous Cell Carcinoma. *Int J Cancer* (2015) 136(6):E569–E77. doi: 10.1002/ijc.29211

24. Zhang Z, Chen C, Fang Y, Li S, Wang X, Sun L, et al. Development of a Prognostic Signature for Esophageal Cancer Based on Nine Immune Related Genes. *BMC Cancer* (2021) 21(1):113. doi: 10.1186/s12885-021-07813-9
25. Huang TX, Fu L. The Immune Landscape of Esophageal Cancer. *Cancer Commun (Lond)* (2019) 39(1):79. doi: 10.1186/s40880-019-0427-z
26. Vrana D, Matzenauer M, Neoral C, Aujesky R, Vrba R, Melichar B, et al. From Tumor Immunology to Immunotherapy in Gastric and Esophageal Cancer. *Int J Mol Sci* (2018) 20(1):13. doi: 10.3390/ijms20010013
27. Marconcini R, Spagnolo F, Stucci LS, Ribero S, Marra E, Rosa FD, et al. Current Status and Perspectives in Immunotherapy for Metastatic Melanoma. *Oncotarget* (2018) 9(15):12452–70. doi: 10.18632/oncotarget.23746
28. Santoni M, Massari F, Di Nunno V, Conti A, Cimadamore A, Scarpelli M, et al. Immunotherapy in Renal Cell Carcinoma: Latest Evidence and Clinical Implications. *Drugs Context* (2018) 7:212528. doi: 10.7573/dic.212528
29. Ohtani H, Jin Z, Takegawa S, Nakayama T, Yoshie O. Abundant Expression of CXCL9 (MIG) by Stromal Cells That Include Dendritic Cells and Accumulation of CXCR3+ T Cells in Lymphocyte-Rich Gastric Carcinoma. *J Pathol* (2009) 217(1):21–31. doi: 10.1002/path.2448
30. Thompson ED, Zahurak M, Murphy A, Cornish T, Cuka N, Abdelfatah E, et al. Patterns of PD-L1 Expression and CD8 T Cell Infiltration in Gastric Adenocarcinomas and Associated Immune Stroma. *Gut* (2017) 66(5):794–801. doi: 10.1136/gutjnl-2015-310839
31. Zu Y, Ping W, Deng T, Zhang N, Fu X, Sun W. Lipopolysaccharide-Induced Toll-Like Receptor 4 Signaling in Esophageal Squamous Cell Carcinoma Promotes Tumor Proliferation and Regulates Inflammatory Cytokines Expression. *Dis Esophagus* (2017) 30(2):1–8. doi: 10.1111/dote.12466
32. Jones DM, Read KA, Oestreich KJ. Dynamic Roles for IL-2-STAT5 Signaling in Effector and Regulatory CD4 T Cell Populations. *J Immunol* (2020) 205 (7):1721–30. doi: 10.4049/jimmunol.2000612
33. Slattery ML, Lundgreen A, Kadlubar SA, Bondurant KL, Wolff RK. JAK/STAT/SOCS-Signaling Pathway and Colon and Rectal Cancer. *Mol Carcinog* (2013) 52(2):155–66. doi: 10.1002/mc.21841
34. Xiong H, Zhang Z-G, Tian X-Q, Sun D-F, Liang Q-C, Zhang Y-J, et al. Inhibition of JAK1, 2/STAT3 Signaling Induces Apoptosis, Cell Cycle Arrest, and Reduces Tumor Cell Invasion in Colorectal Cancer Cells. *Neoplasia* (2008) 10(3):287–97. doi: 10.1593/neo.07971
35. Dias Carvalho P, Guimarães CF, Cardoso AP, Mendonça S, Costa ÂM, Oliveira MJ, et al. KRAS Oncogenic Signaling Extends Beyond Cancer Cells to Orchestrate the Microenvironment. *Cancer Res* (2018) 78(1):7–14. doi: 10.1158/0008-5472.CAN-17-2084
36. Hamarsheh Sa, Groß O, Brummer T, Zeiser R. Immune Modulatory Effects of Oncogenic KRAS in Cancer. *Nat Commun* (2020) 11(1):5439. doi: 10.1038/s41467-020-19288-6
37. Ostuni R, Kratochvill F, Murray PJ, Natoli G. Macrophages and Cancer: From Mechanisms to Therapeutic Implications. *Trends Immunol* (2015) 36(4):229–39. doi: 10.1016/j.it.2015.02.004
38. Ramesh A, Brouillard A, Kumar S, Nandi D, Kulkarni A. Dual Inhibition of CSF1R and MAPK Pathways Using Supramolecular Nanoparticles Enhances Macrophage Immunotherapy. *Biomaterials* (2020) 227:119559. doi: 10.1016/j.biomaterials.2019.119559
39. Pedersen MB, Danielsen AV, Hamilton-Dutoit SJ, Bendix K, Nørgaard P, Møller MB, et al. High Intratumoral Macrophage Content is an Adverse Prognostic Feature in Anaplastic Large Cell Lymphoma. *Histopathology* (2014) 65(4):490–500. doi: 10.1111/his.12407
40. Cannarile MA, Weisser M, Jacob W, Jegg A-M, Ries CH, Rüttinger D. Colony-Stimulating Factor 1 Receptor (CSF1R) Inhibitors in Cancer Therapy. *J Immunother Cancer* (2017) 5(1):53. doi: 10.1186/s40425-017-0257-y
41. Shabo I, Olsson H, Stål O, Svanvik J. Breast Cancer Expression of DAP12 is Associated With Skeletal and Liver Metastases and Poor Survival. *Clin Breast Cancer* (2013) 13(5):371–7. doi: 10.1016/j.clbc.2013.05.003
42. Diefenbach A, Tomasello E, Lucas M, Jamieson AM, Hsia JK, Vivier E, et al. Selective Associations With Signaling Proteins Determine Stimulatory Versus Costimulatory Activity of NKG2D. *Nat Immunol* (2002) 3(12):1142–9. doi: 10.1038/ni858
43. Chanmee T, Ontong P, Konno K, Itano N. Tumor-Associated Macrophages as Major Players in the Tumor Microenvironment. *Cancers (Basel)* (2014) 6 (3):1670–90. doi: 10.3390/cancers6031670
44. Hong Q, Sze C-I, Lin S-R, Lee M-H, He R-Y, Schultz L, et al. Complement C1q Activates Tumor Suppressor WWOX to Induce Apoptosis in Prostate Cancer Cells. *PloS One* (2009) 4(6):e5755. doi: 10.1371/journal.pone.0005755
45. Agostinis C, Vidergar R, Belmonte B, Mangogna A, Amadio L, Geri P, et al. Complement Protein C1q Binds to Hyaluronic Acid in the Malignant Pleural Mesothelioma Microenvironment and Promotes Tumor Growth. *Front Immunol* (2017) 8:1559. doi: 10.3389/fimmu.2017.01559
46. Mangogna A, Belmonte B, Agostinis C, Zacchi P, Iacopino DG, Martorana A, et al. Prognostic Implications of the Complement Protein C1q in Gliomas. *Front Immunol* (2019) 10:2366. doi: 10.3389/fimmu.2019.02366
47. Benoit ME, Clarke EV, Morgado P, Fraser DA, Tenner AJ. Complement Protein C1q Directs Macrophage Polarization and Limits Inflammasome Activity During the Uptake of Apoptotic Cells. *J Immunol* (2012) 188 (11):5682–93. doi: 10.4049/jimmunol.1103760
48. Kemp SB, Steele NG, Carpenter ES, Donahue KL, Bushnell GG, Morris AH, et al. Pancreatic Cancer is Marked by Complement-High Blood Monocytes and Tumor-Associated Macrophages. *Life Sci Alliance* (2021) 4(6): e202000935. doi: 10.26508/lsa.202000935
49. Maher SG, McDowell DT, Collins BC, Muldoon C, Gallagher WM, Reynolds JV. Serum Proteomic Profiling Reveals That Pretreatment Complement Protein Levels are Predictive of Esophageal Cancer Patient Response to Neoadjuvant Chemoradiation. *Ann Surg* (2011) 254(5):809–16. doi: 10.1097/SLA.0b013e31823699f2
50. Sheen J-H, Strainic MG, Liu J, Zhang W, Yi Z, Medof ME, et al. TLR-Induced Murine Dendritic Cell (DC) Activation Requires DC-Intrinsic Complement. *J Immunol* (2017) 199(1):278–91. doi: 10.4049/jimmunol.1700339
51. Yang H, Li L, Liu X, Zhao Y. High Expression of the Component 3a Receptor 1 (C3AR1) Gene in Stomach Adenocarcinomas Infers a Poor Prognosis and High Immune-Infiltration Levels. *Med Sci Monit* (2021) 27:e927977. doi: 10.12659/MSM.927977
52. Lawal B, Tseng S-H, Olugbodi JO, Iamsaard S, Ilesanmi OB, Mahmoud MH, et al. Pan-Cancer Analysis of Immune Complement Signature C3/C5/C3AR1/C5AR1 in Association With Tumor Immune Evasion and Therapy Resistance. *Cancers (Basel)* (2021) 13(16):4124. doi: 10.3390/cancers13164124
53. Cook WD, McCaw BJ, Herring C, John DL, Foote SJ, Nutt SL, et al. PU.1 is a Suppressor of Myeloid Leukemia, Inactivated in Mice by Gene Deletion and Mutation of its DNA Binding Domain. *Blood* (2004) 104(12):3437–44. doi: 10.1182/blood-2004-06-2234
54. Wu G, Suo C, Yang Y, Shen S, Sun L, Li S-T, et al. MYC Promotes Cancer Progression by Modulating M A Modifications to Suppress Target Gene Translation. *EMBO Rep* (2021) 22(3):e51519. doi: 10.15252/embr.202051519
55. Roos-Weil D, Decaudin C, Armand M, Della-Valle V, MbK D, Ghamlouch H, et al. A Recurrent Activating Missense Mutation in Waldenström Macroglobulinemia Affects the DNA Binding of the ETS Transcription Factor SPI1 and Enhances Proliferation. *Cancer Discovery* (2019) 9(6):796–811. doi: 10.1158/2159-8290.CD-18-0873
56. Scott EW, Simon MC, Anastasi J, Singh H. Requirement of Transcription Factor PU.1 in the Development of Multiple Hematopoietic Lineages. *Science* (1994) 265(5178):1573–7. doi: 10.1126/science.8079170
57. McKercher SR, Torbett BE, Anderson KL, Henkel GW, Vestal DJ, Baribault H, et al. Targeted Disruption of the PU.1 Gene Results in Multiple Hematopoietic Abnormalities. *EMBO J* (1996) 15(20):5647–58.
58. Anderson KL, Perkin H, Surh CD, Venturini S, Maki RA, Torbett BE. Transcription Factor PU.1 is Necessary for Development of Thymic and Myeloid Progenitor-Derived Dendritic Cells. *J Immunol* (2000) 164(4):1855–61. doi: 10.4049/jimmunol.164.4.1855
59. Gao N, Ye B. SPI1-Induced Upregulation of lncRNA SNHG6 Promotes non-Small Cell Lung Cancer *via* miR-485-3p/VPS45 Axis. *BioMed Pharmacother* (2020) 129:110239. doi: 10.1016/j.biopha.2020.110239
60. Siggs OM, Miosge LA, Daley SR, Asquith K, Foster PS, Liston A, et al. Quantitative Reduction of the TCR Adapter Protein SLP-76 Unbalances Immunity and Immune Regulation. *J Immunol* (2015) 194(6):2587–95. doi: 10.4049/jimmunol.1400326
61. Liu M, Gou L, Xia J, Wan Q, Jiang Y, Sun S, et al. LncRNA ITGB2-AS1 Could Promote the Migration and Invasion of Breast Cancer Cells Through Up-Regulating Itgb2. *Int J Mol Sci* (2018) 19(7):1866. doi: 10.3390/ijms19071866
62. Zhang X, Dong Y, Zhao M, Ding L, Yang X, Jing Y, et al. ITGB2-Mediated Metabolic Switch in CAFs Promotes OSCC Proliferation by Oxidation of NADH in Mitochondrial Oxidative Phosphorylation System. *Theranostics* (2020) 10(26):12044–59. doi: 10.7150/thno.47901
63. Sun Z, Dang Q, Liu Z, Shao B, Chen C, Guo Y, et al. LINC01272/miR-876/ITGB2 Axis Facilitates the Metastasis of Colorectal Cancer *via* Epithelial-

Mesenchymal Transition. *J Cancer* (2021) 12(13):3909–19. doi: 10.7150/jca.55666

Conflict of Interest: The authors declare that the research was conducted in the absence of any commercial or financial relationships that could be construed as a potential conflict of interest.

Publisher's Note: All claims expressed in this article are solely those of the authors and do not necessarily represent those of their affiliated organizations, or those of the publisher, the editors and the reviewers. Any product that may be evaluated in this article, or claim that may be made by its manufacturer, is not guaranteed or endorsed by the publisher.

frontiers in Oncology

REVIEW
published: 03 January 2022
doi: 10.3389/fonc.2021.803974

Cancer Stem Cells and the Tumor Microenvironment in Gastric Cancer

Ying Yang, Wen-Jian Meng and Zi-Qiang Wang*

Department of Gastrointestinal Surgery, West China Hospital, Sichuan University, Chengdu, China

Gastric cancer (GC) remains one of the leading causes of cancer-related death worldwide. Cancer stem cells (CSCs) might be responsible for tumor initiation, relapse, metastasis and treatment resistance of GC. The tumor microenvironment (TME) comprises tumor cells, immune cells, stromal cells and other extracellular components, which plays a pivotal role in tumor progression and therapy resistance. The properties of CSCs are regulated by cells and extracellular matrix components of the TME in some unique manners. This review will summarize current literature regarding the effects of CSCs and TME on the progression and therapy resistance of GC, while emphasizing the potential for developing successful anti-tumor therapy based on targeting the TME and CSCs.

Keywords: gastric cancer, cancer stem cells (CSC), tumor microenvironment, mesenchymal stem cells, cancer associated fibroblasts (CAFs), tumor-associated macrophages (TAMs)

OPEN ACCESS

Edited by:
Nathaniel Weygant, Fujian University of Traditional Chinese Medicine, China

Reviewed by:
Qianqian Song, Wake Forest School of Medicine, United States
Ghmkin Hassan, Hiroshima University, Japan
Dong-Joo (Ellen) Cheon, Albany Medical College, United States

****Correspondence:***
Wen-Jian Meng
mengwenjian@126.com

Specialty section:
This article was submitted to Gastrointestinal Cancers: Gastric Esophageal Cancers, a section of the journal Frontiers in Oncology

Received: *28 October 2021*
Accepted: *08 December 2021*
Published: *03 January 2022*

Citation:
Yang Y, Meng W-J and Wang Z-Q (2022) Cancer Stem Cells and the Tumor Microenvironment in Gastric Cancer. Front. Oncol. 11:803974. doi: 10.3389/fonc.2021.803974

INTRODUCTION

Gastric cancer (GC) is the fifth most commonly diagnosed cancer and the fourth leading cause of cancer-associated mortality with an estimated more than one million new cases and 769,000 deaths worldwide in 2020 (1). Despite advancements in clinical treatment and technologies, the prognosis of GC remains poor, mainly due to relapse, metastasis and therapy resistance, and the median survival of patients with advanced GC is less than one year (2). Cancer stem cells (CSCs) are a minor subpopulation of uniquely tumorigenic cells exhibiting the capacity for self-renewal, unlimited proliferating and maintenance of a relatively dormant state. Since the first identification of CSCs in acute myeloid leukemia (3), increasing evidence suggests that CSCs may be responsible for tumor (including GC) progression, relapse, metastasis and therapy resistance (4–6).

Abbreviations: Ad5/35-DKK1, Adenovirus-mediated Dickkopf-1; ALDH, Aldehyde dehydrogenase; ALOX15, Arachidonate lipoxygenase 15; anti-PD-1, Anti-programmed cell death 1; anti-PD-L1, Anti-PD-1 ligand; ASIC1a, Acid-sensitive ion channel 1a; BM-MSCs, Bone marrow-derived MSCs; CAFs, Cancer associated fibroblasts; CagA, Cytotoxin-associated gene A; CaMKs, Calcium/calmodulin-dependent protein kinases; CSCs, Cancer stem cells; CTL, Cytotoxic T cells; DGCs, Diffuse-type gastric cancers; ECM, Extracellular matrix; EMT, Epithelial-mesenchymal transformation; EpCAM, Epithelial cellular adhesion molecule; FAK, Focal adhesion kinase; FAO, Fatty acid oxidation; FAP, Fibroblast activating protein; FDA, Food and Drug Administration; FGF, Fibroblast growth factor; GC, Gastric cancer; GCAFs, Gastric CAFs; GC-MSCs, GC-derived MSCs; GCSCs, Gastric CSCs; GEO, Gene Expression Omnibus; GNF, Gastric normal fibroblast; HH, Hedgehog; HIF, Hypoxia-inducible factor; HP, Helicobacter pylori; IL, Interleukin; MCP-1, Monocyte chemoattractant protein-1; MDR, Multi-drug resistance; MSCs, Mesenchymal stem cells; NK, Natural killer; PD-1, Programmed cell death 1; PDGF, Platelet-derived growth factor; PD-L1, PD-1 ligand; RHBDF2, Rhomboid 5 Homolog 2; ROS, Reactive oxygen species; SCID, Severe combined immunodeficiency; SP, Side population; TAMs, Tumor-associated macrophages; TCGA, The Cancer Genome Atlas; TGF, Transforming growth factor; Th, Helper T cells; TILs, Tumor-infiltrating lymphocytes; TME, The tumor microenvironment; TNF, Tumor necrosis factor; Treg, Regulatory T cells; VCAM1, Vascular adhesion molecule 1; VEGF, Vascular endothelial growth factor.

The cellular environment in which tumor cells reside is called the tumor microenvironment (TME), which consists of cellular and non-cellular components. It includes many types of stromal cells (fibroblasts, lymphocytes, macrophages, and endothelial cells), immune cells (such as T and B lymphocytes), and extracellular components (for instance: cytokines, growth factors, hormones and extracellular matrix), which surround tumor cells and are nourished by blood vessels around the tumor (**Figure 1**). The TME provides a suitable living environment for cancer cells to develop, escape from host immune surveillance and resist to anticancer drugs (7–10). With the continuous progress in the study of CSCs and TME, the microenvironment of CSC has gradually entered the vision of researchers. CSCs microenvironment (CSCs niche) is a special microenvironment for the survival of CSCs, which can regulate the characteristics of CSCs *via* cell-to-cell contact and secreted factors (11). Therefore, a precise and meticulous understanding of CSCs, TME and the relationship between them in GC will have a profound impact on the treatment of GC in the future. This review summarized current findings regarding the role of CSCs and TME in the progression of GC, which may facilitate the understanding of CSCs and TME of GC, as well as provide a potential therapeutic strategy based on targeting TME and CSCs for GC.

IDENTIFICATION AND ISOLATION OF CSCs

The study of CSCs may play a critical role in eradicating tumors and solving clinical problems such as tumor recurrence and

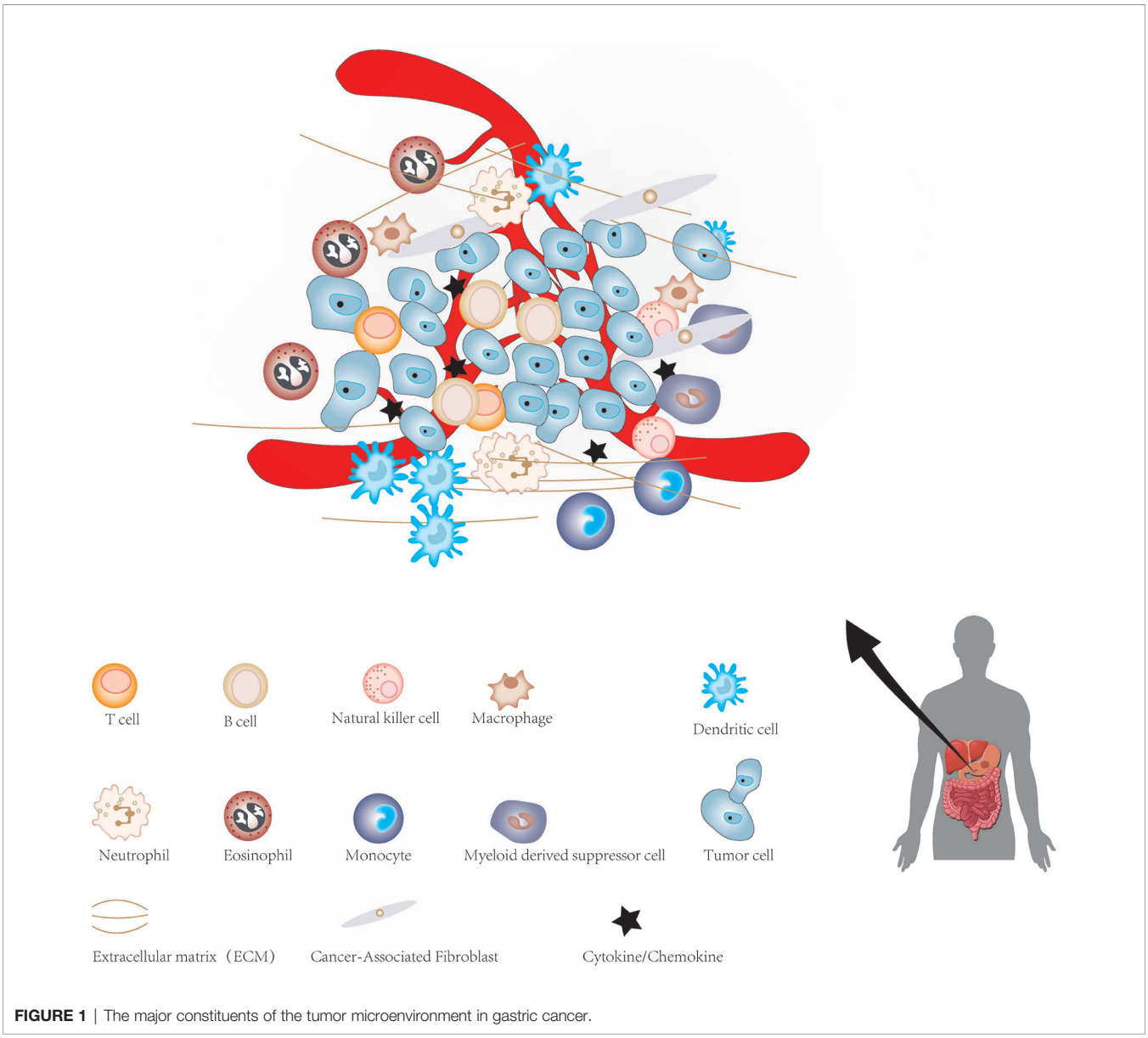

FIGURE 1 | The major constituents of the tumor microenvironment in gastric cancer.

distant metastasis. However, the number of CSCs in cancer cells is extremely small (typically <1% in solid tumors) (12). Therefore, the main difficulty in studying CSCs is how to identify and isolate them from a large number of tumor cells. At present, the most efficacious and commonly used method to isolate CSCs from a large number of tumor cells is by using specific cell surface markers of CSCs.

CSCs can be isolated and identified by combining specific cell surface markers of CSCs with corresponding monoclonal antibodies or fluorescein markers, and then applying some isolation techniques such as flow cytometry and magnetic-activated cell sorting. Therefore, finding specific and effective cell surface markers of CSCs is critical for isolating and identifying CSCs. An increasing number of evidence has confirmed the existence of some specific cell surface markers in gastric CSCs (GCSCs). CD44 was the first confirmed potential GCSCs-specific cell surface marker. Takaishi et al. (13) found a considerable number of CD44 (+) cells in GC cell lines (MKN-45, MKN-74, and NCI-N87), and these CD44 (+) cells showed spheroid colony formation in serum-free media *in vitro*. And when these cells were injected into the stomach and skin (around 30,000 cells per site) of severe combined immunodeficiency (SCID) mice, the significant tumorigenic ability *in vivo* was showed. However, only about 5% of the CD44 (+) cells were ultimately identified as true CSCs. In addition, CD44 is also widely expressed by nonmalignant tumors. Hence, it seems unlikely that a single cell surface marker of CD44 could detect all cells with the characteristics of GCSCs. Lau et al. (14) identified CD44v8-10 (the predominant CD44variant expressed in GC cells) as another potential cell surface marker of GCSCs. The results showed that the expression of CD44v8-10 was significantly upregulated in gastric tumor sites and that exogenous expression of CD44v8-10 contributed to tumor initiation in immunocompromised mice, possibly by improving oxidative stress defense. As a family of intracellular enzymes, aldehyde dehydrogenase (ALDH) enzymes are responsible for cell differentiation, detoxification and drug resistance through the oxidation of cellular aldehydes. Katsuno et al. (15) demonstrated that ALDH1(+) cells possess the characteristics of CSCs, accounting for about 5-8% of the human diffuse-type gastric carcinoma cells and displaying a higher tumorigenicity than ALDH1(-) cells. These findings indicate that ALDH1 is a potential specific cell surface marker for GCSCs. Numerous other molecules or proteins have also been suggested as potential cell surface markers for GCSCs. For instance, Jiang et al. (16). found that CD90(+) cells possessed an increased capacity of tumorigenicity *in vivo* compared with CD90(-) cells, and the expression level of CD90(+) cells was positively correlated with the tumorigenicity of GC cells *in vivo*. In addition, a combination therapy of trastuzumab with conventional chemotherapy is able to suppress tumor growth by reducing the proportion of CD90 (+) cells. These findings suggest that CD90 may be a potential cell surface marker for GCSCs. Ohkuma et al. (17) have investigated the role of CSCs in gastric adenocarcinoma using MKN-1 cells, which showed that CD71 (−) cells were more tumorigenic than CD71 (+) cells in the gastric adenosquamous carcinoma model and that most CD71 (−) cells were dormant (G1/G0 cell cycle phase) and resistant to 5-FU. These characteristics of CD71 (−) cells were highly consistent with the characteristics of CSCs. Wenqi et al. (18) demonstrated that the epithelial cellular adhesion molecule (EpCAM) was overexpressed by gastric cancer cells and down-regulation of EpCAM was able to inhibit tumor formation, reduce cell proliferation, and reduce the proportion of cells in a relatively dormant state. However, there are still some limitations and controversies about the use of these molecules as separate markers. Combining several molecular as cell surface markers to improve the ability of specifically identifying and isolating GCSCs has also been confirmed by some studies. For instance, CD44 was combined with other molecules as a specific cell surface marker for GCSCs, including CD24 (19), CD54 (20) and EpCAM (21). **Table 1** summarizes the current specific cell surface markers for GCSCs.

In addition to the isolation of CSCs by cell surface markers, some characteristics of CSCs also have been applied to isolate and identify CSCs. In serum-free medium supplemented with growth factors, most non-CSCs cannot survive, while CSCs can survive and maintain their self-renewal characteristics. Therefore, serum-free medium containing growth factors can enrich and isolate CSCs, and Li et al. (23) used serum-free medium to enrich and isolate potential GCSCs. Side population (SP) cell isolation also can be applied to sort and enrich GCSCs by taking advantage of efflux characteristics of CSCs for Hoechst33342(a nucleic acid dye) (24, 25). Traditional two-dimensional (2D) cell cultures do not mimic TME *in vivo* due to the lack of cell-extracellular matrix interactions. Animal models may also not adequately mimic the characteristics of human cancers. Therefore, the 3-dimensional (3D) culture

TABLE 1 | Cell surface markers of gastric cancer stem cells (GCSCs).

GCSCs surface marker	Characteristic of stem cell	Reference
CD44(+)	Tumorigenicity, self-renewal, multipotent differentiation, chemoresistance, colony-forming ability	(13)
CD44v8-10	Tumorigenicity,	(14)
ALDH	Chemoresistance, self-renewal, colony-forming ability, generate heterogeneity	(15, 22)
CD90	Tumorigenicity, self-renewal	(16)
CD71 (–)	Tumorigenicity, self-renewal, relatively dormant state	(17)
EpCAM	Tumorigenicity, relatively dormant state	(18)
CD44(+)/CD24(+)	Tumorigenicity, self-renewal, multipotent differentiation	(19)
CD44(+)/CD54(+)	Tumorigenicity, self-renewal	(20)
EpCAM(+)/CD44(+)	Tumorigenicity, chemoresistance	(21)

system, which can better simulate *in vivo* cancer environment, has been widely used in cancer research. In addition, 3D culture systems can simulate the TME of CSCs by controlling the mechanical properties of materials and then effectively isolate CSCs. Recently, increasing studies have also used 3D culture systems to isolate and culture GCSCs (26–30).

With the continual development of single cell technologies, it is possible to identify CSCs from cancer cells. CSCs are usually difficult to isolate owing to their low abundance and similarity to other stem cells. Single-cell sequencing technologies are able to detect extremely trace amounts of nucleic acid sequences, which may assist in the identification and study of CSCs (31). For instance, Velten et al. (32) successfully identified leukemic stem cells from acute myeloid leukemia by clonal tracking from single-cell transcriptomics. Yang et al. (33) performed single-cell RNA sequencing of 59 cells from three bladder cancer samples, and finally found six key modifier genes (ETS1, GPRC5A, MKL1, PAWR, PITX2, and RGS9BP) in bladder CSCs that have never been reported. However, with the wide application of single-cell sequencing in the study of tumors, a large quantities of single-cell genomics data also makes it tricky to study. Therefore, Song et al. (34, 35) developed two research models of single-cell genomics data (single-cell Latent-variable Mode and Single-Cell Graph Convolutional Network) for better mining and understanding these data, which will aid in the understanding the complex mechanisms of cancer and CSCs. However, the high price of single-cell sequencing and the complexity of sample handling and operational procedures limit its application, and current studies identifying GCSCs by single-cell sequencing have not been reported.

THE TME IN GC

The TME favors the survival of tumor cells and provides an excellent shelter for them to escape host immune surveillance and resist anti-tumor drugs. Meanwhile, cancer cells in the TME can also affect and change their surrounding cells in an autocrine and a paracrine manner to maintain the TME required for the survival of cancer cells. This section will summarize the effects of the main components of TME on GC and the features of gastric TME.

Cancer Associated Fibroblasts

Cancer associated fibroblasts (CAFs) are the most abundant stromal cells in the TME, accounting for about 50% of the total number of tumor tissue cells (36). CAFs can promote tumor development, proliferation, drug resistance, invasion and metastasis through direct contact or secretion of a variety of cytokines and metabolites in a paracrine manner, thereby affecting the prognosis of tumors. There are several controversies about the origins of CAFs, but an increasing number of evidence shows that CAFs originate from a variety of cells, such as bone marrow-derived cells, CSCs, epithelial cells through epithelial-mesenchymal transformation (EMT) and normal fibroblasts. The diversity of origins of CAFs also contributes to the heterogeneity of CAFs (37–40) (**Figure 2**). CAFs not only provide physical support for epithelial cells in TME, but also are key factors for EMT of GC cells (41). EMT is a pathological process closely related to tumor invasion and metastasis. The main changes were that the cells changed from closely arranged epithelial cells to loosely structured interstitial cells, which weakened the adhesion between cells and increased the invasion and metastasis of the tumor. Angiogenesis is considered to be critical for tumor proliferation and metastasis, and vascular endothelial growth factor (VEGF) plays a crucial role in promoting angiogenesis. In GC cells, CAFS has been shown to promote angiogenesis by secreting FGF, IL-6, PDGF and VEGF and promote EMT by secreting transforming growth factor beta (TGF-β), FGF, TNF-α, and IL-1β, in turn leading to proliferation, invasion and metastasis of GC (39, 42–49)(**Figure 2**).

CSCs have been shown to be capable of converting mesenchymal stem cells (MSCs) into CAFs in GC *via* exosome-mediated TGF- transfer and activation of TGF-/Smad pathways (50). In turn, CAFs are also able to maintain the stem-like properties of GC, promote the progression of GC and predict the prognosis of GC patients using the characteristics of CAFs. Hasegawa et al. (42) showed that CAFs may be able to maintain the stemness of sclerosing GC cells through TGF-β signaling. And Spondin-2 secreted by CAFs in GC is positively correlated with peritoneal dissemination, tumor size and poor prognosis of GC (51). Ishimoto et al. (52) isolated CAFs and adjacent non-cancer fibroblasts from resected specimens of 110 patients with diffuse-type GCs (DGCs) to investigated the characteristics and functions of CAFs in DGCs by analyzing the features of their genome and gene expression patterns. They found that DGCs cells cultured with CAFs were also more aggressive and invasive *in vitro* than those not cultured with CAFs. Further work using quantitative reverse PCR revealed that the expression of the Rhomboid 5 Homolog 2 (RHBDF2) gene associated with TGF-β1 activity was increased in DGC cells, and increased expression of RHBDF2 gene was observed after incubation of non-cancer fibroblasts with interleukin 1 alpha (IL-1α), IL-β or TNF, secreted by DGCs. In view of the above findings, it was concluded that CAFs were able to activate TGF-β1 signaling by increasing the expression of RHBDF2. And the activation of TGF-β1 was demonstrated to increase the motility and invasiveness of GC cells. Fibroblast activating protein (FAP) is a member of the TME, Wen et al. (53) found that overexpression of FAP was negatively correlated with the survival rate of GC patients, and FAP combined with CAFs could promote the proliferation and invasiveness of GC cells and induce the development of chemoresistance of GC cells *in vitro*. In a xenograft model of GC, combined targeted inhibition of FAP and CAFs enhanced the antitumor immunity of immune checkpoint inhibitors. In addition, the characteristics of CAFs can also be used to predict the prognosis of GC patients and estimate the response of GC patients to clinical immunotherapy. Zheng et al. (54) constructed a 4-gene (COL8A1, SPOCK1, AEBP1, and TIMP2) prognostic CAFs model by analyzing mRNA expression and clinical information of GC samples

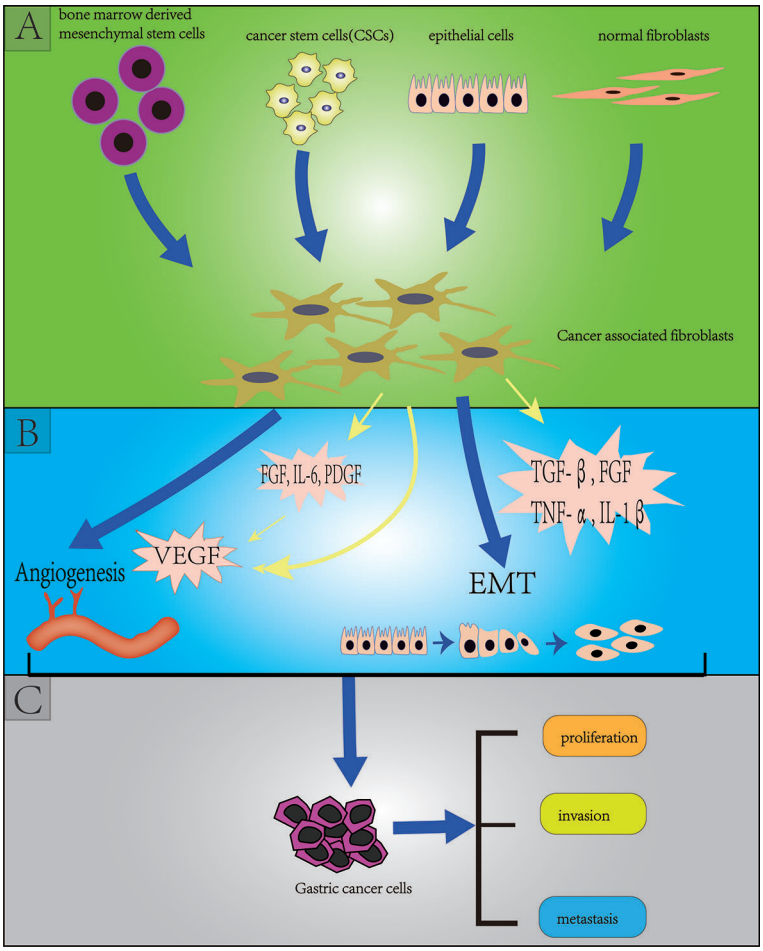

FIGURE 2 | Section **(A)** (green background) indicates the origins of cancer-associated fibroblasts (CAFs) including bone marrow derived mesenchymal stem cells, cancer stem cells, endothelial cells (through endothelial mesenchymal transition: EMT), normal fibroblasts; Section **(B)** (blue background) indicates the effect of CAFs on gastric cancer stem cells (GCSCs) including angiogenesis and EMT; Section **(C)** (grey background) indicates the effect of (GCSCs) on gastric cancer cells including proliferation, invasion and metastasis.

from GEO (Gene Expression Omnibus) and TCGA (Cancer Genome Atlas) databases. The results showed a positive correlation between CAFs risk score and stromal and CAFs infiltrations in GC, and patients in the high-CAF-risk group were less likely to respond to immunotherapy.

Tumor-Associated Macrophages

The most abundant immune cells in the TME are composed of macrophages or monocytes, which are called tumor-associated macrophages (TAMs). TAMs promote tumor progression by secreting a variety of factors, including growth factors, chemokines, cytokines, proteases and so on. Monocytes or macrophages are usually polarized into two main types: M1 and M2 (55). M1 macrophages enhance the function of T cells by releasing proinflammatory cytokines, such as TNF-α, IL-1 and IL-12 and participate in type I helper T cell (Th) responses, which are crucial components involved in inflammatory responses and anti-tumor immunity (56). TAMs frequently exhibit an M2-like phenotype in the microenvironment of cancer, including GC, and express anti-inflammatory cytokines such as IL-10, TGF-β and arginase (57). These anti-inflammatory cytokines inhibit T cell-mediated anti-tumor immunity and provide tumors with an immunosuppressive microenvironment, allowing tumors to evade host immune surveillance and promote tumor growth and metastasis (58). In addition, Oishi et al. (59) demonstrated that intraperitoneal presentation of M2-polarized macrophages was able to inhibit T cell proliferation *in vitro*. In a mouse model of GC, TAMs were demonstrated to be able to secrete the proinflammatory factor TNF-α, which contributes to the formation and development of GC by activating the Wnt signaling pathway (60, 61). Yamanaka et al. (62) showed that IL-1β secreted by TAMs of GC could increase the invasiveness of GC cells by activating NF-κB and expressing MMP-9. In addition, TAMs can also promote tumor angiogenesis and provides nutrition for tumor growth. Some studies have shown that the level of TAMs is closely associated

with the number of blood vessels surrounding the GC cells. Ohta et al. (63) found that expression level of monocyte chemoattractant protein-1 (MCP-1) was significantly increased compared with negative tumors in human GC cell lines, and its expression level was closely related to the secretion of VEGF. And the counts of TAMs are positively correlated with the counts of vessel. They concluded that MCP-1 induced by human GC cells may promote angiogenesis of GC cells by recruiting and activating TAMs. Then, Kuroda et al. (64) further confirmed that MCP-1 also has a similar effect and mechanism (by activating and recruiting TAMs) in a mouse xenograft model of GC. In addition to promoting angiogenesis in GC through MCP-1, TAMs may also directly promote angiogenesis and lymphangiogenesis of GC possibly by enhancing the expression of VEGF and VEGF-C (65).

Mesenchymal Stem Cells

As an important part of the TME, MSCs play a key role in the process of tumor development, including tumor neovascularization, metastasis, maintenance of the stemness of CSCs and the formation of an immunosuppressive TME by activating signaling pathway and secreting a variety of regulatory factors (66). During the growth of GC, MSCs are recruited into the TME of GC, and they are able to alter the TME and promote tumor growth by secreting a variety of factors. GC-derived MSCs (GC-MSCs) were reported to enhance the proliferation, migration, and promotion of angiogenesis of GC cells by secreting considerable the proinflammatory cytokine interleukin-8 (IL-8) (67). IL-15 secreted by GC-MSCs enhances the stem-like properties of GC cells, induces EMT of GC cells which in turn promotes migration and metastasis of GC cells by upregulating Tregs (Regulatory T cells) ratio and programmed cell death protein-1 expression in CD4 + T Cell (68). Huang et al. (69) found that PDGF-DD secreted by GC-MSCs was capable of promoting the migration and proliferation of GC cells *in vitro* and *in vivo* by phosphorylating PDGF-β. Wang et al. (70) found that GC-MSCs were able to significantly promote the growth and migration of HGC-27 and increase microRNA-221 expression through paracrine secretion. In addition, inhibiting the expression of IL-8, PDGF-DD and microRNA-221 were all able to block its tumor-supporting role on GC cells. Recent studies have demonstrated that MSCs are crucial in the progression of GC. GC-MSCs can promote the growth of GC cells and the polarization of macrophages in the GC microenvironment to the M2 type by considerable secretion of IL-6 and IL-8, and M2 type macrophages can promote GC metastasis by promoting the EMT of GC cells (71). The role of GC-MSCs in promoting GC metastasis and EMT of GC cells was also confirmed in another study (72). In TME, bone marrow-derived MSCs (BM-MSCs) were able to produce CXCL16 through Ror2-mediated signaling. While CXCL16 could induce expression of Ror1 in MKN45 cells, thereby promoting the progression of GC by activating the CXCR6-STAT3 signaling pathway (73). In addition, Wnt5a-Ror2 signaling in BM-MSCs has been shown to promote the proliferation of GC cells (74).

Tumor-Infiltrating Lymphocytes

Recently, the effect of tumor-infiltrating lymphocytes (TILs) on GC has also been reported. TILs refer to lymphocytes that leave the blood and enter the tumor, which are a major component of the TME, including CD8 + T cells, CD4 + T cells, B lymphocytes and natural killer (NK) cells (75). CD8 + T cells, also known as cytotoxic T cells (CTL), are recognized as the main anti-tumor immune effector cells. The subsets of CD4 + T cells are represented by Th1, Th2 and Treg. Th1 cells, which secrete IL-2 and interferon, play a crucial role in activating and promoting the proliferation of CD8 + T cell and NK cell. Th2 enhances humoral immunity by secreting cytokines such as IL-4 and IL-6, which promote maturation and clonal proliferation of B cells. Treg cells can suppress the immune response in the host, including inhibiting the activation of NK cells and the cytotoxic function of CD8 + T cells (76). Kono et al. (77) confirmed that as a kind of Treg, the high expression of CD4 (+) CD25 high T cells was closely related to the worse prognosis of gastric and esophageal cancer. Interestingly, the level of CD4 (+) CD25 high T cells decreased significantly after patients with GC undergoing radical resection. Zhuang et al. (78) revealed that the overexpression of IL-22(+) CD4(+) T cells and Th22 cells were associated with tumor progression and predicted reduced overall survival. In addition, CD8 (+) T cells that produce IL-7 can promote the progression of GC cells by promoting chemotaxis of myeloid-derived suppressor cells (79).

Features of Gastric TME

Helicobacter pylori (HP) was confirmed to be associated with approximately 75% of GC events worldwide as a group 1 carcinogen (80, 81). HP infection is able to significantly affect and change the microenvironment of the stomach by inducing chronic inflammation of the stomach, while the inflammatory response will promote EMT of GC through a variety of mechanisms. Alternatively, HP cytotoxin-associated gene A (CagA) can change many signaling pathways of the host cell by inducing DNA damage and changing DNA methylation, and then induce the production of GC EMT. In addition, it also induces the generation of GC EMT by down-regulating the expression of E-cadherin and up-regulating the expression of vimentin and twist (82–84). CagA is also able to activated NFκB and STAT3 signals and increased the expression of SNAIL1 protein, which is closely related to CAFs activation and EMT in GC cells (85). Zhang et al. (86) found that HP infected gastric epithelial cells could activate and recruit MSCs and promote the conversion of MSCs into CAFs, which may promote the EMT of gastric epithelial cells. Krzysiek-Maczka et al. (87) found that HP strains are not only able to induce EMT of normal rat gastric epithelium cells, but also induce differentiation of rat normal gastric fibroblasts into CAFs.

An acidic microenvironment is a basic characteristic of the metabolic environment of tumor tissue. Tumor cells utilize glycolysis to create an acidic microenvironment conducive to invasion and metastasis (88–90). Current studies suggest that both glycolysis and oxidative phosphorylation may be the

metabolic pathways of CSCs (91, 92), but it is undeniable that the acidic microenvironment favors the progression of malignant tumors and the emergence of CSCs (93). For most normal cells, living in an acidic microenvironment is harmful, while tumor cells can survive in the acidic environment and rely on the acidic microenvironment to maintain their ability to grow and proliferate rapidly (94). An acidic microenvironment and acid-sensitive ion channel 1a (ASIC1a) were confirmed to promote the proliferation and migration of GC cells. Chen et al. (95) found that the expression of ASIC1a was significantly increased in GC tissues with postoperative metastasis compared with GC tissues without postoperative metastasis and non-tumor tissues. In addition, down-regulation of ASIC1a expression by silencing ASIC1a *via* shRNA was able to reduce the migration and invasion of GC cells. However, the regulatory mechanism of the acid-base microenvironment on tumor cell growth and metastasis is still unclear, and regulating the pH value of the GC microenvironment may be an effective measurement to kill GC cells.

INTERACTION BETWEEN CSCs AND TME

With the continuous deepening of research in cancer, it has been slowly discovered that there is a complex dialogue between CSCs and the TME during tumor development. TME can not only affect the self-renewal ability of CSCs, but it may also induce the transformation of its surrounding non-tumor stem cells into CSCs (96). The TME surrounding CSCs can secrete cytokines such as hypoxia-inducible factor (HIF) and IL-1β, activate related signaling pathways, and participate in CSCs invasion and metastasis by inducing angiogenesis, induction of EMT and protecting CSCs from being attacked by the host's immune system. CSCs may also rely on their surrounding microenvironment to maintain their stem

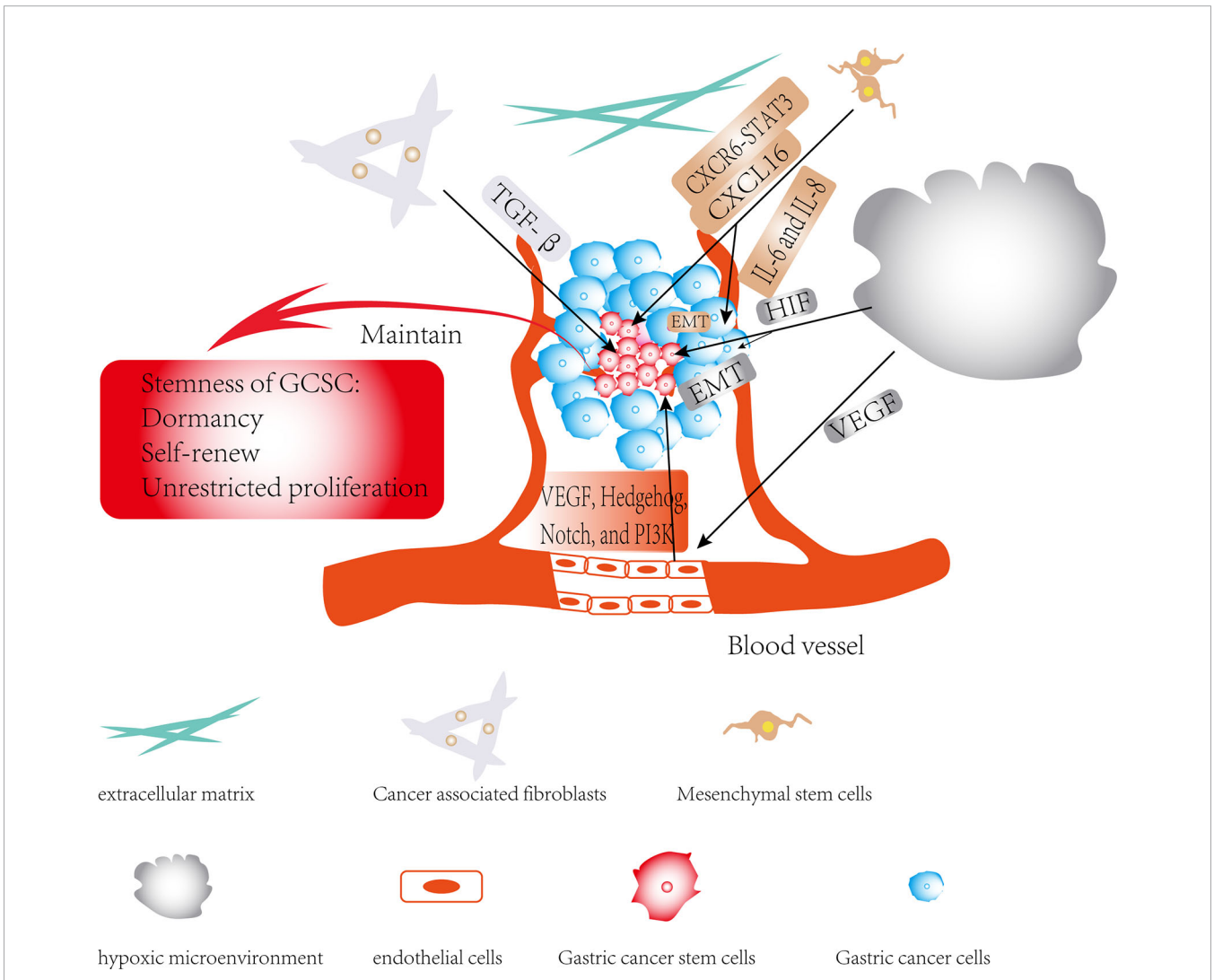

FIGURE 3 | Regulatory role of TME in gastric cancer stem cells (GCSCs): The effects of members of the TME on GCSCs are shown by black arrows; the role of TME in maintaining the stemness of GCSCs is shown by red arrows.

cell characteristics, such as self-renewal, dormancy and multi-lineage differentiation potential (**Figure 3**) (6, 97–101). Furthermore, the CSCs can also affect and modify the nature of the microenvironment. There is increasing evidence that CSCs are able to recruit and activate special types of cells such as MSCs to form a microenvironment suitable for the survival of CSCs, which is commonly known as the CSCs niche. The CSCs niche consists of stromal cells, immune cells, extracellular matrix (ECM), a vascular network and soluble factors (102). At present, there is little literature on exploring the interaction between CSCs and the TME in GC, and this paper only summarizes the existing literatures.

Recent studies have shown that CSCs reside in a vascular microenvironment that provides a suitable environment for the long-term growth of CSCs and maintenance of their stem-like properties. And vascular endothelial cells also play a crucial role in maintaining the stemness and self-renewal of CSCs. Some studies have shown that anti-vascular therapy (such as targeting VEGF) is effective in reducing the counts of CSCs and inhibiting tumor growth (11, 103). These studies demonstrate the critical role of perivascular microenvironment and vascular endothelial cells for the maintenance of the stemness of CSCs. Bevacizumab is a humanized monoclonal antibody that effectively prevents VEGF from binding to VEGFR-1, VEGFR-2, thereby inhibiting vascular endothelial cell proliferation and angiogenesis (104). Several studies have also demonstrated that targeted inhibition of the vascular microenvironment in GC can effectively inhibit the progression of GC. To explore the efficacy of bevacizumab in GC, a study *in vitro* suggested that the use of bevacizumab before chemotherapy can effectively improve the tumor control rate and reduce the tumor volume (105). In addition, it has been found that the combination of bevacizumab, docetaxel/oxaliplatin/5-FU can increase the R0 resection rate of initially unresectable GC, indicating that bevacizumab is effective in the treatment of advanced gastric cancer (106). In addition, treatment with trastuzumab in combination with VEGF-Trap can effectively inhibit the development of HER2-overexpressing GC (107).

Although the perivascular microenvironment of CSCs is increasingly studied, recent studies have found that many CSCs also reside inside tumors that are far from blood vessels and in a hypoxic state, which is known as the hypoxic microenvironment of CSCs. It has been reported that hypoxia can maintain the stemness of CSCs and induce tumor cells to become biologically more aggressive such as invasion, metastasis and therapeutic resistance. These effects are mainly attributed to HIF (108, 109). However, the hypoxic microenvironment and perivascular microenvironment of CSCs are not hostile, and the hypoxic microenvironment is also able to promote angiogenesis. In addition, both endothelial cells and CSCs can produce VEGF to stimulate angiogenesis under a hypoxic environment. Hypoxia can protect CSCs from DNA-damaging agents including chemotherapy and radiation therapy, and also promote the survival and EMT of CSCs through reactive oxygen species (ROS)-activated stress pathway and TGF-β signaling pathway. And hypoxia possess the ability of maintaining the self-renewal, tumorigenicity and the undifferentiated state of CSCs (110, 111). GCSCs microenvironment can also affect the characteristics of stem cells by regulating the expression of some transcription factors and tumor-related genes, and then affect the biological characteristics of tumor cells. For instance, Hasegawa et al. (42) confirmed that TGF-β could blocks the effects of CAFs on GCSCs, reducing the number of SP cells in GCSCs and the level of surface marker expression of GCSCs. Maeda et al. (112) found that Wnt5a gene involved in stem cell niche may promote the invasive properties of GCSCs. It was reported that hypoxia is able to confer a stem cell-like phenotype on GC, enhancing drug resistance, radiation resistance, and EMT of GC cells (113–115). However, the specific mechanism of hypoxia affecting the characteristics of CSCs is still unclear and needs further research.

ANTI-CANCER THERAPY TARGETING GC MICROENVIRONMENT AND GCSCs

Strategies for Targeting GC Microenvironment

Most of the existing clinical drugs for GC treatment are aimed at the characteristics of rapid proliferation of tumor cells, such as cytotoxic chemotherapeutic drugs. Recently, with the in-depth understanding of the role and mechanism of TME in tumor progression, great progress has also been made in the study of targeted TME therapy for tumors including GC. Here, we will show some strategies based on targeting the GC microenvironment for the treatment of GC.

Immune checkpoints are pathways that inhibit the immune system through interactions between ligand and receptor and can regulate the immune system to avoid damage to normal cells and tissues. Cancer cells, on the other hand, evade the surveillance and killing of the immune system by using immune checkpoints, leading to the continuous progression of cancer. Recently, anti-programmed cell death 1 (anti-PD-1) and anti-PD-1 ligand (anti-PD-L1) antibodies with good anti-tumor effect have gradually attracted much attention (116). Briefly, PD-1 is a transmembrane protein on the surface of T cells, and T cells will not kill cancer cells when PD-1 binds to PD-L1 expressed on the surface of cancer cells. Anti-PD-1 antibody can bind to PD-1 expressed on T cells, while anti-PD-L1 antibody can bind to PD-L1 expressed on cancer cells, thus preventing PD-1 expressed on T cells from binding to PD-L1 expressed on tumor cells, allowing T cells to kill cancer cells (117). For instance, pembrolizumab (anti-PD-1 antibody) has been shown a significant survival benefit in the treatment of GC in many studies and has been approved by the Food and Drug Administration (FDA) as a third-line treatment for PD-L1-positive GC patients as well as patients with unresectable or metastatic, highly microsatellite instability or mismatch repair-deficient (118).

CAFs have already been recognized to play a key role in promoting GC progression. Therefore, drugs that inhibit the function of CAFs may potentially prevent the progression of GC. Wang et al. (119) cultured gastric CAFs (GCAFs) and gastric normal fibroblast (GNF) with BGC-823 human GC cells, respectively. The results of this study showed that GCAFs

could significantly promote the proliferation, migration and invasion of BGC-823 cells by down-regulating microRNA-214 and up-regulating microRNA-301a compared with GNFs. And astragaloside IV, a main component of nontoxic Chinese herb, can inhibit the proliferation and invasion of GC by inhibiting the pathological function of CAFs through regulation of microRNA expression. Ferroptosis is a form of regulatory cell necrosis induced by lipid peroxidation (lipid-ROS), iron and reactive oxygen species. Zhang et al. (120) demonstrated that exosomal microRNA-522 secreted by CAFs was able to inhibit ferroptosis in GC cells by inhibiting arachidonate lipoxygenase 15 and reducing lipid-ROS production. In addition, cisplatin and paclitaxel were also demonstrated to be able to increase the secretion of microRNA-522 from CAFs by activating the USP7/hnRNPA1axis, resulting in decreased chemosensitivity of GC cells. And in another study, Uchihara et al. (121) showed Annexin A6 in extracellular vesicles (EV) from CAFs induced drug resistance of GC by activation of β1 integrin-focal adhesion kinase (FAK)-YAP. They also revealed that inhibition of FAK or YAP was able to effectively attenuate drug resistance of GC in a mouse model of peritoneal metastasis. Shen et al. (122) showed HP infection can increase expression of vascular adhesion molecule 1 (VCAM1) in CAFs of GC by activating the JAK/STAT1 signaling pathway, and the expression level of VCAM1 is positively correlated with the progression of GC and the poor prognosis of patients with GC. In addition, the interaction between CAFs-derived VCAM1 and integrin αvβ1/5 can promote the invasiveness of GC *in vivo* and *in vitro*. These findings facilitate us to further understand the mechanism of how CAFs promote GC progression and drug resistance, and provide potential targeted therapeutic strategies for GC treatment and overcoming GC drug resistance.

As an essential component of TME, TAMs are considered to be closely associated with the progression, metastasis and drug resistance of GC. Among TAMs, those of the M2 type are responsible for inhibiting T cell function and promoting tumor growth. Therefore, several potential therapeutic strategies have been proposed to work on eradicating M2 TAMs or converting M2 TAMs into M1 TAMs. Miao et al. (123) performed an immunohistochemical analysis of STING expression in 200 pairs of GC cells and its surrounding normal tissues and detected the effects of STING on cancer cell apoptosis and T cell differentiation by flowcytometry. They also verified the results in a spontaneous GC model of p53+/- mice and cell line-based xenografts. The results of this study suggest that down-regulation of STING expression is able to promote TAMs polarizing into the M1 as well as induce apoptosis in GC cells through the IL6R-JAK-IL24 pathway. Zheng et al. (124) found that M2-type TAMs were able to promote cisplatin resistance in CG cells. Further analysis using the microRNA profiles assay confirmed that exosomal microRNA-21 derived from M2-type TAMs conferred cisplatin resistance in GC cells. Wang et al. (125) confirmed *in vitro* that the expression levels of Legumain in TAMs were positively correlated with the proliferation and angiogenesis of GC. Further experiments *in vivo* also confirmed that GC cells injected with Legumain-knockdown TAMs showed slower growth and less angiogenesis compared with GC cells injected with TAMs. These studies showed that targeting exosomes associated with TAMs may be a promising new therapeutic strategy for the therapy of GC and overcoming drug resistance of GC.

Another important component in TME, MSCs plays a key role in the progression of GC and may be a promising therapeutic target for GC. Accumulating evidence indicates that MSCs contribute to progression and chemotherapy resistance of GC by secreting soluble molecules and regulating various signaling pathways. GC-MSCs have been confirmed to promote immune escape by secreting IL-8 and can induce the expression of PD-L1 in GC cells. Sun et al. (126) further confirmed that GC-MSCs were able to enhance the stemness and self-renewal of GC cells through PD-L1, leading to chemoresistance of GC. It has also been confirmed that MSCs can promote the stemness and chemoresistance of GC cells both *in vivo* and *in vitro* through fatty acid oxidation (FAO). And FAO inhibitors have been demonstrated to reduce MSCs induced resistance to FOLFOX chemotherapy regimens in GC cells. These results of this study suggested that FAO was a key factor in MSC-induced stemness and chemoresistance of GC cell and inhibitors targeting FAO combined with conventional chemotherapy regimens may be a promising therapeutic strategy to overcome GC chemoresistance (127). In addition, exosomes secreted by MSC are responsible for 5-FU resistance in GC cells both *in vivo* and *in vitro*. Ji et al. (128) revealed that MSC-derived exosomes can prevent 5-FU -induced apoptosis of GC cells and increase the expression of multi-drug resistance (MDR)-associated proteins, such as MDR by activating the calcium/calmodulin-dependent protein kinases (CaM-Ks) and Raf/MEK/ERK signaling pathway. And inhibition of CaM-Ks/Raf/MEK/ERK signaling pathway is also able to inhibit GC chemoresistance induced by MSC-exosomes. These findings suggest that targeting MSCs-related soluble molecules and signaling pathways combined with conventional chemotherapy may provide a promising new strategy to overcome the resistance of GC cells to conventional chemotherapy.

At present, surgical resection and chemoradiotherapy are the main therapeutic strategies for the treatment of GC, and molecular targeted drugs are an emerging therapeutic strategy for the treatment of GC. Increasing studies have shown that targeting key signaling pathways and molecules of the TME in GC may be a new promising therapeutic strategy for the treatment of GC. While knowledge is emerging regarding preclinical studies of the GC microenvironment, data from clinical studies on targeting the GC microenvironment in the therapy of GC is still limited. Thus, there is still a long way to go before the therapy of targeting the GC microenvironment can be applied in the treatment of GC. The underlying specific mechanisms involved in TME affecting the progression, recurrence, metastasis and drug resistance of GC remain poorly understood and further studies are still warranted.

Strategies for Targeting GCSCs

GCSCs are considered to be responsible for the development, recurrence, metastasis and drug resistance of GC. Therefore, therapeutic strategies for the targeted elimination of CSCs are

considered to be one of the promising approaches for the treatment of GC. However, there are methodological dilemmas in the current therapeutic strategy for targeting CSCs, including the lack of detection methods to specifically identify and isolate CSCs from tumor cells. This paper summarizes the current promising strategies for targeting GCSCs.

There are some specific surface markers in the surface of GCSCs. Targeting these specific surface markers is an important way to kill GCSCs and improve the prognosis of GC. Many investigators have searched for specific surface markers of GCSCs for a long time, and CD44 has been confirmed in some studies as a specific surface marker of GCSCs. Yao et al. (129) developed a gastric CSCs-specifically targeting drug delivery system (SAL-SWNT-CHI-HA complexes) that can inhibit the self-renewal ability of CD44 (+) cells in serum-free medium, which in turn reduces the formation of GCSCs. Through the eradication of GCSCs, it can effectively eradicate GC cells and block the migration and invasion of GC cells. Liang et al. (130) developed a nanoprobe against CD44v6 (a surface marker of GCSCs), which specifically targets GCSCs. In orthotopic and subcutaneous xenograft models of GC, this nanoprobe actively targets the vascular system of GC and significantly inhibits the growth of GC at 4 hours post-injection. In addition, aberrant activation of signaling pathways is present in GCSCs, and a therapeutic strategy for targeting key signaling pathways in GCSCs appears theoretically feasible in reducing GCSCs and improving GC patient prognosis. GSI, a γ-secretase inhibitor IX, was reported to be capable of inhibiting the proliferation, migration, invasion, and tumor sphere formation of CD44 (+) GCSCs by inhibiting the Notch signaling pathway (131). Feng et al. (132) found that in a GCSCs model, pantoprazole was able to increase the therapeutic sensitivity of GC to 5-fluorouracil, decrease the capacity of generating tumor spheres and the expression levels of GCSCs markers such as CD44, CD24, and Lgr5 by inhibiting the EMT/β–catenin pathways. In a study (133), CD44 (+) GC cells were shown to be resistant to 5-FU and cisplatin chemotherapy. In this study, Hedgehog (HH) signaling played an important role in maintaining the stem-like properties of CD44 (+) GC cells, and inhibition of HH could increase the sensitivity of CD44 (+) GC cells to chemotherapy. Mao et al. (134) found that activation of Wnt signaling can promote the self-renewal and proliferation of GCSCs, and salinomycin can inhibit the growth of GC by inhibiting Wnt signaling in GCSCs. The chimeric 5/35 adenovirus-mediated Dickkopf-1(Ad5/35-DKK1) that could effectively attenuate Wnt signaling of GCSCs was developed by Wang et al. (135). And in preclinical experiments, Ad5/35-DKK1 was demonstrated to be able to inhibit the invasion of CD44 (+) GC cells. Although research on targeting GCSCs is accumulating, more studies, especially clinically relevant studies, are needed to demonstrate the clinical significance of therapeutic strategy for targeting CSCs.

CONCLUSION AND FUTURE PERSPECTIVES

The TME is a complex biological system composed of a variety of cells, extracellular matrix and biological molecules. It is closely related to tumorigenesis, invasion, metastasis, and immune evasion of GC cells by secreting a variety of factors and regulating signaling pathways. CSCs are a small population of tumor cells with stem-like characteristics, which also play a crucial role in the progression, metastasis and drug resistance of GC. On the one hand, TME and CSCs may synergistically contribute the progression of GC. On the other hand, TME and CSCs may mutually promote each other. And future studies to investigate the relationship among them will provide a new idea for the cancer progression and novel therapeutic targets in GC. Because various current targeted therapeutic strategies for GC are mainly to kill non-CSCs, and the residual CSCs of GC after current therapy are implicated in tumor recurrence and metastasis. Consequently, the development of therapy targeting CSCs is warranted for the effective treatment of GC. In addition, studies focusing on targeting TME in the progression and drug resistance of GC have also confirmed that TME may provide new targets for the treatment of GC. In the future, further study on the microenvironment of CSCs in GC should be carried out to clarify the different components and functions of the microenvironment of CSCs in GC. Which will be helpful to understand the mechanism underlying the pathogenesis of GC, develop new therapy to kill CSCs in GC and change GC microenvironment, leading to promote the clinical treatment of GC.

AUTHOR CONTRIBUTIONS

Literature review, data analysis, and manuscript preparation were performed by YY. W-JM and Z-QW contributed for the study conception, design, and revision. All authors contributed to the article and approved the submitted version.

REFERENCES

1. Sung H, Ferlay J, Siegel RL, Laversanne M, Soerjomataram I, Jemal A, et al. Global Cancer Statistics 2020: GLOBOCAN Estimates of Incidence and Mortality Worldwide for 36 Cancers in 185 Countries. *CA Cancer J Clin* (2021) 71(3):209–49. doi: 10.3322/caac.21660. 10.3322/caac.21660.
2. Smyth EC, Nilsson M, Grabsch HI, van Grieken NC, Lordick F. Gastric Cancer. *Lancet* (2020) 396:635–48. doi: 10.1016/S0140-6736(20)31288-5
3. Bonnet D, Dick JE. Human Acute Myeloid Leukemia Is Organized as a Hierarchy That Originates From a Primitive Hematopoietic Cell. *Nat Med* (1997) 3:730–7. doi: 10.1038/nm0797-730
4. Zhang L, Guo X, Zhang D, Fan Y, Qin L, Dong S, et al. Upregulated miR-132 in Lgr5 Gastric Cancer Stem Cell-Like Cells Contributes to Cisplatin-Resistance *via* SIRT1/CREB/ABCG2 Signaling Pathway. *Mol Carcinog* (2017) 56:2022–34. doi: 10.1002/mc.22656
5. Shibue T, Weinberg RA. EMT, CSCs, and Drug Resistance: The Mechanistic Link and Clinical Implications. *Nat Rev Clin Oncol* (2017) 14:611–29. doi: 10.1038/nrclinonc.2017.44
6. Batlle E, Clevers H. Cancer Stem Cells Revisited. *Nat Med* (2017) 23:1124–34. doi: 10.1038/nm.4409
7. Cai W-Y, Dong Z-N, Fu X-T, Lin L-Y, Wang L, Ye G-D, et al. Identification of a Tumor Microenvironment-Relevant Gene Set-Based Prognostic

Signature and Related Therapy Targets in Gastric Cancer. *Theranostics* (2020) 10:8633–47. doi: 10.7150/thno.47938
8. Choi H, Na KJ. Integrative Analysis of Imaging and Transcriptomic Data of the Immune Landscape Associated With Tumor Metabolism in Lung Adenocarcinoma: Clinical and Prognostic Implications. *Theranostics* (2018) 8:1956–65. doi: 10.7150/thno.23767
9. Wang M, Zhao J, Zhang L, Wei F, Lian Y, Wu Y, et al. Role of Tumor Microenvironment in Tumorigenesis. *J Cancer* (2017) 8:761–73. doi: 10.7150/jca.17648
10. Mashukov A, Shapochka D, Seleznov O, Kobyliak N, Falalyeyeva T, Kirkilevsky S, et al. Histological Differentiation Impacts the Tumor Immune Microenvironment in Gastric Carcinoma: Relation to the Immune Cycle. *World J Gastroenterol* (2021) 27:5259–71. doi: 10.3748/wjg.v27.i31.5259
11. Plaks V, Kong N, Werb Z. The Cancer Stem Cell Niche: How Essential Is the Niche in Regulating Stemness of Tumor Cells? *Cell Stem Cell* (2015) 16:225–38. doi: 10.1016/j.stem.2015.02.015
12. Ishizawa K, Rasheed ZA, Karisch R, Wang Q, Kowalski J, Susky E, et al. Tumor-Initiating Cells Are Rare in Many Human Tumors. *Cell Stem Cell* (2010) 7:279–82. doi: 10.1016/j.stem.2010.08.009
13. Takaishi S, Okumura T, Tu S, Wang SSW, Shibata W, Vigneshwaran R, et al. Identification of Gastric Cancer Stem Cells Using the Cell Surface Marker CD44. *Stem Cells* (2009) 27:1006–20. doi: 10.1002/stem.30
14. Lau WM, Teng E, Chong HS, Lopez KAP, Tay AYL, Salto-Tellez M, et al. CD44v8-10 Is a Cancer-Specific Marker for Gastric Cancer Stem Cells. *Cancer Res* (2014) 74:2630–41. doi: 10.1158/0008-5472.CAN-13-2309
15. Katsuno Y, Ehata S, Yashiro M, Yanagihara K, Hirakawa K, Miyazono K. Coordinated Expression of REG4 and Aldehyde Dehydrogenase 1 Regulating Tumourigenic Capacity of Diffuse-Type Gastric Carcinoma-Initiating Cells Is Inhibited by TGF-β. *J Pathol* (2012) 228:391–404. doi: 10.1002/path.4020
16. Jiang J, Zhang Y, Chuai S, Wang Z, Zheng D, Xu F, et al. Trastuzumab (Herceptin) Targets Gastric Cancer Stem Cells Characterized by CD90 Phenotype. *Oncogene* (2012) 31:671–82. doi: 10.1038/onc.2011.282
17. Ohkuma M, Haraguchi N, Ishii H, Mimori K, Tanaka F, Kim HM, et al. Absence of CD71 Transferrin Receptor Characterizes Human Gastric Adenosquamous Carcinoma Stem Cells. *Ann Surg Oncol* (2012) 19:1357–64. doi: 10.1245/s10434-011-1739-7
18. Wenqi D, Li W, Shanshan C, Bei C, Yafei Z, Feihu B, et al. EpCAM Is Overexpressed in Gastric Cancer and Its Downregulation Suppresses Proliferation of Gastric Cancer. *J Cancer Res Clin Oncol* (2009) 135:1277–85. doi: 10.1007/s00432-009-0569-5
19. Zhang C, Li C, He F, Cai Y, Yang H. Identification of CD44+CD24+ Gastric Cancer Stem Cells. *J Cancer Res Clin Oncol* (2011) 137:1679–86. doi: 10.1007/s00432-011-1038-5
20. Chen T, Yang K, Yu J, Meng W, Yuan D, Bi F, et al. Identification and Expansion of Cancer Stem Cells in Tumor Tissues and Peripheral Blood Derived From Gastric Adenocarcinoma Patients. *Cell Res* (2012) 22:248–58. doi: 10.1038/cr.2011.109
21. Han M-E, Jeon T-Y, Hwang S-H, Lee Y-S, Kim H-J, Shim H-E, et al. Cancer Spheres From Gastric Cancer Patients Provide an Ideal Model System for Cancer Stem Cell Research. *Cell Mol Life Sci CMLS* (2011) 68:3589–605. doi: 10.1007/s00018-011-0672-z
22. Nishikawa S, Konno M, Hamabe A, Hasegawa S, Kano Y, Ohta K, et al. Aldehyde Dehydrogenase High Gastric Cancer Stem Cells Are Resistant to Chemotherapy. *Int J Oncol* (2013) 42:1437–42. doi: 10.3892/ijo.2013.1837
23. Li G, Su Q, Liu H, Wang D, Zhang W, Lu Z, et al. Frizzled7 Promotes Epithelial-To-Mesenchymal Transition and Stemness *Via* Activating Canonical Wnt/β-Catenin Pathway in Gastric Cancer. *Int J Biol Sci* (2018) 14:280–93. doi: 10.7150/ijbs.23756
24. Wolmarans E, Nel S, Durandt C, Mellet J, Pepper MS. Side Population: Its Use in the Study of Cellular Heterogeneity and as a Potential Enrichment Tool for Rare Cell Populations. *Stem Cells Int* (2018) 2018:2472137. doi: 10.1155/2018/2472137
25. Haraguchi N, Utsunomiya T, Inoue H, Tanaka F, Mimori K, Barnard GF, et al. Characterization of a Side Population of Cancer Cells From Human Gastrointestinal System. *Stem Cells* (2006) 24:506–13. doi: 10.1634/stemcells.2005-0282
26. Courtois S, Durán RV, Giraud J, Sifré E, Izotte J, Mégraud F, et al. Metformin Targets Gastric Cancer Stem Cells. *Eur J Cancer (Oxford Engl 1990)* (2017) 84:193–201. doi: 10.1016/j.ejca.2017.07.020
27. Chen S, Chen C, Hu Y, Zhu C, Luo X, Wang L, et al. Three-Dimensional Culture for Drug Responses of Patient-Derived Gastric Cancer Tissue. *Front Oncol* (2020) 10:614096. doi: 10.3389/fonc.2020.614096
28. Magalhães L, Quintana LG, Lopes DCF, Vidal AF, Pereira AL, D'Araujo Pinto LC, et al. APC Gene Is Modulated by hsa-miR-135b-5p in Both Diffuse and Intestinal Gastric Cancer Subtypes. *BMC Cancer* (2018) 18:1055. doi: 10.1186/s12885-018-4980-7
29. Kim D-H, Lee S, Kang HG, Park H-W, Lee H-W, Kim D, et al. Synergistic Antitumor Activity of a DLL4/VEGF Bispecific Therapeutic Antibody in Combination With Irinotecan in Gastric Cancer. *BMB Rep* (2020) 53:533–8. doi: 10.5483/BMBRep.2020.53.10.103
30. Takeuchi A, Yokoyama S, Nakamori M, Nakamura M, Ojima T, Yamaguchi S, et al. Loss of CEACAM1 Is Associated With Poor Prognosis and Peritoneal Dissemination of Patients With Gastric Cancer. *Sci Rep* (2019) 9:12702. doi: 10.1038/s41598-019-49230-w
31. Chen T, Li J, Jia Y, Wang J, Sang R, Zhang Y, et al. Single-Cell Sequencing in the Field of Stem Cells. *Curr Genomics* (2020) 21:576–84. doi: 10.2174/1389202921999200624154445
32. Velten L, Story BA, Hernández-Malmierca P, Raffel S, Leonce DR, Milbank J, et al. Identification of Leukemic and Pre-Leukemic Stem Cells by Clonal Tracking From Single-Cell Transcriptomics. *Nat Commun* (2021) 12:1366. doi: 10.1038/s41467-021-21650-1
33. Yang Z, Li C, Fan Z, Liu H, Zhang X, Cai Z, et al. Single-Cell Sequencing Reveals Variants in ARID1A, GPRC5A and MLL2 Driving Self-Renewal of Human Bladder Cancer Stem Cells. *Eur Urol* (2017) 71:8–12. doi: 10.1016/j.eururo.2016.06.025
34. Song Q, Su J, Miller LD, Zhang W. scLM: Automatic Detection of Consensus Gene Clusters Across Multiple Single-Cell Datasets. *Genomics Proteomics Bioinf* (2021) 19:330–41. doi: 10.1016/j.gpb.2020.09.002
35. Song Q, Su J, Zhang W. scGCN Is a Graph Convolutional Networks Algorithm for Knowledge Transfer in Single Cell Omics. *Nat Commun* (2021) 12:3826. doi: 10.1038/s41467-021-24172-y
36. De P, Aske J, Dey N. Cancer-Associated Fibroblast Functions as a Road-Block in Cancer Therapy. *Cancers (Basel)* (2021) 13(20):5246. doi: 10.3390/cancers13205246
37. Gunaydin G. CAFs Interacting With TAMs in Tumor Microenvironment to Enhance Tumorigenesis and Immune Evasion. *Front Oncol* (2021) 11:668349. doi: 10.3389/fonc.2021.668349
38. Nair N, Calle AS, Zahra MH, Prieto-Vila M, Oo AKK, Hurley L, et al. A Cancer Stem Cell Model as the Point of Origin of Cancer-Associated Fibroblasts in Tumor Microenvironment. *Sci Rep* (2017) 7:6838. doi: 10.1038/s41598-017-07144-5
39. Quante M, Tu SP, Tomita H, Gonda T, Wang SSW, Takashi S, et al. Bone Marrow-Derived Myofibroblasts Contribute to the Mesenchymal Stem Cell Niche and Promote Tumor Growth. *Cancer Cell* (2011) 19:257–72. doi: 10.1016/j.ccr.2011.01.020
40. Sugimoto H, Mundel TM, Kieran MW, Kalluri R. Identification of Fibroblast Heterogeneity in the Tumor Microenvironment. *Cancer Biol Ther* (2006) 5:1640–6. doi: 10.4161/cbt.5.12.3354
41. Kobayashi H, Enomoto A, Woods SL, Burt AD, Takahashi M, Worthley DL. Cancer-Associated Fibroblasts in Gastrointestinal Cancer. *Nat Rev Gastroenterol Hepatol* (2019) 16:282–95. doi: 10.1038/s41575-019-0115-0
42. Hasegawa T, Yashiro M, Nishii T, Matsuoka J, Fuyuhiro Y, Morisaki T, et al. Cancer-Associated Fibroblasts Might Sustain the Stemness of Scirrhous Gastric Cancer Cells *via* Transforming Growth Factor-β Signaling. *Int J Cancer* (2014) 134:1785–95. doi: 10.1002/ijc.28520
43. Karakasheva TA, Lin EW, Tang Q, Qiao E, Waldron TJ, Soni M, et al. IL-6 Mediates Cross-Talk Between Tumor Cells and Activated Fibroblasts in the Tumor Microenvironment. *Cancer Res* (2018) 78:4957–70. doi: 10.1158/0008-5472.CAN-17-2268
44. Wang X, Zhou Q, Yu Z, Wu X, Chen X, Li J, et al. Cancer-Associated Fibroblast-Derived Lumican Promotes Gastric Cancer Progression *via* the Integrin β1-FAK Signaling Pathway. *Int J Cancer* (2017) 141:998–1010. doi: 10.1002/ijc.30801

45. Shibata W, Ariyama H, Westphalen CB, Worthley DL, Muthupalani S, Asfaha S, et al. Stromal Cell-Derived Factor-1 Overexpression Induces Gastric Dysplasia Through Expansion of Stromal Myofibroblasts and Epithelial Progenitors. *Gut* (2013) 62:192–200. doi: 10.1136/gutjnl-2011-301824
46. Huang L, Xu AM, Liu S, Liu W, Li T-J. Cancer-Associated Fibroblasts in Digestive Tumors. *World J Gastroenterol* (2014) 20:17804–18. doi: 10.3748/wjg.v20.i47.17804
47. Bockerstett KA, DiPaolo RJ. Regulation of Gastric Carcinogenesis by Inflammatory Cytokines. *Cell Mol Gastroenterol Hepatol* (2017) 4:47–53. doi: 10.1016/j.jcmgh.2017.03.005
48. Li P, Shan J-X, Chen X-H, Zhang D, Su L-P, Huang X-Y, et al. Epigenetic Silencing of microRNA-149 in Cancer-Associated Fibroblasts Mediates Prostaglandin E2/interleukin-6 Signaling in the Tumor Microenvironment. *Cell Res* (2015) 25:588–603. doi: 10.1038/cr.2015.51
49. Kinoshita H, Hirata Y, Nakagawa H, Sakamoto K, Hayakawa Y, Takahashi R, et al. Interleukin-6 Mediates Epithelial-Stromal Interactions and Promotes Gastric Tumorigenesis. *PLoS One* (2013) 8:e60914. doi: 10.1371/journal.pone.0060914
50. Gu J, Qian H, Shen L, Zhang X, Zhu W, Huang L, et al. Gastric Cancer Exosomes Trigger Differentiation of Umbilical Cord Derived Mesenchymal Stem Cells to Carcinoma-Associated Fibroblasts Through TGF-β/Smad Pathway. *PLoS One* (2012) 7:e52465. doi: 10.1371/journal.pone.0052465
51. Kuramitsu S, Masuda T, Hu Q, Tobo T, Yashiro M, Fujii A, et al. Cancer-Associated Fibroblast-Derived Spondin-2 Promotes Motility of Gastric Cancer Cells. *Cancer Genomics Proteomics* (2021) 18:521–9. doi: 10.21873/cgp.20277
52. Ishimoto T, Miyake K, Nandi T, Yashiro M, Onishi N, Huang KK, et al. Activation of Transforming Growth Factor Beta 1 Signaling in Gastric Cancer-Associated Fibroblasts Increases Their Motility, *via* Expression of Rhomboid 5 Homolog 2, and Ability to Induce Invasiveness of Gastric Cancer Cells. *Gastroenterology* (2017) 153:191–204. doi: 10.1053/j.gastro.2017.03.046
53. Wen X, He X, Jiao F, Wang C, Sun Y, Ren X, et al. Fibroblast Activation Protein-α-Positive Fibroblasts Promote Gastric Cancer Progression and Resistance to Immune Checkpoint Blockade. *Oncol Res* (2017) 25:629–40. doi: 10.3727/096504016X14768383625385
54. Zheng H, Liu H, Li H, Dou W, Wang X. Weighted Gene Co-Expression Network Analysis Identifies a Cancer-Associated Fibroblast Signature for Predicting Prognosis and Therapeutic Responses in Gastric Cancer. *Front Mol Biosci* (2021) 8:744677. doi: 10.3389/fmolb.2021.744677
55. Li Y, Li J-Q, Jiang H-P, Li X. The Upregulation of PLXDC2 Correlates With Immune Microenvironment Characteristics and Predicts Prognosis in Gastric Cancer. *Dis Markers* (2021) 2021:5669635. doi: 10.1155/2021/5669635
56. Rihawi K, Ricci AD, Rizzo A, Brocchi S, Marasco G, Pastore LV, et al. Tumor-Associated Macrophages and Inflammatory Microenvironment in Gastric Cancer: Novel Translational Implications. *Int J Mol Sci* (2021) 22 (8):3805. doi: 10.3390/ijms22083805
57. Gambardella V, Castillo J, Tarazona N, Gimeno-Valiente F, Martínez-Ciarpaglini C, Cabeza-Segura M, et al. The Role of Tumor-Associated Macrophages in Gastric Cancer Development and Their Potential as a Therapeutic Target. *Cancer Treat Rev* (2020) 86:102015. doi: 10.1016/j.ctrv.2020.102015
58. Petersen CP, Meyer AR, De Salvo C, Choi E, Schlegel C, Petersen A, et al. A Signalling Cascade of IL-33 to IL-13 Regulates Metaplasia in the Mouse Stomach. *Gut* (2018) 67:805–17. doi: 10.1136/gutjnl-2016-312779
59. Oishi S, Takano R, Tamura S, Tani S, Iwaizumi M, Hamaya Y, et al. M2 Polarization of Murine Peritoneal Macrophages Induces Regulatory Cytokine Production and Suppresses T-Cell Proliferation. *Immunology* (2016) 149:320–8. doi: 10.1111/imm.12647
60. Oguma K, Oshima H, Aoki M, Uchio R, Naka K, Nakamura S, et al. Activated Macrophages Promote Wnt Signalling Through Tumour Necrosis Factor-Alpha in Gastric Tumour Cells. *EMBO J* (2008) 27:1671–81. doi: 10.1038/emboj.2008.105
61. Oshima H, Hioki K, Popivanova BK, Oguma K, Van Rooijen N, Ishikawa T-O, et al. Prostaglandin E_2 Signaling and Bacterial Infection Recruit Tumor-Promoting Macrophages to Mouse Gastric Tumors. *Gastroenterology* (2011) 140:596–607. doi: 10.1053/j.gastro.2010.11.007
62. Yamanaka N, Morisaki T, Nakashima H, Tasaki A, Kubo M, Kuga H, et al. Interleukin 1beta Enhances Invasive Ability of Gastric Carcinoma Through Nuclear factor-kappaB Activation. *Clin Cancer Res* (2004) 10:1853–9. doi: 10.1158/1078-0432.CCR-03-0300
63. Ohta M, Kitadai Y, Tanaka S, Yoshihara M, Yasui W, Mukaida N, et al. Monocyte Chemoattractant Protein-1 Expression Correlates With Macrophage Infiltration and Tumor Vascularity in Human Gastric Carcinomas. *Int J Oncol* (2003) 22:773–8. doi: 10.3892/ijo.22.4.773
64. Kuroda T, Kitadai Y, Tanaka S, Yang X, Mukaida N, Yoshihara M, et al. Monocyte Chemoattractant Protein-1 Transfection Induces Angiogenesis and Tumorigenesis of Gastric Carcinoma in Nude Mice *via* Macrophage Recruitment. *Clin Cancer Res* (2005) 11:7629–36. doi: 10.1158/1078-0432.CCR-05-0798
65. Wu H, Xu J-B, He Y-L, Peng J-J, Zhang X-H, Chen C-Q, et al. Tumor-Associated Macrophages Promote Angiogenesis and Lymphangiogenesis of Gastric Cancer. *J Surg Oncol* (2012) 106:462–8. doi: 10.1002/jso.23110
66. Jiménez G, Hackenberg M, Catalina P, Boulaiz H, Griñán-Lisón C, García MÁ, et al. Mesenchymal Stem Cell's Secretome Promotes Selective Enrichment of Cancer Stem-Like Cells With Specific Cytogenetic Profile. *Cancer Lett* (2018) 429:78–88. doi: 10.1016/j.canlet.2018.04.042
67. Li W, Zhou Y, Yang J, Zhang X, Zhang H, Zhang T, et al. Gastric Cancer-Derived Mesenchymal Stem Cells Prompt Gastric Cancer Progression Through Secretion of Interleukin-8. *J Exp Clin Cancer Res* (2015) 34:52. doi: 10.1186/s13046-015-0172-3
68. Sun L, Wang Q, Chen B, Zhao Y, Shen B, Wang X, et al. Human Gastric Cancer Mesenchymal Stem Cell-Derived IL15 Contributes to Tumor Cell Epithelial-Mesenchymal Transition *via* Upregulation Tregs Ratio and PD-1 Expression in CD4T Cell. *Stem Cells Dev* (2018) 27:1203–14. doi: 10.1089/scd.2018.0043
69. Huang F, Wang M, Yang T, Cai J, Zhang Q, Sun Z, et al. Gastric Cancer-Derived MSC-Secreted PDGF-DD Promotes Gastric Cancer Progression. *J Cancer Res Clin Oncol* (2014) 140:1835–48. doi: 10.1007/s00432-014-1723-2
70. Wang M, Zhao C, Shi H, Zhang B, Zhang L, Zhang X, et al. Deregulated microRNAs in Gastric Cancer Tissue-Derived Mesenchymal Stem Cells: Novel Biomarkers and a Mechanism for Gastric Cancer. *Br J Cancer* (2014) 110:1199–210. doi: 10.1038/bjc.2014.14
71. Li W, Zhang X, Wu F, Zhou Y, Bao Z, Li H, et al. Gastric Cancer-Derived Mesenchymal Stromal Cells Trigger M2 Macrophage Polarization That Promotes Metastasis and EMT in Gastric Cancer. *Cell Death Dis* (2019) 10:918. doi: 10.1038/s41419-019-2131-y
72. Yin L, Zhang R, Hu Y, Li W, Wang M, Liang Z, et al. Gastric-Cancer-Derived Mesenchymal Stem Cells: A Promising Target for Resveratrol in the Suppression of Gastric Cancer Metastasis. *Hum Cell* (2020) 33:652–62. doi: 10.1007/s13577-020-00339-5
73. Ikeda T, Nishita M, Hoshi K, Honda T, Kakeji Y, Minami Y. Mesenchymal Stem Cell-Derived CXCL16 Promotes Progression of Gastric Cancer Cells by STAT3-Mediated Expression of Ror1. *Cancer Sci* (2020) 111:1254–65. doi: 10.1111/cas.14339
74. Takiguchi G, Nishita M, Kurita K, Kakeji Y, Minami Y. Wnt5a-Ror2 Signaling in Mesenchymal Stem Cells Promotes Proliferation of Gastric Cancer Cells by Activating CXCL16-CXCR6 Axis. *Cancer Sci* (2016) 107:290–7. doi: 10.1111/cas.12871
75. Han J, Khatwani N, Searles TG, Turk MJ, Angeles CV. Memory CD8 T Cell Responses to Cancer. *Semin Immunol* (2020) 49:101435. doi: 10.1016/j.smim.2020.101435
76. Liu X, Zhang Z, Zhao G. Recent Advances in the Study of Regulatory T Cells in Gastric Cancer. *Int Immunopharmacol* (2019) 73:560–7. doi: 10.1016/j.intimp.2019.05.009
77. Kono K, Kawaida H, Takahashi A, Sugai H, Mimura K, Miyagawa N, et al. CD4(+)CD25high Regulatory T Cells Increase With Tumor Stage in Patients With Gastric and Esophageal Cancers. *Cancer Immunol Immunother* (2006) 55:1064–71. doi: 10.1007/s00262-005-0092-8
78. Zhuang Y, Peng L-S, Zhao Y-L, Shi Y, Mao X-H, Guo G, et al. Increased Intratumoral IL-22-Producing CD4(+) T Cells and Th22 Cells Correlate With Gastric Cancer Progression and Predict Poor Patient Survival. *Cancer Immunol Immunother* (2012) 61:1965–75. doi: 10.1007/s00262-012-1241-5
79. Zhuang Y, Peng L-S, Zhao Y-L, Shi Y, Mao X-H, Chen W, et al. CD8(+) T Cells That Produce Interleukin-17 Regulate Myeloid-Derived Suppressor

Cells and Are Associated With Survival Time of Patients With Gastric Cancer. *Gastroenterology* (2012) 143:951–62. doi: 10.1053/j.gastro.2012.06.010
80. Sitarz R, Skierucha M, Mielko J, Offerhaus GJA, Maciejewski R, Polkowski WP. Gastric Cancer: Epidemiology, Prevention, Classification, and Treatment. *Cancer Manage Res* (2018) 10:239–48. doi: 10.2147/CMAR.S149619
81. Amieva M, Peek RM. Pathobiology of Helicobacter Pylori-Induced Gastric Cancer. *Gastroenterology* (2016) 150:64–78. doi: 10.1053/j.gastro.2015.09.004
82. Baj J, Brzozowska K, Forma A, Maani A, Sitarz E, Portincasa P. Immunological Aspects of the Tumor Microenvironment and Epithelial-Mesenchymal Transition in Gastric Carcinogenesis. *Int J Mol Sci* (2020) 21 (7):2544. doi: 10.3390/ijms21072544
83. Soundararajan R, Fradette JJ, Konen JM, Moulder S, Zhang X, Gibbons DL, et al. Targeting the Interplay Between Epithelial-To-Mesenchymal-Transition and the Immune System for Effective Immunotherapy. *Cancers (Basel)* (2019) 11(5):714. doi: 10.3390/cancers11050714
84. Ma H-Y, Liu X-Z, Liang C-M. Inflammatory Microenvironment Contributes to Epithelial-Mesenchymal Transition in Gastric Cancer. *World J Gastroenterol* (2016) 22:6619–28. doi: 10.3748/wjg.v22.i29.6619
85. Krzysiek-Maczka G, Targosz A, Szczyrk U, Strzalka M, Brzozowski T, Ptak-Belowska A. Involvement of Epithelial-Mesenchymal Transition-Inducing Transcription Factors in the Mechanism of Helicobacter Pylori-Induced Fibroblasts Activation. *J Physiol Pharmacol* (2019) 70:727–36. doi: 10.26402/jpp.2019.5.08
86. Zhang Q, Wang M, Huang F, Yang T, Cai J, Zhang X, et al. H. Pylori Infection-Induced MSC Differentiation Into CAFs Promotes Epithelial-Mesenchymal Transition in Gastric Epithelial Cells. *Int J Mol Med* (2013) 32:1465–73. doi: 10.3892/ijmm.2013.1532
87. Krzysiek-Maczka G, Targosz A, Szczyrk U, Strzałka M, Sliwowski Z, Brzozowski T, et al. Role of Helicobacter Pylori Infection in Cancer-Associated Fibroblast-Induced Epithelial-Mesenchymal Transition In Vitro. *Helicobacter* (2018) 23:e12538. doi: 10.1111/hel.12538
88. Zhang X, Ashcraft K, Betof Warner A, Nair S, Dewhirst M. Can Exercise-Induced Modulation of the Tumor Physiologic Microenvironment Improve Antitumor Immunity? *Cancer Res* (2019) 79:2447–56. doi: 10.1158/0008-5472.Can-18-2468
89. Varisli L, Cen O, Vlahopoulos S. Dissecting Pharmacological Effects of Chloroquine in Cancer Treatment: Interference With Inflammatory Signaling Pathways. *Immunology* (2020) 159:257–78. doi: 10.1111/imm.13160
90. Lai Y, Huang H, Abudoureyimu M, Lin X, Tian C, Wang T, et al. Non-Coding RNAs: Emerging Regulators of Glucose Metabolism in Hepatocellular Carcinoma. *Am J Cancer Res* (2020) 10:4066–84.
91. Yadav UP, Singh T, Kumar P, Sharma P, Kaur H, Sharma S, et al. Metabolic Adaptations in Cancer Stem Cells. *Front Oncol* (2020) 10:1010. doi: 10.3389/fonc.2020.01010
92. Nimmakayala RK, Leon F, Rachagani S, Rauth S, Nallasamy P, Marimuthu S, et al. Metabolic Programming of Distinct Cancer Stem Cells Promotes Metastasis of Pancreatic Ductal Adenocarcinoma. *Oncogene* (2021) 40:215–31. doi: 10.1038/s41388-020-01518-2
93. Hu P-S, Li T, Lin J-F, Qiu M-Z, Wang D-S, Liu Z-X, et al. VDR-SOX2 Signaling Promotes Colorectal Cancer Stemness and Malignancy in an Acidic Microenvironment. *Signal transduction targeted Ther* (2020) 5:183. doi: 10.1038/s41392-020-00230-7
94. Wojtkowiak JW, Gillies RJ. Autophagy on Acid. *Autophagy* (2012) 8:1688–9. doi: 10.4161/auto.21501
95. Chen X, Sun X, Wang Z, Zhou X, Xu L, Fe Li, et al. Involvement of Acid-Sensing Ion Channel 1a in Gastric Carcinoma Cell Migration and Invasion. *Acta Biochim Biophys Sin* (2018) 50:440–6. doi: 10.1093/abbs/gmy026
96. Chen L, Kasai T, Li Y, Sugii Y, Jin G, Okada M, et al. A Model of Cancer Stem Cells Derived From Mouse Induced Pluripotent Stem Cells. *PLoS One* (2012) 7:e33544. doi: 10.1371/journal.pone.0033544
97. Nguyen LV, Vanner R, Dirks P, Eaves CJ. Cancer Stem Cells: An Evolving Concept. *Nat Rev Cancer* (2012) 12:133–43. doi: 10.1038/nrc3184
98. Nassar D, Blanpain C. Cancer Stem Cells: Basic Concepts and Therapeutic Implications. *Annu Rev Pathol* (2016) 11:47–76. doi: 10.1146/annurev-pathol-012615-044438
99. Najafi M, Farhood B, Mortezaee K. Cancer Stem Cells (CSCs) in Cancer Progression and Therapy. *J Cell Physiol* (2019) 234:8381–95. doi: 10.1002/jcp.27740
100. Huang T, Song X, Xu D, Tiek D, Goenka A, Wu B, et al. Stem Cell Programs in Cancer Initiation, Progression, and Therapy Resistance. *Theranostics* (2020) 10:8721–43. doi: 10.7150/thno.41648
101. Dzobo K, Senthebane DA, Ganz C, Thomford NE, Wonkam A, Dandara C. Advances in Therapeutic Targeting of Cancer Stem Cells Within the Tumor Microenvironment: An Updated Review. *Cells* (2020) 9(8):1896. doi: 10.3390/cells9081896
102. Borovski T, De Sousa E Melo F, Vermeulen L, Medema J. Cancer Stem Cell Niche: The Place to Be. *Cancer Res* (2011) 71:634–9. doi: 10.1158/0008-5472.Can-10-3220
103. Sottoriva A, Sloot PMA, Medema JP, Vermeulen L. Exploring Cancer Stem Cell Niche Directed Tumor Growth. *Cell Cycle (Georgetown Tex.)* (2010) 9:1472–9. doi: 10.4161/cc.9.8.11198
104. Zhang J, Gao B, Zhang W, Qian Z, Xiang Y. Monitoring Antiangiogenesis of Bevacizumab in Zebrafish. *Drug Design Dev Ther* (2018) 12:2423–30. doi: 10.2147/DDDT.S166330
105. Lv Y, Song L, Chang L, Zhang X, Liu Y, Liu W. Effect of Bevacizumab Combined With Chemotherapy at Different Sequences in the Gastric-Cancer-Bearing Nude Mice. *J Cancer Res Ther* (2018) 14:S190–6. doi: 10.4103/0973-1482.171364
106. Ma J, Yao S, Li X-S, Kang H-R, Yao F-F, Du N. Neoadjuvant Therapy of DOF Regimen Plus Bevacizumab Can Increase Surgical Resection Ratein Locally Advanced Gastric Cancer: A Randomized, Controlled Study. *Medicine* (2015) 94:e1489. doi: 10.1097/MD.0000000000001489
107. Singh R, Kim WJ, Kim P-H, Hong HJ. Combined Blockade of HER2 and VEGF Exerts Greater Growth Inhibition of HER2-Overexpressing Gastric Cancer Xenografts Than Individual Blockade. *Exp Mol Med* (2013) 45:e52. doi: 10.1038/emm.2013.111
108. Das B, Tsuchida R, Malkin D, Koren G, Baruchel S, Yeger H. Hypoxia Enhances Tumor Stemness by Increasing the Invasive and Tumorigenic Side Population Fraction. *Stem Cells* (2008) 26:1818–30. doi: 10.1634/stemcells.2007-0724
109. Pistollato F, Rampazzo E, Persano L, Abbadi S, Frasson C, Denaro L, et al. Interaction of Hypoxia-Inducible Factor-1α and Notch Signaling Regulates Medulloblastoma Precursor Proliferation and Fate. *Stem Cells* (2010) 28:1918–29. doi: 10.1002/stem.518
110. Scheel C, Eaton EN, Li SH-J, Chaffer CL, Reinhardt F, Kah K-J, et al. Paracrine and Autocrine Signals Induce and Maintain Mesenchymal and Stem Cell States in the Breast. *Cell* (2011) 145:926–40. doi: 10.1016/j.cell.2011.04.029
111. Man J, Yu X, Huang H, Zhou W, Xiang C, Huang H, et al. Hypoxic Induction of Vasorin Regulates Notch1 Turnover to Maintain Glioma Stem-Like Cells. *Cell Stem Cell* (2018) 22:104–18. doi: 10.1016/j.stem.2017.10.005
112. Maeda M, Takeshima H, Iida N, Hattori N, Yamashita S, Moro H, et al. Cancer Cell Niche Factors Secreted From Cancer-Associated Fibroblast by Loss of H3k27me3. *Gut* (2020) 69:243–51. doi: 10.1136/gutjnl-2018-317645
113. Kato Y, Yashiro M, Fuyuhiro Y, Kashiwagi S, Matsuoka J, Hirakawa T, et al. Effects of Acute and Chronic Hypoxia on the Radiosensitivity of Gastric and Esophageal Cancer Cells. *Anticancer Res* (2011) 31:3369–75.
114. Liu L, Ning X, Sun L, Zhang H, Shi Y, Guo C, et al. Hypoxia-Inducible Factor-1 Alpha Contributes to Hypoxia-Induced Chemoresistance in Gastric Cancer. *Cancer Sci* (2008) 99:121–8. doi: 10.1111/j.1349-7006.2007.00643.x
115. Matsuoka J, Yashiro M, Doi Y, Fuyuhiro Y, Kato Y, Shinto O, et al. Hypoxia Stimulates the EMT of Gastric Cancer Cells Through Autocrine Tgfβ Signaling. *PLoS One* (2013) 8:e62310. doi: 10.1371/journal.pone.0062310
116. Pardoll DM. The Blockade of Immune Checkpoints in Cancer Immunotherapy. *Nat Rev Cancer* (2012) 12:252–64. doi: 10.1038/nrc3239
117. Wu X, Gu Z, Chen Y, Chen B, Chen W, Weng L, et al. Application of PD-1 Blockade in Cancer Immunotherapy. *Comput Struct Biotechnol J* (2019) 17:661–74. doi: 10.1016/j.csbj.2019.03.006
118. Sundar R, Smyth E, Peng S, Yeong J, Tan P. Predictive Biomarkers of Immune Checkpoint Inhibition in Gastroesophageal Cancers. *Front Oncol* (2020) 10:763. doi: 10.3389/fonc.2020.00763

119. Wang Z-F, Ma D-G, Zhu Z, Mu Y-P, Yang Y-Y, Feng L, et al. Astragaloside IV Inhibits Pathological Functions of Gastric Cancer-Associated Fibroblasts. *World J Gastroenterol* (2017) 23:8512–25. doi: 10.3748/wjg.v23.i48.8512
120. Zhang H, Deng T, Liu R, Ning T, Yang H, Liu D, et al. CAF Secreted miR-522 Suppresses Ferroptosis and Promotes Acquired Chemo-Resistance in Gastric Cancer. *Mol Cancer* (2020) 19:43. doi: 10.1186/s12943-020-01168-8
121. Uchihara T, Miyake K, Yonemura A, Komohara Y, Itoyama R, Koiwa M, et al. Extracellular Vesicles From Cancer-Associated Fibroblasts Containing Annexin A6 Induces FAK-YAP Activation by Stabilizing β1 Integrin, Enhancing Drug Resistance. *Cancer Res* (2020) 80:3222–35. doi: 10.1158/0008-5472.CAN-19-3803
122. Shen J, Zhai J, You Q, Zhang G, He M, Yao X, et al. Cancer-Associated Fibroblasts-Derived VCAM1 Induced by H. Pylori Infection Facilitates Tumor Invasion in Gastric Cancer. *Oncogene* (2020) 39:2961–74. doi: 10.1038/s41388-020-1197-4
123. Miao L, Qi J, Zhao Q, Wu Q-N, Wei D-L, Wei X-L, et al. Targeting the STING Pathway in Tumor-Associated Macrophages Regulates Innate Immune Sensing of Gastric Cancer Cells. *Theranostics* (2020) 10:498–515. doi: 10.7150/thno.37745
124. Zheng P, Chen L, Yuan X, Luo Q, Liu Y, Xie G, et al. Exosomal Transfer of Tumor-Associated Macrophage-Derived miR-21 Confers Cisplatin Resistance in Gastric Cancer Cells. *J Exp Clin Cancer Res* (2017) 36:53. doi: 10.1186/s13046-017-0528-y
125. Wang H, Chen B, Lin Y, Zhou Y, Li X. Legumain Promotes Gastric Cancer Progression Through Tumor-Associated Macrophages and. *Int J Biol Sci* (2020) 16:172–80. doi: 10.7150/ijbs.36467
126. Sun L, Huang C, Zhu M, Guo S, Gao Q, Wang Q, et al. Gastric Cancer Mesenchymal Stem Cells Regulate PD-L1-CTCF Enhancing Cancer Stem Cell-Like Properties and Tumorigenesis. *Theranostics* (2020) 10:11950–62. doi: 10.7150/thno.49717
127. He W, Liang B, Wang C, Li S, Zhao Y, Huang Q, et al. MSC-Regulated lncRNA MACC1-AS1 Promotes Stemness and Chemoresistance Through Fatty Acid Oxidation in Gastric Cancer. *Oncogene* (2019) 38:4637–54. doi: 10.1038/s41388-019-0747-0
128. Ji R, Zhang B, Zhang X, Xue J, Yuan X, Yan Y, et al. Exosomes Derived From Human Mesenchymal Stem Cells Confer Drug Resistance in Gastric Cancer. *Cell Cycle (Georgetown Tex.)* (2015) 14:2473–83. doi: 10.1080/15384101.2015.1005530
129. Yao H-J, Zhang Y-G, Sun L, Liu Y. The Effect of Hyaluronic Acid Functionalized Carbon Nanotubes Loaded With Salinomycin on Gastric Cancer Stem Cells. *Biomaterials* (2014) 35:9208–23. doi: 10.1016/j.biomaterials.2014.07.033
130. Liang S, Li C, Zhang C, Chen Y, Xu L, Bao C, et al. CD44v6 Monoclonal Antibody-Conjugated Gold Nanostars for Targeted Photoacoustic Imaging and Plasmonic Photothermal Therapy of Gastric Cancer Stem-Like Cells. *Theranostics* (2015) 5:970–84. doi: 10.7150/thno.11632
131. Barat S, Chen X, Cuong Bui K, Bozko P, Götze J, Christgen M, et al. Gamma-Secretase Inhibitor IX (GSI) Impairs Concomitant Activation of Notch and Wnt-Beta-Catenin Pathways in CD44 Gastric Cancer Stem Cells. *Stem Cells Trans Med* (2017) 6:819–29. doi: 10.1002/sctm.16-0335
132. Feng S, Zheng Z, Feng L, Yang L, Chen Z, Lin Y, et al. Proton Pump Inhibitor Pantoprazole Inhibits the Proliferation, Self–Renewal and Chemoresistance of Gastric Cancer Stem Cells *via* the EMT/β–Catenin Pathways. *Oncol Rep* (2016) 36:3207–14. doi: 10.3892/or.2016.5154
133. Yoon C, Park DJ, Schmidt B, Thomas NJ, Lee H-J, Kim TS, et al. CD44 Expression Denotes a Subpopulation of Gastric Cancer Cells in Which Hedgehog Signaling Promotes Chemotherapy Resistance. *Clin Cancer Res* (2014) 20:3974–88. doi: 10.1158/1078-0432.CCR-14-0011
134. Mao J, Fan S, Ma W, Fan P, Wang B, Zhang J, et al. Roles of Wnt/β-Catenin Signaling in the Gastric Cancer Stem Cells Proliferation and Salinomycin Treatment. *Cell Death Dis* (2014) 5:e1039. doi: 10.1038/cddis.2013.515
135. Wang B, Liu J, Ma LN, Xiao HL, Wang YZ, Li Y, et al. Chimeric 5/35 Adenovirus-Mediated Dickkopf-1 Overexpression Suppressed Tumorigenicity of $CD44^+$ Gastric Cancer Cells *via* Attenuating Wnt Signaling. *J Gastroenterol* (2013) 48:798–808. doi: 10.1007/s00535-012-0711-z

Conflict of Interest: The authors declare that the research was conducted in the absence of any commercial or financial relationships that could be construed as a potential conflict of interest.

Publisher's Note: All claims expressed in this article are solely those of the authors and do not necessarily represent those of their affiliated organizations, or those of the publisher, the editors and the reviewers. Any product that may be evaluated in this article, or claim that may be made by its manufacturer, is not guaranteed or endorsed by the publisher.

frontiers in Oncology

CASE REPORT
published: 01 March 2022
doi: 10.3389/fonc.2022.829235

A Metastatic Intrahepatic Cholangiocarcinoma With HPCs Features: Report of a Case

Qiang Fu[1†], Pan Liu[1†], Shangkun Jin[2], Xu Zhang[1], Chuanjiang Liu[1], Mingxing Hu[1,2], Yuzhu Wang[1,2], Hongwei Zhang[1] and Tao Qin[1*]*

[1] Department of Hepato-Biliary-Pancreatic Surgery, Henan Provincial People's Hospital (People's Hospital of Zhengzhou University), Zhengzhou, China, [2] Department of Hepato-Biliary-Pancreatic Surgery, People's Hospital of Henan University, Zhengzhou, China

Intrahepatic cholangiocarcinoma (ICC) is a highly lethal hepatobiliary neoplasm, which originates from the bile ducts proximal to the second-order division. ICC can be anatomically divided into two subtypes: the large duct type (mucin-production ICC, muc-ICC) and the small duct type (mixed-ICC) origins from hepatic progenitor cells (HPCs). The immunoreactivity of S100P and neural cell adhesion molecule (NCAM) are useful biomarkers to distinguish the two subtypes. In this study, we report a difficult-to-diagnose case of metastatic retroperitoneal tumor of occult hepatolithiasis-associated ICC. Besides, this case was both positive for S100P and NCAM, considered as a rare muc-ICC with the HPCs features. Tumor whole exome sequencing detection results by Genetron (China) revealed that there were 41 gene mutations in this patient. The SMAD4-p.His530ThrfsTer47 and KRAS-p.Gly12Val mutation might promote the occurrence and distant metastasis of the tumor.

Keywords: intrahepatic cholangiocarcinoma, muc-ICC, mixed ICC, hepatic progenitor cells, gene mutation

OPEN ACCESS

Edited by:
Jiannan Yao,
Capital Medical University, China

Reviewed by:
Seogsong Jeong,
Seoul National University, South Korea
Evin Iscan,
Dokuz Eylül University, Turkey

****Correspondence:***
Hongwei Zhang
hwzhang666@126.com
Tao Qin
goodfreecn@163.com

[†]These authors have contributed equally to this work and share first authorship

Specialty section:
This article was submitted to Gastrointestinal Cancers: Gastric & Esophageal Cancers, a section of the journal Frontiers in Oncology

Received: *05 December 2021*
Accepted: *27 January 2022*
Published: *01 March 2022*

Citation:
Fu Q, Liu P, Jin S, Zhang X, Liu C, Hu M, Wang Y, Zhang H and Qin T (2022) A Metastatic Intrahepatic Cholangiocarcinoma With HPCs Features: Report of a Case. Front. Oncol. 12:829235. doi: 10.3389/fonc.2022.829235

INTRODUCTION

Intrahepatic cholangiocarcinoma (ICC) has an increasing incidence worldwide and is the second most common primary hepatic malignancy after hepatocellular carcinoma. Cirrhosis, viral hepatitis, obesity-associated liver disease, diabetes, and the diseases leading to hepatobiliary fibrosis, such as primary sclerosing cholangitis, Caroli's disease, hepatolithiasis, and liver fluke infractions, are risk factors for ICC. However, only 50% of ICC patients have identifiable risk factors (1). Surgery is still the only curative treatment for ICC, but only a minority of patients are suitable for surgery, and the current 5-year survival rate is to be only 25%–40% after surgery (2). The main reason for the low surgical resection rate is that ICC cannot be diagnosed in the early stage because ICC patients do not have specific early symptoms. Therefore, most ICC patients are already at the advanced stage when they go to the hospital (3). ICC patients usually present with intrahepatic mass lesions and symptoms such as abdominal pain, weight loss, and jaundice (4). Parts of ICC patients are misdiagnosed as carcinoma of unknown primary, such as hepatocellular carcinoma, lymphoma, and carcinoma of other types. Here, we present a rare case of metastatic ICC with specific pathological findings that is difficult to diagnose.

CASE PRESENTATION

A 63-year-old woman was admitted to our hospital for having intermittent and severe mid-upper abdominal pain, along with the symptoms of back pain, anorexia, and weight loss of 15 kg for 1 month. This patient denied the history of cancer, surgery, smoking, alcohol drinking, illicit drug use, and blood transfusion. There was no similar patient in her family. Her BMI = 17.72 kg/m^2. On physical exam, she was of middle nutrition and had no jaundice. Her abdomen was soft, while an approximately 6 cm hard mass without clear boundaries in mid-upper abdomen was found. The laboratory data revealed that the patient had normal routine blood test, hepatic function, renal function, and coagulation function. The serum levels of carbohydrate antigen 19-9 (CA19-9) (8.01 U/ml), cancer embryonic antigen (CEA) (2.24 ng/ml), CA-125 (19.71 U/ml), CA-242 (1.24 U/ml), alpha-fetoprotein (AFP) (1.39 ng/ml) were all within the normal range. Intraoperative ultrasonography did not detect fatty liver. The abdominal contrast-enhanced computed tomography (CT) scan and CT angiography showed a huge irregular neoplasm located at the retroperitoneum with edge intensifying (**Supplementary Figure 1A**). Furthermore, the left renal vessel and ureter were invaded combined with left uronephrosis (**Supplementary Figures 1B, E**). Besides, there was atrophy of the left hepatic lobe, and choledocholithiasis was accompanied by intra- and extrahepatic bile duct dilatation (**Supplementary Figures 1C, D**). The patient underwent the surgery of retroperitoneal tumor resection, left nephrectomy, splenectomy, left hepatic lobectomy, cholecystectomy, choledocholithotomy, and T tube drainage, which continued about 360 min, and 525 ml of blood was lost. No tumor mass was found in the left hepatic lobe under naked eye, and the retroperitoneal tumor was solid, not encapsulated, whitish in color, and had an irregular margin.

HE Staining and Immunohistochemistry

All specimens were cut into 5-μm sections and stained with hematoxylin and eosin (HE) after fixation. Tissue sections were deparaffinized, subjected to antigen retrieval, and blocked with 5% bovine serum albumin (BSA) in phosphate-buffered saline (PBS) for 30 min. CA19-9, CK19, CK7, neural cell adhesion molecule (NCAM), S100P, CK20, AFP, and GATA-3 primary antibodies were purchased from Abcam Plc (Cambridge, UK). CEA, Muc-1, CK8/18, Ki67, P40, P53, c-kit, Mucin-2, SATB, and Villin primary antibodies were purchased from Cell Signaling Technology (Danvers, MA, USA) and Hep-par1primary antibody was purchased from Affinity Biosciences (Cincinnati, OH, USA). The sections were incubated with primary antibody overnight at 4°C, followed by the appropriate secondary antibody at room temperature for 1 h. All images were captured by confocal microscopy. Hematoxylin and eosin (HE) staining revealed that chronic inflammation of the intrahepatic bile duct and high-grade intraepithelial neoplasia of the glandular epithelium were commonly seen in the left hepatic lobe of 10 different layers (**Supplementary Figure 2A**). The retroperitoneal tumor was epithelial-derived malignancy with necrosis, considered poorly differentiated adenocarcinoma combined with extensive squamousness (**Supplementary Figure 2B**). Besides, scattered mucin-production adenocarcinoma areas (**Supplementary Figure 3A**) and hyperplastic ductular areas, characterized by ductular reaction-like anastomosing glands in fibrous stroma with mild atypia (**Supplementary Figure 3B**), were seen. Clear-cut hepatocellular differentiation was not seen. Tumor cells invaded the left renal hilum, ureter, and peripheral fibrous adipose tissue. Adenocarcinoma tissue is seen in perirenal lymph nodes (1/9), while Group 12/13/16 lymph nodes were negative (0/18). Immunohistochemistry of retroperitoneal tumor was positive for CA19-9, CEA, Muc-1, CK19, CK7, CK8/18, Ki67 (60%), P40, P53 (partial), c-kit, NCAM, and S100P (**Supplementary Figures 4A–L**) and negative for CK20, GATA-3, Mucin-2, SATB, Villin, AFP, and Hep-par1 (**Supplementary Figures 4M–S**).

Tumor Whole Exome Sequencing Detection

After genomic DNA was extracted from the samples, the library was constructed by fragment and targeted capture of the target region. DNA sequencing was performed based on NovaSeq high-throughput sequencing platform. It was revealed that there were 41 gene mutations but no gene rearrangement and no gene copy number variation. The mutational genes included nonsense mutation (ACHE), frame shift mutation (ADAM7, ANXA5, C13orf45, KLRC4, SMAD4, USP32, and VPS13C), missense mutation (ADAMTS17, ADAMTS9, BCOR, CA12, CASZ1, CEACAM21, CECR6, DAB1, DHCR24, DICER1, FAM57B, HIST1H4J, HTR5A, IGDCC4, IRF2BP2, KLHL36, KRAS, LRRC8D, LSS, MEX3B, MGA, MICAL2, OLFML2B, PZP, REXO4, SEMA5B, SH3PXD2A, SH3TC2, SLC25A37, SYNE1, SYNGR3, and ZFHX4) and splicing mutation (KCND2) (**Supplementary Table 1**).

DISCUSSION

The immunohistochemical results of the retroperitoneal tumor of this case indicated that Muc-1, CK7, CK19, and CEA were positive, which suggested that the tumor might originate from the biliary tract system. Extensive sampling by the pathologist and surgical clinicians of the hole left hepatic lobe was proceeded, and an about 0.4 mm local invasion adenoma with malignant transformation was seen at last (**Supplementary Figure 2C**). After a multidisciplinary discussion of the pathologist, oncologist, and surgical clinicians, this case was diagnosed as a hepatolithiasis-associated intrahepatic cholangiocarcinoma (ICC) accompanied by retroperitoneal metastasis. Hepatolithiasis is a major risk factor of ICC (5). Approximately 5.3%–12.9% of hepatolithiasis cases are complicated with ICC (6).The incidence of hepatolithiasis-associated ICC is relatively insidious, and the clinical symptoms are often hepatolithiasis, biliary infection, or hepatatrophia, which are easy to cause clinically missed diagnosis. The surgical resection rate is low, and the overall prognosis is poor. It has been reported that the 5-year postoperative survival rate of hepatobiliary cholangiolithiasis combined with hepatobiliary carcinoma is only 3.0%–18.4% (7).

ICC can be anatomically divided into two subtypes, namely, the large duct type and the small duct type, which have different etiologies, molecular alteration, growth patterns, and clinical behaviors (8).The large duct type iCCA, which originate from large intrahepatic bile duct (such as segmental, area, and septal bile duct) lining of mucin-producing cylindrical cells, resembles extrahepatic cholangiocarcinoma. Thus, this subtype can also be called mucin-production ICC (muc-ICC). On the other hand, the small intrahepatic bile duct, such as interlobular bile duct and ductules, contains hepatic progenitor cells (HPCs), which have the ability of differentiating into hepatocytes and cholangiocytes and causing tumors during the differentiation process. HPCs-derived tumors (mixed-ICC) display varying hepatocytic and/or cholangiocytic differentiation characteristics within the same tumor (9). Even with the presence of diffuse dilation of the left intrahepatic bile duct, the local invasion adenoma in our case was initially considered to be located at the segmental or area bile duct. Because the primary tumor was too small for further immunohistochemical detection of markers of stem/HPCs, we could further analyze the characteristic and origin from the metastatic tumor. As shown in **Supplementary Figures 3A, B**, the immunohistochemistry of mucin-production adenocarcinoma areas was positive for S100P and NCAM, and the ductular areas were also positive for NCAM and S100P (partial). The immunoreactivity of S100P and NCAM represents a useful tool to distinguish mixed-ICC from muc-ICC. S100P expression is only seen in mucin-positive ICC areas in muc-ICC but not in the mixed-ICC, whereas NCAM is only immunoreactive in the hep-dif and ductular areas in mixed-ICC but not in muc-ICC (10, 11). This case was positive both for S100P and NCAM. Combining the local invasion adenoma with malignant transformation most probably located at the segmental or area bile duct, the patient was considered as a rarely particular subtype of muc-ICC with the HPCs features.

Among the mutation genes of this patient, the mutations of SMAD4 and KRAS were reported to be associated with the genesis and invasion of cholangiocarcinoma. The SMAD4-p.His530ThrfsTer47 mutation of this patient leads to the premature generation of a stop codon, which results in the impact of SMAD4. SMAD4 is the central molecule of the TGF-β signal pathway, which is related to the occurrence, development, and metastasis of cancer (12). Loss expression of SMAD4 promotes the transition from stone-containing intrahepatic bile ducts (IHD) to ICC. SMAD4 expression is related to the histological grade, clinical stage, and metastasis of ICC. The loss of SMAD4 expression in metastatic ICCs was significantly more severe compared with non-metastatic ICC (13). Besides, the KRAS-p.Gly12Val mutation ($KRAS^{G12D}$) of this patient, in the conserved G box domain of KRAS protein, results in the activation of KRAS. $KRAS^{G12D}$ activation leads to the development of invasive ICC with low penetrance and long latency. Latency was shortened by combining $KRAS^{G12D}$ activation with heterozygous or homozygous deletion of p53, which also resulted in widespread local and distant metastasis (14). Until now, there are several drugs targeting KRAS in clinical trials for the treatment of cholangiocarcinoma, such as Trametinib, Binimetinib, and Selumetinib.

In conclusion, we here presented a rarely metastatic occult ICC with the stem/PSC features, which is valuable in terms of examining a rare phenomenon of ICC at the molecular level. It is a pity that we cannot assess the systemic metastases for the absence of PET-CT and just rely on the feedback provided by the patient to know the progress of the disease. The SMAD4-p.His530ThrfsTer47 and KRAS-p.Gly12Val mutation of this patient might promote the occurrence and distant metastasis of the tumor.

DATA AVAILABILITY STATEMENT

The original contributions presented in the study are included in the article/**Supplementary Material**. Further inquiries can be directed to the corresponding authors.

ETHICS STATEMENT

Written informed consent was obtained from the individual(s) for the publication of any potentially identifiable images or data included in this article.

AUTHOR CONTRIBUTIONS

CL and SJ were involved in histopathological diagnosis. QF and PL wrote the first draft of the manuscript. TQ and MH were involved in surgery and tissue collection. YW and XZ performed laboratory experiment. TQ and HZ reviewed and edited the manuscript before submission. All authors contributed to the article and approved the submitted version.

FUNDING

The prevalence study was funded by the National Natural Science Foundation of China (31671440).

ACKNOWLEDGMENTS

We thank Dr. Xianwei Zhang, from the Department of Pathology, Henan Provincial People's Hospital Affiliated to Zhengzhou University, Zhengzhou, China, for his generous help.

SUPPLEMENTARY MATERIAL

The Supplementary Material for this article can be found online at: https://www.frontiersin.org/articles/10.3389/fonc.2022.829235/full#supplementary-material

REFERENCES

1. Kelley RK, Bridgewater J, Gores GJ, Zhu AX. Systemic Therapies for Intrahepatic Cholangiocarcinoma. *J Hepatol* (2020) 72:353–63. doi: 10.1016/j.jhep.2019.10.009
2. Mazzaferro V, Gorgen A, Roayaie S, Droz Dit Busset M, Sapisochin G. Liver Resection and Transplantation for Intrahepatic Cholangiocarcinoma. *J Hepatol* (2020) 72:364–77. doi: 10.1016/j.jhep.2019.11.020
3. Zhang XF, Xue F, Dong DH, Weiss M, Popescu I, Marques HP, et al. Number and Station of Lymph Node Metastasis After Curative-Intent Resection of Intrahepatic Cholangiocarcinoma Impact Prognosis. *Ann Surg* (2021) 274: e1187–95. doi: 10.1097/SLA.0000000000003788
4. Bridgewater J, Galle PR, Khan SA, Llovet JM, Park JW, Patel T, et al. Guidelines for the Diagnosis and Management of Intrahepatic Cholangiocarcinoma. *J Hepatol* (2014) 60:1268–89. doi: 10.1016/j.jhep.2014.01.021
5. Nagtegaal ID, Odze RD, Klimstra D, Paradis V, Rugge M, Schirmacher P, et al. The 2019 WHO Classification of Tumours of the Digestive System. *Histopathology* (2020) 76(2):182–8. doi: 10.1111/his.13975
6. Nishikawa Y, Hirata A, Uza. Hepatobiliary N. And Pancreatic: Intrahepatic Cholangiocarcinoma With Intratumoral Calcification Mimicking Hepatolithiasis. *J Gastroenterol Hepatol* (2019) 34:2060. doi: 10.1111/jgh.14726
7. Choi S-B, Kim K-S, Choi J-Y, Park S-W, Choi J-S, Lee W-J, et al. The Prognosis and Survival Outcome of Intrahepatic Cholangiocarcinoma Following Surgical Resection: Association of Lymph Node Metastasis and Lymph Node Dissection With Survival. *Ann Surg Oncol* (2009) 16:3048–56. doi: 10.1245/s10434-009-0631-1
8. Nagtegaal ID, Odze RD, Klimstra D, Paradis V, Rugge M, Schirmacher P, et al. WHO Classification of Tumours Editorial Board. The 2019 WHO Classification of Tumours of the Digestive System. *Histopathology* (2020) 76:182–8. doi: 10.1111/his.13975
9. Van Haele M, Roskams T. Hepatic Progenitor Cells: An Update. *Gastroenterol Clin North Am* (2017) 46:409–20. doi: 10.1016/j.gtc.2017.01.011
10. Komuta M, Spee B, Vander Borght S, De Vos R, Verslype C, Aerts R, et al. Clinicopathological Study on Cholangiolocellular Carcinoma Suggesting Hepatic Progenitor Cell Origin. *Hepatology* (2008) 47:1544–56. doi: 10.1002/hep.22238
11. Komuta M, Govaere O, Vandecaveye V, Akiba J, Van Steenbergen W, Verslype C, et al. Histological Diversity in Cholangiocellular Carcinoma Reflects the Different Cholangiocyte Phenotypes. *Hepatology* (2012) 55:1876–88. doi: 10.1002/hep.25595
12. David CJ, Huang Y-H, Chen MO, Su J, Zou Y, Bardeesy N, et al. TGF-β Tumor Suppression Through a Lethal EMT. *Cell* (2016) 164:1015–30. doi: 10.1016/j.cell.2016.01.009
13. Yan X-q, Zhang W, Zhang B-x, Liang H-f, Zhang W-g, Chen X-p. Inactivation of Smad4 is a Prognostic Factor in Intrahepatic Cholangiocarcinoma. *Chin Med J (Engl)* (2013) 126:3039–43. doi: 10.3760/cma.j.issn.0366-6999.20121235
14. O'Dell MR, Huang JL, Whitney-Miller CL, Deshpande V, Rothberg P, Grose V, et al. Kras(G12D) and P53 Mutation Cause Primary Intrahepatic Cholangiocarcinoma. *Cancer Res* (2012) 72:1557–67. doi: 10.1158/0008-5472.CAN-11-3596

Conflict of Interest: The authors declare that the research was conducted in the absence of any commercial or financial relationships that could be construed as a potential conflict of interest.

frontiers in Oncology

ORIGINAL RESEARCH
published: 08 March 2022
doi: 10.3389/fonc.2022.825783

Upregulation of MTA1 in Colon Cancer Drives A CD8$^+$ T Cell-Rich But Classical Macrophage-Lacking Immunosuppressive Tumor Microenvironment

Yantong Zhou[1], Peng Nan[1], Chunxiao Li[1], Hongnan Mo[2], Ying Zhang[3], Haijuan Wang[4], Dongkui Xu[5], Fei Ma[2]* and Haili Qian[1]**

[1] State Key Laboratory of Molecular Oncology, National Cancer Center/National Clinical Research Center for Cancer/Cancer Hospital, Chinese Academy of Medical Sciences and Peking Union Medical College, Beijing, China, [2] Department of Medical Oncology, National Cancer Center/National Clinical Research Center for Cancer/Cancer Hospital, Chinese Academy of Medical Sciences and Peking Union Medical College, Beijing, China, [3] Department of Gynecological Minimal Invasive Center, Beijing Obstetrics and Gynecology Hospital, Capital Medical University, Beijing Maternal and Child Health Care Hospital, Beijing, China, [4] The Editorial Office of Infectious Diseases & Immunity, Chinese Medical Journals Publishing House Co., Ltd, Beijing, China, [5] Department of VIP, National Cancer Center/National Clinical Research Center for Cancer/Cancer Hospital, Chinese Academy of Medical Sciences and Peking Union Medical College, Beijing, China

Background: The MTA1 protein encoded by metastasis-associated protein 1 (MTA1) is a key component of the ATP-dependent nucleosome remodeling and deacetylase (NuRD) complex, which is widely upregulated in cancers. MTA1 extensively affects downstream gene expression by participating in chromatin remodeling. Although it was defined as a metastasis-associated gene in first reports and metastasis is a process prominently affected by the tumor microenvironment, whether it affects the microenvironment has not been investigated. In our study, we elucidated the regulatory effect of MTA1 on tumor-associated macrophages (TAMs) and how this regulation affects the antitumor effect of cytotoxic T lymphocytes (CTLs) in the tumor microenvironment of colorectal cancer.

Methods: We detected the cytokines affected by MTA1 expression *via* a cytokine antibody array in control HCT116 cells and HCT116 cells overexpressing MTA1. Multiplex IHC staining was conducted on a colorectal cancer tissue array from our cancer cohort. Flow cytometry (FCM) was performed to explore the polarization of macrophages in the coculture system and the antitumor killing effect of CTLs in the coculture system. Bioinformatics analysis was conducted to analyze the Cancer Genome Atlas (TCGA) colorectal cancer cohort and single-cell RNA-seq data to assess the immune infiltration status of the TCGA colorectal cancer cohort and the functions of myeloid cells.

Results: MTA1 upregulation in colorectal cancer was found to drive an immunosuppressive tumor microenvironment. In the tumor microenvironment of MTA1-upregulated colorectal cancer, although CD8$^+$ T cells were significantly enriched, macrophages were significantly decreased, which impaired the CTL effect of the CD8$^+$

OPEN ACCESS

Edited by:
Nathaniel Weygant, Fujian University of Traditional Chinese Medicine, China

Reviewed by:
Youping Deng, Rush University Medical Center, United States
Zhang Xiaotian, Peking University Cancer Hospital, China
Rathindranath Baral, Chittaranjan National Cancer Institute, India

****Correspondence:***
Haili Qian
qianhaili001@163.com
Fei Ma
drmafei@126.com
Dongkui Xu
13691583382@163.com

Specialty section:
This article was submitted to Gastrointestinal Cancers: Colorectal Cancer, a section of the journal Frontiers in Oncology

Received: *30 November 2021*
Accepted: *28 January 2022*
Published: *08 March 2022*

Citation:
Zhou Y, Nan P, Li C, Mo H, Zhang Y, Wang H, Xu D, Ma F and Qian H (2022) Upregulation of MTA1 in Colon Cancer Drives A CD8$^+$ T Cell-Rich But Classical Macrophage-Lacking Immunosuppressive Tumor Microenvironment. Front. Oncol. 12:825783. doi: 10.3389/fonc.2022.825783

T cells on tumor cells. Moreover, upregulated MTA1 in tumor cells significantly induced infiltrated macrophages into tumor-associated macrophage phenotypes and further weakened the cytotoxic effect of $CD8^+$ T cells.

Conclusion: Upregulation of MTA1 in colorectal cancer drives an immunosuppressive tumor microenvironment by decreasing the microphages from the tumor and inducing the residual macrophages into tumor-associated microphage phenotypes to block the activation of the killing CTL, which contributes to cancer progression.

Keywords: MTA1, immune infiltration, tumor associated macrophage (TAM), tumor microenvironment, colorectal cancer

INTRODUCTION

With the development of cancer research, the concept of the tumor microenvironment and its importance in tumor progression and tumor treatment is increasingly being recognized (1). In the process of cancer development, all types of cells and products in the tumor microenvironment influence tumorigenesis and tumor progression. The composition and functional status of immune cells in the tumor microenvironment are the focus of studies in both fields of basic immunotherapy research and clinical application. Accordingly, immunosignature-based stratification of patients to optimize the treatment response is becoming central to cancer immunotherapy. Preliminarily, the tumor immune microenvironment has been defined as cold versus hot tumors based on their CTL infiltration. An immunologically cold microenvironment is primarily associated with the exclusion of cytotoxic $CD8^+$ T cells in tumors (2). However, hot tumors rich in infiltrated $CD8^+$ T cells may still fail to respond to the immune checkpoint blockade (ICB) if these cells are dysfunctional or become exhausted (3). An inflamed but still immunosuppressive microenvironment can be potentially fueled by various myeloid cells, particularly tumor-associated macrophages (TAMs) (4, 5). Unfortunately, drivers of these different immunomodulatory scenarios are not well defined. Therefore, it is critical to define the mechanisms of immune aberrance in terms of not only the accounts but also the functions of immune cells in the tumor microenvironment to design further optimized cancer immunotherapy strategies.

MTA1, as an important component of the nucleosome-remodeling complex (6), widely participates in gene expression regulation. MTA1 was first discovered as a gene related to tumor metastasis in breast cancer, and more of its biological function was revealed in subsequent studies. It widely regulates the biological behaviors of tumor cells. In our investigation, we found clues about MTA1 involved in the regulation of the immune state in the tumor microenvironment and contributed to an important regulatory link between macrophages and $CD8^+$ T cells, which has been known as a core process in tumor microenvironment regulation but is still poorly understood.

In the current study, we sought to investigate the influence of MTA1 overexpression on the antitumor immune response. Based on the clue that MTA1 has been associated with inflammation in colorectal cancer, we primarily tried to explore how overexpressed MTA1 influences the immune infiltration states and immune response in the tumor microenvironment of a TCGA colorectal cancer cohort. Then, we analyzed the function of macrophages modulated by MTA1-overexpressing colorectal cancer cells. To determine their relevance to overexpressed MTA1, a multiplex immunohistochemistry (m-IHC) panel consisting of surface and intracellular markers was designed to perform on clinical colorectal cancer samples. Using this panel, we described predominant TAM populations, T cell populations and B cell populations characterized by specific markers on individual cells. Finally, we performed a cytotoxicity assay to explore the influence of MTA1 overexpression on the antitumor immune response. Based on the above experimental results, we set out to illustrate how MTA1 affected the interactions between cancer cells, macrophages, and cytotoxic T lymphocytes to contribute to an immunosuppressive microenvironment.

MATERIALS AND METHODS

Cell Culture

Mouse colorectal cancer CT26 cells and human colorectal cancer HCT116 cells were used as models to express high and low MTA1. RAW264.7 cells were used as an *in vitro* model of murine macrophages. Mouse spleen lymphocytes were isolated to perform an *in vitro* cytotoxicity assay for T cell functions. HCT116 cells and RAW264.7 cells were cultured in Dulbecco's modified Eagle's medium (DMEM; CELL Technologies) with 100 μg/ml penicillin/streptomycin supplemented with 10% fetal bovine serum (FBS; Gibco). CT26 cells were cultured in Roswell Park Memorial Institute (RPMI-1640; CELL Technologies) supplemented with 100 μg/ml penicillin/streptomycin and 10% fetal bovine serum (FBS; Gibco).

Study Cohort

The Molecular Analysis of Colorectal Cancer (CRC) cohort consisted of 180 colorectal cancer patients from the Cancer Hospital, Chinese Academy of Medical Sciences. Written informed consent was obtained from all patients prior to sample collection. All procedures were ethically approved by The Independent Ethics Committee of Cancer Hospital, Chinese Academy of Medical Sciences.

Multiplex IHC Staining Protocol

An Opal 7-color kit (PANOVUE) was used for multiplex IHC. Four micrometers of FFPE sections were dewaxed and rehydrated. In the first round, antigen was retrieved with a microwave oven (EDTA pH 8.0) at 70% power for 15 min (Galanz, G80F23CN2P-BM1). Slides were cooled to room temperature (RT) and washed with PBST/0.5% Tween (3 times, 5 min). Slides were washed and blocked with goat serum blocking buffer (zsbio) for 10 min. Primary antibody was incubated at RT for 1 h or at 4 °C overnight. Slides were washed, and an HRP-conjugated secondary antibody was incubated at RT for 10 min. TSA dye (1:100) was applied for 10 min after washing. These procedures were repeated five more times using the following antibodies: CD8a (Cell Signaling Technology, 1:500), CD4 (zsbio, ZA-0519, 1:1), MTA1 (Abcam, AB71153, 1:1,000), CD20 (Cell Signaling Technology, #3958, 1:200), CD163 (Abcam, ab182422, 1:200), CD206 (Abcam, ab64693, 1:500), CD86 (Abcam, ab269587, 1:200), CD68 (Abcam, ab955, 1:1,000), and PD-L1 (Cell Signaling Technology, E1L3N, 1:200).

Multiplex IHC Imaging and Analysis

Stained tissue arrays were imaged using a PerkinElmer Vectra Polaris microscope. Whole slide scans were performed using the ×20 objective lens. ROIs were selected in Phenochart (PerkinElmer) based on the images previously captured on the whole slide scan. For selecting ROIs, 2 × 2 core stamps were used. The image analysis was performed in inForm2.2.4 (PerkinElmer). Tissue component segmentation was conducted to label tumor tissue (α-SMA) and stromal tissue (α-SMA+) regions. Cell phenotyping was performed using previously reported markers (CD8, CD4, CD20, CD163, CD206, CD86, CD68). The density of cells in each tissue type was calculated by normalizing the cell counts from all images by the total area.

Quantification of MTA1-Associated Secretion

HCT116 cells were incubated in DMEM with 10% FBS before collection, and MTA1-associated secretion was estimated by cytokine antibody array (CAA) following the manufacturer's instructions.

Coculture System

CT26–MTA1-knockdown, -overexpressing or control cells (2×10^5) were seeded in 6-well culture dishes for 48 h. RAW264.7 cells were then seeded together with these CT26 cell populations at a 1:2 ratio in RMPI medium with 100 μg/ml penicillin/streptomycin (Gibco) containing 10% heat-inactivated FBS (Gibco) and 200 nM glutamine. After 48 h, cells were trypsinized and then underwent flow cytometry assay or qRT–PCR assay.

RNA Extraction and qRT–PCR

Total RNA was extracted and purified from cell pellets using an RNeasy Mini-Kit (Qiagen) following the manufacturer's instructions. The RNA concentration was determined by a NanoDrop Spectrophotometer ND-1000 (NanoDrop Biotechnologies). Total RNA (1–2 μg) was retrotranscribed into cDNA using a High-Capacity cDNA Reverse Transcriptase Kit (Thermo Fisher Scientific) according to the manufacturer's protocol. Then, 20 ng of the total cDNA was subjected to qRT–PCR (at an annealing temperature of 60°C) using Power SYBR Green PCR Master Mix (TAKARA). Assays were performed in triplicate on a QuantStudio 5 Flex Real-Time PCR System (Applied Biosystems). The forward and reverse primer sequences were as follows: Arg-1(forward: 5′- CCACAGTC TGGCAGTTGGAAG; reverse: 5′- GGTTGTCAGGGG AGTGTTGATG); Ym-1 (forward: 5′- CCCTTCTCATCT GCATCTCC; reverse: 5′- AGTAGCAGTCATCCCAGCA); IL-6 (forward: 5′- GGACCAAGACCATCCAATTC; reverse: 5′- ACCACAGTGAGGAATGTCCA); Saa3 (forward: 5′- GCC TGGGCTGCTAAAGTCAT; reverse: 5′- TGCTCCAT GTCCCGTGAAC); Gapdh (forward: 5′- AATGTGTCC GTCGTGGATCTGA; reverse: 5′- GATGCCTGCTTCA CCACCTTCT); TNF-α (forward: 5′- AGCCCACGTCGTAG CAAACCAC; reverse: 5′- AGGTACAACCCATCGGCTGGCA); CD206 (forward: 5′- GGCAGGATCTTGGCAACCTAGTA; reverse: 5′- GTTTGGATCGGCACACAAAGTC); iNOS (forward: 5′- TCCTGGACATTACGACCCCT; reverse: 5′- CTCTGAGGGCTGACACAAGG);

T Cell Cytotoxicity Assay

CT26–MTA1-knockdown, -overexpressing or control cells (2×10^5) were seeded in 24-well culture dishes for 48 h. RAW264.7 cells were then seeded together with these CT26 cell populations at a 1:2 ratio in RPMI medium with 100 μg ml^{-1} penicillin/streptomycin (Gibco) containing 10% heat-inactivated FBS (Gibco) and 200 nM glutamine. After 48 h, 4×10^5 CD3- and IL-2-activated T effector cells were added to the culture for an additional 6 h. Cells were trypsinized and stained with Annexin-V, as described below, and analyzed by flow cytometry. Before staining with annexin V, CD45 (Invitrogen, 12-0451-81, 0.015 μg/100 μl) was stained to identify macrophages and lymphocytes from the tumor cells. FSC-A and SSC-A, representing volume and granularity, were used to distinguish macrophages from lymphocytes. In addition, CD11b (Invitrogen, 25-0112-81, 0.06 μg/100 μl) was used to identify macrophages in the coculture system.

Immune Profiling by Flow Cytometry

For the coculture experiment for cell surface staining, 1×10^6 cells were incubated with anti-Fc receptor blocking antibody and stained with the indicated antibodies in PBS, 2% bovine serum albumin and 5 mM EDTA for 30 min on ice. All flow cytometry was performed on a BD flow cytometer (BD FACS ARIA II). Analysis of flow cytometry data was performed using FlowJo_v10.6.2. Flow cytometry antibodies were used as follows: CD45 (Invitrogen, 12-0451-81, 0.015 μg/100 μl), CD11b (Invitrogen, 25-0112-81, 0.06 μg/100 μl), PD-L1 (Biolegend, 124307, 1:50), PD-1 (Biolegend, 114117, 1:50), Ifng (Biolegend, 505809, 1:50), Tigit (Biolegend, 142105, 1:50), CD206 (Abcam, ab64693, 1 μg/ml), CD86 (Abcam, ab269587, 1:50), and CD163 (Abcam, ab182422, 1:60). Cells were

discriminated using the following combinations of cell markers after gating on single cells (discriminated by forward scatter area and forward scatter width). CD45 was labeled to select macrophages and T cells. FSC-A, SSC-A and CD11b were labeled to distinguish T cells and macrophages. CD86, CD163 and CD206 were labeled to detect the polarization phenotypes of macrophages.

Bioinformatics Analysis: GSVA and Score Generation

For gene set enrichment analysis (GSEA), we used the Broad Institute Molecular Signatures Database (MSigDB) (https://www.gsea-msigdb.org/gsea/msigdb) to obtain gene annotations of the pathways of interest as the background. In addition, we mapped the collected genes to the background. The R package clusterProfiler (Version 3.14.3) was used for enrichment analysis to obtain the results of gene set enrichment. The minimum gene set included 5 genes, the maximum gene set included 5,000 genes, and a P-value <0.05 and FDR <0.01 were considered statistically significant.

For differential expression analysis, we used the R package limma (version 3.40.6) to obtain differentially expressed genes between groups. For gene set variation analysis (GSVA), we used the R package GSVA (version 1.40.1) (7). Based on RNA expression profiling, we used the Broad Institute Molecular Signatures Database (MSigDB) (https://www.gsea-msigdb.org/gsea/msigdb) to obtain gene annotations of the pathways of interest as the background to score pathways and molecular mechanisms in each sample.

For survival analysis, we used the R package Survival after integrating overall survival time, survival state and expression data of MTA1. In addition, the significance was assessed by COX (8).

Single-cell RNA-seq data were extracted from the Gene Expression Omnibus (accession code GSE132465), comprising 63,687 cells from 23 patients with colorectal cancer, using the provided normalization and cell labels (9). Bulk RNA-seq data of the TCGA colorectal cancer cohort were downloaded from the cBioPortal (http://www.cbioportal.org/).

Statistical Analysis

Two-sided *p*-values of less than 0.05 were considered statistically significant (ns, not significant; *p <0.05; **p <0.01; ***p <0.001; ****p <0.0001). All statistical analyses were performed in GraphPad 8.3.

RESULTS

The High Level of MTA1 Expression in the TCGA Colorectal Cancer Cohort was Significantly Associated With the Immunosuppressive Signature

MTA1 is generally overexpressed in tumors, and also in colorectal cancer (**Figure 1A**), and the MTA1 expression level is negatively correlated with the overall survival of the patients in the colorectal cancer cohort (**Figure 1B**). To explore the effect of MTA1 expression on colorectal cancer immune cell infiltration in the tumor microenvironment, we used the TIMER 2.0 (10) database to evaluate the correlation between the MTA1 expression level and immune cell infiltration score in the colorectal cancer cohort of the TCGA (The Cancer Genome Atlas, TCGA) database. Among the results derived from various immune infiltration evaluation algorithms, the expression level of MTA1 in colorectal cancer was significantly positively correlated with the level of $CD8^+$ T cell infiltration and negatively correlated with macrophage infiltration (**Figure 1C**). To further evaluate the influence of the MTA1 expression level on the status of the immune response in colorectal cancer, we used ssGSVA to evaluate the innate immunomodulation enrichment score and adaptive immunomodulation enrichment score of each colorectal cancer patient cohort in the TCGA database. The results showed that colorectal cancer patients with high levels of MTA1 expression tended to be enriched with lower immunomodulation enrichment scores, which reflects an immunosuppressive status in their tumor tissues (**Figure 1D**). Gene set enrichment analysis of the top 500 MTA1 coexpression genes analyzed by the cluster profiler revealed immune biological processes at the top of the list, suggesting that MTA1 may be immune signature-related in colorectal cancer. In the results derived from the Gene Ontology (GO, **Figure 1E**, left) database and the Kyoto Encyclopedia of Genes and Genomes (KEGG, **Figure 1E**, right) database, the MTA1 expression level may significantly affect the NF-κB pathway and the NOD-like receptor signaling pathway (**Figure 1E**). The immune cell infiltration status and immune response status were based on the recruitment and activation of immune cells. In the tumor microenvironment, the recruitment and activation of immune cells rely mostly on cytokines and chemokines. We then analyzed the correlation between the levels of chemokines and MTA1 in colorectal cancer cell lines in the Cancer Cell Line Encyclopedia (CCLE) database, and there was a significant negative correlation between the levels of MTA1 and the panel of chemokines. Most of the chemokines were downregulated with MTA1 overexpression in colorectal cancer cell lines (**Figure 1F**).

We then performed a more detailed deconvolution of 22 immune cell types with CIBERSORTx (11), which showed significantly enriched scores for $CD8^+$ T cells, memory resting $CD4^+$ T cells, activated NK cells, DC cells, mast cells, and regulatory T cells (Treg cells) and, more notably, for macrophages in the MTA1-high group versus the MTA1-low group of colorectal cancers (**Figure 1G**). Among the significantly affected immune cells, direct tumor killers, $CD8^+$ T cells and NK cells were enhanced with MTA1 upregulation. The immune cells supporting the effect of cytotoxic cells were generally decreased with MTA1 upregulation.

The differentially expressed gene sets between patient populations within the top and bottom 25th percentiles of the MTA1 expression level mainly fell in the family of chemokines (**Figure 1H**, left), common immunostimulators (**Figure 1H**, middle), and immunosuppressors (**Figure 1H**, right), as shown. Thus, we found that in MTA1-upregulated colorectal

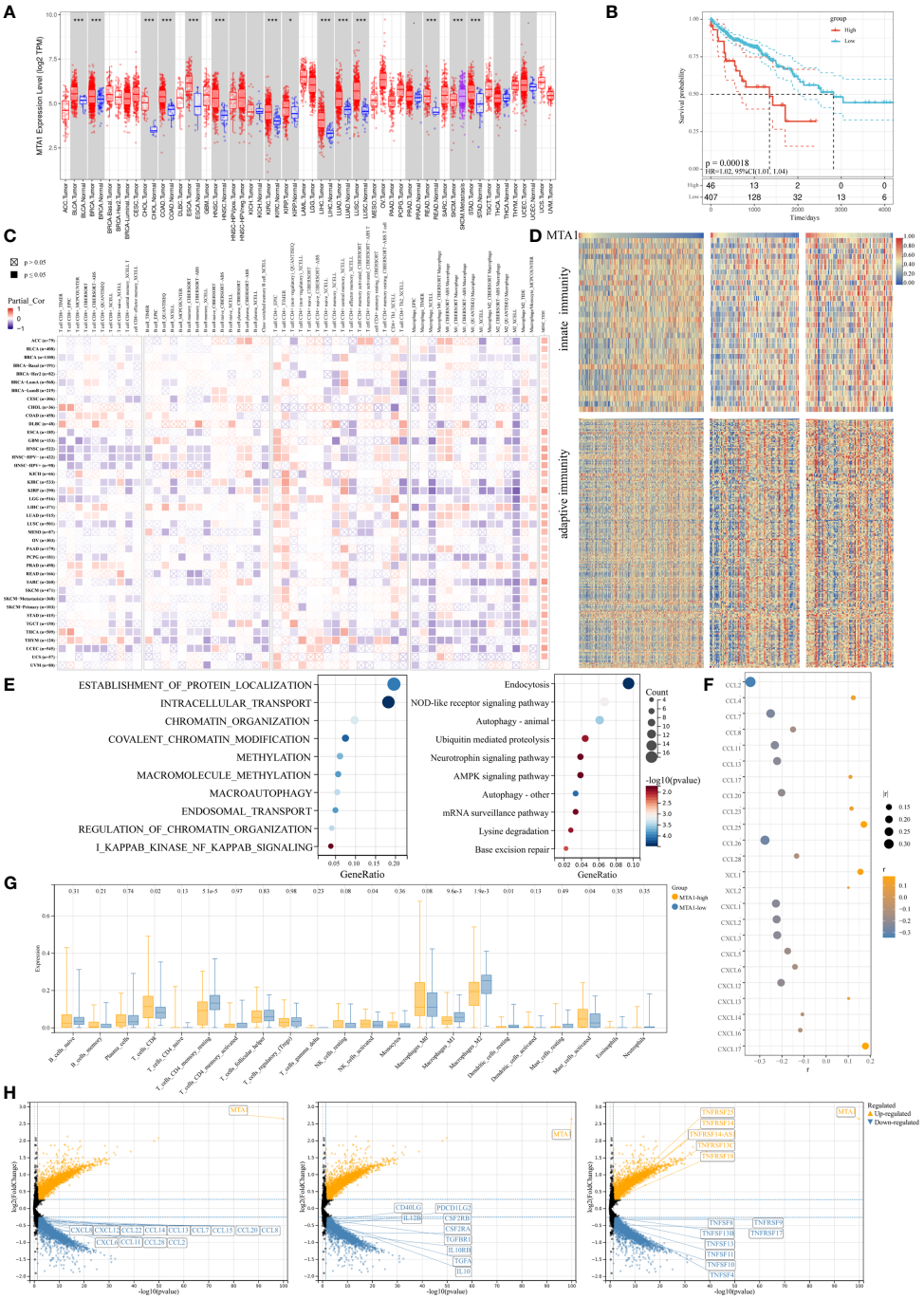

FIGURE 1 | MTA1-driven immunosuppressive tumor microenvironment in colorectal cancer. **(A)** Pan-cancer expressional characterization of MTA1 in tumor and normal tissues from the TCGA database. **(B)** Kaplan–Meier curves of overall survival of patients with MTA1-high and MTA1-low tumors. The MTA1-high group included patients whose tumors expressed MTA1 mRNA at the level of the upper 25%. The MTA1-low group included patients whose tumors expressed MTA1 mRNA at the level of the lower bottom 25%. COAD and colon adenocarcinoma were defined in the TCGA dataset. P-values correspond to two-sided log-rank analyses. **(C)** Immune infiltration based on bulk RNA-seq transcriptome data from the TCGA database assessed by different algorithms. **(D)** Heatmap representing the correlation between MTA1 expression level and enrichment score defined by GSVA of signaling cascades from MSigDB related to immunomodulation in the TCGA colon adenocarcinoma cohort. **(E)** Gene set enrichment of the top 500 MTA1 coexpression genes (p-adjust <0.05; cluster Profiler). **(F)** Pearson correlation between the expression of MTA1 and chemokines in colon cancer cell lines in the CCLE database (p-value <0.05). **(G)** Enrichments of the indicated immune cell populations calculated *via* the Cibersortx algorithm in MTA1-high versus MTA1-low populations (low: n = 92; high: n = 87; unpaired two-tailed t test). **(H)** Differentially expressed gene (DEG) in MTA1-high versus MTA1-low populations (low: n = 128; high: n = 128; limma). The meaning of symbols was provided in Statistical Analysis.

cancer, immune factors were generally downregulated. Altogether, these above data suggest that the expression of MTA1 significantly affects the immune status in colorectal cancers.

Colorectal Cancer Cells Expressing High Levels of MTA1 Downregulate the Expression of Cytokines Recruiting Monocytes and Macrophages

We found that chemokines were mostly downregulated in the MTA1-high group, among which CCL2 was one of the most prominent chemokines. The results derived from CCLE database analysis also displayed a significant difference in the expression of CCL2 between tumor cells with high or low MTA1 levels. Solid tumors are continuously seeded by blood monocytes to sustain large intratumoral macrophage populations (12), and monocyte recruitment to the tumor bed is dependent on the CCL2–CCR2 axis (13–16). The downregulation of CCL2 in MTA1-overexpressing colorectal cancer impaired the recruitment of monocytes and finally formed macrophages with a relatively decreased tumor microenvironment.

To confirm the results derived from the TCGA COAD cohort, we performed a cytokine antibody array to detect cytokine secretion in HCT116 human colon cancer cells of the control group and MTA1-overexpressing group (**Figure 2A**). Consistent with the results derived from bioinformatic analysis, CCL2, CCL7, CCL20, and CXCL12 were all downregulated in MTA1-overexpressing cells. In particular, the downregulation of CCL2 was significantly associated with the absence of macrophages in the MTA1-high tumor group. In addition to the downregulation of cytokines, the inflammatory stimulators IL-6 and SAA3P were also downregulated in MTA1-overexpressing CT26 mouse colon cancer cells (**Figure 2B**). Gene set enrichment analysis was performed to analyze the differentially expressed genes in the MTA1-knockdown HCT116 cells versus the control HCT116 cells, and the NF-κB pathway was also enriched, as shown by the TCGA results (**Figure 2C**).

To illustrate the effect of MTA1 expression in cancer cells on the function of macrophages, we analyzed single-cell RNA-seq data from the GEO database. In this analysis, tumor cells, DCs and macrophages were the main cell types of concern. We aimed to explore how MTA1-overexpressing tumors affected the function of DCs and macrophages; therefore, we divided the samples into the MTA1-high group and the MTA1-low group based on the MTA1 expression level in tumor cells. Then, we assessed the enrichment score of antigen presentation-associated pathways in DCs and macrophages by the GSVA algorithm. Finally, we compared the enrichment score of antigen presentation-associated pathways in the MTA1-high group with the MTA1-low group. The results revealed a significant downregulation of antigen presentation-associated pathways in the MTA1-high group (**Figure 2D**). In addition, we found that markers of M2-like markers for tumor-associated macrophages were significantly upregulated in macrophages in the MTA1-high samples (**Figure 2E**) (17, 18).

The preliminary analysis of colon cancer cells and single-cell RNA-seq data revealed that high-level MTA1 tends to transform the function and quantity of macrophages into an immunosuppressive state.

Higher MTA1 Expression in Colorectal Cancer was Linked to Lower Macrophage Density and Higher Density of CD8$^+$ T Populations

To investigate the immune landscape within colorectal cancer, tissue arrays from 180 patients were prepared from paraffin-embedded (FFPE) tumor samples (**Supplementary Table 1**; see *Materials and Methods* section). A set of H&E-stained tissue sections was reviewed by an anatomical pathologist (CM) to identify tumor (T) and nontumor normal (N) regions, which we referred to as regions of interest (ROIs) (**Figure 3A**; see *Materials and Methods*). The serially sectioned tissue arrays were stained with the m-IHC panel (**Figure 3B**, HE) to distinguish ROIs. A supervised image analysis system (inForm33) was used to identify every single cell by the positive index of DAPI (**Figure 3B**) and to segment each image into tumor areas (α-SMA−), nontumor (α-SMA+) areas and blank areas (**Figure 3B**). In addition, cell phenotyping data were obtained based on the patterns of marker expression (**Figures 3C–E**).

Macrophages in the tumor microenvironment are roughly classified into three populations: tumor-associated macrophages (TAMs) derived from recruited monocytes, tissue-resident macrophages and myeloid-derived suppressor cells (MDSCs). TAMs are the most abundant population in the tumor microenvironment. The polarization status of macrophages is roughly classified as classically activated M1 and alternatively activated M2. Classically activated M1 subtypes are recognized as proinflammatory and express markers such as MHC II, CD68, CD80, CD86 and INOS (19). Alternatively, activated M2 subtypes are recognized as anti-inflammatory and express markers, such as CD206, CD163 and Arg-1. The markers expressed by subtypes displayed differential metabolizing status. CD206 is a marker of glutamine metabolism (20), CD163 is a marker of iron metabolism (21), and ARG1 is associated with tumor-derived lactic acid (22). Therefore, three macrophage markers were analyzed at the single-cell level, and three typical populations were characterized and validated (**Figure 3D**). CD68 positivity was used as the criterion to identify macrophages (**Figure 3D**). Macrophages were further subdivided based on the positivity and relative intensity of other markers. M1-like TAM populations were identified by the CD163$^-$/CD206$^-$/CD86$^+$ phenotype. M2-like TAM populations were identified by the presence of CD163$^+$ or CD206$^+$ (23).

We also stained CD8, CD4 and CD20 to monitor the infiltration of CD8$^+$ T cells, CD4$^+$ T cells and B cells (**Figure 3E**). The results showed that MTA1 expression was significantly negatively correlated with the infiltration density of CD68$^+$/CD86$^+$ macrophages, while it was significantly positively correlated with the infiltration of CD8$^+$ T cells and CD68$^+$/CD206$^+$ macrophages. In addition, we found a significant correlation between CD4$^+$ T cell infiltration density and CD20$^+$ B cell infiltration density in the clinical colorectal cancer cohort (**Figure 3F**). Although the infiltration of CD4$^+$ T

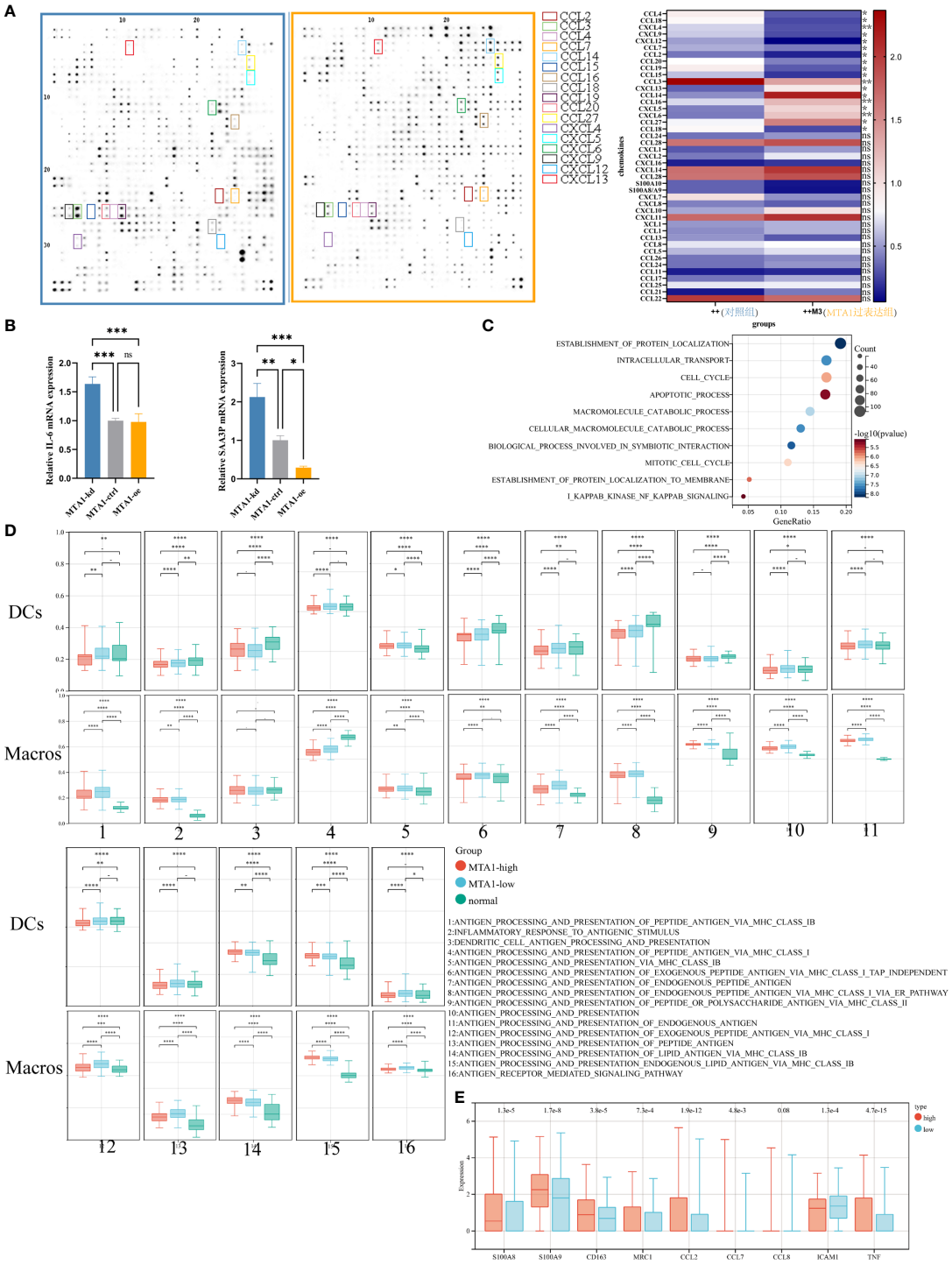

FIGURE 2 | MTA1-driven immunosuppressive secretome and educated myeloid cells in colorectal cancer. **(A)** Expressional characterization of chemokines in MTA1-overexpressing and control HCT116 human colorectal cancer cells. **(B)** qRT–PCR detected the expression of cytokines, the inflammation stimulators IL-6 and SAA3P, in MTA1-knockdown, MTA1-overexpressing and control CT26 mouse colorectal cancer cells. **(C)** Gene set enrichment analysis of differentially expressed genes between MTA1-knockdown and control HCT116 cells. **(D)** Antigen presentation-associated gene set enrichment scores of dendritic cells (DCs) and macrophages (Macros) in the MTA1-high tumor group, MTA1-low tumor group and normal tissue group. The expression profiles of single DCs or macrophages were used to perform GSVA. **(E)** Tumor-associated macrophage expressional features of macrophages in the MTA1-high tumor group versus the MTA1-low tumor group. The expression profiles of single macrophages were used to perform differential analysis. The meaning of symbols was provided in Statistical Analysis.

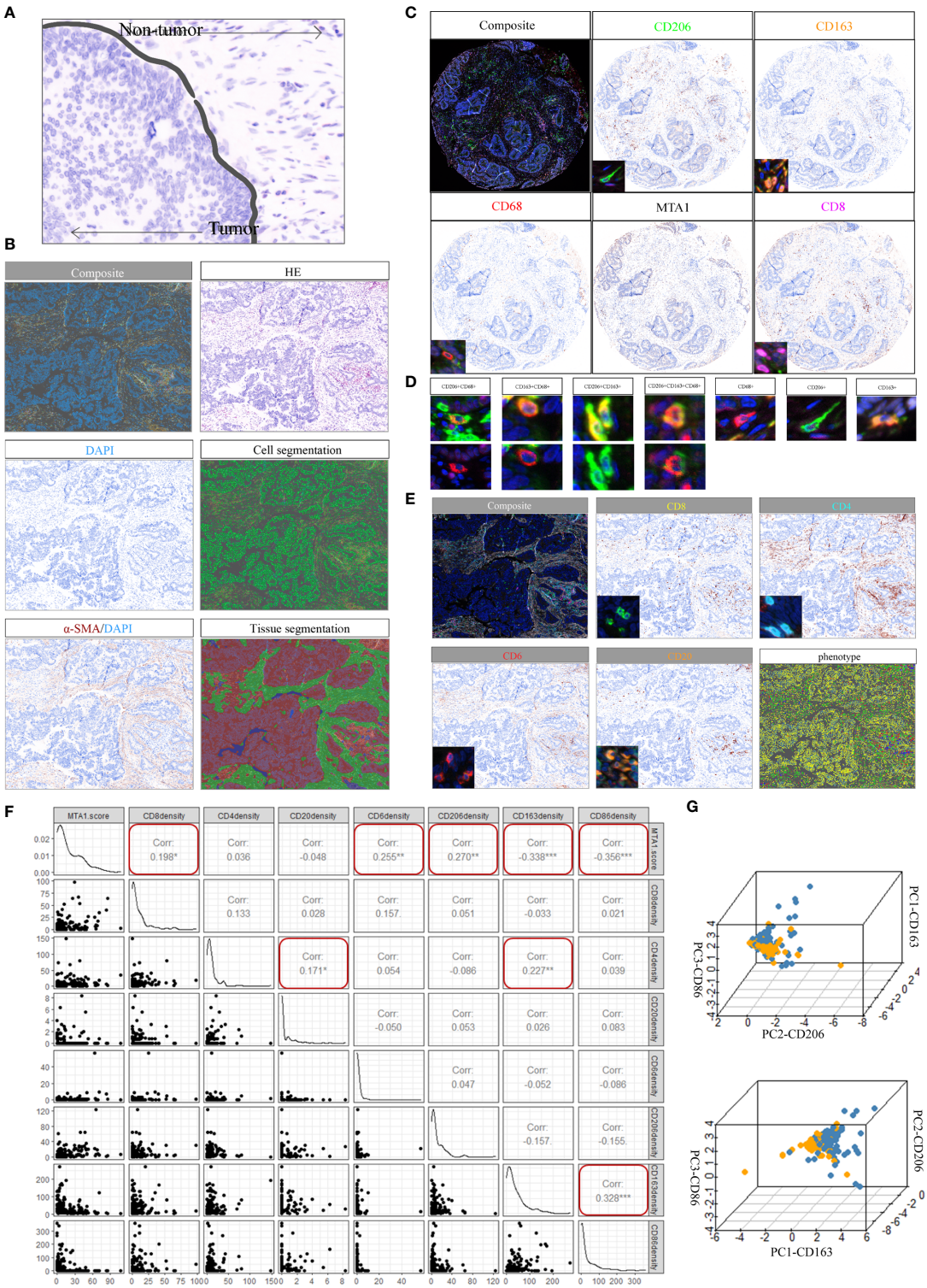

FIGURE 3 | Spectrum landscape of the MTA1-driven tumor microenvironment. **(A)** Regions of interest (ROIs): tumor tissue and nontumor tissue. **(B)** Composite image (unfiltered image), H&E, single-stained DAPI, cell segmentation of single cells, single-stained α-SMA, and tissue-component segmentation of the same region. **(C)** Representative composite and single-stained IHC images of multiplex IHC panel No. 1. **(D)** Major TAM populations. Positivity (+) of corresponding markers and relative intensity between populations are indicated. **(E)** Representative composite and single-stained IHC images of multiplex IHC panel No. 2. **(F)** Pearson correlation between MTA1 score and immune cell infiltration density in colorectal cancer patients. (*p-value <0.05, **p-value <0.01, ***p-value <0.001). **(G)** 3D plots showing the intensities of TAM populations per group.

cells and $CD20^+$B cells was not significantly associated with the expression of MTA1, but the significant correlation and intercellular interaction between $CD4^+$ T and B cells have been mentioned in numerous studies. B cells was generally recognized as a positive factor for immunotherapy response, especially B cells which are localized in lymphoid follicles of tertiary lymphoid structures (TLS) that increased percentages of tumor antigen-specific B cells and induced antitumor responses of T cells. These B cells are critically dependent on their interactions with $CD4^+$ follicular helper T cells (Tfh) which provide signals necessary for the survival and proliferation of these B cells (24–26).

The individual macrophages for all patients were plotted based on the intensity of CD86, CD163, and CD206 (**Figure 3G**), providing a spectrum of macrophage populations according to MTA1 levels. These data clearly displayed evidence of differential macrophage polarization between the MTA1-high and MTA1-low groups.

Colorectal Cancer Cells Expressing Higher Levels of MTA1 Induced Macrophage Polarization Into M2-Like Tumor-Associated Macrophage (TAM) Phenotypes

To explore the influence of MTA1 expression in tumor cells on the polarization of macrophages in the tumor microenvironment, we separately cocultured MTA1-knockdown, MTA1-overexpressing and control CT26 mouse colorectal cancer cells with mouse macrophages. Macrophages cocultured with MTA1-overexpressing colorectal cancer cells significantly upregulated the M2-like macrophage markers Arg-1, CD206 and Ym1 (**Figure 4A**) but significantly downregulated the expression of the immunostimulator IL-6 (**Figure 4A**). The differences in the expression of the M1-like macrophage marker INOS and the immunoinhibitors TNF-α and IL-10 were not significant between the groups (**Figure 4A**) (27). In the results of phenotype analysis by flow cytometry, colorectal cancer cells expressing higher MTA1 promoted the polarization of macrophages to the $CD206^+$ phenotype (**Figure 4C**) while inhibiting $CD163^+$ polarization (**Figure 4D**) without affecting the polarization of the $CD86^+$ phenotype (**Figure 4B**). In addition, we found that CT26 colorectal cancer cells barely expressed PD-L1 (**Figure 4F**). In the coculture system, PD-L1 was mainly expressed on macrophages, and CT26 cells expressing lower MTA1 expression promoted macrophages to express significantly upregulated PD-L1 in comparison with other groups (**Figure 4E**). By staining PD-L1 expression on the cancer tissue array from our clinical colorectal cohort, we confirmed the expression pattern of PD-L1 in colorectal cancer. The expression of PD-L1 in tumor cells was relatively lower than that in macrophages. The expression of PD-L1 was relatively higher in macrophages and other cells that were not stained in our panels (**Figure 4G**). Analysis of the correlation of the PD-L1 immunohistochemical score and the macrophage infiltration density revealed a significant positive/negative correlation between PD-L1 expression and macrophage infiltration density in colorectal cancer (**Figures 4H, I**).

In total, MTA1-overexpressing colorectal cancer cells significantly induced polarization of macrophages into M2 tumor-associated macrophage (TAM) phenotypes. In addition, we found that colorectal cancer cells rarely expressed PD-L1, suggesting that PD-L1 in the colorectal tumor microenvironment was mainly produced by macrophages and other nontumor cells.

Macrophages Help Kill T Cells in Colorectal Cancer Models

As above, we found a positive correlation between the MTA1 expression level and $CD8^+$ T cell infiltration. $CD8^+$ T cells are the main immune cells that directly exert antitumor effects. Therefore, we focused on the influence of MTA1 expression and its influence on macrophages on the activation of T cells. The results from flow cytometry showed that higher MTA1 expression in CT26 colorectal cancer cells promoted the secretion of Ifng in T cells (**Figure 5B**), reflecting T cell activation (28). In addition, we detected the immune checkpoints PD-1 and Tigit in T cells (29) and found that the expression of PD-1 (**Figure 5C**) and Tigit (**Figure 5A**) was not significantly different between the groups. However, the presence of macrophages in the coculture system significantly upregulated PD-1 expression levels (**Figure 5C**) and downregulated the expression of Ifng (**Figure 5B**) and Tigit (**Figure 5A**) in T cells. This suggests that macrophages suppress the activation of T cells. However, the presence of macrophages significantly decreased the apoptosis of T cells in the coculture system (**Figure 5D**), especially in the MTA1 knockdown group (**Figure 5D**).

Next, we performed a T cell cytotoxicity assay to further investigate the effect of MTA1 expression in colorectal cancer cells on T cell cytotoxicity in the tumor microenvironment (**Figure 5E**). Macrophages alone did not show a tumor-killing effect, while they enhanced the killing effects of T cells on tumor cells in the coculture system. In the coculture system, cancer cells expressing higher MTA1 suppressed the tumor-killing effect of T cells, and additional macrophages increased the killing effects of T cells on cancers.

These results indicated that MTA1 overexpression-correlated macrophage exclusion in tumor cells exacerbates the immunosuppressive state of the tumor macroenvironment.

MTA1 Overexpression Attenuated the Interaction Between Cancer Cells and Effector T Cells, Which Could be Rescued by Macrophage Completion

The most important manner in which effector T cells kill cancer cells is to directly interact with tumor cells and establish immunological synapses to perform accurately polarized secretion, ensuring that CTLs destroy only the recognized cells but not neighboring bystanders (30). Thus, we analyzed the interaction between tumor cells and T cells under various conditions with or without macrophages. First, we primarily compared the detection index of FCS, which represents the volume of cells, to exclude potential fluorescence crosstalk signals. The average FSC-A was equally increased in the cancer cell-T cell coculture system compared with the single cancer cell groups, indicating the

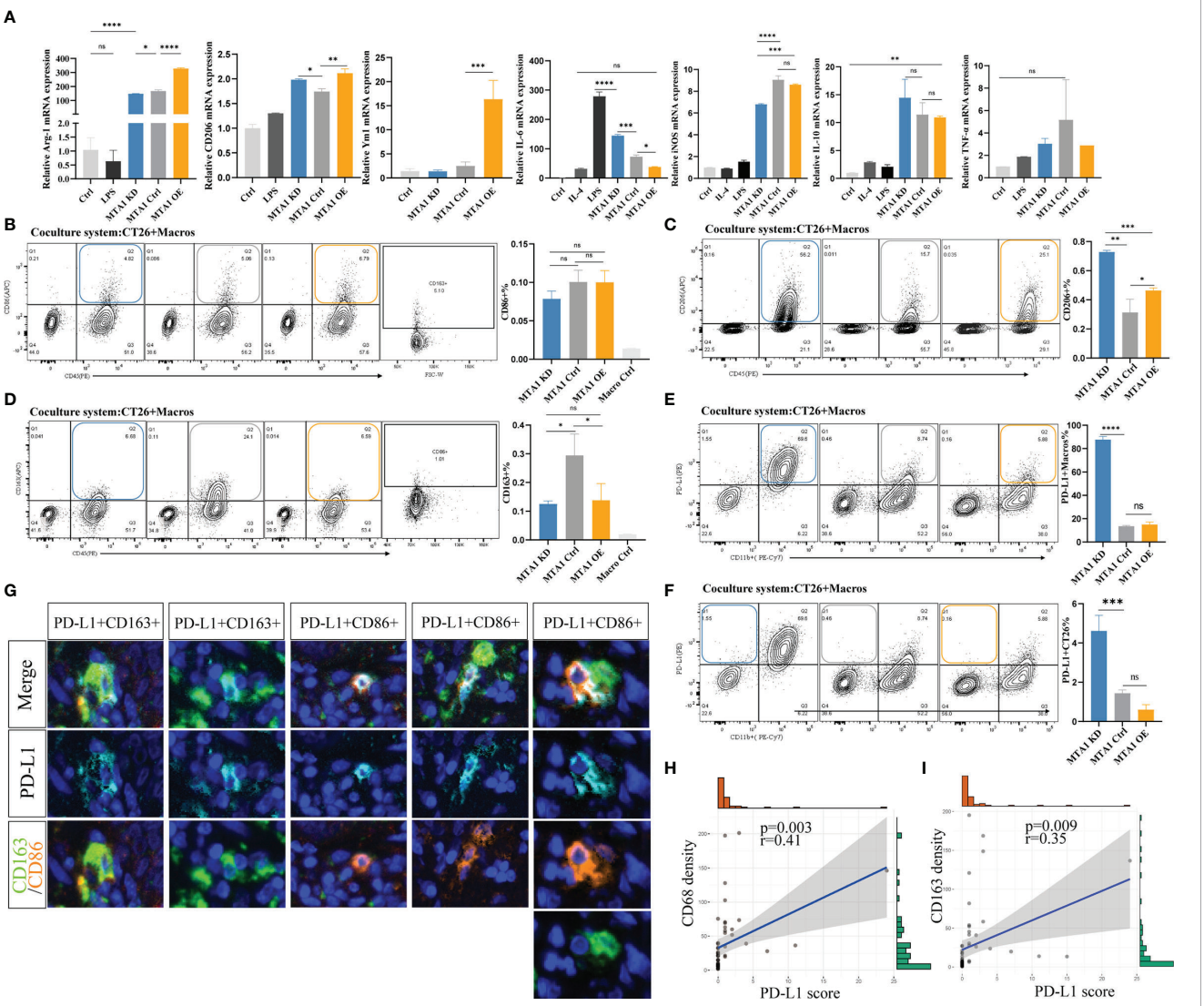

FIGURE 4 | MTA1 drives the polarization of macrophages in colorectal cancer. **(A)** qRT–PCR analysis of macrophage polarization-related genes in cell line Raw264.7 cocultured with cell line CT26 (MTA1-ctrl), and CT26 depleted for MTA1 (MTA1-KD) or enforced to express MTA1(MTA1-OE) for 48 h. **(B)** Flow cytometry analysis of macrophage polarization-related marker CD86 in cell line Raw264.7 cocultured with cell line CT26 of the control (MTA1-ctrl) and CT26 depleted of MTA1 (MTA1-KD) or enforced to express MTA1(MTA1-OE) for 48 h. **(C)** Flow cytometry analysis of macrophage polarization-related marker CD206 in cell line Raw264.7 cocultured with cell line CT26 (MTA1-ctrl), CT26 depleted of MTA1 (MTA1-KD) or CT26-overexpressing MTA1(MTA1-OE) for 48 h. **(D)** Flow cytometry analysis of macrophage polarization-related marker CD163 in cell line Raw264.7 cocultured with cell line CT26 (MTA1-ctrl), CT26 depleted of MTA1 (MTA1-KD) or CT26-overexpressing MTA1 (MTA1-OE) for 48 h. **(E)** Flow cytometry analysis of immune checkpoint, PD-L1, in cell line Raw264.7 cocultured with cell line CT26 (MTA1-ctrl), CT26 depleted of MTA1 (MTA1-KD) or CT26-overexpressing MTA1(MTA1-OE) for 48 h. **(F)** Flow cytometry analysis of immune checkpoint PD-L1 in cell line CT26 (MTA1-ctrl), CT26 depleted of MTA1 (MTA1-KD) or CT26-overexpressing MTA1(MTA1-OE) cocultured with cell line Raw264.7for 48 h. **(G)** The expression pattern of PD-L1 in clinical colorectal cancer tissue array. **(H)** Correlation between PD-L1 score and infiltration density of $CD68^+$ macrophages in colorectal cancer tissue array. **(I)** Correlation between PD-L1 score and infiltration density $CD163^+$ macrophages in colorectal cancer tissue array. The meaning of symbols was provided in Statistical Analysis.

reliability of the system to detect the interaction between T cells and cancer cells (**Figure 6A**). We found that the interaction between tumor cells and T cells in the MTA1-overexpressing group was significantly decreased compared to that of the control and MTA1-knockdown groups. Furthermore, when labeling the T cells with the immune markers Ifng or Tigit, the interaction between tumor cells and both T cells expressing Ifng (**Figure 6B**) or T cells expressing the immune checkpoint Tigit was significantly decreased in the MTA1-overexpressing group (**Figure 6C**). When macrophages were added to the coculture system, the difference in the interaction between different groups became insignificant. In addition, the interaction between macrophages and $PD\text{-}1^+$ T cells was significantly increased by MTA1 overexpression (**Figure 6D**). However, the addition of macrophages enhanced the interaction

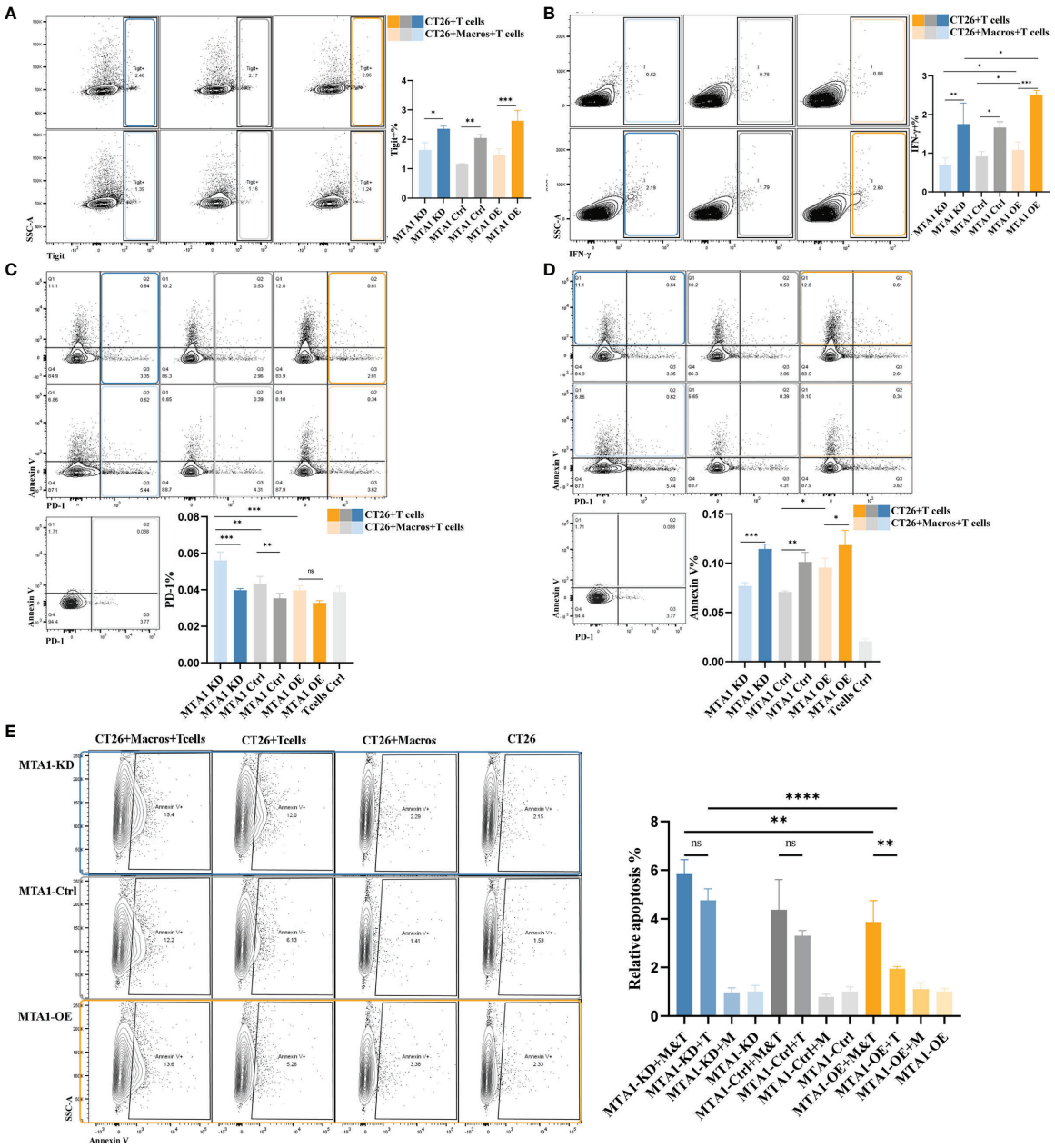

FIGURE 5 | MTA1-driven functional activation of T cells in colorectal cancer. **(A)** Flow cytometry analysis of immune checkpoint Tigit in T cells isolated from mouse spleen and cocultured with cell line CT26 (MTA1-ctrl), CT26 depleted of MTA1 (MTA1-KD) or CT26 overexpressing MTA1(MTA1-OE) for 6 h. **(B)** Flow cytometry analysis of activation marker of T cell, Ifng, in T cells isolated from mouse spleen cocultured with cell line CT26 (MTA1-ctrl), CT26 depleted of MTA1 (MTA1-KD) or CT26 overexpressing MTA1(MTA1-OE) for 6 h. **(C)** Flow cytometry analysis of immune checkpoint PD1 in T cells isolated from mouse spleen cocultured with cell line CT26 (MTA1-ctrl), CT26 depleted of MTA1 (MTA1-KD) or CT26 overexpressing (MTA1-OE) for 6 h. **(D)** Flow cytometry analysis of apoptosis using Annexin V in T cells isolated from mouse spleen cocultured with cell line CT26 ((MTA1-ctrl), CT26 depleted of MTA1 (MTA1-KD) or CT26 overexpressing MTA1(MTA1-OE) for 6 h. **(E)** Flow cytometry analysis of apoptosis marker, Annexin V, in cell line CT26 ((MTA1-ctrl), depleted of MTA1 (MTA1-KD) or overexpression for MTA1(MTA1-OE) cocultured with T cells isolated from mouse spleen for 6 h. (M, Macrophages; T, T cells). The meaning of symbols was provided in Statistical Analysis.

between T cells and MTA1-overexpressing tumor cells, eliminating the difference between the interaction of T cells with MTA1-high and MTA1-low cancer cells (**Figure 6E**).

In summary, the high expression of MTA1 in colorectal cancer decreased the interaction between tumor cells and T cells, which can be rescued by the presence of classical macrophages. Unfortunately, with still unverified mechanisms, macrophages were always lacking in the tumor microenvironment with MTA1 overexpression. The combinational consequence of MTA1 overexpression is a markedly suppressed immune microenvironment.

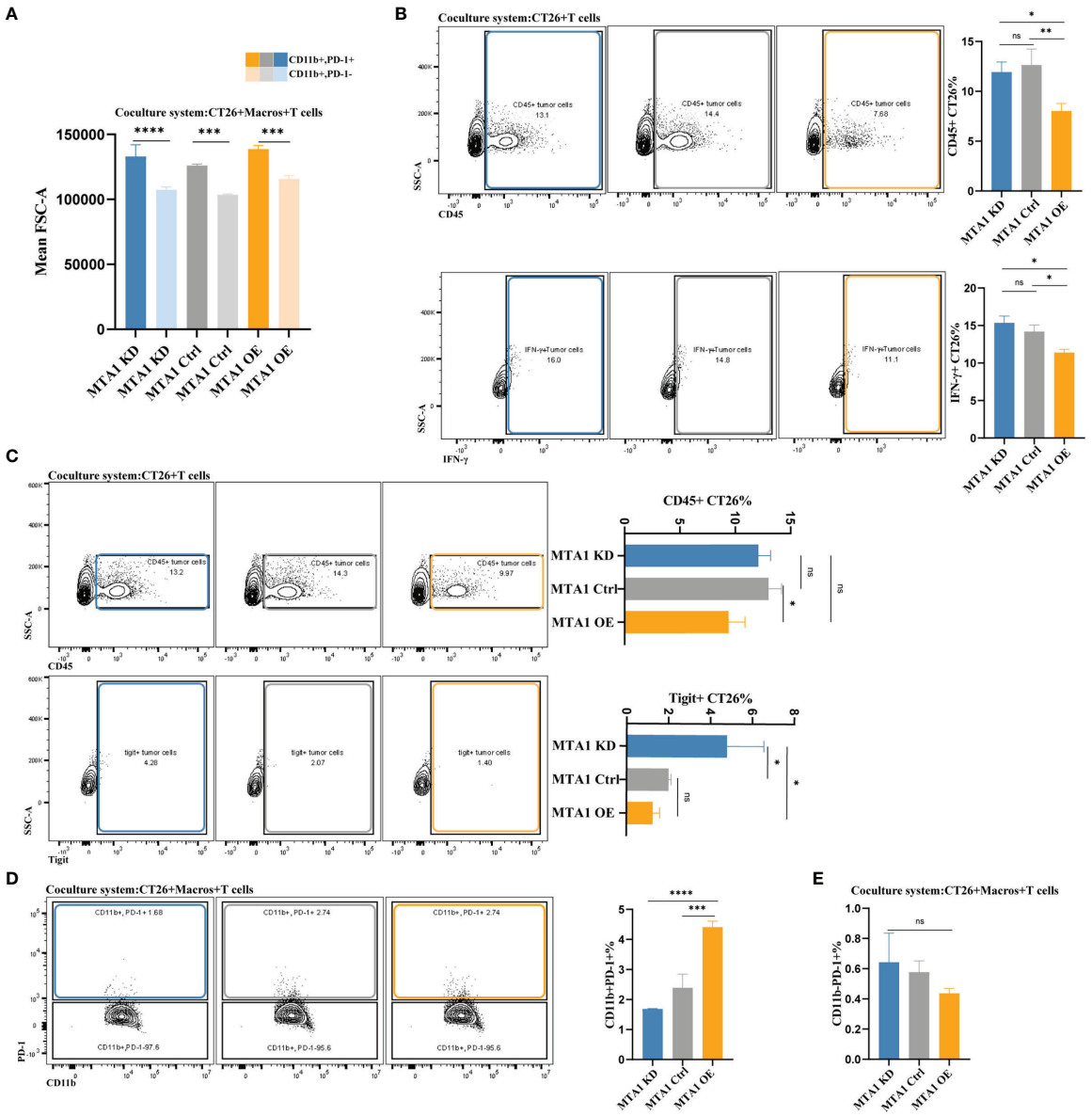

FIGURE 6 | MTA1-driven difference in interaction between tumor cells, macrophages and T cells in colorectal cancer. **(A)** The average volume variation of a single macrophage or object of interacting T cells and macrophages. **(B)** Flow cytometry analysis of the interaction between T cells (all CD45-positive T cells and Tigit-positive T cells) and CT26 tumor cells (MTA1-ctrl), CT26 cells depleted of MTA1 (MTA1-KD) or CT26 cells overexpressing MTA1 (MTA1-OE). **(C)** Flow cytometry analysis of interaction between T cells (all the CD45 positive T cells and Ifng positive T cells) and tumor cells, CT26 (MTA1-ctrl), depleted of MTA1 (MTA1-KD) or overexpression of MTA1 (MTA1-OE). **(D)** Flow cytometry analysis of the interaction between T cells (all the CD45 positive T cells and Tigit positive T cells) and macrophages cocultured with CT26 (MTA1-ctrl), depleted of MTA1 (MTA1-KD) or overexpression for MTA1 (MTA1-OE) for 6 h. **(E)** Flow cytometry analysis of interaction between T cells (PD1 positive T cells) and tumor cells, CT26 (MTA1-ctrl), depleted of MTA1 (MTA1-KD) or overexpression of MTA1 (MTA1-OE) in the cocultured system with macrophages. The meaning of symbols was provided in Statistical Analysis.

DISCUSSION

As we recognize tumors as a complex microenvironment in which various cell types interact with each other, contributing to the phenotypes of the entire tumor, we are facing the new challenge of understanding the mechanisms of the interaction network between cell types and how they influence cancer treatment practice (1, 31, 32).

Due to progress in biological technologies, it has been possible to identify different subclasses in the immune microenvironment (TIME) of tumors. The immune signatures in the microenvironment are predictive of patient outcomes and the response to immunotherapy and leads to novel therapeutic strategies (33–35). Therefore, it is urgent to interpret the immune profiles in cancer.

In our previous research, we reported overexpression of MTA1 in the majority of cancer types, which contributes to the malignant phenotypes of cancers, especially metastatic behaviors (36–39). We found clues that highly expressed MTA1 is associated with immune signatures in the tumor microenvironment. Here, we report the ability of MTA1 to rewire the transcriptome and proteome of colorectal cancer cells, resulting in an immunosuppressive microenvironment. Mechanistically, we described that the chemokines and cytokines downregulated by MTA1 in cancer cells may result in decreased macrophages in the tumor microenvironment. We also found that macrophage polarization was affected. Colorectal cancer cells expressing high levels of MTA1 tend to induce M2-like macrophages. The polarization phenotypes were significantly different in MTA1-high versus MTA1-tumors.

In addition, we found enrichment of CD8+ T cells in the MTA1-high patient group. However, the enrichment of $CD8^+$ T cells was not significantly correlated with patient survival. We hypothesized that the enriched $CD8^+$ T cells were functionally impaired or that cancer cells expressing high levels of MTA1 may be intrinsically resistant to the killing effects of $CD8^+$ T cells. Subsequent investigation showed that decreased macrophages at high MTA1 levels significantly affected the tumor killing of T cells. The completion of macrophages into the coculture system significantly restored the tumor-killing function of T cells. The existence of macrophages in the microenvironment significantly improved the interaction between T cells and cancer cells. Numerous studies have also mentioned the essential crosstalk between myeloid cells and T cells in the antitumor immune response (40–43). Activated T cells stimulated by aPD-1 or other cytokines expressed IFN-γ and other proinflammatory cytokines; however, the antitumor effect of activated T cells was dependent on the presence of myeloid cells, such as DCs, $CD14^+$ macrophages and $CXCL9^+$ macrophages. Not only the presence of myeloid cells but also crosstalk between myeloid cells and T cells were necessary for the antitumor effect of T cells. In our study, we also emphasized that the relatively decreased macrophages impaired the antitumor effect in MTA1-overexpressing colorectal cancer. However, the crosstalk network between myeloid cells and T cells still needs to be solved, and the detailed mechanisms by which myeloid cells stimulate antitumor phenotypes should be further clarified to design clinical therapeutic strategies.

MTA1 was first reported as a metastasis-associated molecule in breast cancer, and then, the functions and tumorigenic potential of MTA1 were gradually recognized. MTA1 affects the biological behaviors of tumors from genetic and epigenetic aspects (36–39). In this study, the results suggested an MTA1-derived immunosuppressive signature in the tumor microenvironment. In more detail, MTA1 remodeled the tumor microenvironment into a $CD8^+$ T cell-enriched and classical macrophage-lacking microenvironment (**Figure 7**). Based on the characteristics of the MTA1-derived immunosuppressive microenvironment, we can further focus on enhancing the tumor-killing effect of $CD8^+$ T cells by interfering with the MTA1 level since it intermediates the interaction between $CD8^+$ T cells and tumor cells.

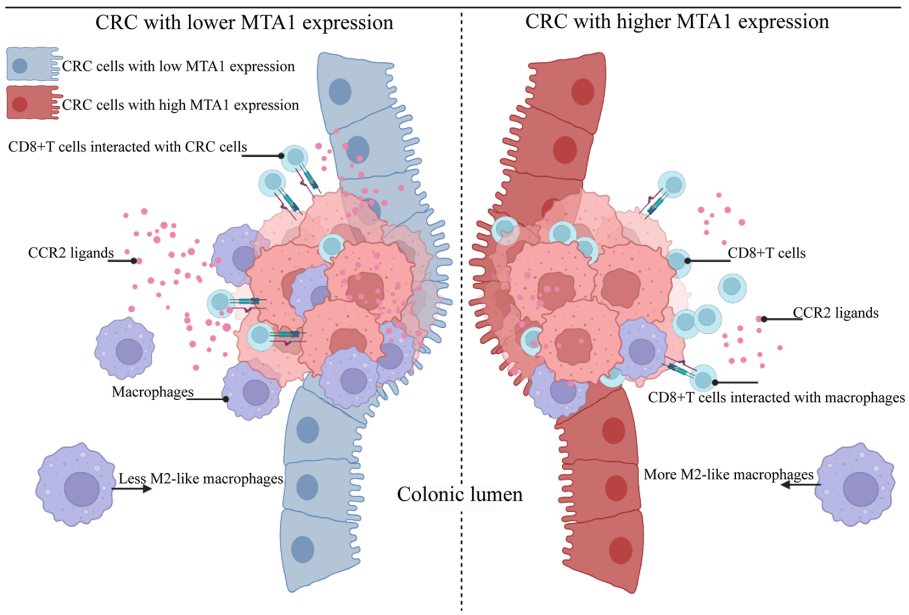

FIGURE 7 | Schematic model of colorectal cancer with lower and higher MTA1 expression. Summary of the main conclusions from this study. In brief, MTA1 was found to rewire the transcriptome and proteome of colorectal cells to promote an immunosuppressive tumor microenvironment. MTA1-overexpressing colon cancer cells significantly decreased the expression levels of the CCR2 ligands CCL2 and CCL7, among others, which were able to attract macrophages. This microenvironment of MTA1-overexpressing colorectal cancer ultimately leads to CD8 T cell enrichment but a lack of classical macrophages. Macrophages enhanced the cytotoxic effect of T cells while enhancing the interaction of T cells and cancer cells. In MTA1-overexpressing colorectal cancer, the absence of macrophages impaired the cytotoxic effect of T cells, decreased the interaction of T cells and cancer cells, and finally resulted in an immunosuppressive tumor microenvironment.

There are certain limitations to roundly defining the detailed functions of $CD8^+$ T cell subtypes and macrophage subtypes induced by MTA1-high tumor cells. In this study, we only focused on the tumor-killing pathway by cytotoxicity. This research suggested that the absence of macrophages significantly decreased the cytotoxicity of $CD8^+$ T cells. Limited by the complex interaction and secretion in the tumor microenvironment, we have not yet defined the core chemokine regulation networks between tumor cells, $CD8^+$ T cells and macrophages derived by MTA1. According to the results in this study, it is highly probable that macrophages enhance cytotoxicity by maintaining the survival of $CD8^+$ T cells and antigen presentation (44), and it is worth elucidating the detailed mechanism in further studies.

In conclusion, our results show that MTA1 overexpression in colon cancer drives a $CD8^+$ T cell-rich but exhausted phenotype by decreasing macrophage intensity and inducing M2-like macrophage polarization. The importance of MTA1 on macrophages for the antitumor effects of $CD8^+$ T cells implies an immunosuppressive tumor microenvironment by MTA1 overexpression in cancers. Our report guarantees further study on whether MTA1 can serve as a marker for the sensitivity of cancers to immunotherapy or even as an immunotherapy target in combination with current immune checkpoint blockers.

DATA AVAILABILITY STATEMENT

The datasets presented in this study can be found in online repositories. The names of the repository/repositories and accession number(s) can be found in the article/**Supplementary Material**.

ETHICS STATEMENT

The studies involving human participants were reviewed and approved by the Cancer Hospital, Chinese Academy of Medical Sciences National GCP Center for Anticancer Drug, The Independent Ethics Committee. The patients/participants provided their written informed consent to participate in this study. The animal study was reviewed and approved by the Animal Control Committee of National Cancer Center/National Clinical Research Center for Cancer/Cancer Hospital, Chinese Academy of Medical Sciences and Peking Union Medical College.

AUTHOR CONTRIBUTIONS

Conceptualization: HQ, FM, and DX Experiment: YZhou and PN. Data analysis: YZhou, CL, PN, HM, YZhang, and HW. Resources: HQ and DX. Manuscript writing: YZhou. Manuscript editing: HQ. Visualization: YZhou, CL, PN, HM, HW, and YZhang. Supervision: HQ, FM, and DX. Project Administration: HQ. Funding Acquisition: HQ. All authors listed have made a substantial, direct, and intellectual contribution to the work and approved it for publication.

FUNDING

This work was financially supported by grants from the National Key Research and Development Program of China (2021YFF1201302), the National Natural Science Foundation of China (No. 81872280, 82073094), the CAMS Innovation Fund for Medical Sciences (CIFMS)(2021-I2M-014), the Open Issue of State Key Laboratory of Molecular Oncology (No. SKL-KF-2021-16), and the Independent Issue of State Key Laboratory of Molecular Oncology (No. SKL-2021-16).

SUPPLEMENTARY MATERIAL

The Supplementary Material for this article can be found online at: https://www.frontiersin.org/articles/10.3389/fonc.2022.825783/full#supplementary-material

REFERENCES

1. Hanahan D, Weinberg RA. Hallmarks of Cancer: The Next Generation. *Cell* (2011) 144:646–74. doi: 10.1016/J.CELL.2011.02.013
2. Jerby-Arnon L, Shah P, Cuoco MS, Rodman C, Su MJ, Melms JC, et al. A Cancer Cell Program Promotes T Cell Exclusion and Resistance to Checkpoint Blockade. *Cell* (2018) 175:984–97.E24. doi: 10.1016/J.CELL.2018.09.006
3. Jiang P, Gu S, Pan D, Fu J, Sahu A, Hu X, et al. Signatures of T Cell Dysfunction and Exclusion Predict Cancer Immunotherapy Response. *Nat Med* (2018) 24:1550–8. doi: 10.1038/S41591-018-0136-1
4. Neubert NJ, Schmittnaegel M, Bordry N, Nassiri S, Wald N, Martignier C, et al. T Cell-Induced Csf1 Promotes Melanoma Resistance To Pd1 Blockade. *Sci Transl Med* (2018) 10:eaan3311. doi: 10.1126/SCITRANSLMED.AAN3311
5. Pathria P, Louis TL, Varner JA. Targeting Tumor-Associated Macrophages in Cancer. *Trends Immunol* (2019) 40:310–27. doi: 10.1016/J.IT.2019.02.003
6. Torchy MP, Hamiche A, Klaholz BP. Structure and Function Insights Into The Nurd Chromatin Remodeling Complex. *Cell Mol Life Sci* (2015) 72:2491–507. doi: 10.1007/S00018-015-1880-8
7. Hänzelmann S, Castelo R, Guinney J. Gsva: Gene Set Variation Analysis for Microarray And Rna-Seq Data. *BMC Bioinf* (2013) 14:7. doi: 10.1186/1471-2105-14-7
8. Wu WT, Li YJ, Feng AZ, Li L, Huang T, Xu AD, et al. Data Mining In Clinical Big Data: The Frequently Used Databases, Steps, And Methodological Models. *Mil Med Res* (2021) 8:44. doi: 10.1186/S40779-021-00338-Z
9. Lee HO, Hong Y, Etlioglu HE, YB C, Pomella V, Van Den Bosch B, et al. Lineage-Dependent Gene Expression Programs Influence The Immune Landscape Of Colorectal Cancer. *Nat Genet* (2020) 52:594–603. doi: 10.1038/S41588-020-0636-Z
10. Li T, Fu J, Zeng Z, Cohen D, Li J, Chen Q, et al. Timer2.0 For Analysis of Tumor-Infiltrating Immune Cells. *Nucleic Acids Res* (2020) 48:W509–509W514. doi: 10.1093/NAR/GKAA407
11. Steen CB, Liu CL, Alizadeh AA, Newman AM. Profiling Cell Type Abundance and Expression In Bulk Tissues With Cibersortx. *Methods Mol Biol* (2020) 2117:135–57. doi: 10.1007/978-1-0716-0301-7_7
12. Okamoto Y, Devoe S, Seto N, Minarchick V, Wilson T, Rothfuss HM, et al. Association of Sputum Neutrophil Extracellular Trap Subsets With Iga Anti-Citrullinated Protein Antibodies In Subjects At Risk For Rheumatoid Arthritis. *Arthritis Rheumatol* (2022) 74:38–48. doi: 10.1002/ART.41948

13. Movahedi K, Laoui D, Gysemans C, Baeten M, Stangé G, Van Den Bossche J, et al. Different Tumor Microenvironments Contain Functionally Distinct Subsets of Macrophages Derived From Ly6c(High) Monocytes. *Cancer Res* (2010) 70:5728–39. doi: 10.1158/0008-5472.CAN-09-4672
14. Qian BZ, Li J, Zhang H, Kitamura T, Zhang J, Campion LR, et al. Ccl2 Recruits Inflammatory Monocytes to Facilitate Breast-Tumour Metastasis. *Nature* (2011) 475:222–5. doi: 10.1038/NATURE10138
15. Haverkamp JM, Smith AM, Weinlich R, Dillon CP, Qualls JE, Neale G, et al. Myeloid-Derived Suppressor Activity Is Mediated By Monocytic Lineages Maintained By Continuous Inhibition Of Extrinsic And Intrinsic Death Pathways. *Immunity* (2014) 41:947–59. doi: 10.1016/J.IMMUNI.2014.10.020
16. Kratochvill F, Neale G, Haverkamp JM, Van De Velde LA, Smith AM, Kawauchi D, et al. Tnf Counterbalances the Emergence Of M2 Tumor Macrophages. *Cell Rep* (2015) 12:1902–14. doi: 10.1016/J.CELREP.2015.08.033
17. Liou GY, Bastea L, Fleming A, Döppler H, Edenfield BH, Dawson DW, et al. The Presence of Interleukin-13 At Pancreatic Adm/Panin Lesions Alters Macrophage Populations And Mediates Pancreatic Tumorigenesis. *Cell Rep* (2017) 19:1322–33. doi: 10.1016/J.CELREP.2017.04.052
18. Perrotta C, Cervia D, Di Renzo I, Moscheni C, Bassi MT, Campana L, et al. Nitric Oxide Generated By Tumor-Associated Macrophages Is Responsible For Cancer Resistance To Cisplatin And Correlated With Syntaxin 4 And Acid Sphingomyelinase Inhibition. *Front Immunol* (2018) 9:1186. doi: 10.3389/FIMMU.2018.01186
19. Chen Y, Song Y, Du W, Gong L, Chang H, Zou Z. Tumor-Associated Macrophages: An Accomplice In Solid Tumor Progression. *J BioMed Sci* (2019) 26:78. doi: 10.1186/S12929-019-0568-Z
20. Arief Waskito B, Sargowo D, Kalsum U, Tjokroprawiro A. Anti-Atherosclerotic Activity of Aqueous Extract of Ipomoea Batatas (L.) Leaves in High-Fat Diet-Induced Atherosclerosis Model Rats. *J Basic Clin Physiol Pharmacol* (2022). doi: 10.1515/JBCPP-2021-0080
21. Recalcati S, Locati M, Marini A, Santambrogio P, Zaninotto F, De Pizzol M, et al. Differential Regulation of Iron Homeostasis During Human Macrophage Polarized Activation. *Eur J Immunol* (2010) 40:824–35. doi: 10.1002/EJI.200939889
22. Colegio OR, Chu NQ, Szabo AL, Chu T, Rhebergen AM, Jairam V, et al. Functional Polarization of Tumour-Associated Macrophages By Tumour-Derived Lactic Acid. *Nature* (2014) 513:559–63. doi: 10.1038/NATURE13490
23. Murray PJ. Macrophage Polarization. *Annu Rev Physiol* (2017) 79:541–66. doi: 10.1146/ANNUREV-PHYSIOL-022516-034339
24. Linterman MA, Liston A, Vinuesa CG. T-Follicular Helper Cell Differentiation and The Co-Option Of This Pathway By Non-Helper Cells. *Immunol Rev* (2012) 247:143–59. doi: 10.1111/J.1600-065X.2012.01121.X
25. Allen CD, Okada T, Cyster JG. Germinal-Center Organization and Cellular Dynamics. *Immunity* (2007) 27:190–202. doi: 10.1016/J.IMMUNI.2007.07.009
26. Wennhold K, Thelen M, Lehmann J, Schran S, Preugszat E, Garcia-Marquez M, et al. Cd86(+) Antigen-Presenting B Cells Are Increased In Cancer, Localize In Tertiary Lymphoid Structures, and Induce Specific T-Cell Responses. *Cancer Immunol Res* (2021) 9:1098–108. doi: 10.1158/2326-6066.CIR-20-0949
27. Spranger S, Gajewski TF. Impact of Oncogenic Pathways On Evasion of Antitumour Immune Responses. *Nat Rev Cancer* (2018) 18:139–47. doi: 10.1038/NRC.2017.117
28. St Paul M, Ohashi PS. The Roles of Cd8(+) T Cell Subsets In Antitumor Immunity. *Trends Cell Biol* (2020) 30:695–704. doi: 10.1016/J.TCB.2020.06.003
29. Chauvin JM, Zarour HM. Tigit In Cancer Immunotherapy. *J Immunother Cancer* (2020) 8:e000957. doi: 10.1136/JITC-2020-000957
30. Ritter AT, Asano Y, Stinchcombe JC, Dieckmann NM, Chen BC, Gawden-Bone C, et al. Actin Depletion Initiates Events Leading To Granule Secretion At The Immunological Synapse. *Immunity* (2015) 42:864–76. doi: 10.1016/J.IMMUNI.2015.04.013
31. Soysal SD, Tzankov A, Muenst SE. Role of The Tumor Microenvironment In Breast Cancer. *Pathobiology* (2015) 82:142–52. doi: 10.1159/000430499
32. Arneth B. Tumor Microenvironment. *Medicina (Kaunas)* (2019) 56:15. doi: 10.3390/MEDICINA56010015
33. Binnewies M, Roberts EW, Kersten K, Chan V, Fearon DF, Merad M, et al. Understanding The Tumor Immune Microenvironment (Time) For Effective Therapy. *Nat Med* (2018) 24:541–50. doi: 10.1038/S41591-018-0014-X
34. Wu T, Dai Y. Tumor Microenvironment and Therapeutic Response. *Cancer Lett* (2017) 387:61–8. doi: 10.1016/J.CANLET.2016.01.043
35. Jin MZ, Jin WL. The Updated Landscape of Tumor Microenvironment and Drug Repurposing. *Signal Transduct Target Ther* (2020) 5:166. doi: 10.1038/S41392-020-00280-X
36. Zhou N, Wang H, Liu H, Xue H, Lin F, Meng X, et al. Mta1-Upregulated Epcam Is Associated With Metastatic Behaviors And Poor Prognosis In Lung Cancer. *J Exp Clin Cancer Res* (2015) 34:157. doi: 10.1186/S13046-015-0263-1
37. Liu J, Li C, Wang J, Xu D, Wang H, Wang T, et al. Chromatin Modifier Mta1 Regulates Mitotic Transition and Tumorigenesis By Orchestrating Mitotic Mrna Processing. *Nat Commun* (2020) 11:4455. doi: 10.1038/S41467-020-18259-1
38. Nan P, Wang T, Li C, Li H, Wang J, Zhang J, et al. Mta1 Promotes Tumorigenesis and Development Of Esophageal Squamous Cell Carcinoma *Via* Activating The Mek/Erk/P90rsk Signaling Pathway. *Carcinogenesis* (2020) 41:1263–72. doi: 10.1093/CARCIN/BGZ200
39. Li L, Liu J, Xue H, Li C, Liu Q, Zhou Y, et al. A Tgf-B-Mta1-Sox4-Ezh2 Signaling Axis Drives Epithelial-Mesenchymal Transition In Tumor Metastasis. *Oncogene* (2020) 39:2125–39. doi: 10.1038/S41388-019-1132-8
40. Garris CS, Arlauckas SP, Kohler RH, Trefny MP, Garren S, Piot C, et al. Successful Anti-Pd-1 Cancer Immunotherapy Requires T Cell-Dendritic Cell Crosstalk Involving The Cytokines Ifn-Γ And Il-12. *Immunity* (2018) 49:1148–61.E7. doi: 10.1016/J.IMMUNI.2018.09.024
41. Rubin J, Mansoori S, Blom K, Berglund M, Lenhammar L, Andersson C, et al. Mebendazole Stimulates Cd14+ Myeloid Cells To Enhance T-Cell Activation And Tumour Cell Killing. *Oncotarget* (2018) 9:30805–13. doi: 10.18632/ONCOTARGET.25713
42. Qing X, Koo GC, Salmon JE. Complement Regulates Conventional Dc-Mediated Nk-Cell Activation By Inducing Tgf-B1 In Gr-1+ Myeloid Cells. *Eur J Immunol* (2012) 42:1723–34. doi: 10.1002/EJI.201142290
43. Zhang Y, Chen H, Mo H, Hu X, Gao R, Zhao Y, et al. Single-Cell Analyses Reveal Key Immune Cell Subsets Associated With Response To Pd-L1 Blockade In Triple-Negative Breast Cancer. *Cancer Cell* (2021) 39:1578–93.E8. doi: 10.1016/J.CCELL.2021.09.010
44. Lecoultre M, Dutoit V, Walker PR. Phagocytic Function Of Tumor-Associated Macrophages As A Key Determinant Of Tumor Progression Control: A Review. *J Immunother Cancer* (2020) 8:e001408. doi: 10.1136/JITC-2020-001408

Conflict of Interest: Author HW was employed by Chinese Medical Journals Publishing House Co., Ltd.

The remaining authors declare that the research was conducted in the absence of any commercial or financial relationships that could be construed as a potential conflict of interest.

Publisher's Note: All claims expressed in this article are solely those of the authors and do not necessarily represent those of their affiliated organizations, or those of the publisher, the editors and the reviewers. Any product that may be evaluated in this article, or claim that may be made by its manufacturer, is not guaranteed or endorsed by the publisher.

frontiers | Frontiers in Oncology

REVIEW
published: 22 June 2022
doi: 10.3389/fonc.2022.911285

The Role of Tumor Microenvironment in Invasion and Metastasis of Esophageal Squamous Cell Carcinoma

Shuyue Zheng[1,2], *Beilei Liu*[1,2] *and Xinyuan Guan*[1,2,3]*

[1] Department of Clinical Oncology, Li Ka Shing Faculty of Medicine, The University of Hong Kong, Hong Kong, Hong Kong SAR, China, [2] Department of Clinical Oncology, The University of Hong Kong-Shenzhen Hospital, Shenzhen, China, [3] State Key Laboratory of Oncology in Southern China, Sun Yat-sen University Cancer Center, Guangzhou, China

Esophageal squamous cell carcinoma (ESCC) is one of the most common cancers in the world, with a high rate of morbidity. The invasion and metastasis of ESCC is the main reason for high mortality. More and more evidence suggests that metastasized cancer cells require cellular elements that contribute to ESCC tumor microenvironment (TME) formation. TME contains many immune cells and stromal components, which are critical to epithelial–mesenchymal transition, immune escape, angiogenesis/lymphangiogenesis, metastasis niche formation, and invasion/metastasis. In this review, we will focus on the mechanism of different microenvironment cellular elements in ESCC invasion and metastasis and discuss recent therapeutic attempts to restore the tumor-suppressing function of cells within the TME. It will represent the whole picture of TME in the metastasis and invasion process of ESCC.

Keywords: esophageal squamous cell carcinoma, tumor microenvironment, invasion, metastasis, immune regulation

OPEN ACCESS

Edited by:
Nathaniel Weygant, Fujian University of Traditional Chinese Medicine, China

Reviewed by:
Zhong-Xi Huang, Southern Medical University, China
Ting Zhuang, Xinxiang Medical University, China

***Correspondence:**
Xinyuan Guan
xyguan@hku.hk

Specialty section:
This article was submitted to Gastrointestinal Cancers: Gastric and Esophageal Cancers, a section of the journal Frontiers in Oncology

Received: *02 April 2022*
Accepted: *18 May 2022*
Published: *22 June 2022*

Citation:
Zheng S, Liu B and Guan X (2022) The Role of Tumor Microenvironment in Invasion and Metastasis of Esophageal Squamous Cell Carcinoma. Front. Oncol. 12:911285. doi: 10.3389/fonc.2022.911285

1 INTRODUCTION

Esophageal squamous cell carcinoma (ESCC) is one of the most common cancers in the world, with high rates of morbidity and mortality (1). More than half of the ESCC patients are in advanced stages when they are first diagnosed. Extensive metastases prevent patients from having radical surgery, which is the only clinical method of curing ESCC currently (2). The Food and Drug Administration (FDA) has approved a number of new immune and targeted drugs, such as programmed cell death protein 1 (PD-1) inhibitors and human epidermal growth factor receptor-2 (Her-2) inhibitors for advanced ESCC treatment, but the survival rate of those advanced patients is still low (3, 4). It is reported that the 5-year survival rate for advanced esophageal cancer (19%) was on par with lung cancer (19%) and next only to liver cancer (18%) and pancreatic cancer (9%) (5, 6). Local invasion and distant metastasis of ESCC are the main reasons for the failure of treating these advanced patients. Therefore, further molecular research of the ESCC landscape has the potential to ascertain new biomarkers and molecular targets that affect ESCC progression and enable the design of new therapeutic strategies (7).

Recently, the central role of the tumor microenvironment (TME) in the invasion and metastasis of *de novo* ESCC has been identified. TME includes immune cells, fibroblasts, endothelial cells, perivascular cells, neurons, and extracellular matrix. There is increasing evidence that TME plays an important role in cell proliferation, cell survival, epithelial–mesenchymal transition (EMT), angiogenesis/lymphangiogenesis immunosuppression, invasion, and metastasis (8, 9). TME is a dynamic environment constantly reshaped by tumor and tumor-associated cells to make tumor cells survive well (10). Thus, TME is now regarded as a target-rich environment for the development of novel anticancer drugs in ESCC. Actually, many drugs that focus on diverse components of TME, including vascular endothelial growth factor (VEGF) and immune checkpoints, have been approved for clinical use (11, 12).

In this review, we summarize recent advances in how ESCC cells recruit and modify cells in the immune microenvironment to make them more conducive to metastasize and how those factors in the TME support the ESCC invasion and metastasis. Also, we discuss the regulation of abnormal molecular signaling pathways and networks stimulated by tumor and TME interactions, which might provide new diagnostic, prognostic, or therapeutic opportunities.

2 INVASION AND METASTASIS PROCESS OF ESOPHAGEAL SQUAMOUS CELL CARCINOMA

Metastasis is the process by which circulating tumor cells colonize in other tissues or organs and become diffuse tumor cells. However, only 0.01% of circulating tumor cells have been reported to successfully colonize and grow into diffuse tumor cells (13, 14). It is because the circulating tumor cells are seriously influenced by the human local microenvironment. The "seed and soil" hypothesis raised by Paget can be used to well characterize this process (15). Tumor cells *in situ* ("seeds") tend to stay on some specific target organs ("soil"), which have TME beneficial to the survival of tumor cells. At present, it is supposed that there are three main steps for the formation of a metastasis niche: first, the primary tumors secrete some factors around them (invasion), exosomes, and micro-vesicles (metastasis) to create the pre-metastatic niche (16, 17). Then, those factors induce immune cells, such as marrow-derived suppressor cells (MDSCs), macrophages, dendritic cells (DCs), neutrophils (18, 19), and regulatory T cells (Tregs) to polarize into tumor-promoting cells. Also, some stromal components such as cancer-associated fibroblasts (CAFs) promoting angiogenesis, secreting cytokines, inducing EMT, recombining matrix components, recruiting inflammatory cells to help ESCC cells invade and metastasize (20, 21), and other factors (hypoxia, etc.) (17). Finally, all those factors remodel the microenvironment into TME, and invasion and metastasis occur (**Figure 1**).

Lymphatic metastasis is the most common way of ESCC metastasis, which is determined by the characteristics of lymphatic reflux in the esophageal wall (22, 23). Also, lymph node metastasis is the most important prognostic factor of ESCC. As to the "seeds and soil" hypothesis, lymph node metastasis is not a simple process of direct migration of ESCC cells. Many kinds of literature have reported that the niche of ESCC lymph nodes has changed significantly before metastasis (24, 25). It has been shown that the lymph node immune status of pN0 and pN1 patients is completely different. There is an obvious activated pattern of immune response in the pN0 patients. On the contrary, pN1 patients show a distinct pattern of inhibition, such as reduced immune response, immune cell proliferation, and increased immune cell apoptosis (26, 27). It means that in the early stage of ESCC metastasis, drainage of tumor antigens to lymph nodes results in the antitumor status. However, as time goes on, more and more tumor secretory factors and immunosuppressive cells will accumulate. Then, the immune state of lymph nodes will change from antitumor to pro-tumor mode until the tumor cells first colonize and metastasize (28). Therefore, an in-depth study of the interaction between tumor cells and the immune microenvironment and how it promotes the ESCC invasion and metastasis will guide the development of future diagnosis and treatment strategies.

3 THE ROLE OF TUMOR MICROENVIRONMENT IN ESOPHAGEAL SQUAMOUS CELL CARCINOMA INVASION AND METASTASIS

3.1 Immune Modulation Promotes Esophageal Squamous Cell Carcinoma Invasion and Metastasis

Tumors escaping from the immune system are the key to tumor invasion and metastasis. Tumor cells can form specific TME that inhibits antitumor immune response by recruiting various alternative tumor-associated immune cells or expressing inhibitory molecular factors (**Figure 2**). Specific immune cell types and influencing factors in ESCC will be discussed below.

3.1.1 Myeloid-Derived Suppressor Cells

Myeloid-derived suppressor cells (MDSCs) are the suppressive cell population of the immune system, which play a pivotal role in the TME (29). MDSCs can greatly inhibit the cytotoxic function of T cells and NK cells during circulation and support ESCC progression (30). The specific markers of MDSCs are most often identified by the expression of CD11b and lack of HLA-DR expression (31). In ESCC, MDSCs produce reactive oxygen species (ROS) and peroxynitrite ($ONOO^-$), which block the activation and proliferation of T cells to disrupt immune responses (32). Also, MDSCs inhibit the proliferation of $CD8^+$ T cells by phosphorylating T-cell receptor (TCR) and CD8 molecules during direct interaction with T cells, which results in the downregulation of immune activity (33, 34). In addition, VEGF produced by MDSCs promotes tumor angiogenesis, creates a pre-metastasis environment, and

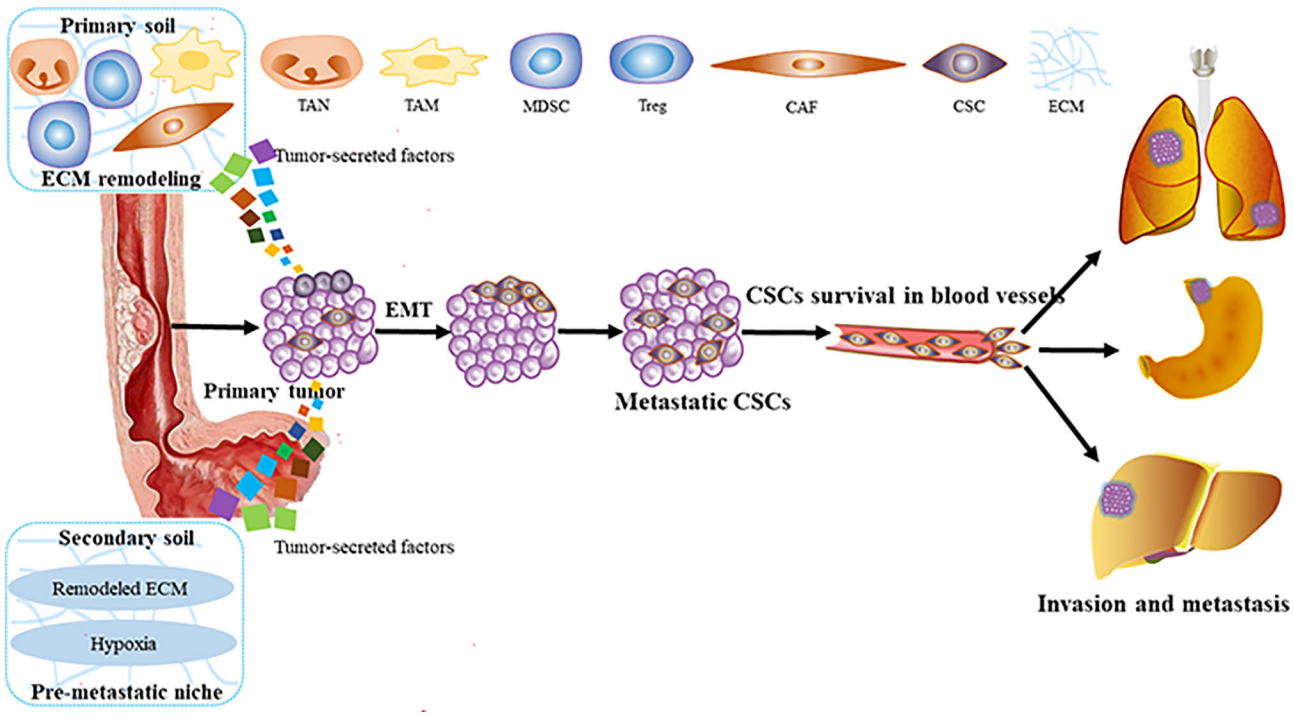

FIGURE 1 | The process of ESCC invasion and metastasis. ESCC, esophageal squamous carcinoma; MDSC, marrow-derived suppressor cell; Tregs, regulatory T cells; CAFS, cancer associated fibroblasts; EMT, epithelial—mesenchymal transition; TAM, tumor-associated macrophage; TAN, tumor-related neutrophil; ECM, extracellular matrix; CSCs, cancer stem cells.

prolongs immunosuppression (35, 36). Furthermore, it has been demonstrated recently that MDSCs could paralyze T cells by cell–cell transfer of the metabolite methylglyoxal, which would reduce the antitumor immunity of T cells and promote invasion and metastasis (37). Further research into the biology of MDSCs, especially the functions of specific population cells, will provide directions for therapeutic development.

3.1.2 Regulatory T Cells

Tregs, a subgroup of $CD4^+$ helper T cells identified by CD25 and Foxp3 expression, play an immunosuppressive role in cancer. Tregs attenuate antitumor immunity by secreting immunosuppressive cytokines, interfering with tumor-associated antigen presentation, and inhibiting cytotoxic cell function (38, 39). It has been demonstrated that Foxp3 expression in ESCC means a poor prognosis (40, 41). It is reported that FOXP3 might directly inhibit the IL-2 and promote cytotoxic T lymphocyte-associated antigen 4 (CTLA4) and CD25 expression (42). In ESCC, increased recruitment of Tregs is mediated, at least in part, by chemokines CCL17 and CCL22, secreted by tumor cells and macrophages (43). It has been reported that IL-33, which has a high expression in ESCC, could promote CCL2 expression *via* the NF-κB pathway and then recruit Tregs to promote ESCC migration (44, 45). Treg infiltration has been found to be prognostic, and more Tregs are often associated with deeper tumor invasion, extensive metastasis, and reduced survival (46, 47). Tregs have several context-dependent functions that are not well described, which poses challenges for ESCC invasion and migration.

3.1.3 Tumor-Associated Macrophages

Tumor-associated macrophages (TAMs) promote various pro-tumor mechanisms. Macrophages are classified into M1 and M2 types, of which M2 macrophages secreted type II cytokines to facilitate various pro-tumorigenic mechanisms (48). The specific markers of TAMs are most often identified by expression of iNOS for M1 type and CD163 for M2 type. Hypoxia can induce M2 polarization, and then TAMs will produce growth factors and proteases that promote tumorigenesis and inhibit the immune system, angiogenesis, invasion, and metastasis (49, 50). $CD68^+$ $PD\text{-}1^+$ TAMs in ESCC TME tend to be of M2 phenotype, which can result in the upregulation of PD-L1 expression in tumor cells and promote ESCC invasion and migration (51, 52). Activation of the AKT/ERK pathway is a driving force for ESCC cell invasion and migration, and this pathway can be triggered by a variety of factors produced by TAMs or cancer cells themselves (53, 54). $CD163^+$ TAMs can also promote ESCC cell invasion and migration by releasing thymidine phosphorylase (TP) to augment angiogenesis and produce IL-1β to enhance EMT (55, 56). The M2/M1 macrophage ratio of ESCC patients has also been used as a predictor of lymph node metastasis (57). All of these suggest potential intervention and immunotherapy strategies for TAMs in the invasion and migration of ESCC patients.

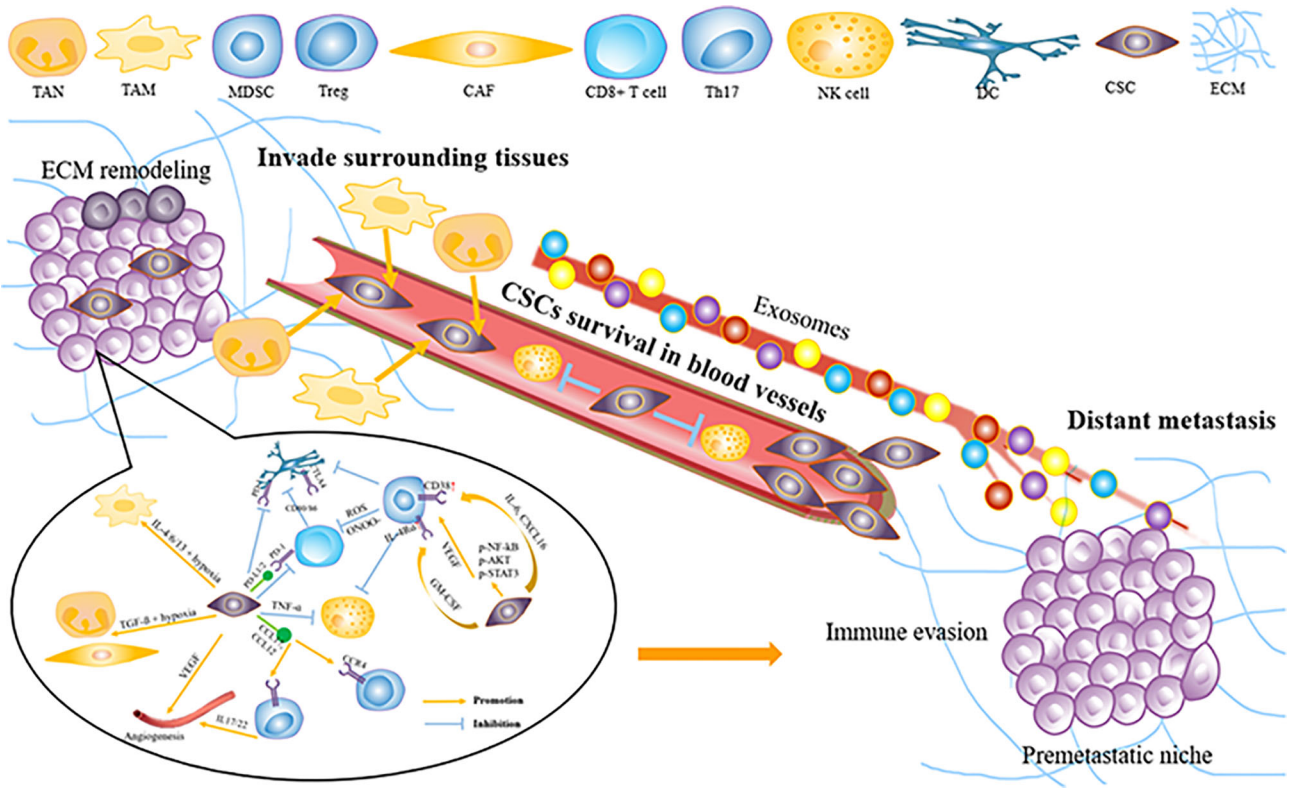

FIGURE 2 | How tumor microenvironment support ESCC invasion and metastasis. ESCC, esophageal squamous carcinoma; MD.SC, man-our-derived suppressor cell; DC, dendritic cell; Treg, regulatory T cell; CAE, Cancer associated fibroblast; VEGF, vascular endothelial growth factor; NK cell, natural killer cell; TAM, tumor-associated macrophage; TAN, tumor-related neutrophil; ECM, extracellular matrix; CSCs, cancer Stem cells.

3.1.4 Tumor-Associated Neutrophils

Tumor-associated neutrophils (TANs) are completely different from circulating neutrophils (58). Transforming growth factor-β (TGF-β) in TME promotes the transformation of neutrophils from antitumor N1 to pro-tumor N2 (59). Unlike M1 and M2, there is no suitable marker to indicate the N1 and N2 neutrophils in the tumor (60). The study of TANs mainly focuses on the neutrophil-to-lymphocyte ratio (NLR) (60). It has been reported that preoperative NLR elevation was associated with lymph node metastasis, deeper tumor invasion, and advanced TNM stage (61). Neutrophils will undergo apoptosis after activation, forming neutrophil extracellular traps (NETs), which have been shown to predict the lymph node and distant metastasis (62, 63). All of these indicate that TANs can be a good predictor of ESCC invasion and migration.

3.1.5 Mast Cells and Eosinophils

Mast cells (MCs) and eosinophils often co-participate in response to parasitic infections and allergic diseases (64). In the TME of ESCC, high MC density has been found to be closely associated with tumor angiogenesis, invasion, and metastasis and predicts poor survival in ESCC patients (65, 66). It is reported that trypsin release from MCs promotes tumor cell metastasis through exosomes (67). Yet the high expression of eosinophils has been reported to be positively associated with low rates of metastasis in early ESCC patients (68). Also, it has been reported recently that metastasis-entrained eosinophils could promote lymphocyte-mediated antitumor immunity (69). A large number of new studies are needed for the mechanism of eosinophil in ESCC, which will provide new ideas for the ESCC invasion and metastasis and eosinophil-based immunotherapy.

3.1.6 Th17 Lymphocytes

Th17 lymphocytes are a branch of $CD4^+$ helper T cells, and IL-17 is its main effector molecule. IL-17A expressed by Th17 cells can induce the production of chemokines in ESCC cells, such as CCL20, CXCL-9, CXCL-10, and CXCL13 (70, 71). These chemokines could promote the proliferation and differentiation of Th17 lymphocytes in ESCC TME (72). Also, increased Th17 lymphocytes are positively associated with more lymph node metastasis (73). It has been reported that IL-17A can activate MMP-2 and MMP-9 through the ROS/NF-κB signaling pathway (74), while matrix metalloproteinases (MMPs) could catalyze the degradation of extracellular matrix and promote ESCC migration and metastasis (75, 76). The role of Th17 lymphocytes in ESCC invasion and metastasis needs to be further investigated.

3.2 Stromal Components Facilitate Esophageal Squamous Cell Carcinoma Invasion and Metastasis

In addition to immune cells, stromal components and CAFs play a critical role in ESCC invasion and metastasis (77) (**Figure 2**). Fibroblast activation protein-α (FAP) and α-smooth muscle actin (α-SMA) are often used as the markers for the activated phenotype of CAFs, of which the process is induced by ESCC secreting TGF-β (78, 79).

CAFs have been proved to promote ESCC invasion and metastasis by secretion of cytokines, induction of EMT, recruitment of immune cells, and other mechanisms to reconstruct TME (80). IL-6 secreted by FAP^+ CAFs not only can promote ESCC cell invasion and EMT but also can recruit $FoxP3^+$ T cells and induce TAM M2 polarization to promote metastasis (81, 82). The presence of CAFs in ESCC patients is associated with increased micro-vessel density, TAMs, and EMT, which are critical for ESCC invasion and metastasis (83, 84). A number of genes have been shown to promote ESCC invasion and metastasis *via* the CAF transformation and EMT process (85, 86). Also, it has been demonstrated that CAFs promote ESCC invasion by secreting hepatocyte growth factor (HGF) and infiltrating MDSCs (87, 88). Also, CAFs have been reported to be associated with low 3-year survival and ESCC progression after chemoradiotherapy (89). FAP-α has been reported to be an important regulator in ESCC lymph node metastasis (90). HGF and TGF-β are closely related to tumor invasion and metastasis (91). It has been demonstrated that CAFs could express HGF and TGF-β1 and then promote ESCC invasion and metastasis *via* the HGF/Met and TGFβ1/Smad pathways, respectively (92, 93). It has been confirmed that infiltrating MDSCs activate CAFs to promote ESCC invasion (94). Interaction between CAFs and immune cells to promote ESCC invasion and metastasis needs further research.

Due to the high heterogeneity of ESCC, traditional genomic and transcriptome analyses tend to ignore some signals displayed by specific cell populations or cell states. However, with the development of single-cell sequencing technology, several single-cell studies about ESCC and TME have been published in recent years. It has been reported that single-cell transcriptome sequencing was performed in 11 ESCC patients to analyze the TME. Heterogeneity was found in most ESCC interstitial cell types, particularly between fibroblasts and immune cells. Also, tumor-specific $CST1^+$ myofibroblast subpopulations had been identified to have prognostic values and potential biological significance (95). Also, the main association framework between cancer cells and various non-cancer cells in TME has been established *via* single-cell transcriptome sequencing, which contributes to the further investigation of ESCC progression and prognosis (96). Furthermore, a comparison between esophagus non-malignant tissues and ESCC tissues *via* single-cell transcriptome network analysis has shown that energy supply-related pathways are pivotal in cancer metabolic reprogramming for TME. Immune checkpoints, which are potential targets for ESCC immunotherapy, have been found to be significantly overexpressed in ESCC, including LAG3 and HAVCR2 (97). At present, there are no single-cell studies specifically for ESCC invasion and metastasis, which needs further investigation.

4 THE ROLE OF CELLULAR COMMUNICATION IN ESOPHAGEAL SQUAMOUS CELL CARCINOMA INVASION AND METASTASIS

4.1 Tumor Cells Remodel Tumor Microenvironment to Promote Esophageal Squamous Cell Carcinoma Invasion and Metastasis

4.1.1 Cytokine/Chemokine Network

Metastasis is a multistep process that requires tumor cells to separate from the primary tumor and migrate through the lymphatic or blood circulatory system to target distant organs (98). There is increasing evidence that primary tumors can prepare the cytokine/chemokine network for invasion and metastasis (99, 100) (**Figure 2**).

CXCL12 is a chemokine that functions through CXCR4 and plays an important role in ESCC invasion and metastasis (101). It is noteworthy that CXCR4 is expressed only in ESCC tissues but not in the normal esophageal epithelium (102). Expression of CXCL12 or CXCR4 in ESCC patients is significantly related to ESCC invasion, lymph node metastasis, and poor survival (103, 104). It has been shown that ESCC cells could secrete large amounts of CXCL12 *via* an autocrine way and increase their receptor CXCR4 expression compared with normal cells (105). Also, ESCC cells could enhance the activation of the p-ERK1/2 pathway *via* the CXCL12/CXCR4 axis to promote ESCC invasion and metastasis (106).

It has been reported that CCR7, combined with CCL21, supports a metastatic niche directly (107). A number of studies have shown that high levels of CCR7 are related to ESCC metastasis and poor survival (108). It has been investigated that co-expressed CCR7 and MUC1 could facilitate ESCC invasion and metastasis *via* the ERK1/2 pathway (109, 110). Some studies have also demonstrated that there is an interaction between CCR7 and VEGF-C, and their expression can be used as the predictor for ESCC lymphatic metastasis (111).

Many studies have indicated that high levels of CXCL8 and CXCR2 in ESCC patients are associated with metastasis and poor prognosis (112). It has been shown that CXCL8 is upregulated in TAMs and promotes ESCC invasion and metastasis *via* CXCR1/CXCR2 receptors to activate AKT and ERK1/2 signaling pathways (52). Also, a clinical study has shown that CXCL8 expression is significantly associated with metastasis and the increase of CXCR2- and CD204-positive macrophages (108, 113). It is necessary to further investigate the biological significance of cytokine/chemokine networks in ESCC and their potential use as future drug targets.

4.1.2 Exosome

Exosomes are nanovesicles (30–150-nm diameter) that are secreted by various cell types (114). Recently, it has been shown that exosomes play important roles in ESCC invasion and metastasis (115). It is reported that exosomes released by ESCC can enrich miR-320b and promote ESCC lymph node metastasis *via* programmed cell death 4 (PDCD4) through the AKT signaling pathway (116). Exosome-shuttling miR-21 has been shown to promote ESCC invasion and metastasis by targeting PDCD4 *via* the c-Jun N-terminal kinase (JNK) signaling pathway (117). Clinical data have also displayed that serum exosomal hsa_circ_0026611 expression is significantly upregulated with ESCC lymph node metastasis (118). Exosome long non-coding RNA (lncRNA) LINC01711 promotes ESCC invasion *via* FSCN1 upregulation and miR-326 downregulation (119). Also, it has been reported that T cell-derived exosomes promote ESCC metastasis *via* promoting EMT by β-catenin and NF-κB/snail signaling pathways upregulation (120). However, there is still a long way to the mechanisms of how these exosomes are involved in ESCC invasion and metastasis.

4.1.3 Vascular Endothelial Growth Factor

VEGF is the key mediator of angiogenesis, which has the function of triggering endothelial cell proliferation, migration, and breakdown of the extracellular matrix for new blood vessels. It has been reported that when tumor cells overexpressing HMGB1 co-cultured with B cells, the proliferating B cells can be induced to express VEGF and then elevate angiogenesis (121). A significant decrease in VEGF-C has been found in high tumor lymphocytic infiltration (122). It is reported that low expression of CD80 can be associated with VEGF overexpression. CD80 impairment in the ESCC tissues is correlated with poor survival, which indicates the dysfunction of the immune system and promotes the ESCC progression (123). Some studies have confirmed that VEGF-C, a lymphangiogenic factor, is associated with survival, tumor depth, stage, and lymph node metastasis of ESCC (124, 125). Also, many genes have been reported to promote ESCC invasion and metastasis *via* VEGF-related pathways or axis (126, 127). Development of new angiogenesis inhibitors and regulation of tumor vascular microenvironment are still possible ways to treat ESCC invasion and metastasis.

4.2 The Interaction Between Immune Cells Promotes Esophageal Squamous Cell Carcinoma Invasion and Metastasis

In addition to the interaction between various immune cells and ESCC cells, there is an important interaction among various immune cells, which indirectly promotes ESCC invasion and metastasis. For example, Th-2 could secrete many cytokines (IL-6 and IL-13) to recruit MDSCs in the ESCC TME (128, 129). Also, IL-4 and IL-13 derived from Th-2 could promote macrophages polarizing into M2 macrophages (130). MDSCs with high CD38 levels have been reported to inhibit the cytotoxic effect of ESCC-activated T cells (131). MDSCs could also induce Tregs and CAFs to inhibit the antigen-presenting cells (APCs) and indirectly inhibit the cytotoxic effect of ESCC-activated T cells (42, 132). In addition, ESCC cells could produce RCAS1 to induce DC, promote tumor-infiltrating lymphocyte apoptosis, and inhibit $CD8^+$ T-cell activity (133). IL-17A-producing cells could enhance $CD1a^+$ DC infiltration of TME *via* the release of CCL2 or CCL20, which is associated with better survival in ESCC patients (134). Th17 cells and MCs in ESCC TME have been shown to secrete IL-17 to promote ESCC cells to release CXCL9/10, CXCL2/3, and CCL2/20, which could facilitate NK cell infiltration and activity (66). PD-1, a member of the CD28 family, is mainly expressed on activated T cells (135). When PD-1 is combined with its ligand (PD-L1 or PD-L2), which can be expressed by tumor cells, immune cells (i.e., macrophages), and endothelial cells, then T-cell activation will be inhibited (136, 137). TME contains a variety of immune cells, which form a complex regulatory network through receptor-ligand binding or the release of various immune factors, thus affecting the invasion and metastasis of ESCC.

5 TARGETING TUMOR MICROENVIRONMENT FOR ESOPHAGEAL SQUAMOUS CELL CARCINOMA INVASION AND METASTASIS

Targeting approaches using different methods to remodel the TME and then inhibit ESCC invasion and metastasis are discussed as follows (**Figure 3**).

5.1 Targeting Angiogenesis for Esophageal Squamous Cell Carcinoma Invasion and Metastasis

Angiogenesis plays a crucial role in the development of ESCC, by delivering oxygen and nutrients to tumors, and its key mediator is VEGF (138). Distant vascular metastasis is another way of tumor progression. Many VEGF/VEGFR inhibitors have been developed to induce vascular normalization and make patients more sensitive to chemotherapy (139). It has been found that low doses of VEGF inhibitor (apatinib) could regulate the TME, relieve hypoxia, and increase the number of T cells at the tumor site, thereby enhancing the efficacy of PD-1/PD-L1 inhibitors, while excessive doses do not produce such an effect (140). However, this theory has not been tested in ESCC. The development of new angiogenesis inhibitors and regulation of vascular TME are still possible ways to avoid ESCC invasion and metastasis.

5.2 Targeting Immune Markers for Esophageal Squamous Cell Carcinoma Invasion and Metastasis

5.2.1 Immune Checkpoint Inhibitors

PD-1 is an immune checkpoint that inactivates T-cell immune function. Its two ligands, PD-L1 and PD-L2, combined with the PD-1 receptor, could induce depletion of PD-1 signaling pathways and associated T cells and inhibit T-cell activation and proliferation reversibly (141). Many studies have reported

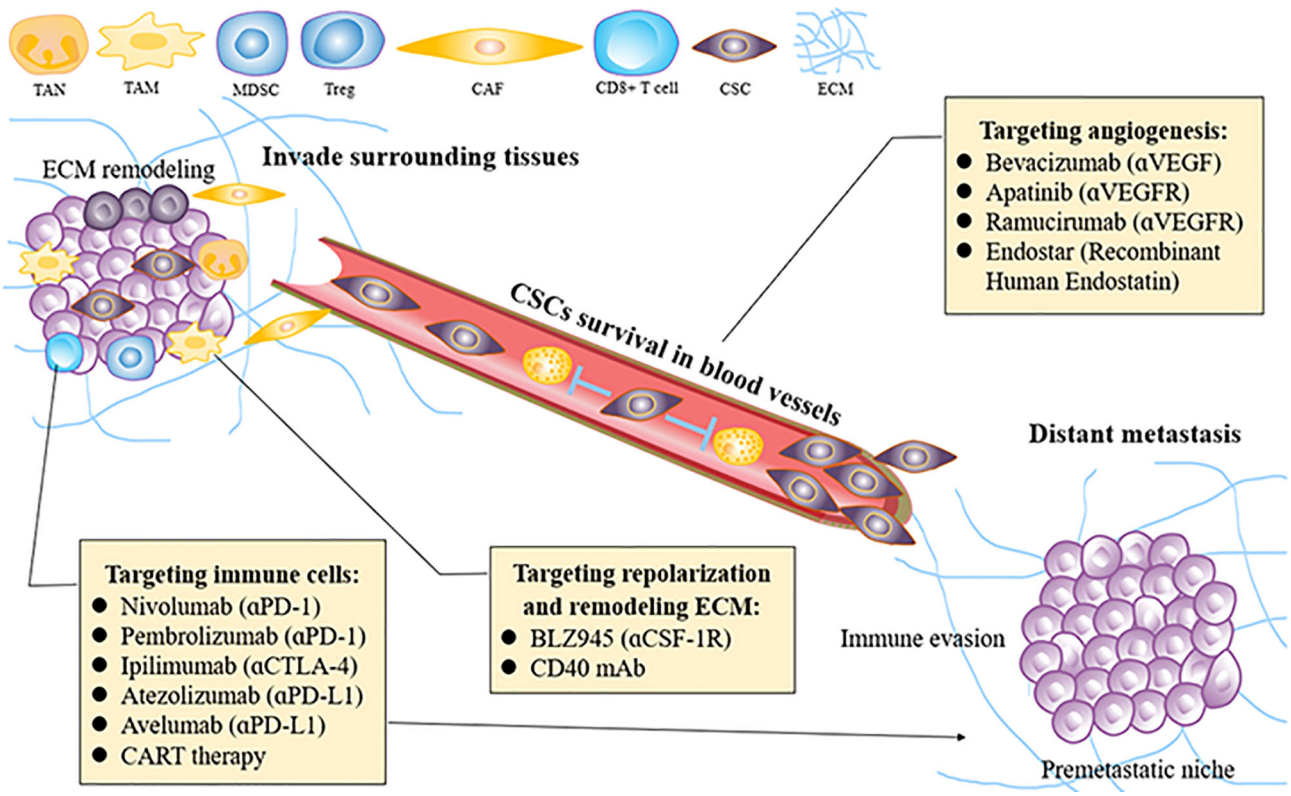

FIGURE 3 | How to re-educate the tumor microenvironment for treating ESCC invasion and metastasis. ESCC, esophageal squamous carcinoma; MDSC, mallow-derived suppressor cell; Treg, regulatory T cell; CAF, cancer associated fibroblast; VEGF, vascular endothelial growth factor; TAM, tumor-associated macrophage; TAN, tumor-related neutrophil; ECM, extracellular matrix; CSCs, cancer stem cells; PID-1, programmed cell death protein 1; CTLA4, T lymphocyte-associated antigen 4; CSF-1, colony-stimulating factor-1.

that the expression of both PD-L1 and PD-L2 is elevated in ESCC. In fact, in ESCC patients, increased PD-L1 or PD-L2 expression in ESCC cells is correlated with reduced survival, while increased PD-L1 expression is associated with increased depth of tumor invasion and worse survival (142, 143). In addition, the expression of PD-L2 is related to decreased $CD8^+$ T-cell infiltration. The increased PD-L2 expression is induced by tumor-promoting Th2 cytokines such as IL-13 or IL-4 (144).

The expression of CTLA4 is another immune checkpoint that inactivates by inhibiting TCR signaling (145). CTLA4 is expressed not only in tumor-infiltrating immune cells but also in cancer cells, which is a key part of immune escape (146). Existing evidence already suggests that PD-1 inhibitors show therapeutic promise in lung cancer and melanoma and might also be used in ESCC (147). Also, many studies are targeted at how to regulate other immune cells in TME to improve the efficacy of immunotherapy (148, 149).

5.2.2 Other Immune Cells

TAMs can produce a variety of tumor-promoting factors, such as colony-stimulating factor-1 (CSF-1), so they might be attractive targets for remodeling immune responses within TME (150). In recent years, targeting TAM therapies such as CSF-1 or CSF-1R blockade have attracted extensive attention in tumor research. The combination of CSF-1R blockade and PD-1/PD-L1 inhibitors is underway (NCT02323191) (151). IL-6 secreted by FAP^+ CAFs not only can promote ESCC cell invasion and EMT but also can recruit $FoxP3^+$ T cells and induce TAM M2 polarization to promote metastasis (81, 82). Using CAF-targeted NIR-PIT to eliminate CAFs could interfere with ESCC invasion and metastasis effectively. The combination of the CAF-targeted NIR-PIT with traditional anticancer drugs might be a promising choice (152).

5.3 T-Cell Modification for Esophageal Squamous Cell Carcinoma Invasion and Metastasis

Chimeric antigen receptor (CAR) T-cell therapy means that T cells are modified into CAR T cells by genetic engineering to specifically recognize and attack tumor cells (153). Ephrin type A receptor 2 (EphA2) and HER-2, highly expressed in ESCC, are common targets of CAR T-cell therapy and have been verified to effectively kill esophageal cancer cells (154, 155). Enhanced MUC1-CAR T cells have been shown to have better antitumor activity because they can survive longer *in vivo*, which means they have long-lasting antitumor effects (156). Also, it has been recently reported that IDO1 inhibitor-loaded nanosheets could enhance CAR T-cell

effectiveness in ESCC and CD276 suppress CAR T-cell function (157, 158). The selection of different solid tumor-specific antigens and the delivery of CAR T cells are still the disadvantages of CAR T-cell therapy (159).

6 CONCLUSION

In this review, we have summarized how ESCC invasion and metastasis occur and discussed how the major cell populations, stromal components, and their interaction in the TME promote ESCC invasion and metastasis. Also, we summarized recent therapies targeting TME for ESCC invasion and metastasis. Looking forward, it is critical to further investigate how cancer cells transfer to the new environment and adapt surrounding cells and components into a suitable environment for tumor invasion and metastasis. At present, there are few diagnostic methods and new drugs targeted for ESCC invasion and metastasis. Advances in these areas promise improved treatment options and better outcomes for this deadly disease.

AUTHOR CONTRIBUTIONS

XYG and BLL supervised and reviewed the manuscript. SYZ conducted the literature review and wrote the manuscript. All authors contributed to the article and approved the submitted version.

FUNDING

This work was supported by grants from the Hong Kong Research Grant Council (RGC) grants including Collaborative Research Funds (C7065-18GF, C7026-18GF, and C4039-19GF), Research Impact Funds (R4017-18, R1020-18F, and R7022-20), Shenzhen Fundamental Research Program (JCYJ20180508 153249223), The Shenzhen Science and Technology program (KQTD20180411185028798), and the Program for Guangdong Introducing Innovative and Entrepreneurial Teams (2019BT02Y198). XYG is the Sophie YM Chan Professor in Cancer Research.

REFERENCES

1. Bray F, Ferlay J, Soerjomataram I, Siegel RL, Torre LA, Jemal A, et al. Global Cancer Statistics 2018: GLOBOCAN Estimates of Incidence and Mortality Worldwide for 36 Cancers in 185 Countries. *CA Cancer J Clin* (2018) 68 (6):394–424. doi: 10.3322/caac.21492
2. Ajani JA, D'Amico TA, Bentrem DJ, Chao J, Corvera C, Das P, et al. Esophageal and Esophagogastric Junction Cancers, Version 2.2019, NCCN Clinical Practice Guidelines in Oncology. *J Natl Compr Canc Netw* (2019) 17 (7):855–83. doi: 10.6004/jnccn.2019.0033
3. Creemers A, Ebbing EA, Hooijer GKJ, Stap L, Jibodh-Mulder RA, Gisbertz SS, et al. The Dynamics of HER2 Status in Esophageal Adenocarcinoma. *Oncotarget* (2018) 9(42):26787–99. doi: 10.18632/oncotarget.25507
4. Barsouk A, Rawla P, Hadjinicolaou AV, Aluru JS, Barsouk A. Targeted Therapies and Immunotherapies in the Treatment of Esophageal Cancers. *Med Sci (Basel)* (2019) 7(10):100. doi: 10.3390/medsci7100100
5. Siegel RL, Miller KD, Jemal A. Cancer Statistics, 2019. *CA Cancer J Clin* (2019) 69(1):7–34. doi: 10.3322/caac.21551
6. Jin Z, Chen D, Chen M, Wang C, Zhang B, Zhang J, et al. Neoadjuvant Chemoradiotherapy Is Beneficial to the Long-Term Survival of Locally Advanced Esophageal Squamous Cell Carcinoma: A Network Meta-Analysis. *World J Surg* (2022) 46(1):136–46. doi: 10.1007/s00268-021-06301-2
7. Guccione C, Yadlapati R, Shah S, Shah S, Knight R, Curtius K, et al. Challenges in Determining the Role of Microbiome Evolution in Barrett's Esophagus and Progression to Esophageal Adenocarcinoma. *Microorganisms* (2021) 9(10):2003. doi: 10.3390/microorganisms9102003
8. Klein S, Duda DG. Machine Learning for Future Subtyping of the Tumor Microenvironment of Gastro-Esophageal Adenocarcinomas. *Cancers (Basel)* (2021) 13(19):4919. doi: 10.3390/cancers13194919
9. Nienhüser H, Wirsik N, Schmidt T. Esophageal Tumor Microenvironment. *Adv Exp Med Biol* (2020) 1296:103–16. doi: 10.1007/978-3-030-59038-3_6
10. Han P, Cao P, Hu S, Kong K, Deng Y, Zhao B, et al. Esophageal Microenvironment: From Precursor Microenvironment to Premetastatic Niche. *Cancer Manag Res* (2020) 12:5857–79. doi: 10.2147/CMAR.S258215
11. Wang L, Han H, Wang Z, Shi L, Yang M, Qin Y, et al. Targeting the Microenvironment in Esophageal Cancer. *Front Cell Dev Biol* (2021) 9:684966. doi: 10.3389/fcell.2021.684966
12. Lv X, Xu G. Regulatory Role of the Transforming Growth Factor-β Signaling Pathway in the Drug Resistance of Gastrointestinal Cancers. *World J Gastrointest Oncol* (2021) 13(11):1648–67. doi: 10.4251/wjgo.v13.i11.1648
13. Cheung KJ, Ewald AJ. A Collective Route to Metastasis: Seeding by Tumor Cell Clusters. *Science* (2016) 352(6282):167–9. doi: 10.1126/science.aaf6546
14. Doglioni G, Parik S, Fendt SM. Interactions in the (Pre)metastatic Niche Support Metastasis Formation. *Front Oncol* (2019) 9:219. doi: 10.3389/fonc.2019.00219
15. Akhtar M, Haider A, Rashid S, Al-Nabet ADMH. Paget's "Seed and Soil" Theory of Cancer Metastasis: An Idea Whose Time has Come. *Adv Anat Pathol* (2019) 26(1):69–74. doi: 10.1097/PAP.0000000000000219
16. Wortzel I, Dror S, Kenific CM, Lyden D. Exosome-Mediated Metastasis: Communication From a Distance. *Dev Cell* (2019) 49(3):347–60. doi: 10.1016/j.devcel.2019.04.011
17. Sun H, Meng Q, Shi C, et al. Hypoxia-Inducible Exosomes Facilitate Liver-Tropic Premetastatic Niche in Colorectal Cancer. *Hepatology* (2021) 74 (5):2633–51. doi: 10.1002/hep.32009
18. Tang F, Tie Y, Hong W, Wei Y, Tu C, Wei X, et al. Targeting Myeloid-Derived Suppressor Cells for Premetastatic Niche Disruption After Tumor Resection. *Ann Surg Oncol* (2021) 28(7):4030–48. doi: 10.1245/s10434-020-09371-z
19. Paiva AE, Lousado L, Guerra DAP, Azevedo PO, Sena IFG, Andreotti JP, et al. Pericytes in the Premetastatic Niche. *Cancer Res* (2018) 78(11):2779–86. doi: 10.1158/0008-5472.CAN-17-3883
20. Maughan BL, Pal SK, Gill D, Boucher K, Martin C, Salgia M, et al. Modulation of Premetastatic Niche by the Vascular Endothelial Growth Factor Receptor Tyrosine Kinase Inhibitor Pazopanib in Localized High-Risk Prostate Cancer Followed by Radical Prostatectomy: A Phase II Randomized Trial. *Oncologist* (2018) 23(12):1413–e151. doi: 10.1634/theoncologist.2018-0652
21. Kwa MQ, Herum KM, Brakebusch C. Cancer-Associated Fibroblasts: How Do They Contribute to Metastasis? *Clin Exp Metastasis* (2019) 36(2):71–86. doi: 10.1007/s10585-019-09959-0
22. Chen D, Mao Y, Zheng Y, Wen J, Song P, Xue Y, et al. Extracapsular Lymph Node Involvement Is a Robust Survival Predictor in Esophageal Cancer Patients: A Pooled Analysis. *Eur J Surg Oncol* (2021) 47(8):1875–82. doi: 10.1016/j.ejso.2021.03.247
23. Rani P, Gupta AJ, Mehrol C, Singh M, Khurana N, Passey JC, et al. Clinicopathological Correlation of Tumor-Stroma Ratio and Inflammatory Cell Infiltrate With Tumor Grade and Lymph Node Metastasis in Squamous

Cell Carcinoma of Buccal Mucosa and Tongue in 41 Cases With Review of Literature. *J Cancer Res Ther* (2020) 16(3):445–51. doi: 10.4103/0973-1482.193113
24. Patel S, Raghavan S, Prem A. Prognostic Impact of Pathological Response in Lymph Nodes in Esophageal Squamous Cell Cancers: Is It Over-Rated? *Eur J Surg Oncol* (2021) 47(11):2959. doi: 10.1016/j.ejso.2021.07.031
25. Zhong J, Wang K, Fang S, Fu J. Prognostic Impact of Sterilized Lymph Nodes in Esophageal Squamous Cell Carcinomas After Neoadjuvant Chemoradiotherapy. *Eur J Surg Oncol* (2021) 47(12):3074–80. doi: 10.1016/j.ejso.2021.04.026
26. Otto B, Koenig AM, Tolstonog GV, Jeschke A, Klaetschke K, Vashist YK, et al. Molecular Changes in Pre-Metastatic Lymph Nodes of Esophageal Cancer Patients. *PloS One* (2014) 9(7):e102552. doi: 10.1371/journal.pone.0102552
27. Wakita A, Motoyama S, Sato Y, Kawakita Y, Nagaki Y, Terata K, et al. Evaluation of Metastatic Lymph Nodes in Cn0 Thoracic Esophageal Cancer Patients With Inconsistent Pathological Lymph Node Diagnosis. *World J Surg Oncol* (2020) 18(1):111. doi: 10.1186/s12957-020-01880-1
28. Zhou L, Zhao Y, Zheng Y, Wang M, Tian T, Lin S, et al. The Prognostic Value of the Number of Negative Lymph Nodes Combined With Positive Lymph Nodes in Esophageal Cancer Patients: A Propensity-Matched Analysis. *Ann Surg Oncol* (2020) 27(6):2042–50. doi: 10.1245/s10434-019-08083-3
29. Ma T, Renz BW, Ilmer M, Koch D, Yang Y, Werner J, et al. Myeloid-Derived Suppressor Cells in Solid Tumors. *Cells* (2022) 11(2):310. doi: 10.3390/cells11020310
30. Xu J, Peng Y, Yang M, Guo N, Liu H, Gao H, et al. Increased Levels of Myeloid-Derived Suppressor Cells in Esophageal Cancer Patients is Associated With the Complication of Sepsis. *BioMed Pharmacother* (2020) 125:109864. doi: 10.1016/j.biopha.2020.109864
31. Hegde S, Leader AM, Merad M. MDSC: Markers, Development, States, and Unaddressed Complexity. *Immunity* (2021) 54(5):875–84. doi: 10.1016/j.immuni.2021.04.004
32. Li R, Jia Z, Trush MA. Defining ROS in Biology and Medicine. *React Oxyg Species (Apex)* (2016) 1(1):9–21. doi: 10.20455/ros.2016.803
33. Zhou H, Yang P, Li H, Zhang L, Li J, Zhang T, et al. Carbon Ion Radiotherapy Boosts Anti-Tumour Immune Responses by Inhibiting Myeloid-Derived Suppressor Cells in Melanoma-Bearing Mice. *Cell Death Discovery* (2021) 7(1):332. doi: 10.1038/s41420-021-00731-6
34. Wang Y, Sun H, Zhu N, Wu X, Sui Z, Gong L, et al. Myeloid-Derived Suppressor Cells in Immune Microenvironment Promote Progression of Esophagogastric Junction Adenocarcinoma. *Front Oncol* (2021) 11:640080. doi: 10.3389/fonc.2021.640080
35. Ren Y, Dong X, Zhao H, Feng J, Chen B, Zhou Y, et al. Myeloid-Derived Suppressor Cells Improve Corneal Graft Survival Through Suppressing Angiogenesis and Lymphangiogenesis. *Am J Transpl* (2021) 21(2):552–66. doi: 10.1111/ajt.16291
36. Horikawa N, Abiko K, Matsumura N, Hamanishi J, Baba T, Yamaguchi K, et al. Expression of Vascular Endothelial Growth Factor in Ovarian Cancer Inhibits Tumor Immunity Through the Accumulation of Myeloid-Derived Suppressor Cells. *Clin Cancer Res* (2017) 23(2):587–99. doi: 10.1158/1078-0432.CCR-16-0387
37. Baumann T, Dunkel A, Schmid C, Schmitt S, Hiltensperger M, Lohr K, et al. Regulatory Myeloid Cells Paralyze T Cells Through Cell-Cell Transfer of the Metabolite Methylglyoxal. *Nat Immunol* (2020) 21(5):555–66. doi: 10.1038/s41590-020-0666-9
38. Huppert LA, Green MD, Kim L, Chow C, Leyfman Y, Daud AI, et al. Tissue-Specific Tregs in Cancer Metastasis: Opportunities for Precision Immunotherapy. *Cell Mol Immunol* (2022) 19(1):33–45. doi: 10.1038/s41423-021-00742-4
39. Yan S, Zhang Y, Sun B. The Function and Potential Drug Targets of Tumour-Associated Tregs for Cancer Immunotherapy. *Sci China Life Sci* (2019) 62(2):179–86. doi: 10.1007/s11427-018-9428-9
40. Xue L, Lu HQ, He J, Zhao XW, Zhong L, Zhang ZZ, et al. Expression of FOXP3 in Esophageal Squamous Cell Carcinoma Relating to the Clinical Data. *Dis Esophagus* (2010) 23(4):340–6. doi: 10.1111/j.1442-2050.2009.01013.x
41. Wang G, Liu G, Liu Y, Liu Y, Li X, Su Z, et al. FOXP3 Expression in Esophageal Cancer Cells Is Associated With Poor Prognosis in Esophageal Cancer. *Hepatogastroenterology* (2012) 59(119):2186–91. doi: 10.5754/hge11961
42. Shitara K, Nishikawa H. Regulatory T Cells: A Potential Target in Cancer Immunotherapy. *Ann N Y Acad Sci* (2018) 1417(1):104–15. doi: 10.1111/nyas.13625
43. Chen BJ, Zhao JW, Zhang DH, Zheng AH, Wu GQ. Immunotherapy of Cancer by Targeting Regulatory T Cells. *Int Immunopharmacol* (2022) 104:108469. doi: 10.1016/j.intimp.2021.108469
44. Yue Y, Lian J, Wang T, Luo C, Yuan Y, Qin G, et al. Interleukin-33-Nuclear Factor-κb-CCL2 Signaling Pathway Promotes Progression of Esophageal Squamous Cell Carcinoma by Directing Regulatory T Cells. *Cancer Sci* (2020) 111(3):795–806. doi: 10.1111/cas.14293
45. Cui G, Li Z, Ren J, Yuan A. IL-33 in the Tumor Microenvironment is Associated With the Accumulation of FoxP3-Positive Regulatory T Cells in Human Esophageal Carcinomas. *Virchows Arch* (2019) 475(5):579–86. doi: 10.1007/s00428-019-02579-9
46. Nabeki B, Ishigami S, Uchikado Y, Sasaki K, Kita Y, Okumura H, et al. Interleukin-32 Expression and Treg Infiltration in Esophageal Squamous Cell Carcinoma. *Anticancer Res* (2015) 35(5):2941–7.
47. Lian J, Liu S, Yue Y, Yang Q, Zhang Z, Yang S, et al. Eomes Promotes Esophageal Carcinoma Progression by Recruiting Treg Cells Through the CCL20-CCR6 Pathway. *Cancer Sci* (2021) 112(1):144–54. doi: 10.1111/cas.14712
48. Zhu S, Yi M, Wu Y, Dong B, Wu K, et al. Roles of Tumor-Associated Macrophages in Tumor Progression: Implications on Therapeutic Strategies. *Exp Hematol Oncol* (2021) 10(1):60. doi: 10.1186/s40164-021-00252-z
49. Zou Y, Zhang J, Xu J, Fu L, Xu Y, Wang X, et al. SIRT6 Inhibition Delays Peripheral Nerve Recovery by Suppressing Migration, Phagocytosis and M2-Polarization of Macrophages. *Cell Biosci* (2021) 11(1):210. doi: 10.1186/s13578-021-00725-y
50. Quail DF, Joyce JA. Microenvironmental Regulation of Tumor Progression and Metastasis. *Nat Med* (2013) 19(11):1423–37. doi: 10.1038/nm.3394
51. Kodaira H, Koma YI, Hosono M, Higashino N, Suemune K, Nishio M, et al. ANXA10 Induction by Interaction With Tumor-Associated Macrophages Promotes the Growth of Esophageal Squamous Cell Carcinoma. *Pathol Int* (2019) 69(3):135–47. doi: 10.1111/pin.12771
52. Hosono M, Koma YI, Takase N, Urakawa N, Higashino N, Suemune K, et al. CXCL8 Derived From Tumor-Associated Macrophages and Esophageal Squamous Cell Carcinomas Contributes to Tumor Progression by Promoting Migration and Invasion of Cancer Cells. *Oncotarget* (2017) 8(62):106071–88. doi: 10.18632/oncotarget.22526
53. Yokozaki H, Koma YI, Shigeoka M, Nishio M. Cancer as a Tissue: The Significance of Cancer-Stromal Interactions in the Development, Morphogenesis and Progression of Human Upper Digestive Tract Cancer. *Pathol Int* (2018) 68(6):334–52. doi: 10.1111/pin.12674
54. Okamoto M, Koma YI, Kodama T, Nishio M, Shigeoka M, Yokozaki H, et al. Growth Differentiation Factor 15 Promotes Progression of Esophageal Squamous Cell Carcinoma *via* TGF-β Type II Receptor Activation. *Pathobiology* (2020) 87(2):100–13. doi: 10.1159/000504394
55. Hu JM, Liu K, Liu JH, Jiang XL, Wang XL, Yang L, et al. The Increased Number of Tumor-Associated Macrophage is Associated With Overexpression of VEGF-C, Plays an Important Role in Kazakh ESCC Invasion and Metastasis. *Exp Mol Pathol* (2017) 102(1):15–21. doi: 10.1016/j.yexmp.2016.12.001
56. Liu J, Li C, Zhang L, Liu K, Jiang X, Wang X, et al. Association of Tumor-Associated Macrophages With Cancer Cell EMT, Invasion, and Metastasis of Kazakh Esophageal Squamous Cell Cancer. *Diagn Pathol* (2019) 14(1):55. doi: 10.1186/s13000-019-0834-0
57. Cao W, Peters JH, Nieman D, Sharma M, Watson T, Yu J, et al. Macrophage Subtype Predicts Lymph Node Metastasis in Esophageal Adenocarcinoma and Promotes Cancer Cell Invasion *In Vitro*. *Br J Cancer* (2015) 113(5):738–46. doi: 10.1038/bjc.2015.292
58. Hurt B, Schulick R, Edil B, El Kasmi KC, Barnett C Jr. Cancer-Promoting Mechanisms of Tumor-Associated Neutrophils. *Am J Surg* (2017) 214(5):938–44. doi: 10.1016/j.amjsurg.2017.08.003

59. Qin F, Liu X, Chen J, Huang S, Wei W, Zou Y, et al. Anti-TGF-β Attenuates Tumor Growth *via* Polarization of Tumor Associated Neutrophils Towards an Anti-Tumor Phenotype in Colorectal Cancer. *J Cancer* (2020) 11 (9):2580–92. doi: 10.7150/jca.38179
60. Wu L, Saxena S, Awaji M, Singh RK. Tumor-Associated Neutrophils in Cancer: Going Pro. *Cancers (Basel)* (2019) 11(4):564. doi: 10.3390/cancers11040564
61. Sun Y, Zhang L. The Clinical Use of Pretreatment NLR, PLR, and LMR in Patients With Esophageal Squamous Cell Carcinoma: Evidence From a Meta-Analysis. *Cancer Manag Res* (2018) 10:6167–79. doi: 10.2147/CMAR.S171035
62. Liew PX, Kubes P. The Neutrophil's Role During Health and Disease. *Physiol Rev* (2019) 99(2):1223–48. doi: 10.1152/physrev.00012.2018
63. Rayes RF, Mouhanna JG, Nicolau I, Bourdeau F, Giannias B, Rousseau S, et al. Primary Tumors Induce Neutrophil Extracellular Traps With Targetable Metastasis Promoting Effects. *JCI Insight* (2019) 5(16):e128008. doi: 10.1172/jci.insight.128008
64. Noto CN, Hoft SG, DiPaolo RJ. Mast Cells as Important Regulators in Autoimmunity and Cancer Development. *Front Cell Dev Biol* (2021) 9:752350. doi: 10.3389/fcell.2021.752350
65. Fakhrjou A, Niroumand-Oscoei SM, Somi MH, Ghojazadeh M, Naghashi S, Samankan S, et al. Prognostic Value of Tumor-Infiltrating Mast Cells in Outcome of Patients With Esophagus Squamous Cell Carcinoma. *J Gastrointest Cancer* (2014) 45(1):48–53. doi: 10.1007/s12029-013-9550-2
66. Wang B, Li L, Liao Y, Li J, Yu X, Zhang Y, et al. Mast Cells Expressing Interleukin 17 in the Muscularis Propria Predict a Favorable Prognosis in Esophageal Squamous Cell Carcinoma. *Cancer Immunol Immunother* (2013) 62(10):1575–85. doi: 10.1007/s00262-013-1460-4
67. Xiao H, He M , Xie G, Liu Y, Zhao Y, Ye X, et al. The Release of Tryptase From Mast Cells Promote Tumor Cell Metastasis *via* Exosomes. *BMC Cancer* (2019) 19(1):1015. doi: 10.1186/s12885-019-6203-2
68. Ohashi Y, Ishibashi S, Suzuki T, Shineha R, Moriya T, Satomi S, et al. Significance of Tumor Associated Tissue Eosinophilia and Other Inflammatory Cell Infiltrate in Early Esophageal Squamous Cell Carcinoma. *Anticancer Res* (2000) ;20(5A):3025–30.
69. Grisaru-Tal S, Dulberg S, Beck L, Zhang C, Itan M, Hediyeh-Zadeh S, et al. Metastasis-Entrained Eosinophils Enhance Lymphocyte-Mediated Antitumor Immunity. *Cancer Res* (2021) 81(21):5555–71. doi: 10.1158/0008-5472.CAN-21-0839
70. Nicola S, Rolla G, Bucca C, Geronazzo G, Ridolfi I, Ferraris A, et al. Gastric Juice Expression of Th-17 and T-Reg Related Cytokines in Scleroderma Esophageal Involvement. *Cells* (2020) 9(9):2106. doi: 10.3390/cells9092106
71. Wang Y, Xu G, Wang J, Li XH, Sun P, Zhang W, et al. Relationship of Th17/Treg Cells and Radiation Pneumonia in Locally Advanced Esophageal Carcinoma. *Anticancer Res* (2017) 37(8):4643–7. doi: 10.21873/anticanres.11866
72. Chen D, Jiang R, Mao C, Shi L, Wang S, Yu L, et al. Chemokine/chemokine Receptor Interactions Contribute to the Accumulation of Th17 Cells in Patients With Esophageal Squamous Cell Carcinoma. *Hum Immunol* (2012) 73(11):1068–72. doi: 10.1016/j.humimm.2012.07.333
73. Chen D, Hu Q, Mao C, Jiao Z, Wang S, Yu L, et al. Increased IL-17-Producing CD4(+) T Cells in Patients With Esophageal Cancer. *Cell Immunol* (2012) 272(2):166–74. doi: 10.1016/j.cellimm.2011.10.015
74. Liu D, Zhang R, Wu J, Pu Y, Yin X, Cheng Y, et al. Interleukin-17A Promotes Esophageal Adenocarcinoma Cell Invasiveness Through ROS-Dependent, NF-κb-Mediated MMP-2/9 Activation. *Oncol Rep* (2017) 37 (3):1779–85. doi: 10.3892/or.2017.5426
75. García-Varona A, Fernández-Vega I, Santos-Juanes J. Immunohistochemical Expression Analysis of MMP-1, TIMP-2 and P53 in Barrett's Esophagus, Dysplasia and Esophageal Adenocarcinoma. *Pol J Pathol* (2021) 72(1):48–56. doi: 10.5114/pjp.2021.106443
76. Chen N, Zhang G, Fu J, Wu Q. Matrix Metalloproteinase-14 (MMP-14) Downregulation Inhibits Esophageal Squamous Cell Carcinoma Cell Migration, Invasion, and Proliferation. *Thorac Cancer* (2020) 11(11):3168–74. doi: 10.1111/1759-7714.13636
77. Mao X, Xu J, Wang W, Liang C, Hua J, Liu J, et al. Crosstalk Between Cancer-Associated Fibroblasts and Immune Cells in the Tumor Microenvironment: New Findings and Future Perspectives. *Mol Cancer* (2021) 20(1):131. doi: 10.1186/s12943-021-01428-1
78. Peng L, Wang D, Han Y, Huang T, He X, Wang J, et al. Emerging Role of Cancer-Associated Fibroblasts-Derived Exosomes in Tumorigenesis. *Front Immunol* (2022) 12:795372. doi: 10.3389/fimmu.2021.795372
79. Kalluri R, Zeisberg M. Fibroblasts in Cancer. *Nat Rev Cancer* (2006) 6 (5):392–401. doi: 10.1038/nrc1877
80. Wang J, Zhang G, Wang J, Wang L, Huang X, Cheng Y, et al. The Role of Cancer-Associated Fibroblasts in Esophageal Cancer. *J Transl Med* (2016) 14:30. doi: 10.1186/s12967-016-0788-x
81. Kato T, Noma K, Ohara T, Kashima H, Katsura Y, Sato H, et al. Cancer-Associated Fibroblasts Affect Intratumoral CD8+ and FoxP3+ T Cells *Via* IL6 in the Tumor Microenvironment. *Clin Cancer Res* (2018) 24(19):4820–33. doi: 10.1158/1078-0432.CCR-18-0205
82. Higashino N, Koma YI, Hosono M, Takase N, Okamoto M, Kodaira H, et al. Fibroblast Activation Protein-Positive Fibroblasts Promote Tumor Progression Through Secretion of CCL2 and Interleukin-6 in Esophageal Squamous Cell Carcinoma. *Lab Invest* (2019) 99(6):777–92. doi: 10.1038/s41374-018-0185-6
83. Shimizu M, Koma YI, Sakamoto H, Tsukamoto S, Kitamura Y, Urakami S, et al. Metallothionein 2a Expression in Cancer-Associated Fibroblasts and Cancer Cells Promotes Esophageal Squamous Cell Carcinoma Progression. *Cancers (Basel)* (2021) 13(18):4552. doi: 10.3390/cancers13184552
84. Du X, Xu Q, Pan D, Xu D, Niu B, Hong W, et al. HIC-5 in Cancer-Associated Fibroblasts Contributes to Esophageal Squamous Cell Carcinoma Progression. *Cell Death Dis* (2019) 10(12):873. doi: 10.1038/s41419-019-2114-z
85. Fang L, Che Y, Zhang C, Huang J, Lei Y, Lu Z, et al. PLAU Directs Conversion of Fibroblasts to Inflammatory Cancer-Associated Fibroblasts, Promoting Esophageal Squamous Cell Carcinoma Progression *via* uPAR/Akt/NF-κb/IL8 Pathway. *Cell Death Discovery* (2021) 7(1):32. doi: 10.1038/s41420-021-00410-6
86. Cai R, Wang P, Zhao X, Lu X, Deng R, Wang X, et al. LTBP1 Promotes Esophageal Squamous Cell Carcinoma Progression Through Epithelial-Mesenchymal Transition and Cancer-Associated Fibroblasts Transformation. *J Transl Med* (2020) 18(1):139. doi: 10.1186/s12967-020-02310-2
87. Grugan KD, Miller CG, Yao Y, Michaylira CZ, Ohashi S, Klein-Szanto AJ, et al. Fibroblast-Secreted Hepatocyte Growth Factor Plays a Functional Role in Esophageal Squamous Cell Carcinoma Invasion. *Proc Natl Acad Sci U S A* (2010) 107(24):11026–31. doi: 10.1073/pnas.0914295107
88. Stairs DB, Bayne LJ, Rhoades B, Vega ME, Waldron TJ, Kalabis J, et al. Deletion of P120-Catenin Results in a Tumor Microenvironment With Inflammation and Cancer That Establishes it as a Tumor Suppressor Gene. *Cancer Cell* (2011) 19(4):470–83. doi: 10.1016/j.ccr.2011.02.007
89. Chen Y, Li X, Yang H, Xia Y, Guo L, Wu X, et al. Expression of Basic Fibroblast Growth Factor, CD31, and α-Smooth Muscle Actin and Esophageal Cancer Recurrence After Definitive Chemoradiation. *Tumor Biol* (2014) 35(7):7275–82. doi: 10.1007/s13277-014-1987-9
90. Li F, Wu X, Sun Z, Cai P, Wu L, Li D, et al. Fibroblast Activation Protein-α Expressing Fibroblasts Promote Lymph Node Metastasis in Esophageal Squamous Cell Carcinoma. *Onco Targets Ther* (2020) 13:8141–8. doi: 10.2147/OTT.S257529
91. Labib PL, Goodchild G, Pereira SP. Molecular Pathogenesis of Cholangiocarcinoma. *BMC Cancer* (2019) 19(1):185. doi: 10.1186/s12885-019-5391-0
92. Xu Z, Wang S, Wu M, Zeng W, Wang X, Dong Z, et al. Tgfβ1 and HGF Protein Secretion by Esophageal Squamous Epithelial Cells and Stromal Fibroblasts in Oesophageal Carcinogenesis. *Oncol Lett* (2013) 6(2):401–6. doi: 10.3892/ol.2013.1409
93. Ozawa Y, Nakamura Y, Fujishima F, Felizola SJ, Takeda K, Okamoto H, et al. C-Met in Esophageal Squamous Cell Carcinoma: An Independent Prognostic Factor and Potential Therapeutic Target. *BMC Cancer* (2015) 15:451. doi: 10.1186/s12885-015-1450-3
94. Xiang H, Ramil CP, Hai J, Zhang C, Wang H, Watkins AA, et al. Cancer-Associated Fibroblasts Promote Immunosuppression by Inducing ROS-Generating Monocytic MDSCs in Lung Squamous Cell Carcinoma. *Cancer Immunol Res* (2020) 8(4):436–50. doi: 10.1158/2326-6066.CIR-19-0507

95. Dinh HQ, Pan F, Wang G, Huang QF, Olingy CE, Wu ZY, et al. Integrated Single-Cell Transcriptome Analysis Reveals Heterogeneity of Esophageal Squamous Cell Carcinoma Microenvironment. *Nat Commun* (2021) 12 (1):7335. doi: 10.1038/s41467-021-27599-5
96. Zhang X, Peng L, Luo Y, Zhang S, Pu Y, Chen Y, et al. Dissecting Esophageal Squamous-Cell Carcinoma Ecosystem by Single-Cell Transcriptomic Analysis. *Nat Commun* (2021) 12(1):5291. doi: 10.1038/s41467-021-25539-x
97. Chen Z, Zhao M, Liang J, Hu Z, Huang Y, Li M, et al. Dissecting the Single-Cell Transcriptome Network Underlying Esophagus non-Malignant Tissues and Esophageal Squamous Cell Carcinoma. *EBioMedicine* (2021) 69:103459. doi: 10.1016/j.ebiom.2021.103459
98. Fares J, Fares MY, Khachfe HH, Salhab HA, Fares Y, et al. Molecular Principles of Metastasis: A Hallmark of Cancer Revisited. *Signal Transduct Target Ther* (2020) 5(1):28. doi: 10.1038/s41392-020-0134-x
99. Bhat AA, Nisar S, Maacha S, Carneiro-Lobo TC, Akhtar S, Siveen KS, et al. Cytokine-Chemokine Network Driven Metastasis in Esophageal Cancer; Promising Avenue for Targeted Therapy. *Mol Cancer* (2021) 20(1):2. doi: 10.1186/s12943-020-01294-3
100. Yao M, Brummer G, Acevedo D, Cheng N. Cytokine Regulation of Metastasis and Tumorigenicity. *Adv Cancer Res* (2016) 132:265–367. doi: 10.1016/bs.acr.2016.05.005
101. Wu X, Zhang H, Sui Z, Wang Y, Yu Z, et al. The Biological Role of the CXCL12/CXCR4 Axis in Esophageal Squamous Cell Carcinoma. *Cancer Biol Med* (2021) 18(2):401–10. doi: 10.20892/j.issn.2095-3941.2020.0140
102. Yang X, Lu Q, Xu Y, Liu C, Sun Q, et al. Clinicopathologic Significance of CXCR4 Expressions in Patients With Esophageal Squamous Cell Carcinoma. *Pathol Res Pract* (2020) 216(1):152787. doi: 10.1016/j.prp.2019.152787
103. Loh CY, Chai JY, Tang TF, Wong WF, Sethi G, Shanmugam MK, et al. The E-Cadherin and N-Cadherin Switch in Epithelial-To-Mesenchymal Transition: Signaling, Therapeutic Implications, and Challenges. *Cells* (2019) 8(10):1118. doi: 10.3390/cells8101118
104. Fedele M, Sgarra R, Battista S, Cerchia L, Manfioletti G. The Epithelial-Mesenchymal Transition at the Crossroads Between Metabolism and Tumor Progression. *Int J Mol Sci* (2022) 23(2):800. doi: 10.3390/ijms23020800
105. Wang X, Cao Y, Zhang S, Chen Z, Fan L, Shen X, et al. Stem Cell Autocrine CXCL12/CXCR4 Stimulates Invasion and Metastasis of Esophageal Cancer. *Oncotarget* (2017) 8(22):36149–60. doi: 10.18632/oncotarget.15254
106. Mortezaee K. CXCL12/CXCR4 Axis in the Microenvironment of Solid Tumors: A Critical Mediator of Metastasis. *Life Sci* (2020) 249:117534. doi: 10.1016/j.lfs.2020.117534
107. Zhang M, Zhou S, Zhang L, Ye W, Wen Q, Wang J, et al. Role of Cancer-Related Inflammation in Esophageal Cancer. *Crit Rev Eukaryot Gene Expr* (2013) 23(1):27–35. doi: 10.1615/CritRevEukarGeneExpr.2013006033
108. Cai QY, Liang GY, Zheng YF, Tan QY, Wang RW, Li K, et al. CCR7 Enhances the Angiogenic Capacity of Esophageal Squamous Carcinoma Cells *In Vitro via* Activation of the NF-κb/VEGF Signaling Pathway. *Am J Transl Res* (2017) 9(7):3282–92.
109. Wang Q, Zou H, Wang Y, Shang J, Yang L, Shen J, et al. CCR7-CCL21 Axis Promotes the Cervical Lymph Node Metastasis of Tongue Squamous Cell Carcinoma by Up-Regulating MUC1. *J Craniomaxillofac Surg* (2021) 49 (7):562–9. doi: 10.1016/j.jcms.2021.02.027
110. Shi M, Chen D, Yang D, Liu XY. CCL21-CCR7 Promotes the Lymph Node Metastasis of Esophageal Squamous Cell Carcinoma by Up-Regulating MUC1. *J Exp Clin Cancer Res* (2015) 34:149. doi: 10.1186/s13046-015-0268-9
111. Song Y, Wang Z, Liu X, Liu X, Jiang W, Shi M., et al. CCR7 and VEGF-C: Molecular Indicator of Lymphatic Metastatic Recurrence in Pn0 Esophageal Squamous Cell Carcinoma After Ivor-Lewis Esophagectomy? *Ann Surg Oncol* (2012) 19(11):3606–12. doi: 10.1245/s10434-012-2419-y
112. Liu Q, Li A, Tian Y, Wu JD, Liu Y, Li T, et al. The CXCL8-CXCR1/2 Pathways in Cancer. *Cytokine Growth Factor Rev* (2016) 25(2):61–71. doi: 10.1016/j.cytogfr.2016.08.002
113. Waugh DJ, Wilson C. The Interleukin-8 Pathway in Cancer. *Clin Cancer Res* (2008) 14(21):6735–41. doi: 10.1158/1078-0432.CCR-07-4843
114. Mathieu M, Martin-Jaular L, Lavieu G, Théry C, et al. Specificities of Secretion and Uptake of Exosomes and Other Extracellular Vesicles for Cell-to-Cell Communication. *Nat Cell Biol* (2019) 21(1):9–17. doi: 10.1038/s41556-018-0250-9
115. Jing Z, Chen K, Gong L. The Significance of Exosomes in Pathogenesis, Diagnosis, and Treatment of Esophageal Cancer. *Int J Nanomed* (2021) 16:6115–27. doi: 10.2147/IJN.S321555
116. Liu T, Li P, Li J, Qi Q, Sun Z, Shi S, et al. Exosomal and Intracellular miR-320b Promotes Lymphatic Metastasis in Esophageal Squamous Cell Carcinoma. *Mol Ther Oncol* (2021) 23:163–80. doi: 10.1016/j.omto.2021.09.003
117. Liao J, Liu R, Shi YJ, Yin LH, Pu YP. Exosome-Shuttling microRNA-21 Promotes Cell Migration and Invasion-Targeting PDCD4 in Esophageal Cancer. *Int J Oncol* (2016) 48(6):2567–79. doi: 10.3892/ijo.2016.3453
118. Liu S, Lin Z, Rao W, Zheng J, Xie Q, Lin Y, et al. Upregulated Expression of Serum Exosomal Hsa_Circ_0026611 is Associated With Lymph Node Metastasis and Poor Prognosis of Esophageal Squamous Cell Carcinoma. *J Cancer* (2021) 12(3):918–26. doi: 10.7150/jca.50548
119. Xu ML, Liu TC, Dong FX, Meng LX, Ling AX, Liu S, et al. Exosomal lncRNA LINC01711 Facilitates Metastasis of Esophageal Squamous Cell Carcinoma *via* the miR-326/FSCN1 Axis. *Aging (Albany NY)* (2021) 13(15):19776–88. doi: 10.18632/aging.203389
120. Min H, Sun X, Yang X, Zhu H, Liu J, Wang Y, et al. Exosomes Derived From Irradiated Esophageal Carcinoma-Infiltrating T Cells Promote Metastasis by Inducing the Epithelial-Mesenchymal Transition in Esophageal Cancer Cells. *Pathol Oncol Res* (2018) 24(1):11–8. doi: 10.1007/s12253-016-0185-z
121. Kam NW, Wu KC, Dai W, Wang Y, Yan LYC, Shakya R, et al. Peritumoral B Cells Drive Proangiogenic Responses in HMGB1-Enriched Esophageal Squamous Cell Carcinoma. *Angiogenesis* (2021), 1–23.doi: 10.1007/s10456-021-09819-0
122. Donlon NE, Sheppard A, Davern M, O'Connell F, Phelan JJ, Power R, et al. Linking Circulating Serum Proteins With Clinical Outcomes in Esophageal Adenocarcinoma-An Emerging Role for Chemokines. *Cancers (Basel)* (2020) 12(11):3356. doi: 10.3390/cancers12113356
123. Yang W, Zhang Y, Yu J, Li S, et al. The Low Expression of CD80 Correlated With the Vascular Endothelial Growth Factor in Esophageal Cancer Tissue. *Eur J Surg Oncol* (2010) 36(5):501–6. doi: 10.1016/j.ejso.2010.01.007
124. Wang M, Li Y, Xiao Y, Yang M, Chen J, Jian Y, et al. Nicotine-Mediated OTUD3 Downregulation Inhibits VEGF-C mRNA Decay to Promote Lymphatic Metastasis of Human Esophageal Cancer. *Nat Commun* (2021) 12(1):7006. doi: 10.1038/s41467-021-27348-8
125. Li J, Xie Y, Wang X, Jiang C, Yuan X, Zhang A, et al. Overexpression of VEGF-C and MMP-9 Predicts Poor Prognosis in Kazakh Patients With Esophageal Squamous Cell Carcinoma. *Peer J* (2019) 7:e8182. doi: 10.7717/peerj.8182
126. Ma S, Lu CC, Yang LY, Wang JJ, Wang BS, Cai HQ, et al. ANXA2 Promotes Esophageal Cancer Progression by Activating MYC-HIF1A-VEGF Axis. *J Exp Clin Cancer Res* (2018) 37(1):183. doi: 10.1186/s13046-018-0851-y
127. Mohammadi F, Javid H, Afshari AR, Mashkani B, Hashemy SI. Substance P Accelerates the Progression of Human Esophageal Squamous Cell Carcinoma *via* MMP-2, MMP-9, VEGF-A, and VEGFR1 Overexpression. *Mol Biol Rep* (2020) 47(6):4263–72. doi: 10.1007/s11033-020-05532-1
128. Chen MF, Kuan FC, Yen TC, Lu MS, Lin PY, Chung YH, et al. IL-6-Stimulated CD11b+ CD14+ HLA-DR- Myeloid-Derived Suppressor Cells, are Associated With Progression and Poor Prognosis in Squamous Cell Carcinoma of the Esophagus. *Oncotarget* (2014) 5(18):8716–28. doi: 10.18632/oncotarget.2368
129. Li J, Zhang BZ, Qin YR, Bi J, Liu HB, Li Y, et al. CD68 and Interleukin 13, Prospective Immune Markers for Esophageal Squamous Cell Carcinoma Prognosis Prediction. *Oncotarget* (2016) 7(13):15525–38. doi: 10.18632/oncotarget.6900
130. Van Dyken SJ, Locksley RM. Interleukin-4- and Interleukin-13-Mediated Alternatively Activated Macrophages: Roles in Homeostasis and Disease. *Annu Rev Immunol* (2013) 31:317–43. doi: 10.1146/annurev-immunol-032712-095906
131. Karakasheva TA, Waldron TJ, Eruslanov E, Kim SB, Lee JS, O'Brien S, et al. CD38-Expressing Myeloid-Derived Suppressor Cells Promote Tumor Growth in a Murine Model of Esophageal Cancer. *Cancer Res* (2015) 75 (19):4074–85. doi: 10.1158/0008-5472.CAN-14-3639

132. Paluskievicz CM, Cao X, Abdi R, Zheng P, Liu Y, Bromberg JS, et al. T Regulatory Cells and Priming the Suppressive Tumor Microenvironment. *Front Immunol* (2019) 10:2453. doi: 10.3389/fimmu.2019.02453
133. Kato H, Nakajima M, Masuda N, Faried A, Sohda M, Fukai Y, et al. Expression of RCAS1 in Esophageal Squamous Cell Carcinoma is Associated With a Poor Prognosis. *J Surg Oncol* (2005) 90(2):89–94. doi: 10.1002/jso.20249
134. Lu L, Pan K, Zheng HX, Li JJ, Qiu HJ, Zhao JJ, et al. IL-17A Promotes Immune Cell Recruitment in Human Esophageal Cancers and the Infiltrating Dendritic Cells Represent a Positive Prognostic Marker for Patient Survival. *J Immunother* (2013) 36(8):451–8. doi: 10.1097/CJI.0b013e3182a802cf
135. Yi M, Zheng X, Niu M, Zhu S, Ge H, Wu K, et al. Combination Strategies With PD-1/PD-L1 Blockade: Current Advances and Future Directions. *Mol Cancer* (2022) 21(1):28. doi: 10.1186/s12943-021-01489-2
136. Siddiqui AZ, Almhanna K. Beyond Chemotherapy, PD-1, and HER-2: Novel Targets for Gastric and Esophageal Cancer. *Cancers (Basel)* (2021) 13 (17):4322. doi: 10.3390/cancers13174322
137. Hong Y, Ding ZY. PD-1 Inhibitors in the Advanced Esophageal Cancer. *Front Pharmacol* (2019) 10:1418. doi: 10.3389/fphar.2019.01418
138. Wang Y, Chen T, Li K, Mu W, Liu Z, Shi A, et al. Recent Advances in the Mechanism Research and Clinical Treatment of Anti-Angiogenesis in Biliary Tract Cancer. *Front Oncol* (2021) 11:777617. doi: 10.3389/fonc.2021.777617
139. Wang K, Chen Q, Liu N, Zhang J, Pan X, et al. Recent Advances in, and Challenges of, Anti-Angiogenesis Agents for Tumor Chemotherapy Based on Vascular Normalization. *Drug Discovery Today* (2021) 26(11):2743–53. doi: 10.1016/j.drudis.2021.07.024
140. Zhao S, Ren S, Jiang T, Zhu B, Li X, Zhao C, et al. Low-Dose Apatinib Optimizes Tumor Microenvironment and Potentiates Antitumor Effect of PD-1/PD-L1 Blockade in Lung Cancer. *Cancer Immunol Res* (2019) 7 (4):630–43. doi: 10.1158/2326-6066.CIR-17-0640
141. Zou W, Wolchok JD, Chen L. PD-L1 (B7-H1) and PD-1 Pathway Blockade for Cancer Therapy: Mechanisms, Response Biomarkers, and Combinations. *Sci Transl Med* (2016) 8(328):328rv4. doi: 10.1126/scitranslmed.aad7118
142. Ohigashi Y, Sho M, Yamada Y, Tsurui Y, Hamada K, Ikeda N, et al. Clinical Significance of Programmed Death-1 Ligand-1 and Programmed Death-1 Ligand-2 Expression in Human Esophageal Cancer. *Clin Cancer Res* (2005) 11(8):2947–53. doi: 10.1158/1078-0432.CCR-04-1469
143. Chen L, Deng H, Lu M, Xu B, Wang Q, Jiang J, et al. B7-H1 Expression Associates With Tumor Invasion and Predicts Patient's Survival in Human Esophageal Cancer. *Int J Clin Exp Pathol* (2014) 7(9):6015–23.
144. Derks S, Nason KS, Liao X, Stachler MD, Liu KX, Liu JB, et al. Epithelial PD-L2 Expression Marks Barrett's Esophagus and Esophageal Adenocarcinoma. *Cancer Immunol Res* (2015) 3(10):1123–9. doi: 10.1158/2326-6066.CIR-15-0046
145. Zhang H, Dai Z, Wu W, Wang Z, Zhang N, Zhang L, et al. Regulatory Mechanisms of Immune Checkpoints PD-L1 and CTLA-4 in Cancer. *J Exp Clin Cancer Res* (2021) 40(1):184. doi: 10.1186/s13046-021-01987-7
146. Huang TX, Fu L. The Immune Landscape of Esophageal Cancer. *Cancer Commun (Lond)* (2019) 39(1):79. doi: 10.1186/s40880-019-0427-z
147. Ri MH, Ma J, Jin X. Development of Natural Products for Anti-PD-1/PD-L1 Immunotherapy Against Cancer. *J Ethnopharmacol* (2021) 281:114370. doi: 10.1016/j.jep.2021.114370
148. Zhulai G, Oleinik E. Targeting Regulatory T Cells in Anti-PD-1/PD-L1 Cancer Immunotherapy. *Scand J Immunol* (2022) 95(3):e13129. doi: 10.1111/sji.13129
149. Tashireva LA, Muravyova DT, Popova NO, Goldberg VE, Vtorushin SV, Perelmuter VM., et al. Parameters of Tumor Microenvironment Determine Effectiveness of Anti-PD-1/PD-L1 Therapy. *Biochem (Mosc)* (2021) 86 (11):1461–8. doi: 10.1134/S0006297921110092
150. Mantovani A, Marchesi F, Malesci A, Laghi L, Allavena P., et al. Tumour-Associated Macrophages as Treatment Targets in Oncology. *Nat Rev Clin Oncol* (2017) 14(7):399–416. doi: 10.1038/nrclinonc.2016.217
151. Conte E. Targeting Monocytes/Macrophages in Fibrosis and Cancer Diseases: Therapeutic Approaches. *Pharmacol Ther* (2021) 108031. doi: 10.1016/j.pharmthera.2021.108031
152. Katsube R, Noma K, Ohara T, Nishiwaki N, Kobayashi T, Komoto S, et al. Fibroblast Activation Protein Targeted Near Infrared Photoimmunotherapy (NIR PIT) Overcomes Therapeutic Resistance in Human Esophageal Cancer. *Sci Rep* (2021) 11(1):1693. doi: 10.1038/s41598-021-81465-4
153. Cui X, Liu R, Duan L, Cao D, Zhang Q, Zhang A, et al. CAR-T Therapy: Prospects in Targeting Cancer Stem Cells. *J Cell Mol Med* (2021) 25 (21):9891–904. doi: 10.1111/jcmm.16939
154. Shi H, Yu F, Mao Y, Ju Q, Wu Y, Bai W, et al. EphA2 Chimeric Antigen Receptor-Modified T Cells for the Immunotherapy of Esophageal Squamous Cell Carcinoma. *J Thorac Dis* (2018) 10(5):2779–88. doi: 10.21037/jtd.2018.04.91
155. Yu F, Wang X, Shi H, Jiang M, Xu J, Sun M, et al. Development of Chimeric Antigen Receptor-Modified T Cells for the Treatment of Esophageal Cancer. *Tumori* (2021) 107(4):341–52. doi: 10.1177/0300891620960223
156. Zhang H, Zhao H, He X, He X, Xi F, Liu J, et al. JAK-STAT Domain Enhanced MUC1-CAR-T Cells Induced Esophageal Cancer Elimination. *Cancer Manag Res* (2020) 12:9813–24. doi: 10.2147/CMAR.S264358
157. Shao J, Hou L, Liu J, Liu Y, Ning J, Zhao Q, et al. Indoleamine 2,3-Dioxygenase 1 Inhibitor-Loaded Nanosheets Enhance CAR-T Cell Function in Esophageal Squamous Cell Carcinoma. *Front Immunol* (2021) 12:661357. doi: 10.3389/fimmu.2021.661357
158. Yue G, Tang J, Zhang L, Niu H, Li H, Luo S, et al. CD276 Suppresses CAR-T Cell Function by Promoting Tumor Cell Glycolysis in Esophageal Squamous Cell Carcinoma. *J Gastrointest Oncol* (2021) 12 (1):38–51. doi: 10.21037/jgo-21-50
159. Akhoundi M, Mohammadi M, Sheykhhasan M, Fayazi N, et al. CAR T Cell Therapy as a Promising Approach in Cancer Immunotherapy: Challenges and Opportunities. *Cell Oncol (Dordr)* (2021) 44(3):495–523. doi: 10.1007/s13402-021-00593-1

Conflict of Interest: The authors declare that the research was conducted in the absence of any commercial or financial relationships that could be construed as a potential conflict of interest.

Publisher's Note: All claims expressed in this article are solely those of the authors and do not necessarily represent those of their affiliated organizations, or those of the publisher, the editors and the reviewers. Any product that may be evaluated in this article, or claim that may be made by its manufacturer, is not guaranteed or endorsed by the publisher.

frontiers | Frontiers in Oncology

ORIGINAL RESEARCH
published: 23 June 2022
doi: 10.3389/fonc.2022.913432

Integrated Multi-Omics Data Analysis Reveals Associations Between Glycosylation and Stemness in Hepatocellular Carcinoma

Peiyan Liu[1,2†], *Qi Zhou*[3,4†] *and Jia Li*[1,2*]

[1] Department of Hepatology, Second People's Clinical College of Tianjin Medical University, Tianjin, China, [2] Department of Hepatology, Tianjin Second People's Hospital, Tianjin, China, [3] Department of Gastroenterology, The Third Affiliated Hospital of Sun Yat-Sen University, Guangzhou, China, [4] Guangdong Provincial Key Laboratory of Liver Disease Research, Guangzhou, China

OPEN ACCESS

Edited by:
Nathaniel Weygant,
Fujian University of Traditional Chinese Medicine, China

Reviewed by:
Ka-wing Fong,
University of Kentucky, United States
Liang Lin,
Cytovia Therapeutics, United States

***Correspondence:**
Jia Li
18622663700@163.com

[†]These authors have contributed equally to this work

Specialty section:
This article was submitted to Gastrointestinal Cancers: Hepato Pancreatic Biliary Cancers, a section of the journal Frontiers in Oncology

Received: 05 April 2022
Accepted: 25 May 2022
Published: 23 June 2022

Citation:
Liu P, Zhou Q and Li J (2022) Integrated Multi-Omics Data Analysis Reveals Associations Between Glycosylation and Stemness in Hepatocellular Carcinoma. Front. Oncol. 12:913432. doi: 10.3389/fonc.2022.913432

Background: Glycosylation plays an essential role in driving the progression and treatment resistance of hepatocellular carcinoma (HCC). However, its function in regulating the acquisition and maintenance of the cancer stemness-like phenotype in HCC remains largely unknown. There is also very little known about how CAD and other potential glycosylation regulators may influence stemness. This study explores the relationship between glycosylation and stemness in HCC.

Methods: Gene set variance analysis (GSVA) was used to assess the TCGA pan-cancer enrichment in glycosylation-related pathways. Univariate, LASSO, and multivariate COX regression were then used to identify prognostic genes in the TCGA-LIHC and construct a prognostic signature. HCC patients were classified into high- and low-risk subgroups based on the signature. The relationship between gene expression profiles and stemness was confirmed using bulk and single-cell RNA-sequencing data. The role of CAD and other genes in regulating the stemness of HCC was also validated by RT-qPCR, CCK-8, and colony formation assay. Copy number variation (CNV), immune infiltration, and clinical features were further analyzed in different subgroups and subsequent gene expression profiles. Sensitive drugs were also screened.

Results: In the pan-cancer analysis, HCC was shown to have specific glycosylation alterations. Five genes, CAD, SLC51B, LGALS3, B3GAT3, and MT3, identified from 572 glycosylation-related genes, were used to construct a gene signature and predict HCC patient survival in the TCGA cohort. The results demonstrated a significant positive correlation between patients in the high-risk group and both elevated gene expression and HCC dedifferentiation status. A significant reduction in the stemness-related markers, CD24, CD44, CD20, FOXM1, and EpCAM, was found after the knockdown of CAD and other genes in HepG2 and Huh7 cells. Frequent mutations increased CNVs, immune-suppressive responses, and poor prognosis were also associated with the high-risk profile. The ICGC-LIRI-JP cohort confirmed a similar relationship between glycosylation-

related subtypes and stemness. Finally, 84 sensitive drugs were screened for abnormal glycosylation of HCC, and carfilzomib was most highly correlated with CAD.

Conclusions: Glycosylation-related molecular subtypes are associated with HCC stemness and disease prognosis. These results provide new directions for further research on the relationship between glycosylation and stemness phenotypes.

Keywords: hepatocellular carcinoma, glycosylation, stemness, copy number variations, immunity, prognosis, CAD

INTRODUCTION

Hepatocellular carcinoma (HCC) accounts for 75–85% of primary liver cancers and is the second leading cause of cancer death, with 5-year survival rates of only 4–17% (1). This disease is highly malignant and progresses rapidly, resulting in almost one million deaths each year (2). Surgical resection of HCC followed by chemotherapy is an ideal curative treatment strategy, but it is limited by advanced stage and metastasized tumor cells. While several new therapeutic agents, including checkpoint or tyrosine kinase inhibitors, have been approved by the FDA for patients who cannot undergo surgery or transplantation, their efficacy is unsatisfactory (3, 4), and HCC patients still have an average survival of only 6 months (5, 6). Liver cancer stem cells (LCSCs) are closely associated with the poor prognosis of HCC because they have more robust metastatic and tumorigenic properties than non-LCSCs. Thus, eliminating LCSCs or reducing tumor size is critical to improving HCC treatment efficacy (7). There is an urgent need to explore the molecular biological features of LCSCs.

Glycosylation is a complex process by which a carbohydrate is added to a protein or lipid carrier and is involved in many cellular mechanisms, including cell–cell adhesion, trafficking, motility, inflammation, signaling, host–pathogen interactions, and innate immune responses. All these processes play an essential role in the development and progression of HCC (8, 9). Aberrant glycosylation is frequently cited as a hallmark of malignancy, and from the perspective of epigenetics, glycosylation is thought to directly impact key processes supporting the stemness of HCC, including cell adhesion, motility, invasion, and evasion (9–11). With the presence of highly expressed glycosyltransferases, altered glycosylation is ubiquitous in HCC cells.

Carbamoyl-phosphate synthetase 2, aspartate transcarbamoylase, and dihydrooro-tase (CAD) are multifunctional proteins that play prominent roles in glycosylation. CAD mutations can significantly reduce glycosylation and angiogenesis (12). A product of CAD, uridine diphosphate (UDP), is a specific target for interventional tumors (13, 14). Numerous drugs and anti-tumor vaccines targeting glycosylation are currently in clinical trials. One drug, trastuzumab, is shown to increase the sensitivity of drug-resistant breast cancer cell lines by removing siglec ligands and boosting antibody-dependent natural killer (NK) cell cytotoxicity (15). More glycomic and glycoproteomic studies will help define novel targets and strategies for improving cancer treatment (16). While the B3GAT3, SLC51B, LGALS3, and MT3 genes also play an essential role in the glycosylation pathway, their relationship with stemness remains unclear.

Because of the Warburg effect, sustained high glucose levels in HCC can promote abnormal glycosylation reactions, activate particular signaling pathways, and produce irreversible toxic products, such as glyoxal, methylglyoxal, and 3-deoxyglucosone, that accelerate HCC proliferation and metastasis (17–20). Glycosylation of the stem cell markers, CD24, CD20, CD44, EpCAM, and FOXM1, plays an important role in regulating LCSCs (21–23). Tumor-related glycoprotein or glycan antigen alterations approved by the Food and Drug Administration (FDA), such as core fucosylated AFP (AFP-L3), are better targets for tumor diagnosis and prognosis than AFP alone (24). Further understanding of HCC-related glycosylation patterns will provide advances in treatment and prognosis and reduce mortality.

In this study, glycosylation-related gene sets were downloaded from the GSEA (http://www.gsea-msigdb.org) and a model of HCC prognosis was constructed. Bulk and single-cell RNA-sequencing revealed that the genes and model correlated closely with the stemness of HCC. A systematic analysis of the multi-omics results, including CNV mutations, transcription factors, immunity, and clinical characteristics, may inform further study of the relationships between glycosylation and the stemness of HCC.

MATERIALS AND METHODS

Pan-Cancer Data Collection and Analysis

All glycosylation-related pathways and relevant gene sets were retrieved from the Molecular Signatures Database (MSigDB, http://www.gsea-msigdb.org/gsea/msigdb/) (**Table S1**). TCGA pan-cancer RNA-seq data (FPKM values) were downloaded from the genomic data common website (https://gdc.cancer.gov/about-data/publications/pancanatlas). Gene set variance analysis (GSVA) was used to assess the enrichment of each pan-cancer sample in glycosylation-related pathways, and the distribution of scores was shown using the R "pheatmap" package. Principal component analysis (PCA) was performed after scaling by Z-score, and the pan-cancer RNA-seq data were projected into two dimensions.

HCC Data Collection

In total, 424 RNA-seq transcriptome cases with corresponding clinical information were extracted from the TCGA-LIHC

database (https://portal.gdc.cancer.gov) using the Genomic Data Commons (GDC) tool. RNA-seq data were normalized by FPKM. The somatic mutation and CNV data were also downloaded from the TCGA. RNA-seq and clinicopathological data from a Japanese HCC cohort were obtained from the ICGC (LIRI-JP, https://dcc.icgc.org/projects/LIRI-JP) as a comparison.

Construction of a Potential Prognostic Signature

First, 143 differentially expressed genes (DEGs) were identified using LIMMA analysis (adjusted P <0.05 and |Log FC| >1). Univariate Cox regression analysis was then performed to identify potential prognostic DEGs (P <0.05). Least absolute shrinkage and selection operator (LASSO) regression analysis and stepwise Cox regression analysis were used to construct a prognostic model. The risk score of each sample was calculated using the following formula:

$$\text{Risk score} = \sum_i^k Xi \times Yi$$

$$(X: coefficients,\ Y: gene\ \ expression\ \ level)\cdot$$

Based on risk scores, the samples were divided into high- and low-risk subgroups.

Calculation of Stemness-Associated Scores

The mRNA-si stemness score (25) and other stemness signatures (Ben-Porath ESC score (26), Wong ESC score (27), and Bhattacharya ESC score (28)) were used to assess stemness in both the TCGA-LIHC and ICGC-LIRI-JP cohorts.

Single-Cell RNA-Sequencing Data Analysis

Smart-seq2 data (GSE103866) from 55 HuH-1 cells, 63 HuH-7 cells, and 12 patient HCC cells were obtained from the Gene Expression Omnibus (GEO) website. After preprocessing, the scRNA-seq data were converted into a Seurat object, and further quality control was conducted. Data were excluded if 1) cells had >30% mitochondrial genes, 2) genes were identified in <3 cells, or 3) cells had <300 detectable genes. Log normalization, centralization, generation of hypervariable genes, PCA, and clustering analysis were used to perform dimensionality reduction. Uniform manifold approximation and projection (UMAP) was used to visualize the cell distribution using EpCAM, CD24, and CD133 as cell surface markers. "FeaturePlot" and "VlnPlot" were also used to visualize the glycosylation-related genes.

Experimental Validation of the Relationship Between Gene Expressions and Stemness Phenotype

The expression of the HepG2, PLC, Huh7, and Hep3B genes in HCC tumors and cells was determined by quantitative real-time PCR (RT-qPCR) according to the protocols of the manufacturer. Cell Counting Kit-8 (CCK-8) and colony formation assays were used to measure cell proliferation. Small interfering RNA (siRNA) was transfected using Lipofectamine 2000 (Invitrogen, Carlsbad, CA, USA) and mRNA levels were assessed after 48 h. The primer and specific siRNA sequences are included in **Table S2**.

Analysis of Somatic Mutations and Gene Copy Number Variations (CNVs)

Somatic mutation and CNV data were extracted from the TCGA. The somatic mutation data were visualized using the R "maftools" package. GISTIC2.0 was used to determine the significantly deleted or amplified genomic regions in low- and high-risk subgroups in TCGA-LIHC, referenced to the Consortium Human build 38 (GRCh38). Gene locations were obtained online (ftp://ftp.ensembl.org/pub/current_gtf).

Analysis of Tumor Immune Infiltration

Six previously reported immune subtypes of TCGA-LIHC were identified (29). Infiltrating immune cell fractions were analyzed in tumor samples using single-sample gene set enrichment analysis (ssGSEA) and cell-type identification. Relative subsets of RNA transcript (CIBERSORT) algorithms were estimated in both the TCGA-LIHC and ICGC-LIRI-JP cohorts. Intratumor heterogeneity, IFN-response, TGF-β response, proliferation, and wound healing scores were estimated in the low- and high-risk groups (29).

Analysis of Clinical Data

Kaplan–Meier survival curves were used to evaluate the overall survival (OS) of risk subgroups from the TCGA-LIHC and ICGC-LIRI-JP cohorts. The predictive sensitivity and specificity of the gene signatures were assessed by receiver operating characteristic (ROC). PCA was conducted using the R "prcomp" function of the "stats" package. Univariate and multivariate Cox regression analyses were performed to identify whether clinical characteristics and risk scores were independent risk factors. A nomogram was established to predict the 1-, 3-, and 5-year OS using the R "rms" package. Calibration plots, concordance index (C-index), and ROC were used to evaluate nomogram performance.

Analysis of Drug Sensitivity

The drug sensitivity inhibitory concentration (IC50) value and the mRNA profiles of NCI60 cell lines were extracted from the Cell-Miner™ database (https://discover.nci.nih.gov/cellminer/home.do). The sensitivity of the five selected genes was tested against 216 FDA-approved drugs. Co-expression network analysis of the genes and drugs was visualized using Cytoscape.

RESULTS

HCC Has Specific Glycosylation Alterations in Human Pan-Cancer

A flowchart of this study is shown in **Figure 1A**. mRNA expression of glycosylation-related genes across 11 cancer types in TCGA was evaluated using PCA. HCC had the most distinct glycosylation patterns (**Figure 1B**). The GSVA value of glycosylation-related pathways was also calculated in different samples of 11 pan-cancers, and HCC had the most specific enrichment of all cancers (**Figure 1C**).

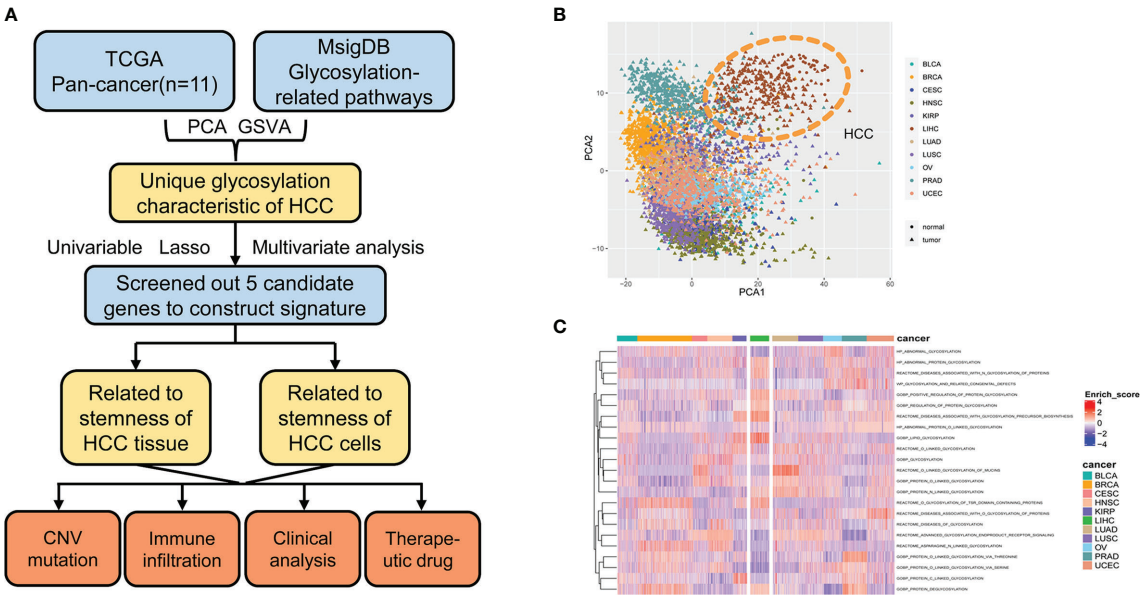

FIGURE 1 | Glycosylation alterations in human pan-cancer. **(A)** Study flowchart. **(B)** PCA projection of paired tumor and normal tissue samples from 11 different cancer types in TCGA. Different colors represent different cancer types. Circles and triangles represent normal and tumor tissue, respectively. **(C)** Heatmap showing glycosylation-related pathway alterations across 11 cancer types. MsigDB, molecular signatures database; PCA, principal component analysis; HCC, hepatocellular carcinoma; GSVA, gene set variance analysis; CNV, copy number variation; BLCA, bladder urothelial carcinoma; BRCA, breast invasive carcinoma; CESC, cervical squamous cell carcinoma and endocervical adenocarcinoma; HNSC, head and neck squamous cell carcinoma; KIRP, kidney renal papillary cell carcinoma; LIHC, liver hepatocellular carcinoma; LUAD, lung adenocarcinoma; LUSC, lung squamous cell carcinoma; OV, ovarian serous cystadenocarcinoma; PRAD, prostate adenocarcinoma; UCEC, uterine corpus endometrial carcinoma.

Identification of the Candidate Genes and Construction of the Prognostic Signature of HCC

Using gene expression profiling and corresponding clinical information from 50 normal and 374 tumor samples in the TCGA-LIHC database, 143 glycosylation-related DEGs were selected (adjusted P <0.05 and |Log FC| >1). Univariate Cox regression, LASSO regression, and stepwise Cox regression analyses were used to further investigate the importance of these DEGs (**Figures 2A, B**; **Table 1**). Five glycosylation-related genes were selected to construct the prognostic signature. Risk score = (0.403 ∗ CAD exp.) + (0.371 ∗ B3GAT3 exp.) + (0.068 ∗ SLC51B exp.) + (0.124 ∗ LGALS3 exp.) + (0.0767 ∗ MT3 exp.).

Based on the median risk score, HCC patients from the TCGA-LIHC and ICGC-LIRI-JP cohorts were classified into high- and low-risk groups. The five selected genes were identified as risk factors and had higher mRNA expressions in tumor tissues (**Figures 2C–E**). The protein expression patterns are presented in **Supplementary Figure 1**.

Gene Expression Profiles of High-Risk Patients Were Enriched With HCC Stemness Markers in TCGC-LIHC and ICGC-LIRI-JP Cohorts

As reported previously, glycosylation is highly correlated with stemness. This study aimed to compare gene expression profiles and risk scores with stemness markers. A mostly positive Spearman's correlation with the stemness-associated transcriptome-based signatures (Ben-Porath, Wong, Bhattacharya, and mRNA-si) was observed in the TCGA-LIHC (**Figure 3A**) and ICGC-LIRI-JP cohorts (**Supplementary Figure 2A**). The stemness markers, CD24, CD44, CD20, FOXM1, and EpCAM, also correlated strongly with gene expression levels and risk scores in both the TCGA-LIHC (**Figure 3B**) and ICGC-LIRI-JP cohorts (**Supplementary Figure 2B**). The high-risk cohorts had significantly higher signature scores (**Figure 3C**; **Supplementary Figure 2C**) and the gene expression profiles in the TCGA-LIHC and ICGC-LIRI-JP high-risk subgroups were significantly enriched in the Bhattacharya ESC signature (**Figure 3D**; **Supplementary Figure 2D**). The TCGA-LIHC and ICGC-LIRI-JP high-risk groups also had a significantly larger proportion of higher stages and grades (**Figure 3E**; **Supplementary Figure 2E**), suggesting the presence of a dedifferentiated phenotype.

Expression Profiles of the Five Glycosylation-Related Genes Were Associated With Stemness Markers in LCSCs

To further define the relationship between gene expression profiles and stemness in terms of stem cells, a single-cell RNA-sequencing dataset (GSE103866) including 55 HuH-1 cells, 63 HuH-7 cells, and 12 patient-derived cancer stem cells (CSCs) was downloaded. The UMAP algorithm was adopted for the three

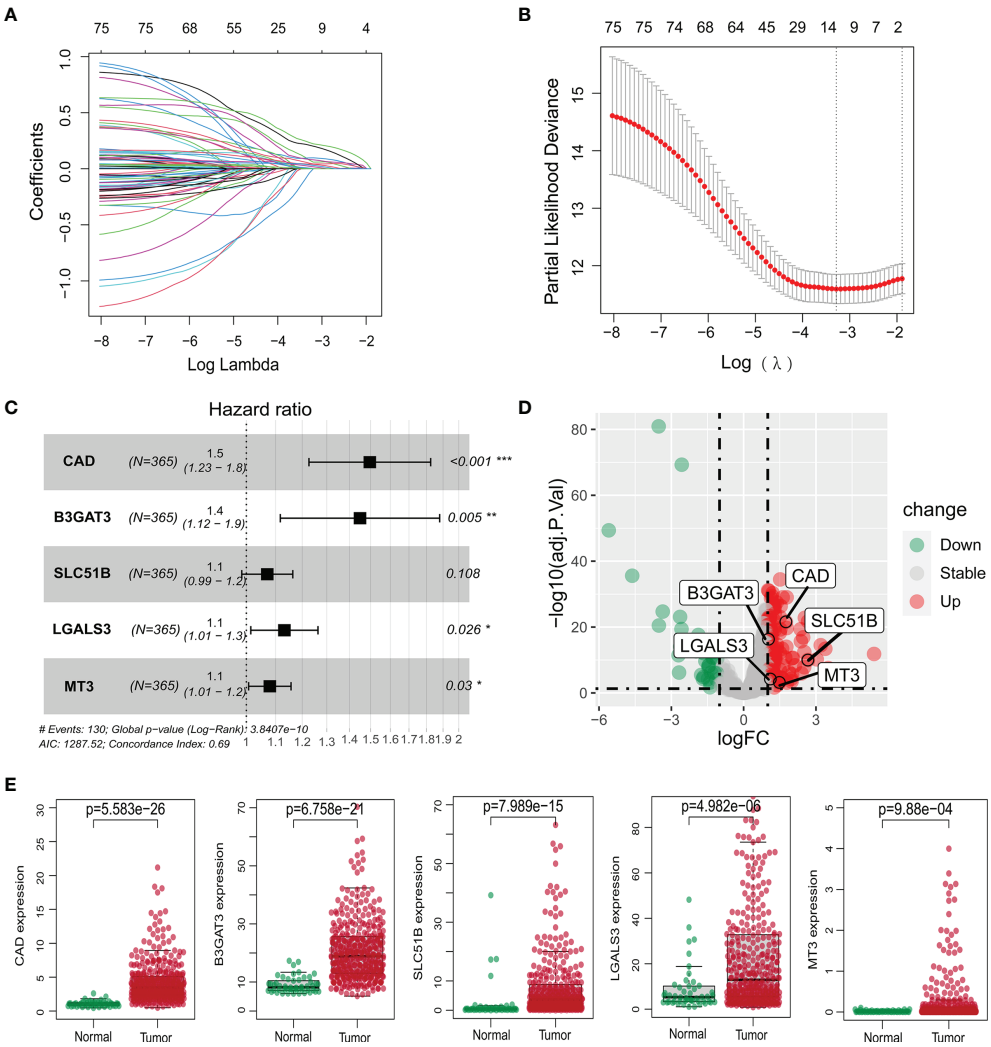

FIGURE 2 | Construction of the prognostic model of the TCGA-LIHC cohort. **(A, B)** Lasso regression analysis of survival-associated genes. **(C)** Multivariate Cox regression confirming five glycosylation-related genes. **(D)** Volcano plot of differentially expressed genes between HCC and non-tumor tissues. The five genes are marked. Red: significant upregulation; blue: significant downregulation; grey: no statistical significance. **(E)** Expression levels of five glycosylation-related genes between normal and HCC samples. *P <0.05; **P <0.01; *** P <0.001.

TABLE 1 | Multivariate Cox analysis results of glycosylation-related genes.

Id	Coef	HR	HR.95L	HR.95H	*P*-value
CAD	0.402886	1.496136	1.226555	1.824968	7.05E−5
B3GAT3	0.370858	1.448978	1.117225	1.879242	0.005181
SLC51B	0.068264	1.070648	0.9851	1.163626	0.108134
LGALS3	0.12411	1.13214	1.014627	1.263264	0.026941
MT3	0.076625	1.079637	1.007436	1.157013	0.023701

HR, hazard ratio; L, low; H, high.

cell types, three CSC markers, and the four gene expression distributions (**Figures 4A, B**). Vlnplot was used to visualize differences in marker gene expression in the distinct immunophenotypes (**Figure 4C**). Compared with the triple-negative CSCs, these genes showed high expression in other groups with stemness phenotypes (**Figure 4D**). These results confirm that high expression of these glycosylation-related genes may enhance the stemness of HCC.

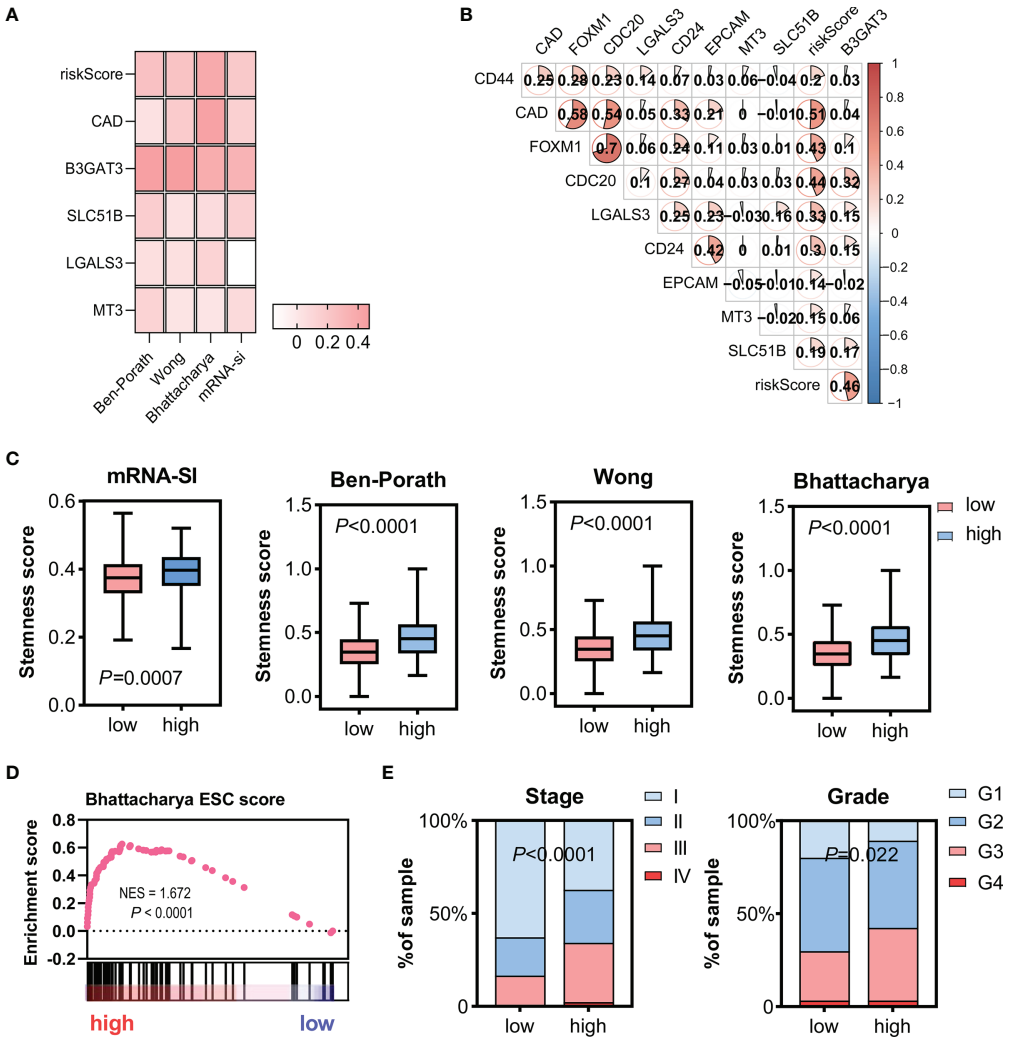

FIGURE 3 | Relationship between gene expression profiles and HCC stemness using HCC bulk data from TCGA-LIHC. **(A)** Heatmap of Spearman's correlation results of the gene expression profiles and four distinct stemness indices (Ben-Porath signature, Wong signature, Bhattacharya signature, and mRNA-si). A darker color represents a stronger correlation. **(B)** Correlation between the CSC markers, CD24, CD44, CD20, FOXM1, and EpCAM, and the gene expression profiles. **(C)** Different scores of the four distinct stemness indices between the low- and high-risk groups. **(D)** The transcriptome profiles of high-risk HCC patients were significantly enriched with stemness markers. **(E)** Among the high-risk patients, the frequency of higher stages and grades was more significantly elevated. Tumor stages and grades were color-coded as shown in the legend. NES, normalized enrichment score; CSC, cancer stem cells.

Experimental Validation of the Relationship Between the Five Glycosylation-Related Genes and Stemness

The relationship between the five genes and stemness was also verified in HCC samples. CAD expression was the most different between HCC and normal tissues in the TCGA-LIHC cohort. HCC patient tissues and cell lines also had significantly higher CAD mRNA levels than normal samples (**Figures 5A, B**). Gene knockdown was conducted in the HepG2 and Huh7 cell lines and the efficiencies were verified (**Figure 5C**). CAD knockdown resulted in a significant decline in tumor cell viability (P <0.05; **Figure 5D**) and a marked decrease in the proliferative capacity (**Figure 5E**). CD24, CD44, CD20, FOXM1, and EpCAM expression were also significantly lower in both si-CAD HepG2 and Huh7 cells than in control cells (**Figure 5F**). Knockdown of the remaining four genes also significantly inhibited CD24, CD44, CD20, FOXM1, and EpCAM expression (**Supplementary Figure 3**).

Somatic Mutation Alterations and CNVs in Different Gene Expression Profiles

Gene mutations in normal stem or progenitor cells may lead to the development and activation of LCSCs and are closely linked to the stemness of HCC. In mutation frequency analyses, a waterfall diagram showed the different status of somatic mutations in the TCGA-LIHC low- and high-risk groups. Sixty

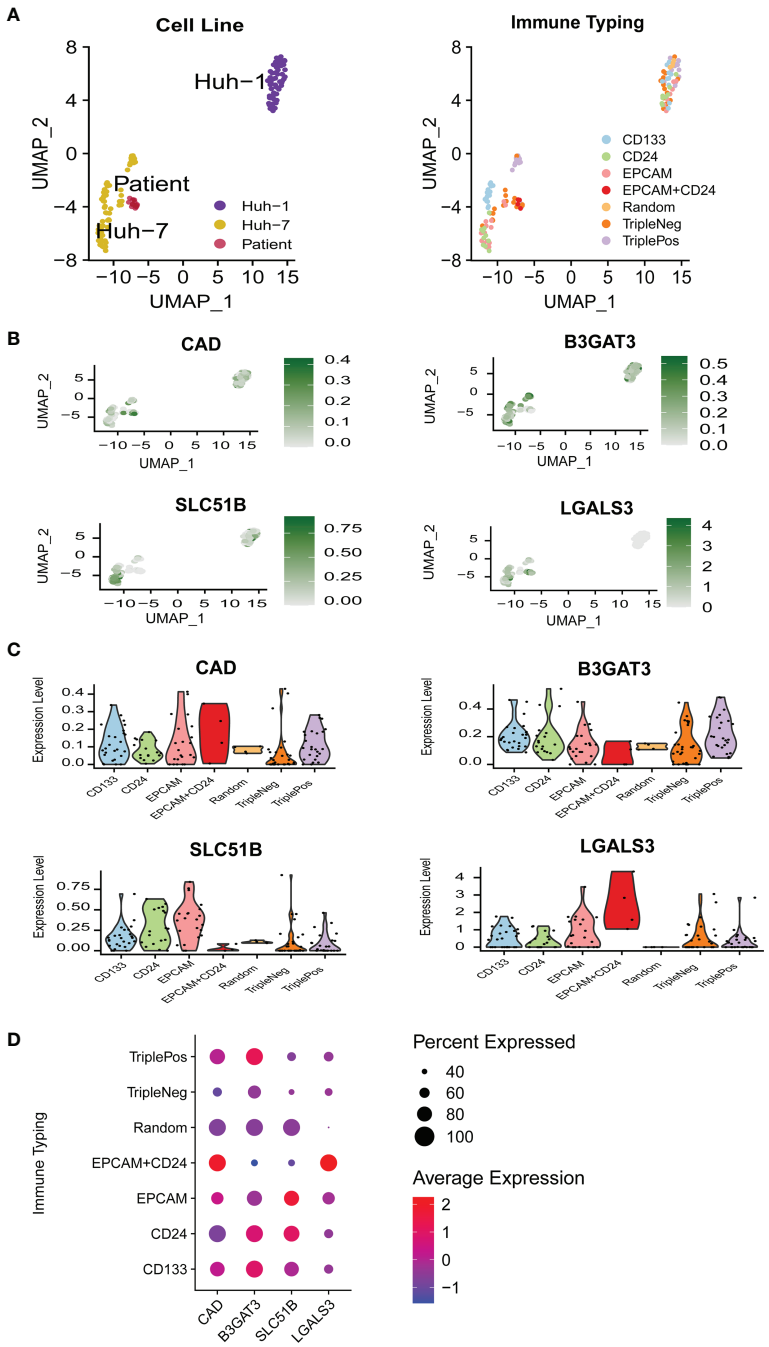

FIGURE 4 | The relationship between gene expression profiles and HCC stemness in single-cell RNA-sequencing data. **(A)** UMAP plots of 130 single cells using different classifications. **(B)** UMAP plots of the four glycosylation-related genes in CSC (MT3 was not detected in GSE 103866). **(C)** Violin plots of the four glycosylation-related gene expressions in CSC. **(D)** Expression of the four glycosylation-related genes in different immune phenotypes. CSC, cancer stem cells.

percent of genes, including TP53, TTN, MUC16, RYR2, LRP1B, OBSCN, CSMD3, XIRP2, FAT3, CACNA1E, HMCN1, and ARID1A, had a higher mutation frequency in the high-risk than in the low-risk group, while only 20%, including CTNNB1, APOB, ALB, and AXIN1, had a higher frequency in the low-risk group (**Figure 6A**). The chromosomal locations and CNV alterations of the glycosylation-related genes are shown in **Figure 6B**. High-risk patients also had a higher number of segments and some mutation scores (29) (**Figure 6C**). Many chromosomal regions showed significant copy amplification and

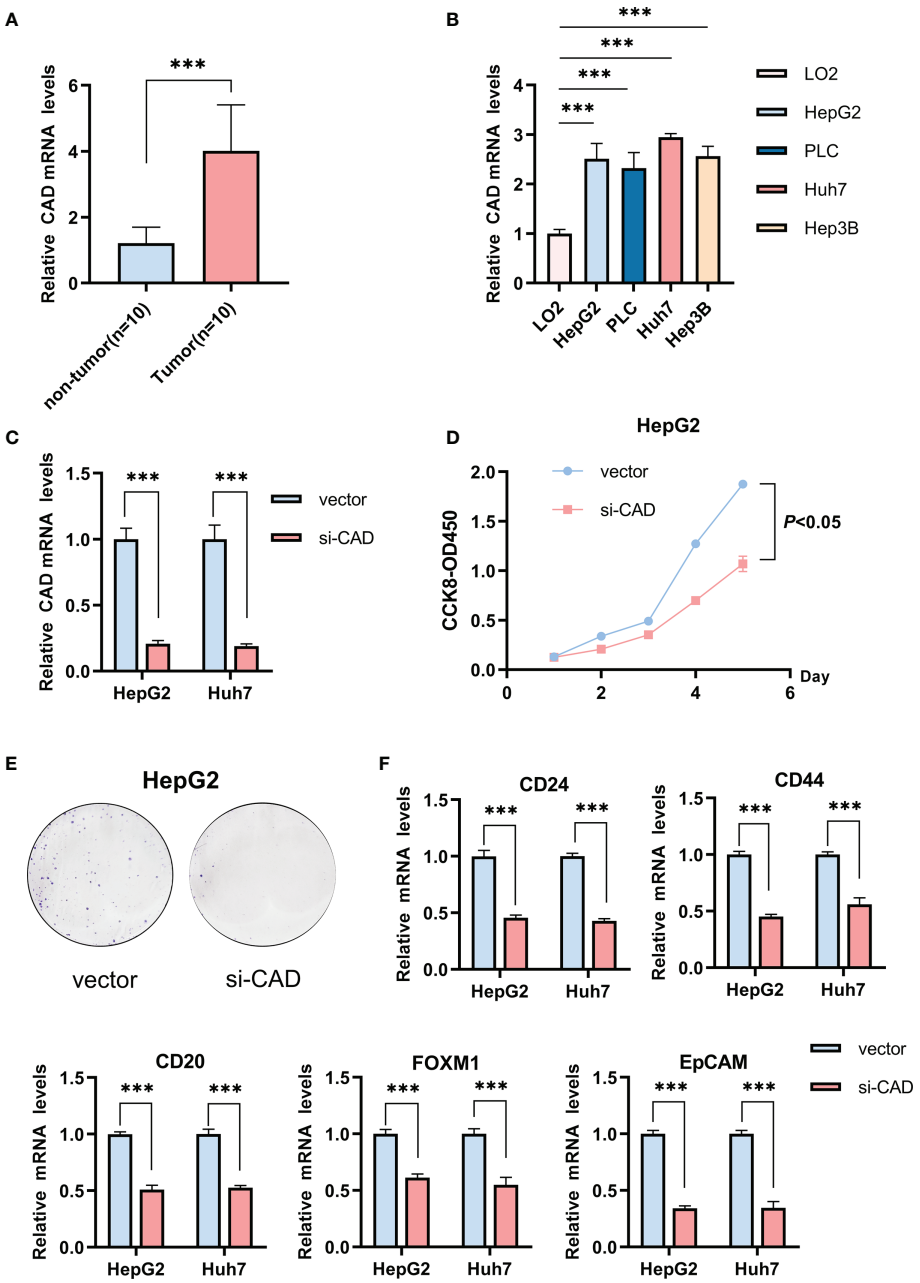

FIGURE 5 | The influence of CAD on the HCC stemness phenotype. **(A)** Differences in CAD expression between normal and HCC tissues. **(B)** Differential expression of CAD in HCC and normal cells. **(C)** The efficiency of CAD knockdown in HepG2 and Huh7 cells. **(D)** CCK-8 experiment comparing the si-CAD and control groups in HepG2 cells. **(E)** Colony formation assay comparing the si-CAD and control group in HepG2 cells. **(F)** Significant decrease in stemness-related markers, CD24, CD44, CD20, FOXM1, and EpCAM, after CAD knockdown in HepG2 and Huh7 cells. ***P <0.001.

gene deletion. CNVs were associated with a high-risk prognosis (**Figure 6D**). GISTIC showed that the scores of both amplification and deletion CNVs were considerably higher in the high-risk group than in the low-risk group (**Figure 6E**). While the low-risk group had a higher frequency of CNVs than the high-risk group, the high-risk group had more variability (**Figure 6F**).

The Landscape of Immune Infiltration in Different Gene Expression Profiles

Immune suppression drives tumor evolution toward a stem cell-like phenotype. This study assessed the correlation between risk classification and immune molecular subtype and found that C4 (lymphocyte-depleted) was the most common subtype (**Figure 7A**). A higher proportion of C1 and C2 subtypes, and

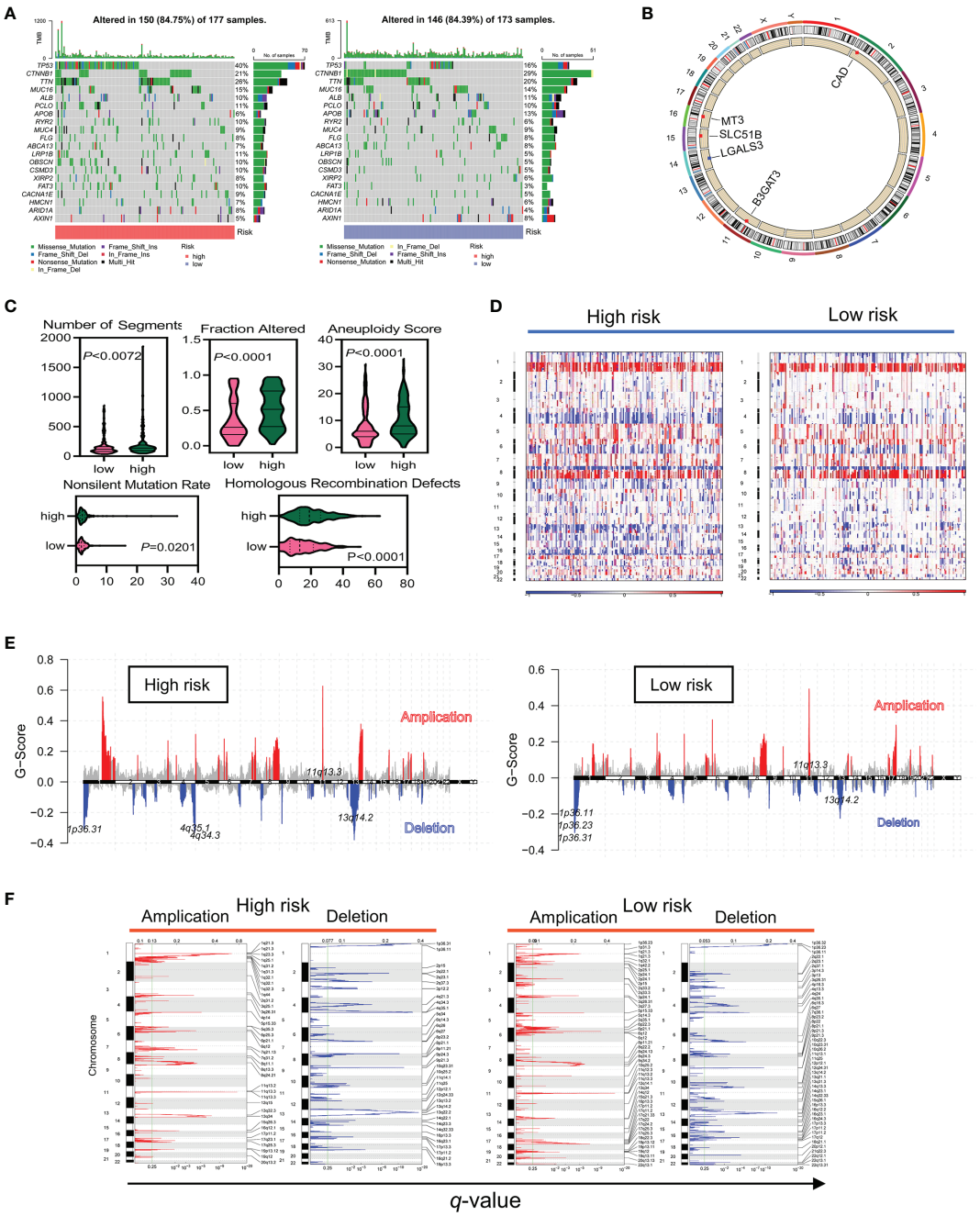

FIGURE 6 | The high-risk group had a higher frequency of somatic mutations and CNVs in TCGA data. **(A)** Differences in somatic mutation frequency in the high- and low-risk groups. **(B)** Five gene copy loss and copy amplification proportion distributions in the genome. **(C)** Scores of the five distinct mutation indices (number of segments, fraction altered, aneuploidy score, nonsilent mutation rate, and homologous recombination defects) in the low- and high-risk groups. **(D–F)** CNVs in different risk subgroups. Red and blue represent the two types of CNVs, amplification and deletion, respectively.

a lower level of the C3 subtype, were associated with a poorer prognosis (P <0.0001; **Figure 7B**). The correlation between immune cell infiltration and glycosylation-related gene expression also varied (**Figure 7C**). In the TCGA-LIHC cohort, correlation analyses further revealed a clear positive association between risk scores and infiltrating Th2 cells (R = 0.33; P = 3.6e−10) and M0 macrophages (R = 0.36; P = 1.2e−12). In contrast, both Th17 cells (R = −0.31; P = 3e−9) and M1 macrophages (R = −0.13; P = 0.018) were negatively associated with risk scores (**Figure 7D**). Similar results were also shown in the ICGC-LIRI-JP cohort (**Supplementary Figure 4A**). Differences in immune cells were also evaluated between the

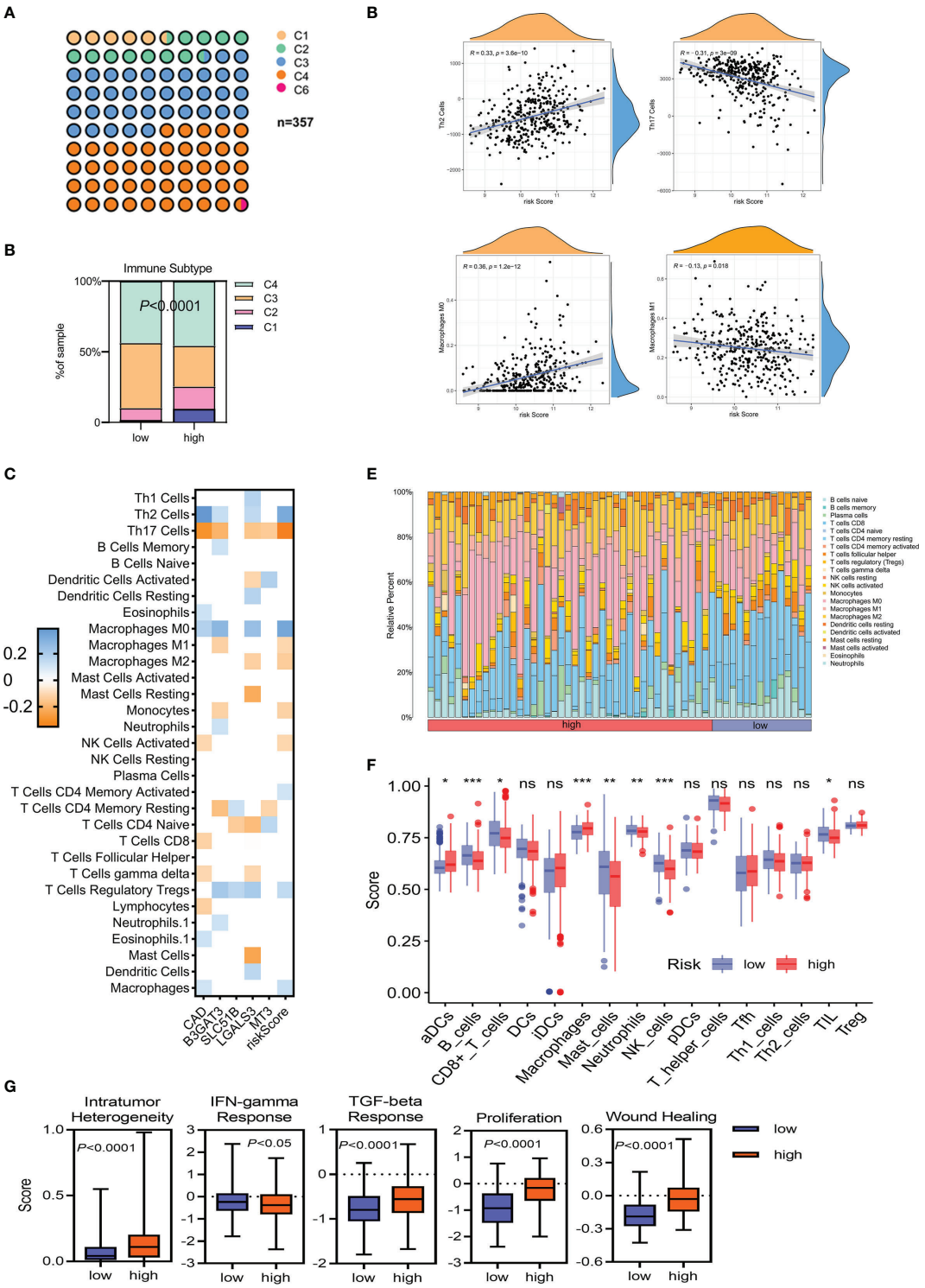

FIGURE 7 | The immune landscape of HCC tumors in TCGA-LIHC. **(A, B)** Classification of low- and high-risk HCC tumors into C1–C6 classes. C1, wound healing; C2, IFN-γ dominant; C3, inflammatory; C4, lymphocyte depleted; C6, TGF-β dominant. **(C)** Heatmap of Spearman's correlation between transcriptome profiles, risk scores, and immune infiltration. Only statistically significant correlations are shown (P <0.05). **(D)** Spearman's correlation of Th2/Th17 infiltration, M0/M1 macrophage infiltration, and the glycosylation-based risk score. **(E, F)** Different relative proportions of immune cells in different groups. **(G)** Scores of the five distinct immune indices between the low- and high-risk groups. *P <0.05; **P <0.01; ***P < 0.001, ns, not significant.

low- and high-risk groups in the TCGA-LIHC and ICGC-LIRI-JP cohorts. While aDCs and macrophages were significantly increased in the high-risk groups in both the TCGA-LIHC and ICGC-LIRI-JP cohorts, B cells, $CD8^+$ T cells, mast cells, neutrophils, NK cells, and TIL were reduced in the high-risk score group in the TCGA-LIHC cohort (**Figures 7E, F**). Meanwhile, only NK cells were reduced in the high-risk group in the ICGC-LIRI-JP cohort (**Supplementary Figures 4B, C**). Some immune-related scores were also assessed in the low- and high-risk groups (**Figure 7G**). Except for a striking negative association between the IFN-γ response score and the high-risk subgroup, other scores were significantly elevated in the high-risk group. These results indicated that high-risk patients had a distinct stemness phenotype associated with the accumulation of immune-suppressive cells.

Validation of the Prognostic Signature and Establishment of a Novel Nomogram

HCC patients in the high-risk group had a significantly poorer prognosis and lower OS than those in the low-risk group (**Figure 8A**; **Supplementary Figure 5A**). The area under the ROC curve (AUC) of the risk score in predicting 1-, 2-, and 3-year survival was 0.747, 0.741, and 0.730, respectively, in the TCGA dataset and 0.672, 0.642, and 0.647, respectively, in the ICGC dataset (**Figure 8B**; **Supplementary Figure 5B**). Compared with the risk subgroups, whole gene expression patterns were separated into two dispersion directions in both the ICGC and TCGA (**Figure 8C**; **Supplementary Figure 5C**). Race, gender, age, stage, fibrosis, and risk score were then included in univariate and multivariate Cox regression analyses. Notably, risk score was found to be an independent risk factor (HR >1, P <0.001) (**Figure 8D**). To further verify the prognostic value of the risk score, a nomogram that included gender, age, stage, and risk score was designed to illustrate patient survival more intuitively (**Figure 8E**). The calibration curves evaluated the predictive power of the nomogram at 1, 3, and 5 years, and the C-indexes were 0.704, 0.705, and 0.703, respectively (**Figure 8F**). The ICGC dataset was used to validate the nomogram and showed better discrimination and calibration ability, with C-indexes of 0.737, 0.739, and 0.739, respectively (**Figure 8G**). The AUC values of the nomogram at 1, 3, and 5 years reached 0.778, 0.748, and 0.741, respectively, which were better than those of the traditional HCC marker, AFP (**Figure 8H**).

Drug Sensitivity Analysis for the Five Glycosylation-Related Prognostic Genes

Glycosylation provides a range of potential targets for therapeutic intervention. However, potential drugs are still in clinical trials. Thus, the drug sensitivity of five selected glycosylation-related genes across diverse human cancer cell lines was further analyzed (correlation coefficient |R| >0.25, P <0.05). Consequently, 84 sensitive drugs were screened for abnormal glycosylation during HCC. Carfilzomib had the most obvious correlation with CAD (R = −0.341, P = 0.008) and mitoxantrone had the most obvious correlation with LGALS3 (R = −0.517, P = 2.36e−5). Dasatinib is associated with several genes. The top 16 strongest negative correlations between gene expression and IC50 are shown in **Figure 9A**. The link between the genes and sensitive drugs with a negative correlation of IC50 is shown in **Figure 9B**.

DISCUSSION

HCC involves complex architecture and heterogeneity and lacks effective individualized treatment targets (30). LCSCs with a specific phenotype are believed to promote HCC relapse, metastasis, and chemoresistance. Recent studies have shown that aberrant glycosylation of signaling pathways and LCSC markers directly impacts key processes that maintain cell survival, self-renewal, and extravasation properties (31–33). This study focused on the importance of glycosylation in promoting the stemness of HCC by assessing alterations in somatic mutations, immune cell infiltration, and clinical characteristics. Potential target drugs that could be used to improve HCC prognosis were selected.

To our knowledge, this is the first integrated multi-omics study in which the association between glycosylation and stemness was shown in HCC patients using bulk and single-cell RNA-sequencing data. A glycosylation-related prognostic signature was constructed consisting of five genes: CAD, B3GAT3, SLC51B, LGALS3, and MT3, using univariate, stepwise, and multivariate Cox regression analysis. Patients were then divided into low- and high-risk subgroups. Gene expression profiles of the high-risk group correlated positively with the upregulation of CSC markers, CD24, CD44, CD20, FOXM1, and EpCAM, and significant enrichment of other ESC signatures, indicating that these were tumor-promoting targets. Several studies have shown that stemness is associated with genetic mutations, epigenetic changes, and differences in the tumor microenvironment (34, 35). Similarly, our study found that the high-risk group had unique somatic mutations, CNVs, and immune patterns as well as enriched stem cell-like characteristics and high levels of gene expression. Clinical information was then combined with the prognostic signature to construct a calibrated nomogram. Finally, the sensitivity of glycosylation-related genes to particular drugs was evaluated, providing novel insight into tumor treatments and the prevention of drug resistance. Among the drug candidates, carfilzomib showed the most obvious correlation with CAD.

The five glycosylation-related genes were identified as significant in HCC. CAD is a multifunctional protein that takes part in *de novo* pyrimidine nucleotide synthesis, protein glycosylation, and phospholipid biosynthesis in mammals (12). This protein must initiate the di-(UDP)-dependent glycosylation process by producing UDP. UDP-N-acetylglucosamine (UDP-GlcNAc), for example, serves as an essential sugar donor substrate for O-GlcNAc, which is involved in a central intracellular protein modification in diverse metabolism, signaling, and disease processes (36). A recent study by Ching-Yu et al. (37) showed that UDP overexpression significantly

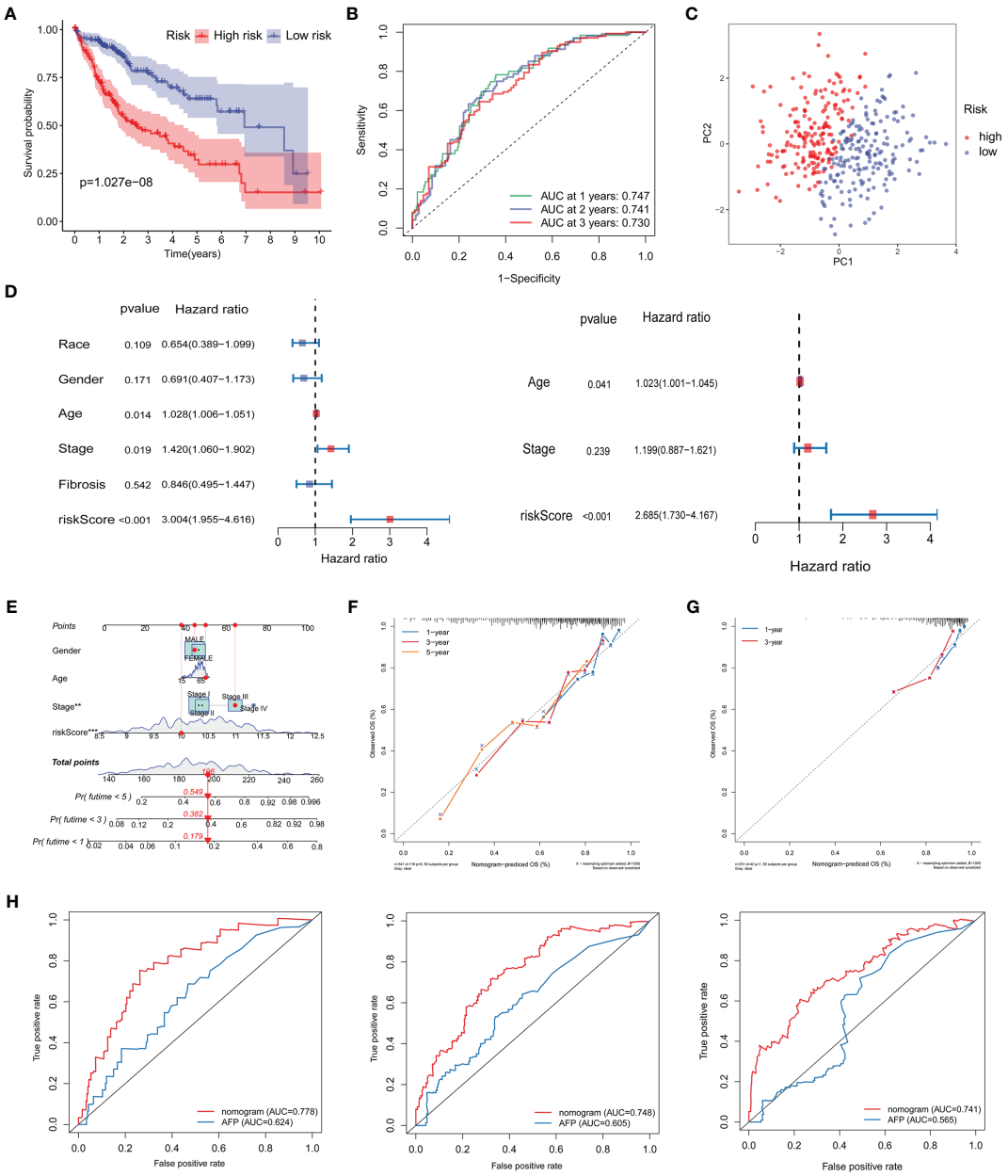

FIGURE 8 | Validation of the prognostic signature and establishment of a novel nomogram. **(A)** Kaplan–Meier curve analysis of the low- and high-risk groups. **(B)** ROC curve showing the prognostic risk model. **(C)** PCA plot of TCGA-LIHC patients in different risk groups. **(D)** Univariate and multivariate independent prognostic analysis of clinical features and risk scores. **(E)** Nomogram for survival prediction in TCGA-LIHC. **(F, G)** Nomogram calibration curves of 1-, 3-, and 5-year survival probabilities in TCGA-LIHC and ICGC-LIRI-JP, respectively. **(H)** ROC curves of the nomogram and AFP for the survival prediction at 1-, 3-, and 5-years. ROC, receiver operating characteristic; AUC, areas under the receiver operating characteristic curve; PCA, Principal component analysis; AFP, alpha-fetoprotein; OS overall survival.

promoted human hepatoma cell proliferation both *in vitro* and *in vivo*. UDP-13C-glucose flux is also responsible for metabolic reprogramming and the expression of key stemness genes in CSCs (38). The expression of LGALS3, a siglec-9 ligand in cancer cells, correlates with tumor progression and increased expression of β-catenin and CSC markers induced through Wnt signaling (39, 40). LGALS3 also helps maintain LSCS stemness, expansion, and aggressiveness and may thus serve as a target for HCC treatment (41). B3GAT3 is a glucuronosyltransferase involved in glycosylation and the proliferation and metastasis of HCC tissues and cells (42). SLC51B is involved in the intestinal reclamation of bile acids and steroids and eicosanoid metabolism, promoting liver cancer cell proliferation and suppressing apoptosis, which is associated with stemness (43). MT3 is a member of the

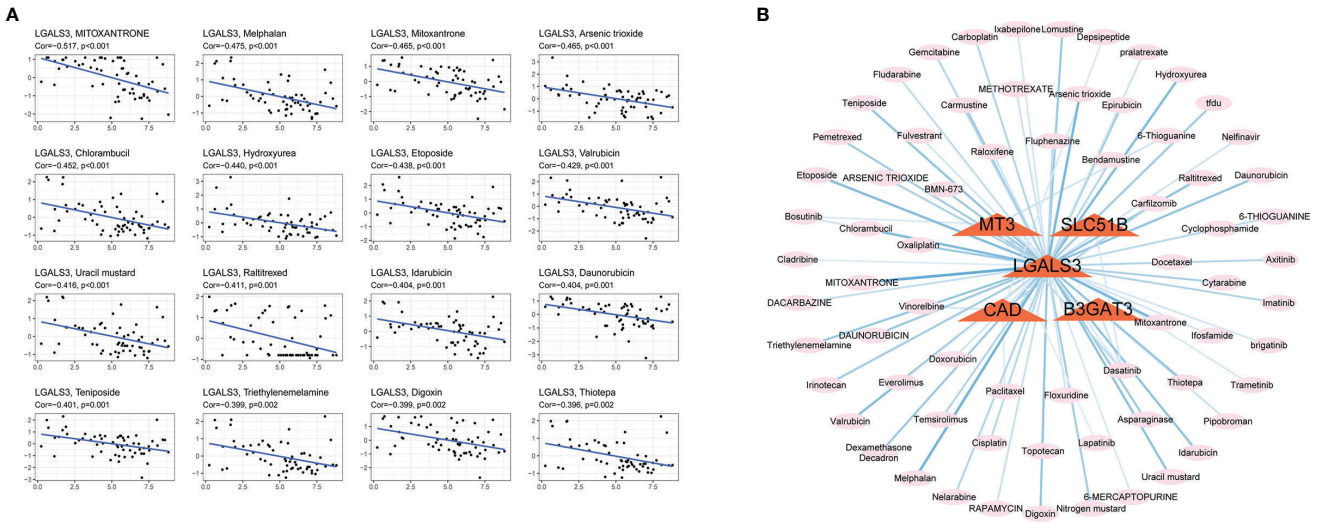

FIGURE 9 | Screening for sensitive drugs. **(A)** The top 16 most relevant negative correlations. **(B)** The network between five genes and sensitive drugs with negative IC50s (R<–0.25, *P* <0.05). Stronger correlations are represented by a thick dark blue line.

metallothionein family that regulates protein glycosylation and is closely linked to HCC progression. Studies indicate that MT overexpression may induce tumor cell differentiation (44, 45), but the mechanism will require further investigation. This study is consistent with the previously reported findings while also furthering our understanding of the relationship between LCSCs and glycosylation.

The production and activation of LCSCs may be induced by a series of gene mutations in normal stem or progenitor cells that disrupt cell metabolism, immune escape, and drug resistance. CNV is a hallmark of amplifications or deletions in the cancer genome, which can inactivate tumor suppressor genes, induce high oncogene expression, and increase stemness. A recent study of CNV showed that increases in the E2f1 or E2f3b loci promoted spontaneous HCC, whereas decreases in these loci suppressed HCC (46). In a genome-wide analysis, TRIM35 was shown as a novel tumor suppressor (47), and COL4A1 on the 13q34 locus was a frequent amplification target, a finding consistent with our results (48). Our study found that the RB1 deletion was most significant in the high-risk group, which supports prior research by Sung-Min et al. (49).

Stemness is significantly associated with immunosuppression in the immune microenvironment. As a result, this study also compared the proportions of immune cells in the high- and low-risk score groups and their gene expression profiles. Interestingly, cancer stem cell-like characteristics were enriched in the high-risk groups. To characterize intratumoral immune states, HCC samples were clustered into six subtypes using definitions developed by Thorsson et al. (29). The C4 subtype, associated with an imbalanced ratio of Th2/Th17 and M0/M1 cells, was the most common. Th2-related cytokines such as IL-4, IL-5, and IL-10 are involved in stimulating B cell proliferation and mediating humoral immunity. Some studies indicate that Th2 cells induce HCC progression (50). Indeed, Th2 cytokines facilitate tumor escape by inhibiting Th1 cytokine production (51) and furthering the progression of liver damage. However, IL-17 production by Th17 cells is generally associated with higher cancer survival (52). After transcatheter arterial embolization (TAE), the number of Th17 cells in the tumor microenvironment increases significantly (53). The Th2/Th17 cytokine profile is unbalanced during HCC and the shift towards Th17 cells can promote anti-tumor effects. Macrophages are key antigen-presenting cells of the innate immune system, and different macrophage phenotypes have distinct functions in regulating the tumor microenvironment. In particular, M1 macrophages are involved in suppressing tumor growth and inducing liver tumor regression. Guerra et al. (54) found that hydrogel-embedded M1 macrophages induced apoptosis of HCC cells and promoted tumor regression. Localization of activated M1 macrophages may be a new novel HCC treatment strategy. Our study also found significant enrichment in intratumor heterogeneity, TGF-β mediated signaling, proliferation, and a cancer stemness phenotype in the high-risk group, while IFN signaling was increased in the low-risk group. Consistent with these results, TGF-β-mediated signaling has been strongly linked to a cancer stem-like phenotype in tumors (55), while IFN signaling has been negatively correlated with stemness and HCC progression (56, 57).

Current chemotherapy drugs remain unable to significantly promote the long-term survival of HCC patients. Thus, this study screened potential target drugs using the Cell-Miner database. Carfilzomib, a second-generation proteasome inhibitor, had the strongest correlation with CAD. This drug exhibits an anti-tumor effect by inhibiting MAPK signaling (58). CAD activation requires MAPK, so it is possible that carfilzomib indirectly inhibits CAD by suppressing MAPK signaling and promoting an anti-tumor response. Mitoxantrone, an antineoplastic drug developed in the 1980s, had the strongest

correlation with genes. A recent study found that mitoxantrone inhibits HCC growth and proliferation by inducing autophagy (59). In the mitoxantrone-resistant cell line, LGALS3 was detected with an abundance ratio well above two (60). Dasatinib, a tyrosine kinase inhibitor that exerts anti-tumor effects by inhibiting glucuronosyltransferase, is associated with the expression of several genes (61). SLC51B is a subtype of the human solute carrier (SLC) and correlates negatively with drug sensitivity (62). MT3 is also involved in SLC synthesis and is negatively associated with Dasatinib. BAGAT3 is an important type of glucuronosyltransferase. However, whether these drugs could be used to treat abnormal glycosylation requires further study.

Glycosylation is a promising target for tumor treatment. However, there are some limitations that should be addressed in our study. First, few studies have assessed the relationship between stemness and glycosylation, especially those involving the development of HCC. This study relied heavily on TCGA, GEO, and ICGC data and lacked experimental evidence. Thus, we could not determine whether the selected genes have corresponding roles in glycosylation pathways. Further functional experiments are necessary to define the molecular mechanisms. Second, CNVs were not available in the ICGC database. A larger CNV sample size would help ensure the reliability of the study. Third, the mechanism of potentially sensitive drugs in abnormal glycosylation during HCC remains unknown and requires further study.

CONCLUSIONS

In conclusion, this study proposed a prognostic signature founded on glycosylation-related gene expression and classified HCC samples into low- and high-risk subgroups. According to bulk and single-cell RNA-sequencing, the high-risk group was most likely to have a stem-like phenotype. This was verified by assessing somatic mutations, CNVs, immune infiltration, and clinical characteristics. These findings will help inform future studies on the relationship between glycosylation and HCC stemness.

DATA AVAILABILITY STATEMENT

The original contributions presented in the study are included in the article/**Supplementary Material**. Further inquiries can be directed to the corresponding author.

ETHICS STATEMENT

The studies involving human participants were reviewed and approved by the Ethics Committee of Tianjin Second People's Hospital. The patients/participants provided their written informed consent to participate in this study.

AUTHOR CONTRIBUTIONS

All authors contributed to the study conception and design. PL and QZ contributed equally to this study. PL and QZ designed and wrote the manuscript. PL and QZ screened the literature and collected data. PL and QZ were responsible for pictures and statistics. PL and QZ polished the article. JL critically revised the manuscript. All authors listed have made a substantial, direct, and intellectual contribution to the work and approved it for publication.

FUNDING

This work was funded by the Natural Science Foundation of Tianjin City (20JCYBJC01150); the Tianjin Health Science and Technology Project (Nos. TJWJ2021QN063, TJWJ2021ZD010, and TJWJ2021MS034), and the Tianjin Key Medical Discipline (Specialty) Construction Project.

ACKNOWLEDGMENTS

The authors acknowledge The Third Affiliated Hospital of Sun Yat-Sen University for their technical assistance.

SUPPLEMENTARY MATERIAL

The Supplementary Material for this article can be found online at: https://www.frontiersin.org/articles/10.3389/fonc.2022.913432/full#supplementary-material

Supplementary Table 1 | Glycosylation-related pathways and genes retrieved from MSigDB. MSigDB, Molecular signatures Database.

Supplementary Table 2 | Primer and specific siRNA sequences were used in this study. siRNA, small interfering RNA.

Supplementary Figure 1 | The representative immunohistochemistry of the five glycosylation-related genes in normal and HCC tissues downloaded from HPA. HPA, The Human Protein Atlas.

Supplementary Figure 2 | Relationship between gene expression profiles and HCC stemness using HCC bulk data from ICGC-LIRI-JP. **(A)** Heatmap of Spearman's correlation results of the gene expression profiles and four distinct stemness indices (Ben-Porath signature, Wong signature, Bhattacharya signature, and mRNA-si). A darker color represents a stronger correlation. **(B)** Correlation between the CSC markers, CD24, CD44, CD20, FOXM1, and EpCAM, and the gene expression profiles. **(C)** Different scores of the four distinct stemness indices between the low- and high-risk groups. **(D)** The transcriptome profiles of high-risk HCC patients were significantly enriched with stemness markers. **(E)** Among the high-risk patients, the frequency of higher stages and grades was more significantly elevated. Tumor stages and grades were color-coded as shown in the legend. NES, normalized enrichment score; CSC, cancer stem cells.

Supplementary Figure 3 | The influence of the remaining four genes on the stemness phenotype of HCC. **(A)** Differential expression in HCC and normal cells. **(B)** Significant decrease in stemness-related markers, CD24, CD44, CD20, FOXM1, and EpCAM, after SLC51B knockdown in HepG2 and Huh7 cells. **(C)** Significant decrease in stemness-related markers, CD24, CD44, CD20, FOXM1,

and EpCAM, after LGALS3 knockdown in HepG2 and Huh7 cells. **(D)** Significant decrease in stemness-related markers, CD24, CD44, CD20, FOXM1, and EpCAM, after B3GAT3 knockdown in HepG2 and Huh7 cells. **(E)** Significant decrease in stemness-related markers, CD24, CD44, CD20, FOXM1, and EpCAM, after MT3 knockdown in HepG2 and Huh7 cells. *** $P < 0.001$.

Supplementary Figure 4 | The immune landscape of HCC tumors in ICGC-LIRI-JP. **(A)** Spearman's correlation of Th2/Th17 infiltration, M0/M1 macrophage infiltration, and the glycosylation-based risk score. **(B, C)** Different relative proportions of immune cells in different groups. *P <0.05; **P <0.01; *** P <0.001.

Supplementary Figure 5 | Validation of the prognostic signature in ICGC-LIRI-JP. **(A)** Kaplan-Meier curve analysis of the low- and high-risk groups. **(B)** ROC curve showing the prognostic risk model. **(C)** PCA plot of TCGA-LIHC patients in different risk groups. ROC, receiver operating characteristic; PCA, principal component analysis.

REFERENCES

1. Emal A, Ward EM, Johnson CJ, Cronin KA, Ma J, Ryerson B, et al. Annual Report to the Nation on the Status of Cancer, 1975-2014, Featuring Survival. *J Natl Cancer Inst* (2017) 109(9):djx030. doi: 10.1093/jnci/djx030
2. Sung H, Ferlay J, Siegel RL, Laversanne M, Soerjomataram I, Jemal A, et al. Global Cancer Statistics 2020: GLOBOCAN Estimates of Incidence and Mortality Worldwide for 36 Cancers in 185 Countries. *CA Cancer J Clin* (2021) 71(3):209–49. doi: 10.3322/caac.21660
3. Yu M, Chen Z, Zhou Q, Zhang B, Huang J, Jin L, et al. PARG InhibitionLimits HCC Progression and Potentiates the Efficacy of Immune CheckpointTherapy. *J Hepatol* (2022) 12:S0168–8278(22)00072. doi: 10.1016/j.jhep.2022.01.026
4. Romito I, Porru M, Braghini MR, Pompili L, Panera N, Crudele A, et al. Focal Adhesion Kinase Inhibitor TAE226 Combined With Sorafenib Slows Down Hepatocellular Carcinoma by Multiple Epigenetic Effects. *J Exp Clin Cancer Res* (2021) 40(1):364. doi: 10.1186/s13046-021-02154-8
5. European Association for the Study of the Liver. EASL-EORTC Clinical Practice Guidelines: Management of Hepatocellular Carcinoma. *J Hepatol* (2012) 56(4):908–43. doi: 10.1016/j.jhep.2011.12.001
6. Bruix J, Reig M, Sherman M. Evidence-Based Diagnosis, Staging, and Treatment of Patients With Hepatocellular Carcinoma. *Gastroenterology* (2016) 150(4):835–53. doi: 10.1053/j.gastro.2015.12.041
7. Tricot T, Verfaillie CM, Kumar M. Current Status and Challenges of Human Induced Pluripotent Stem Cell-Derived Liver Models in Drug Discovery. *Cells* (2022) 11(3):442. doi: 10.3390/cells11030442
8. Zhang S, Cao X, Gao Q, Liu Y. Protein Glycosylation in Viral Hepatitis-Related HCC: Characterization of Heterogeneity, Biological Roles, and Clinical Implications. *Cancer Lett* (2017) 406:64–70. doi: 10.1016/j.canlet.2017.07.026
9. Jia L, Li J, Li P, Liu D, Li J, Shen J, et al. Site-Specific Glycoproteomic Analysis Revealing Increased Core-Fucosylation on FOLR1 Enhances Folate Uptake Capacity of HCC Cells to Promote EMT. *Theranostics* (2021) 11(14):6905–21. doi: 10.7150/thno.56882
10. Zhang Q, Jiang K, Li Y, Gao D, Sun L, Zhang S, et al. Histidine-Rich Glycoprotein Function in Hepatocellular Carcinoma Depends on its N-Glycosylation Status, and it Regulates Cell Proliferation by Inhibiting Erk1/2 Phosphorylation. *Oncotarget* (2015) 6(30):30222–31. doi: 10.18632/oncotarget.4997
11. Zhang C, Niu Y, Wang Z, Xu X, Li Y, Ma L, et al. Corosolic Acid Inhibits Cancer Progression by Decreasing the Level of CDK19-Mediated O-GlcNAcylation in Liver Cancer Cells. *Cell Death Dis* (2021) 12(10):889. doi: 10.1038/s41419-021-04164-y
12. Coxam B, Neyt C, Grassini DR, Le Guen L, Smith KA, Schulte-Merker S, et al. Carbamoyl-Phosphate Synthetase 2, Aspartate Transcarbamylase, and Dihydroorotase (Cad) Regulates Notch Signaling and Vascular Development in Zebrafish. *Dev Dyn* (2015) 244(1):1–9. doi: 10.1002/dvdy.24209
13. Teoh ST, Ogrodzinski MP, Lunt SY. UDP-Glucose 6-Dehydrogenase Knockout Impairs Migration and Decreases *In Vivo* Metastatic Ability of Breast Cancer Cells. *Cancer Lett* (2020) 492:21–30. doi: 10.1016/j.canlet.2020.07.031
14. Wolfe AL, Zhou Q, Toska E, Galeas J, Ku AA, Koche RP, et al. UDP-Glucose Pyrophosphorylase 2, a Regulator of Glycogen Synthesis and Glycosylation, is Critical for Pancreatic Cancer Growth. *Proc Natl Acad Sci U.S.A.* (2021) 118 (31):e2103592118. doi: 10.1073/pnas.2103592118
15. Xiao H, Woods EC, Vukojicic P, Bertozzi CR. Precision Glycocalyx Editing as a Strategy for Cancer Immunotherapy. *Proc Natl Acad Sci U.S.A.* (2016) 113 (37):10304–9. doi: 10.1073/pnas.1608069113
16. Pinho SS, Reis CA. Glycosylation in Cancer: Mechanisms and Clinical Implications. *Nat Rev Cancer* (2015) 15(9):540–55. doi: 10.1038/nrc3982
17. Ashraf JM, Shahab U, Tabrez S, Lee EJ, Choi I, Aslam yusuf M, et al. DNA Glycation From 3-Deoxyglucosone Leads to the Formation of AGEs: Potential Role in Cancer Auto-Antibodies. *Cell Biochem Biophys* (2016) 74(1):67–77. doi: 10.1007/s12013-015-0713-6
18. Khan MS, Rabbani N, Tabrez S, Islam BU, Malik A, Ahmed A, et al. Glycation Induced Generation of Amyloid Fibril Structures by Glucose Metabolites. *Protein Pept Lett* (2016) 23(10):892–7. doi: 10.2174/0929866523666160831153858
19. Ahmad S, Akhter F, Shahab U, Rafi Z, Khan MS, Nabi R, et al. Do All Roads Lead to the Rome? The Glycation Perspective! *Semin Cancer Biol* (2018) 49:9–19. doi: 10.1016/j.semcancer.2017.10.012
20. Ashraf JM, Ahmad S, Rabbani G, Hasan Q, Jan AT, Lee EJ, et al. 3-Deoxyglucosone: A Potential Glycating Agent Accountable for Structural Alteration in H3 Histone Protein Through Generation of Different AGEs. *PloS One* (2015) 10(2):e0116804. doi: 10.1371/journal.pone.0116804
21. Shen YA, Wang CY, Chuang HY, Hwang JJ, Chi WH, Shu CH, et al. CD44 and CD24 Coordinate the Reprogramming of Nasopharyngeal Carcinoma Cells Towards a Cancer Stem Cell Phenotype Through STAT3 Activation. *Oncotarget* (2016) 7(36):58351–66. doi: 10.18632/oncotarget.11113
22. Yamashita T, Honda M, Nakamoto Y, Baba M, Nio K, Hara Y, et al. Discrete Nature of EpCAM+ and CD90+ Cancer Stem Cells in Human Hepatocellular Carcinoma. *Hepatology* (2013) 57(4):1484–97. doi: 10.1002/hep.26168
23. Yuan B, Liu Y, Yu X, Yin L, Peng Y, Gao Y, et al. FOXM1 Contributes to Taxane Resistance by Regulating UHRF1-Controlled Cancer Cell Stemness. *Cell Death Dis* (2018) 9(5):562. doi: 10.1038/s41419-018-0631-9
24. Ahn KS, O'Brien DR, Kim YH, Kim TS, Yamada H, Park JW, et al. Associations of Serum Tumor Biomarkers With Integrated Genomic and Clinical Characteristics of Hepatocellular Carcinoma. *Liver Cancer* (2021) 10 (6):593–605. doi: 10.1159/000516957
25. Malta TM, Sokolov A, Gentles AJ, Burzykowski T, Poisson L, Weinstein JN, et al. Machine Learning Identifies Stemness Features Associated With Oncogenic Dedifferentiation. *Cell* (2018) 173(2):338–354.e15. doi: 10.1016/j.cell.2018.03.034
26. Ben-Porath I, Thomson MW, Carey VJ, Ge R, Bell GW, Regev A, et al. An Embryonic Stem Cell-Like Gene Expression Signature in Poorly Differentiated Aggressive Human Tumors. *Nat Genet* (2008) 40(5):499–507. doi: 10.1038/ng.127
27. Wong DJ, Liu H, Ridky TW, Cassarino D, Segal E, Chang HY. Module Map of Stem Cell Genes Guides Creation of Epithelial Cancer Stem Cells. *Cell Stem Cell* (2008) 2(4):333–44. doi: 10.1016/j.stem.2008.02.009
28. Bhattacharya B, Miura T, Brandenberger R, Mejido J, Luo Y, Yang AX, et al. Gene Expression in Human Embryonic Stem Cell Lines: Unique Molecular Signature. *Blood* (2004) 103(8):2956–64. doi: 10.1182/blood-2003-09-3314
29. Thorsson V, Gibbs DL, Brown SD, Wolf D, Bortone DS, Ou Yang TH, et al. The Immune Landscape of Cancer. *Immunity* (2018) 48(4):812–830.e14. doi: 10.1016/j.immuni.2018.03.023
30. Losic B, Craig AJ, Villacorta-Martin C, Martins-Filho SN, Akers N, Chen X, et al. Intratumoral Heterogeneity and Clonal Evolution in Liver Cancer. *Nat Commun* (2020) 11(1):291. doi: 10.1038/s41467-019-14050-z
31. Li C, Du Y, Yang Z, He L, Wang Y, Hao L, et al. GALNT1-Mediated Glycosylation and Activation of Sonic Hedgehog Signaling Maintains the Self-Renewal and Tumor-Initiating Capacity of Bladder Cancer Stem Cells. *Cancer Res* (2016) 76(5):1273–83. doi: 10.1158/0008-5472.CAN-15-2309
32. Venetz D, Hess C, Lin CW, Aebi M, Neri D. Glycosylation Profiles Determine Extravasation and Disease-Targeting Properties of Armed Antibodies. *Proc Natl Acad Sci U.S.A.* (2015) 112(7):2000–5. doi: 10.1073/pnas.1416694112
33. Zhou B, Zhao YC, Liu H, Luo S, Amos CI, Lee JE, et al. Novel Genetic Variants of ALG6 and GALNTL4 of the Glycosylation Pathway Predict Cutaneous Melanoma-Specific Survival. *Cancers (Basel)* (2020) 12(2):288. doi: 10.3390/cancers12020288

34. Weng CC, Ding PY, Liu YH, Hawse JR, Subramaniam M, Wu CC, et al. Mutant Kras-Induced Upregulation of CD24 Enhances Prostate Cancer Stemness and Bone Metastasis. *Oncogene* (2019) 38(12):2005–19. doi: 10.1038/s41388-018-0575-7
35. Miranda A, Hamilton PT, Zhang AW, Pattnaik S, Becht E, Mezheyeuski A, et al. Cancer Stemness, Intratumoral Heterogeneity, and Immune Response Across Cancers. *Proc Natl Acad Sci U.S.A.* (2019) 116(18):9020–9. doi: 10.1073/pnas.1818210116
36. Winans KA, Bertozzi CR. An Inhibitor of the Human UDP-GlcNAc 4-Epimerase Identified From a Uridine-Based Library: A Strategy to Inhibit O-Linked Glycosylation. *Chem Biol* (2002) 9(1):113–29. doi: 10.1016/s1074-5521(02)00093-5
37. Lai CY, Liu H, Tin KX, Huang Y, Yeh KH, Peng HW, et al. Identification of UAP1L1 as a Critical Factor for Protein O-GlcNAcylation and Cell Proliferation in Human Hepatoma Cells. *Oncogene* (2019) 38(3):317–31. doi: 10.1038/s41388-018-0442-6
38. Bi Z, Zhang Q, Fu Y, Wadgaonkar P, Zhang W, Almutairy B, et al. Nrf2 and HIF1α Converge to Arsenic-Induced Metabolic Reprogramming and the Formation of the Cancer Stem-Like Cells. *Theranostics* (2020) 10(9):4134–49. doi: 10.7150/thno.42903
39. Ilmer M, Mazurek N, Gilcrease MZ, Byrd JC, Woodward WA, Buchholz TA, et al. Low Expression of Galectin-3 is Associated With Poor Survival in Node-Positive Breast Cancers and Mesenchymal Phenotype in Breast Cancer Stem Cells. *Breast Cancer Res* (2016) 18(1):9. doi: 10.1186/s13058-016-0757-6
40. Chung LY, Tang SJ, Wu YC, Sun GH, Liu HY, Sun KH. Galectin-3 Augments Tumor Initiating Property and Tumorigenicity of Lung Cancer Through Interaction With β-Catenin. *Oncotarget* (2015) 6(7):4936–52. doi: 10.18632/oncotarget.3210
41. Tummala KS, Brandt M, Teijeiro A, Graña O, Schwabe RF, Perna C, et al. Hepatocellular Carcinomas Originate Predominantly From Hepatocytes and Benign Lesions From Hepatic Progenitor Cells. *Cell Rep* (2017) 19(3):584–600. doi: 10.1016/j.celrep.2017.03.059
42. Zhang YL, Ding C, Sun L. High Expression B3GAT3 Is Related With Poor Prognosis of Liver Cancer. *Open Med (Wars)* (2019) 14:251–8. doi: 10.1515/med-2019-0020
43. Cheng J, Li Y, Wang X, Dong Z, Chen Y, Zhang R, et al. Response Stratification in the First-Line Combined Immunotherapy of Hepatocellular Carcinoma at Genomic, Transcriptional and Immune Repertoire Levels. *J Hepatocell Carcinoma* (2021) 8:1281–95. doi: 10.2147/JHC.S326356
44. Jin R, Bay BH, Chow VT, Tan PH, Lin VC. Metallothionein 1e mRNA is Highly Expressed in Oestrogen Receptor-Negative Human Invasive Ductal Breast Cancer. *Br J Cancer* (2000) 83(3):319–23. doi: 10.1054/bjoc.2000.1276
45. Sens MA, Somji S, Garrett SH, Beall CL, Sens DA. Metallothionein Isoform 3 Overexpression is Associated With Breast Cancers Having a Poor Prognosis. *Am J Pathol* (2001) 159(1):21–6. doi: 10.1016/S0002-9440(10)61668-9
46. Kent LN, Bae S, Tsai SY, Tang X, Srivastava A, Koivisto C, et al. Dosage-Dependent Copy Number Gains in E2f1 and E2f3 Drive Hepatocellular Carcinoma. *J Clin Invest* (2017) 127(3):830–42. doi: 10.1172/JCI87583
47. Jia D, Wei L, Guo W, Zha R, Bao M, Chen Z, et al. Genome-Wide Copy Number Analyses Identified Novel Cancer Genes in Hepatocellular Carcinoma. *Hepatology* (2011) 54(4):1227–36. doi: 10.1002/hep.24495
48. Lau SH, Guan XY. Cytogenetic and Molecular Genetic Alterations in Hepatocellular Carcinoma. *Acta Pharmacol Sin* (2005) 26(6):659–65. doi: 10.1111/j.1745-7254.2005.00126.x
49. Ahn SM, Jang SJ, Shim JH, Kim D, Hong SM, Sung CO, et al. Genomic Portrait of Resectable Hepatocellular Carcinomas: Implications of RB1 and FGF19 Aberrations for Patient Stratification. *Hepatology* (2014) 60(6):1972–82. doi: 10.1002/hep.27198
50. Gramenzi A, Andreone P, Loggi E, Foschi FG, Cursaro C, Margotti M, et al. Cytokine Profile of Peripheral Blood Mononuclear Cells From Patients With Different Outcomes of Hepatitis C Virus Infection. *J Viral Hepat* (2005) 12(5):525–30. doi: 10.1111/j.1365-2893.2005.00634.x
51. Ji L, Gu J, Chen L, Miao D. Changes of Th1/Th2 Cytokines in Patients With Primary Hepatocellular Carcinoma After Ultrasound-Guided Ablation. *Int J Clin Exp Pathol* (2017) 10(8):8715–20. doi: 10.4161/2162402X.2014.984547
52. Punt S, Langenhoff JM, Putter H, Fleuren GJ, Gorter A, Jordanova ES. The Correlations Between IL-17 vs Th17 Cells and Cancer Patient Survival: A Systematic Review. *Oncoimmunology* (2015) 4(2):e984547. doi: 10.4161/2162402X.2014.984547
53. Avritscher R, Jo N, Polak U, Cortes AC, Nishiofuku H, Odisio BC, et al. Hepatic Arterial Bland Embolization Increases Th17 Cell Infiltration in a Syngeneic Rat Model of Hepatocellular Carcinoma. *Cardiovasc Intervent Radiol* (2020) 43(2):311–21. doi: 10.1007/s00270-019-02343-1
54. Guerra AD, Yeung OWH, Qi X, Kao WJ, Man K. The Anti-Tumor Effects of M1 Macrophage-Loaded Poly (Ethylene Glycol) and Gelatin-Based Hydrogels on Hepatocellular Carcinoma. *Theranostics* (2017) 7(15):3732–44. doi: 10.7150/thno.20251
55. Johnston CJ, Smyth DJ, Dresser DW, Maizels RM. TGF-β in Tolerance, Development and Regulation of Immunity. *Cell Immunol* (2016) 299:14–22. doi: 10.1016/j.cellimm.2015.10.006
56. Shirasaki T, Honda M, Yamashita T, Nio K, Shimakami T, Shimizu R, et al. The Osteopontin-CD44 Axis in Hepatic Cancer Stem Cells Regulates IFN Signaling and HCV Replication. *Sci Rep* (2018) 8(1):13143. doi: 10.1038/s41598-018-31421-6
57. Xing M, Li J. A New Inflammation-Related Risk Model for Predicting Hepatocellular Carcinoma Prognosis. *BioMed Res Int* (2022) 5:5396128. doi: 10.1155/2022/5396128
58. Jiang C, Xu R, Li XX, Zhou YF, Xu XY, Yang Y, et al. Sorafenib and Carfilzomib Synergistically Inhibit the Proliferation, Survival, and Metastasis of Hepatocellular Carcinoma. *Mol Cancer Ther* (2018) 17(12):2610–21. doi: 10.1158/1535-7163.MCT-17-0541
59. Xie B, He X, Guo G, Zhang X, Li J, Liu J, et al. High-Throughput Screening Identified Mitoxantrone to Induce Death of Hepatocellular Carcinoma Cells With Autophagy Involvement. *Biochem Biophys Res Commun* (2020) 521(1):232–7. doi: 10.1016/j.bbrc.2019.10.114
60. Wang J, Gutierrez P, Edwards N, Fenselau C. Integration of 18O Labeling and Solution Isoelectric Focusing in a Shotgun Analysis of Mitochondrial Proteins. *J Proteome Res* (2007) 6(12):4601–7. doi: 10.1021/pr070401e
61. Virakul S, Dalm VA, Paridaens D, van den Bosch WA, Hirankarn N, van Hagen PM, et al. The Tyrosine Kinase Inhibitor Dasatinib Effectively Blocks PDGF-Induced Orbital Fibroblast Activation. *Graefes Arch Clin Exp Ophthalmol* (2014) 252(7):1101–9. doi: 10.1007/s00417-014-2674-7
62. Polillo M, Galimberti S, Baratè C, Petrini M, Danesi R, Di Paolo A. Pharmacogenetics of BCR/ABL Inhibitors in Chronic Myeloid Leukemia. *Int J Mol Sci* (2015) 16(9):22811–29. doi: 10.3390/ijms160922811

Conflict of Interest: The authors declare that the research was conducted in the absence of any commercial or financial relationships that could be construed as a potential conflict of interest.

Publisher's Note: All claims expressed in this article are solely those of the authors and do not necessarily represent those of their affiliated organizations, or those of the publisher, the editors and the reviewers. Any product that may be evaluated in this article, or claim that may be made by its manufacturer, is not guaranteed or endorsed by the publisher.

frontiers | Frontiers in Oncology

ORIGINAL RESEARCH
published: 28 June 2022
doi: 10.3389/fonc.2022.904911

Yiqi Jianpi Huayu Jiedu Decoction Inhibits Metastasis of Colon Adenocarcinoma by Reversing Hsa-miR-374a-3p/Wnt3/β-Catenin-Mediated Epithelial–Mesenchymal Transition and Cellular Plasticity

Yuwen Zhuang[1†], Jinyong Zhou[2†], Shenlin Liu[1], Qiong Wang[2], Jun Qian[1], Xi Zou[1], Haiyan Peng[1], Tian Xue[3], Zhichao Jin[1] and Cunen Wu[1]*

[1] Department of Oncology, Affiliated Hospital of Nanjing University of Chinese Medicine, Jiangsu Province Hospital of Chinese Medicine, Nanjing, China, [2] Central Laboratory, Affiliated Hospital of Nanjing University of Chinese Medicine, Jiangsu Province Hospital of Chinese Medicine, Nanjing, China, [3] Department of Education, Affiliated Hospital of Nanjing University of Chinese Medicine, Jiangsu Province Hospital of Chinese Medicine, Nanjing, China

Colon adenocarcinoma (COAD) accounts for 95% of colon cancer cases, with the 5-year survival rate significantly affected by local or distant metastases. Yiqi Jianpi Huayu Jiedu decoction (YJHJD), based on the theory of "nourish qi, invigorate the spleen, remove blood stasis, and detoxify", has long been applied and shown to be remarkable in the prevention and treatment of gastrointestinal tumors. However, the underlying therapeutic mechanisms of YJHJD have not been fully elucidated. Herein, we first confirmed hsa-miR-374a-3p as a tumor suppressor based on its lower expression in the plasma of patients with COAD with liver metastasis and association with more advanced local progression. We also verified WNT3 as a potential target of hsa-miR-374a-3p and observed its increased expression in COAD tissues. Furthermore, we showed that the hsa-miR-374a-3p/Wnt3/β-catenin axis was responsible for epithelial–mesenchymal transition (EMT) and cellular plasticity in COAD, as well as poorer patient prognosis. Our results showed that YJHJD inhibited motility and colony potential *in vitro*, as well as liver metastasis of COAD *in vivo*. Moreover, YJHJD induced a reversal of EMT and cellular plasticity-related molecular expression, increased hsa-miR-374a-3p, and decreased Wnt3 and β-catenin levels. In addition, silencing of hsa-miR-374a-3p weakened YJHJD inhibition, whereas the β-catenin inhibitor XAV939 partially repaired it. Taken together, these results demonstrated that YJHJD suppressed the EMT and cellular plasticity of COAD by regulating hsa-miR-374a-3p/Wnt3/β-catenin signaling.

Keywords: Yiqi Jianpi Huayu Jiedu decoction, colon adenocarcinoma, epithelial–mesenchymal transition, cellular plasticity, hsa-miR-374a-3p, Wnt3

OPEN ACCESS

Edited by:
Nathaniel Weygant, Fujian University of Traditional Chinese Medicine, China

Reviewed by:
Changyong Luo, Dongfang Hospital of Beijing University of Chinese Medicine, China
Jose Francisco Islas, Autonomous University of Nuevo León, Mexico

****Correspondence:***
Cunen Wu
wucunen@njucm.edu.cn

[†]These authors share first authorship

Specialty section:
This article was submitted to Gastrointestinal Cancers: Colorectal Cancer, a section of the journal Frontiers in Oncology

Received: *26 March 2022*
Accepted: *20 May 2022*
Published: *28 June 2022*

Citation:
Zhuang Y, Zhou J, Liu S, Wang Q, Qian J, Zou X, Peng H, Xue T, Jin Z and Wu C (2022) Yiqi Jianpi Huayu Jiedu Decoction Inhibits Metastasis of Colon Adenocarcinoma by Reversing Hsa-miR-374a-3p/Wnt3/β-Catenin-Mediated Epithelial–Mesenchymal Transition and Cellular Plasticity. Front. Oncol. 12:904911. doi: 10.3389/fonc.2022.904911

INTRODUCTION

Colon cancer is the fifth most common malignancy worldwide, causing nearly 1,150,000 new cases and 580,000 deaths annually. Colon adenocarcinoma (COAD) is one of the most common pathological subtypes, accounting for 95% of colon cancer cases (1). With increased control of high-risk factors and improvements in diagnosis and treatment techniques, the incidence of colon cancer has been declining in recent years; however, more than half of patients have local or distant metastases when diagnosed, severely affecting patient 5-year survival (2, 3). Although intravenous chemotherapy, targeted therapy, radiotherapy, and immunotherapy can control lesions to a certain extent and benefit patients, treatment efficiency is often limited by drug resistance or side effects (4). Therefore, reducing the risk of metastasis is an effective strategy for improving the comprehensive efficacy and prognosis of patients with COAD.

The epithelial–mesenchymal transition (EMT) is an important process by which epithelial cells acquire mesenchymal properties. This process is related to a variety of biological characteristics of tumors, including metastasis. During the EMT, the epithelial molecule E-cadherin is downregulated, and the mesenchymal marker N-cadherin and a series of EMT-activating transcription factors such as Snail are upregulated. Tumor cells lose their original polarity and close intercellular connections, thus acquiring stronger infiltrative and invasive abilities during EMT (5). Furthermore, cancer cell plasticity is necessary for EMT during metastasis (6). EMT-induced cellular plasticity and cancer stem cell (CSC)-related signals are associated with malignant progression (7). CSCs are a small group of tumor-initiating cells (TICs) that can produce multiple cell types through self-renewal and differentiation, subsequently leading to tumor initiation. CSCs are closely related to COAD metastasis due to their insensitivity to traditional treatment methods (8). Reversing the EMT and cellular plasticity to reduce metastatic potential may be an effective method for the treatment of COAD metastasis.

Increasing evidence has shown that microRNAs (miRNAs) are involved in multiple processes, including malignancy genesis and development. By specifically binding to the 3'-UTR region of the target mRNA, miRNAs can regulate mRNA translation or degradation and play a role in carcinogenesis or tumor inhibition (9). Among these miRNAs, hsa-miR-374a was shown to participate in the formation of a negative feedback loop and suppression of downstream signals associated with EMT in nasopharyngeal carcinoma (10). Moreover, hsa-miR-374a suppressed *in vivo* tumorigenicity by reducing the stemness of human glioma stem cells (11). Hsa-miR-374a also directly targeted regulators of the Wnt/β-catenin pathway to regulate EMT in breast cancer (12). Wnt3a can induce β-catenin accumulation and RhoA activation, which is linked to upregulated vimentin expression (13). Therefore, targeted regulation of the hsa-miR-374a-3p/Wnt3 axis may provide a new direction for the prevention and treatment of COAD metastasis.

Traditional Chinese medicine theory states that "spleen deficiency and stasis toxin" are the main pathogenesis of COAD, while the combination of "qi deficiency," "blood stasis", and "cancer toxin" is a key pathological factor. Hence, the treatment principle follows the theory of "nourish qi, invigorate the spleen, remove blood stasis, and detoxify". Based on this, a traditional Chinese medicine compound prescription derived from the classical formula Guishao Liujun decoction, called Yiqi Jianpi Huayu Jiedu decoction (YJHJD), has long been applied for the treatment of COAD. To further explore the mechanism underlying the inhibitory effect of YJHJD on COAD, we investigated the influence of YJHJD on the EMT and cellular plasticity of COAD cells, as well as YJHJD regulation of hsa-miR-374a-3p/Wnt3 signaling.

MATERIALS AND METHODS

RNA Extraction and Small RNA Sequencing Analysis

Peripheral venous blood was collected from each subject early in the morning on an empty stomach. Plasma was isolated within 4 h and stored at −80°C for future analysis. Total cell-free RNA was extracted from the plasma using the miRNeasy Serum/Plasma kit (Qiagen, CA, USA). A small RNA library was established using a TruSeq Small RNA Sample Prep Kit (Illumina, San Diego, CA, USA). The qualified library was loaded onto an Illumina HiSeq 2500 platform for high-throughput sequencing (Lianchuan Biotechnology, Hangzhou, China). Raw data from each sample were filtered using ACGT101-miR (LC Sciences, Houston, Texas, USA) to remove junk sequences, adapter dimers, low-complexity reads, common RNA families, and repeats. Known miRNAs and novel 5p or 3p miRNAs were identified by mapping all 18–26 nucleotide sequences to the miRBase22.0 database (http://www.mirbase.org/). The remaining sequences were aligned to the miRBase miRNA database to identify completely matched sequences that were judged to be conserved *Homo sapiens* miRNAs (14). Differences in miRNA expression were evaluated by analysis of variance (ANOVA) test, with the significance threshold defined as $|\log2\ FC| > 1.0$ and $p < 0.05$.

Plasma and Tissue Samples of Patients With COAD

A total of 66 patients diagnosed with primary COAD by postoperative pathology were recruited for this retrospective study. All plasma specimens were collected by centrifuging peripheral venous blood preoperatively and stored at −80°C. Another three pairs of para-carcinoma, CAOD, and hepatic metastasis tissue samples were collected from three patients who were diagnosed with COAD with hepatic metastasis immediately after surgical resection and frozen in liquid nitrogen within 5 min. Written informed consent was obtained from all the patients.

Data Source and Different Expression Gene Analysis

COAD data containing 41 paracancerous and 480 COAD samples were acquired from The Cancer Genome Atlas (TCGA) database. Annotation information (GENCODE v25) was obtained from the UCSC Xena database. Differentially

expressed genes (DEGs) between paracancerous tissues and tumors were authenticated *via* the classical Bayesian method in the Limma package (Version 3.10.3), with a threshold value of adjusted $p < 0.01$ and $|\log2\ FC| > 1.5$. Heatmaps and volcano figures of DEGs were constructed using the pheatmap and ggplot packages.

Kaplan–Meier Plotter Analysis

The patients with COAD were divided into low and high groups according to the specific miRNA or mRNA expression levels. The relationships between miRNA or mRNA expression and the prognosis of patients with COAD were assessed based on the Kaplan–Meier method using the survival package and visualized using the survminer package. Statistical significance was defined as $p < 0.05$.

Cell Culture

The human COAD cell lines HCT116 and HT29 were obtained from the Type Culture Collection, Chinese Academy of Sciences (Shanghai, China). The mouse colon cancer cell line CT26-GFP was purchased from Cellcook (Guangzhou, China). The cells were cultured in RPMI-1640 medium with 10% fetal bovine serum (FBS, Gibco-BRL, Gaithersburg, USA) in a humidified incubator at 37°C and 5% CO_2.

Fluorescence *In Situ* Hybridization and Immunofluorescence in Human Tissues

FISH experiments were conducted to evaluate hsa-miR-374a-3p expression in human tissues as described previously (15, 16). Hsa-miR-374a-3p probes [5'-AATTACAATACAATCTGATAAG (ttt CATCATCAT ACATCATCAT)30-3', 5'-DIG-tt ATGATGATGT ATGATGATGT-3'] with a double digoxigenin (DIG)-labeled probe against hsa-miR-374a-3p were synthesized (Servicebio Technology, Wuhan, China). For *in situ* hybridization, anti-DIG-horseradish peroxidase (HRP)-conjugated antibody (Jackson, West Grove, USA) and tyramide signal amplification iF647-TSA (Servicebio) were applied and the nuclei were stained with 4′,6-diamidino-2-phenylindole (DAPI). Wnt3 (1:100, Abcam, Cambridge, UK), β-catenin (1:100, Servicebio, Wuhan, China), and Cy3/FITC-labeled anti-rabbit immunoglobulin G (IgG, Servicebio, Wuhan, China) were used for the analysis of human specimens. Fluorescence images were captured using a Nikon imaging system (DS-U3; Tokyo, Japan).

Transfection of COAD Cells With Hsa-miR-374a-3p Mimic/Inhibitor

Hsa-miR-374a-3p mimic/inhibitor and scrambled control plasmids were constructed by Gene Pharma (Shanghai, China). HCT116 and HT29 cells were seeded in 24-well plates and incubated for 24 h. Both cell types were then transfected with miRNA-335-5p mimic/inhibitor using Lipofectamine 3000 Transfection Reagent according to the manufacturer's protocol (Invitrogen, Grand Island, NY, USA). Transfection potency was confirmed 48 h later by RT-PCR.

Wound-Healing Assay

HCT116 and HT29 cells were plated in six-well dishes and incubated overnight to form confluent monolayers. Pipette tips were used to scratch a strip to create a line across the cell monolayers. The remaining cells underwent another 24-h incubation and the relative wounded areas were measured and calculated.

Transwell Assay

Transwell membrane filter inserts (pore size, 8 μm; Costar, Corning, NY, USA) in 24-well dishes were used to test the cell invasive ability. Starved COAD cells were resuspended in serum-free medium (5×10^5/ml). A 200-μl cell suspension was added to the upper inserts and covered with Matrigel. Then, 500 μl of complete medium was added to the lower chambers. After another 24-h incubation, the cells that remained on the upper side were wiped off. The cells were fixed with 95% alcohol and stained with 0.05% crystal violet for further analysis.

Spheroid Formation

HCT116 and HT29 cells (1×10^3/well) were seeded into ultralow attachment six-well plates, filled with serum-free medium containing 1% B27 (Life Technology, Grand Island, USA), 20 ng/ml epidermal growth factor (EGF), and 10 ng/ml basic fibroblast growth factor (bFGF, Peprotech, Rocky Hill, USA) at 37°C in 5% CO_2. The medium was changed every 6 days. Spheroid formation images were obtained 10 or 20 days after culture.

RT-PCR Assay

Total RNA was extracted from COAD cells or liver metastatic tumor tissues using TRIzol reagent (Life Technology, Grand Island, USA) and reverse-transcribed into cDNA using the PrimeScript RT reagent kit with gDNA Eraser (TaKaRa, Dalian, China). The primers used in this experiment are presented in **Table 1**. Gene expression was investigated on an ABI7500 fast RT-PCR System (Applied Biosystems, Waltham, USA) using the DNA-binding SYBR-Green dye and the $\triangle\triangle$Ct analysis method.

Western Blot Assay

Total or nuclear proteins were extracted from COAD cells or liver metastatic tumor tissues and lysed in radioimmunoprecipitation assay (RIPA) buffer. Proteins were separated by sodium dodecyl sulfate-polyacrylamide gel electrophoresis (SDS-PAGE) and transferred to polyvinylidene difluoride (PVDF) membranes (Millipore, Bedford, USA). Membranes were incubated with 5% bovine serum albumin (BSA) for 1 h at room temperature and then incubated with primary antibodies against E-cadherin, N-cadherin, Snail, CD44, Sox2, β-catenin (1:1,000, CST), β-actin, histone H3 (1:2,000, CST), and Wnt3 (1:1,000, Abcam) at 4°C overnight. The membranes were then incubated with secondary antibodies at room temperature for 1 h. Protein signals were probed using an ECL kit (BI, Kibbutz Beit-Haemek, Israel).

Immunofluorescence Analysis

The cells were fixed with 4% paraformaldehyde for 15 min and permeabilized with 0.5% Triton X-100 for 20 min. Subsequently, 5% BSA was used to block the cells for 30 min. The cells were incubated with antibodies against Wnt3 (1:100, Abcam,

TABLE 1 | Primers used for RT-PCR.

Target	Primer sequence
hsa-miR-374a-3p	Forward 5'-TACATCGGCCATTATAATA-3' Reverse 5'-TACACAGAATTACAATAC-3'
U6	Forward 5'-CTCGCTTCGGCAGCACA-3' Reverse 5'-AACGCTTCACGAATTTGCGT-3'
WNT3	Forward 5'-CGTCTTCCACTGGTGCTGC-3' Reverse 5'-CAGTCCATGCTCCTTGCTG-3'
GAPDH	Forward 5'-TGGGTGTGACCATGAGAAGT-3' Reverse 5'-TGAGTCCTTCCACGATACCAA-3'

Cambridge, UK) or β-catenin (1:100; Servicebio, Wuhan, China) overnight at 4°C followed by incubation with Cy3-labeled anti-rabbit IgG (1:200 dilution, Servicebio, Wuhan, China) secondary antibody for 1 h. Next, the nuclei were stained with DAPI for 5 min. Fluorescence images were acquired using a laser scanning confocal microscope (Zeiss LSM710, Jena, Germany).

Immunohistochemistry Analysis

Formaldehyde-fixed portions of the tissues were embedded in paraffin and sectioned into 4-μm thick slices. After deparaffinization in xylene, the sections were hydrated in a series of graded alcohols. A pressure cooker was used to perform antigen retrieval by placing the sections in 10 mM sodium citrate buffer (pH 6.0) for 15 min. The sections were incubated with primary antibodies against β-catenin, α-sma, and CD44 (1:100, Abcam) overnight at 4°C. HRP-linked secondary antibody was used for incubation for 1 h at room temperature, and the nuclei were stained with hematoxylin.

Hematoxylin–Eosin Staining

Mouse livers with metastatic tumor tissue were fixed in formaldehyde, embedded in paraffin, and cut into 4-μm-thick sections. The sections were then dewaxed with xylene and hydrated with gradient ethanol before staining with hematoxylin for 5 min and soaking in tap water for 5 min. The sections were subsequently stained with eosin solution for 2 min before conventional dehydration, vitrification and sealing with neutral resin. A Nikon imaging system (DS-U3, Tokyo, Japan) was used to obtain photos.

Preparation of YJHJD

YJHJD comprises the 10 types of Chinese herbal medicines listed in **Table 2**. All herbs were obtained from the Affiliated Hospital of Nanjing University of Chinese Medicine and Jiangsu Province Hospital of TCM. YJHJD granules were dissolved in 165 ml of double-steamed water, heated, and stirred until boiling for 20 min. The liquid was concentrated to ensure the crude drug concentrations of 1.7–3.4 g/ml. The herb solution was then centrifuged at 10,000 *g*/min for 5 min and the supernatant was collected and subpackaged. The YJHJD drug serum used for the *in vitro* experiments was prepared according to the equivalent dose conversion formula (17). Pathogen-free Sprague–Dawley rats were administered 2 ml of YJHJD solution by gavage twice daily for 14 days (0.85 and 3.4 g/ml, respectively, in the YJHJ low-dose [DL] and YJHJ high-dose [DH] groups). Arterial blood was collected 1 h after the last drug administration and centrifuged at 3,000 r/min. The supernatants were stored at −80°C after inactivation and filtration sterilization.

High-Performance Liquid Chromatography Analysis of YJHJD

A total of 100 μl of YJHJD at a concentration of 2 g/ml was diluted in methanol and then mixed. The solution was then centrifuged at 12,000 r/min for 10 min and the supernatant was collected. Separation was performed on an Agilent SB-C 18 column (100 mm × 4.60 mm, 1.8 μm). The mobile phase consisted of methyl alcohol (A), acetonitrile (B), and 0.1% formic acid. Gradient elution was performed according to the protocol. The temperature of the column was maintained at 40° C, with a sample volume of 10 μl.

In Vivo Liver Metastasis Assay

A total of 30 BALB/c mice (6–8 weeks of age, 15 male and 15 female) were obtained from Beijing Vital River Laboratory Animal Technology Co., Ltd. The mice were anesthetized by intraperitoneal injection of 1% pentobarbital sodium. A total of 10 μl of CT26-GFP cell suspension (5×10^7/ml) was injected under the spleen envelope in each. The mice were randomly divided into three groups (model, YJHJDL, and YJHJDH) on the third day after surgery. Mice in the YJHJDL (1.7 g/ml, 0.2 ml/20 g) and YJHJDH (3.4 g/ml, 0.2 ml/20 g) groups were administered YJHJD by gavage twice daily, while the mice in the model group were administered the same amount of normal saline for 21 days. The mice were sacrificed 2 h after the last drug administration. The livers were removed for photography and immediately frozen in liquid nitrogen for further analysis.

TABLE 2 | Yiqi Jianpi Huayu Jiedu decoction (YJHJD) composition.

Chinese name	Latin name	Doses (g)
Huang Qi	Astragalus Membranaceus	15
Dang Shen	Codonopsis Pilosula	15
Bai Zhu	Rhizomes Atractylodis Macrocephalae	10
Fu Ling	Poria Cocos	15
Shan Yao	Chinese Yam	15
Wu Mei	Smoked Plum	10
Cu San Leng	Vinegar Rhizoma Sparganii	10
Cu E Zhu	Vinegar Curcuma Zedoary	10
Xian He Cao	Herba Agrimoniae	30
Bai Jiang Cao	Defeat Sauce	30
Gan Cao	Radix Glycyrrhizae	5

Statistical Analysis

The results are presented as means ± SD. Statistical analysis was conducted using IBM SPSS Statistics for Windows, version 23.0 (IBM Corp., Armonk, NY, USA) with one-way ANOVA, followed by Duncan's test. Statistical significance was defined as $p < 0.05$ or 0.01.

RESULTS

Hsa-miR-374a-3p Is Downregulated in the Plasma of Patients With Hepatic Metastasis of COAD and Is Correlated to Poorer Prognosis

Plasma from a cohort of six patients diagnosed with COAD (three with hepatic metastasis [COAD_M] and three without) was analyzed to identify expression profiles using miRNA high-throughput RNA-seq analysis. The results showed that compared to the COAD group, the levels of 12 miRNAs increased and 51 miRNAs decreased in patients with COAD_M (**Figures 1A, B**). Subsequently, the Kaplan–Meier plotter was used to analyze the association between these miRNAs and clinical prognosis. Among the eight paracancerous tissues and 457 COAD samples from the TCGA database, low hsa-miR-374a-3p expression in tumor tissues was significantly correlated with worse overall survival (OS) ($p = 0.042$), disease-specific survival (DSS) ($p = 0.022$), and progression-free interval (PFI) ($p = 0.047$) (**Figures 1C–E**).

Decreased Hsa-miR-374a-3p Is Related to the Malignant Progression of COAD

To investigate the clinical significance of hsa-miR-374a-3p, 66 patients were divided into high- and low-expression groups based on the mean plasma hsa-miR-374a-3p expression. The association between clinical or pathological features and hsa-miR-374a-3p expression was further analyzed. The data showed that low expression of miR-374a-3p in the plasma of patients with COAD was significantly related to tumor size ($p = 0.013$), T stage ($p = 0.012$), and lymphatic metastasis ($p = 0.002$), but not to patient age ($p = 0.323$), sex ($p = 0.453$), and tumor location ($p = 0.447$) (**Table 3**).

WNT3 Is Potentially Targeted by and Expresses Inversely to Hsa-miR-374a-3p

Differences in mRNA expression were analyzed using COAD data from TCGA. We discovered 1,078 upregulated and 2,048 downregulated genes in colorectal cancer (CRC) compared to paracancerous tissue (**Figures 2A, B**). Next, we predicted 4,284 and 740 potential target genes of hsa-miR-374a-3p using two public miRNA prediction databases (TargetScan Human 7.2 and ENCORI). Eighteen genes were initially screened based on their identification in the differential expression analysis from TCGA (upregulated) and the miRNA prediction databases (**Figure 2C**). Furthermore, prognostic analysis of 41 paracancerous tissues and 480 COAD samples from TCGA was conducted using the Kaplan–Meier plotter. WNT3 was finally identified as it was the only gene whose high expression was associated with poorer patient PFI ($p = 0.043$) (**Figures 2D, E**).

The TargetScan Human 7.2 database showed that hsa-miR-374a-3p can pair with positions 531–538 and 1772–1778 of the WNT3 mRNA 3'-UTR (**Figure 3A**). In addition, three groups of samples containing tumor-adjacent, COAD, and hepatic metastasis tissues from three patients who underwent surgery were obtained for further exploration. The results showed that hsa-miR-374a-3p was downregulated gradually in the tumor-adjacent, COAD, and hepatic metastasis tissues, while the expression of WNT3 and its downstream molecule β-catenin showed the opposite trend (**Figure 3B**). Thus, *WNT3* is potentially targeted by and has an adverse relationship with hsa-miR-374a-3p in COAD.

Hsa-miR-374a-3p/WNT3 Axis-Mediated β-Catenin Signaling Regulates EMT and Cellular Plasticity in COAD Cells

We performed wound-healing, transwell, and spheroid formation assays to verify that hsa-miR-374a-3p silencing increased cell motility and colony formation, while hsa-miR-374a-3p overexpression inhibited these effects in COAD cells (**Figures 4B–D**). COAD cells showed downregulated E-cadherin and upregulated N-cadherin and CD44 in response to hsa-miR-374a-3p silencing, while overexpression of hsa-miR-374a-3p led to adverse variations in related molecules (**Figure 5E**). Moreover, Wnt3 was upregulated when hsa-miR-374a-3p was silenced but downregulated when hsa-miR-374a-3p was overexpressed at both

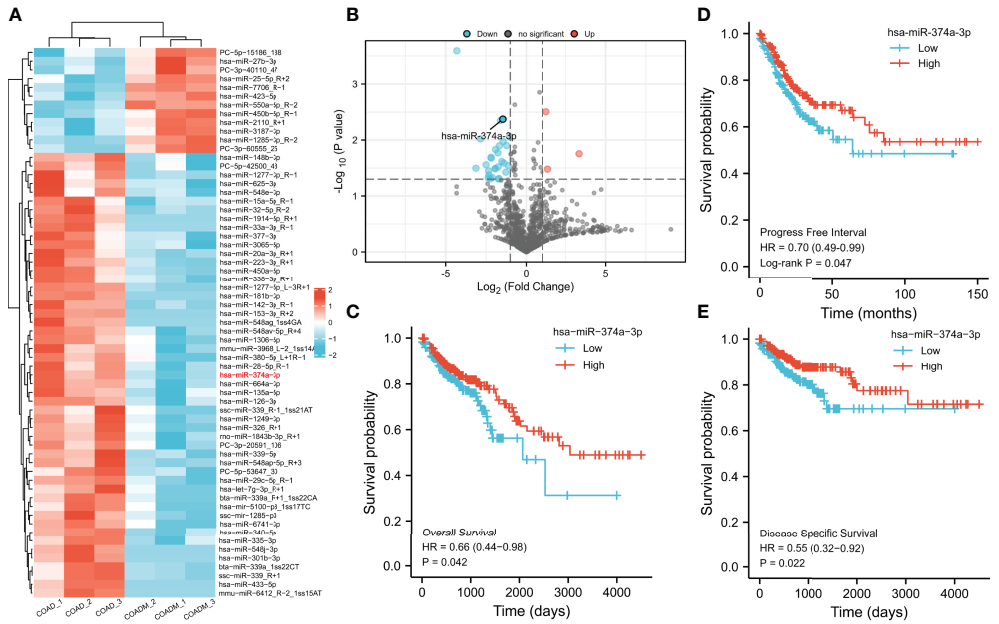

FIGURE 1 | Decreased expression of hsa-miR-374a-3p is bound up with poor prognosis of COAD patients. **(A, B)** Plasma from 6 COAD patients was collected for analysis of microRNA expression profiles by high-throughput RNA-seq. **(C–E)** Data from TCGA was used to verify the association between expression of has-miR-374a-3p and prognosis (PFS, OS, and DSS) of COAD.

the mRNA and protein levels. β-catenin protein expression showed a similar trend in HCT116 and HT29 cells (**Figures 4A, E**).

The Chemical Components of YJHJD

The HPLC fingerprint of the YJHJD decoction was compared to reference standards (**Figure 5A**). Gallic acid, neochlorogenic acid, chlorogenic acid, cryptochlorogenic acid, ferulic acid, licorice glycosides, calycosin-7-glucoside, Dangshen acetylene glycosides, and glycyrrhizic acid were detected, several of which exhibited anticancer activity. Gallic acid induced apoptosis, suppressed proliferation, and decreased cell viability (18, 19). Chlorogenic acid induced reactive oxygen species

TABLE 3 | Relationship between clinical or pathological characteristics and hsa-miR-374a-3p levels.

Variable	hsa-miR-374a-3p			
	N (%)	High expression (*n* = 33)	Low expression (*n* = 33)	*p*-value
Age (years)				0.323
≥60	36 (54.5)	20	16	
<60	30 (45.5)	13	17	
Sex				0.453
Male	39 (59.1)	18	21	
Female	27 (40.9)	15	12	
Location				0.447
Left	25 (37.9)	14	11	
Right	41 (62.1)	19	22	
Tumor size (cm)				0.013*
≥5	38 (57.6)	14	24	
<5	28 (42.4)	19	9	
T stage				0.012*
T 1–2	26 (39.4)	18	8	
T 3–4	40 (60.6)	15	25	
N stage				0.002*
N 0	17 (25.8)	14	3	
N 1–2	49 (74.2)	19	30	

*$P < 0.05$.

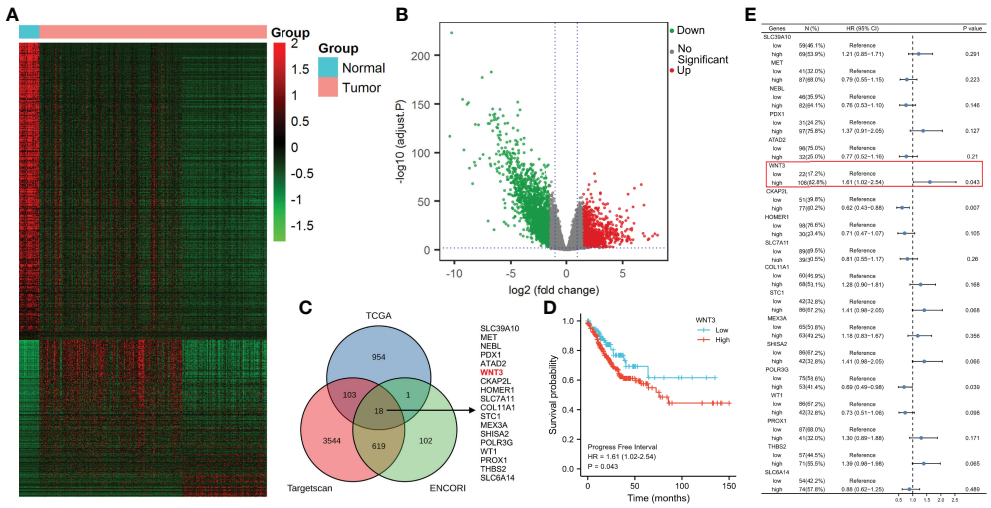

FIGURE 2 | WNT3 is upregulated in COAD tissue and is a predictor of poor prognosis of COAD. **(A, B)** Analysis of mRNA expression profiles was performed through data from TCGA. **(C)** Potential target genes of hsa-miR-374a-3p were predicted *via* taking the intersection of TCGA, TargetScan Human 7.2, and ENCORI. **(D)** Prognostic function of WNT3 in COAD was explored by analyzing data of TCGA. **(E)** PFI of 18 genes was presented by a forest plot.

generation, cell cycle arrest, and apoptosis (20, 21). Ferulic acid induced apoptosis (22). Glycyrrhizic acid treatment decreased cell viability, motility, and cloning ability and increased apoptosis (23). From the literature review, peak 1 (gallic acid) might be derived from *Angelica sinensis* or *Oldenlandia diffusa*; peak 2 (neochlorogenic acid), peak 3 (chlorogenic acid), and peak 4 (cryptochlorogenic acid) might be derived from *Angelica sinensis*; peak 5 (ferulic acid) might be derived from *Angelica sinensis, Rhizoma atractylodis macrocephalae, Rhizoma sparganii*, or *Curcuma zedoary*; peak 6 (licorice glycosides) and peak 9 (glycyrrhizic acid) might be derived from licorice; peak 7 (calycosin-7-glucoside) might be derived from *Astragalus membranaceus*; and peak 8 (Dangshen acetylene glycosides) might be derived from *Codonopsis pilosula*.

YJHJD Inhibits EMT and Colony Formation Ability of COAD cells, and Regulates the Expression of Hsa-miR-374a-3p and WNT3

The migration assay showed a relatively increased wound area, suggesting that YJHJD effectively inhibited the migration ability of HCT116 and HT29 cells (**Figure 5B**). The transwell assay showed a gradual reduction in the number of invading cells, confirming that YJHJD decreased the invasion ability of both types of colon cancer cells (**Figure 5C**). The spheroid formation assay demonstrated that YJHJD inhibited colon cancer cell colony formation in a dose-dependent manner (**Figure 5D**).

The results of Western blotting showed that YJHJD upregulated E-cadherin and downregulated N-cadherin, Snail, CD44, and Sox2 in a dose-dependent manner (**Figure 5F**). Additionally, RT-PCR and Western blot assays showed increased hsa-miR-374a-3p and decreased WNT3 response to YJHJD (**Figure 5E**). In addition, YJHJD significantly reduced cytoplasmic and nuclear β-catenin protein expression in both HCT116 and HT29 cells (**Figure 5F**). The reduced Wnt3 and β-catenin signals were further explored by immunofluorescence (**Figure 5G**).

YJHJD Suppresses EMT and Cellular Plasticity Through Hsa-miR-374a-3p/WNT3 Axis-Mediated β-Catenin Signaling

HCT116 and HT29 cells with hsa-miR-374a-3p silencing showed decreased hsa-miR-374a-3p and increased WNT3 mRNA expression, in contrast to cells without silencing exposed to YJHD (**Figure 6D**). Silencing of hsa-miR-374a-3p also counteracted the inhibitory effect of YJHJD on cell motility and clonality (**Figures 6A–C**), as well as β-catenin, EMT, and cellular plasticity-related molecular changes at the protein level (**Figure 6E**). In addition, the application of the specific β-catenin inhibitor XAV939 partially restored the suppressive effect of YJHJD, which was weakened by transfection silencing of hsa-miR-374a-3p in colon cancer cells (**Figure 6**).

YJHJD Represses Hepatic Metastasis of Colon Cancer by Inhibiting Hsa-miR-374a-3p/WNT3 Axis-Regulated EMT and Cellular Plasticity

A hepatic metastasis model was established by injecting CT26 cells into the spleen of mice to investigate the effect of YJHJD on colon cancer cell invasion *in vivo*. The groups treated with YJHJD showed significantly reduced liver metastases, especially in the high-dose group (**Figure 7A**). HE staining verified the remarkably decreased number and diameter of hepatic metastatic nodules in mice in the YJHJD group as well (**Figure 7B**). The expression of related molecules in liver metastatic tumor tissues was also investigated. RT-PCR assay showed that YJHJD effectively upregulated hsa-miR-374a-3p and

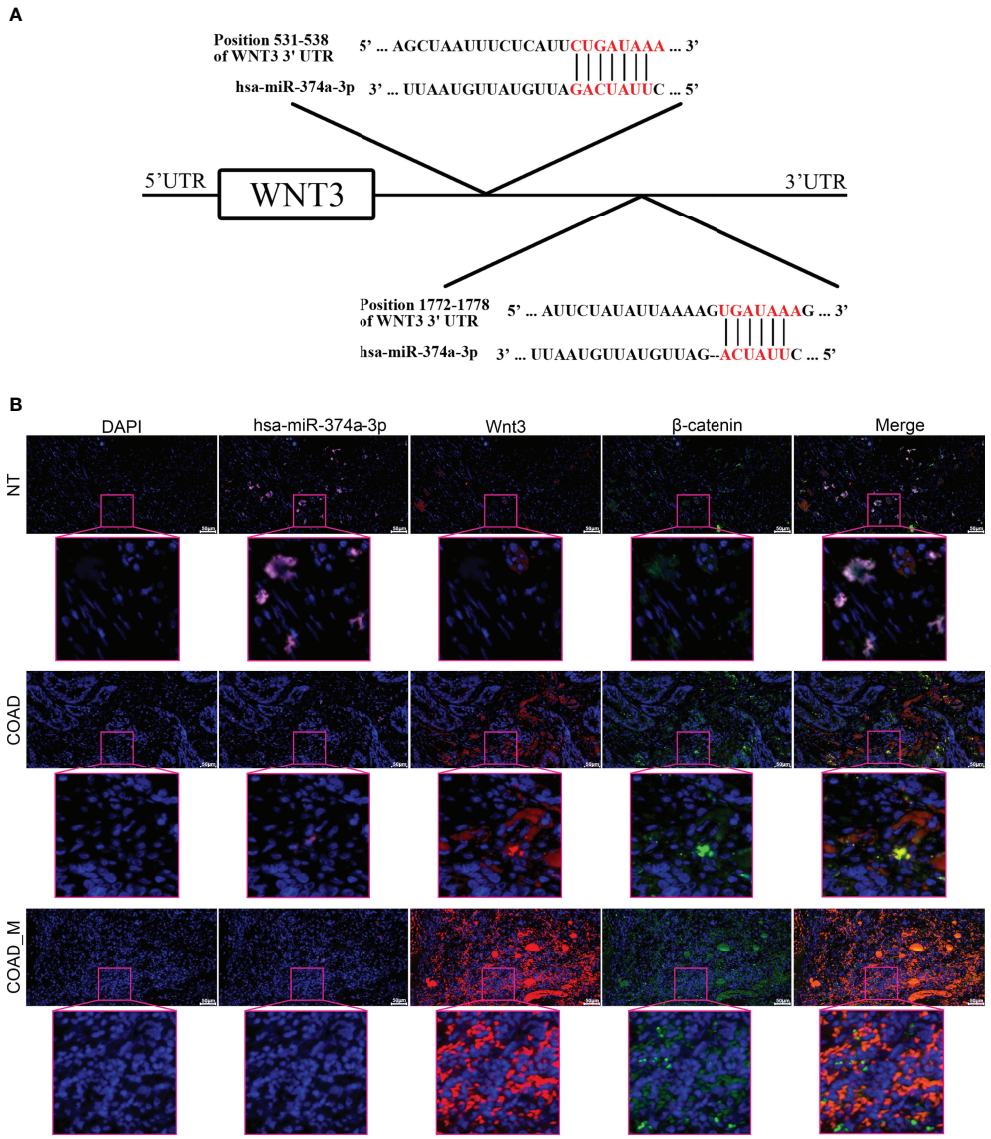

FIGURE 3 | WNT3 is potentially targeted by hsa-miR-374a-3p and expression of WNT3 is negatively linked to hsa-miR-374a-3p in COAD. **(A)** Feasible binding sites were predicted using the TargetScan Human 7.2 database. **(B)** Expression of hsa-miR-374a-3p, Wnt3, and β-catenin in COAD specimens was probed *via* FISH and immunofluorescence experiments.

downregulated WNT3 at the mRNA level (**Figure 7D**). Western blotting confirmed that YJHJD upregulated the protein expression of E-cadherin and downregulated the expression of Wnt3, β-catenin, N-cadherin, Snail, CD44, and Sox2 (**Figure 7C**). Meanwhile, immunohistochemical staining confirmed the decreased expression of β-catenin, α-sma, and CD44 in the liver metastases of colon cancer (**Figure 7E**).

DISCUSSION

Our previous clinical research validated that the Chinese herbal formulation based on the method of "nourish qi, invigorate the spleen, remove blood stasis and detoxify" prolonged disease-free survival (DFS), reduced the risk of recurrence and metastasis, and improved the quality of life of patients with stage II or III gastric cancer after radical gastrectomy (24). In addition, this therapy increased the survival rate and inhibited CRC liver metastasis in a nude mouse model by activating the innate immune system (25). This treatment method also inhibited COAD cell proliferation by inducing G0/G1-phase cell cycle arrest and cell apoptosis (26). The present study further explored the mechanism underlying the inhibitory effects of YJHJD on COAD.

MiRNAs play a vital role in the biological behavior of CRC, as well as in patient prognosis. Hsa-miR-374a is correlated with

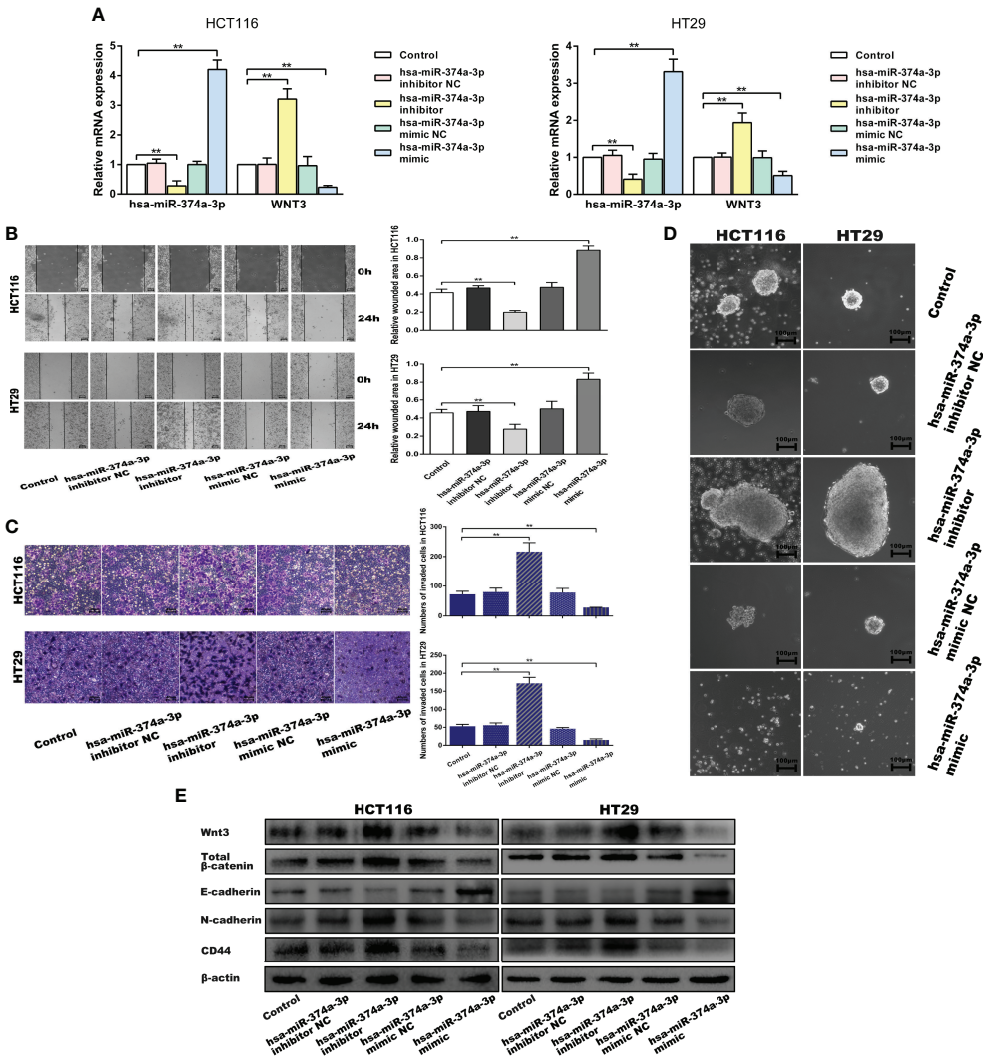

FIGURE 4 | Hsa-miR-374a-3p plays an inhibitive role in the motility and cellular plasticity of COAD cells by suppressing WNT3/β-catenin signaling. **(A)** mRNA expression of hsa-miR-374a-3p and WNT3 was detected by PT-PCR assay. **(B)** Wound-healing assay was performed to assess the migration ability of CAOD cells. **(C)** Transwell assay was used to evaluate the invasion ability. **(D)** Spheroid formation assay proceeded to estimate the cellular plasticity. **(E)** Protein levels of WNT3/β-catenin, EMT, and cellular plasticity-related molecules were tested by Western blot experiment. *P < 0.05, **P < 0.01 compared to control group.

CRC development and prognostic indicators and can significantly reduce the mortality risk despite the tumor site, as high hsa-miR-374a expression is associated with better survival (27, 28). After surgical resection of colorectal advanced adenomas (CAA) or CRC, patients showed upregulated plasma levels of miR-374a (29). We observed that hsa-miR-374a-3p was downregulated in the plasma of patients diagnosed with COAD with liver metastasis compared to those without. Moreover, decreased levels of hsa-miR-374a-3p in COAD tissues were associated with reduced OS, DSS, and PFI. Our retrospective study further indicated that patients with lower plasma expression of miR-374a-3p might have a larger tumor size and more advanced T or N stages of COAD. The sequence of *in vitro* assays showed that hsa-miR-374a-3p silencing enhanced COAD cell migration, invasion ability, and cellular plasticity, whereas hsa-miR-374a-3p overexpression led to the opposite phenotype. Thus, we inferred that hsa-miR-374a-3p may serve as a tumor suppressor that inhibits COAD development and metastasis.

In the canonical Wnt pathway, Wnt ligands bind to the corresponding receptors, leading to the nuclear translocation of β-catenin and activation of target genes (30). Wnt/β-catenin signaling is highly activated in several malignancies, including colon cancer (31). Hyperactivated Wnt/β-catenin signaling is thought to promote CRC progression by regulating the EMT, as overexpression of nuclear β-catenin and continuous activation of Wnt/β-catenin signaling have been reported in aggressive colon cancer (32). The Wnt/β-catenin pathway also plays a major role in maintaining cellular plasticity in colon cancers (33).

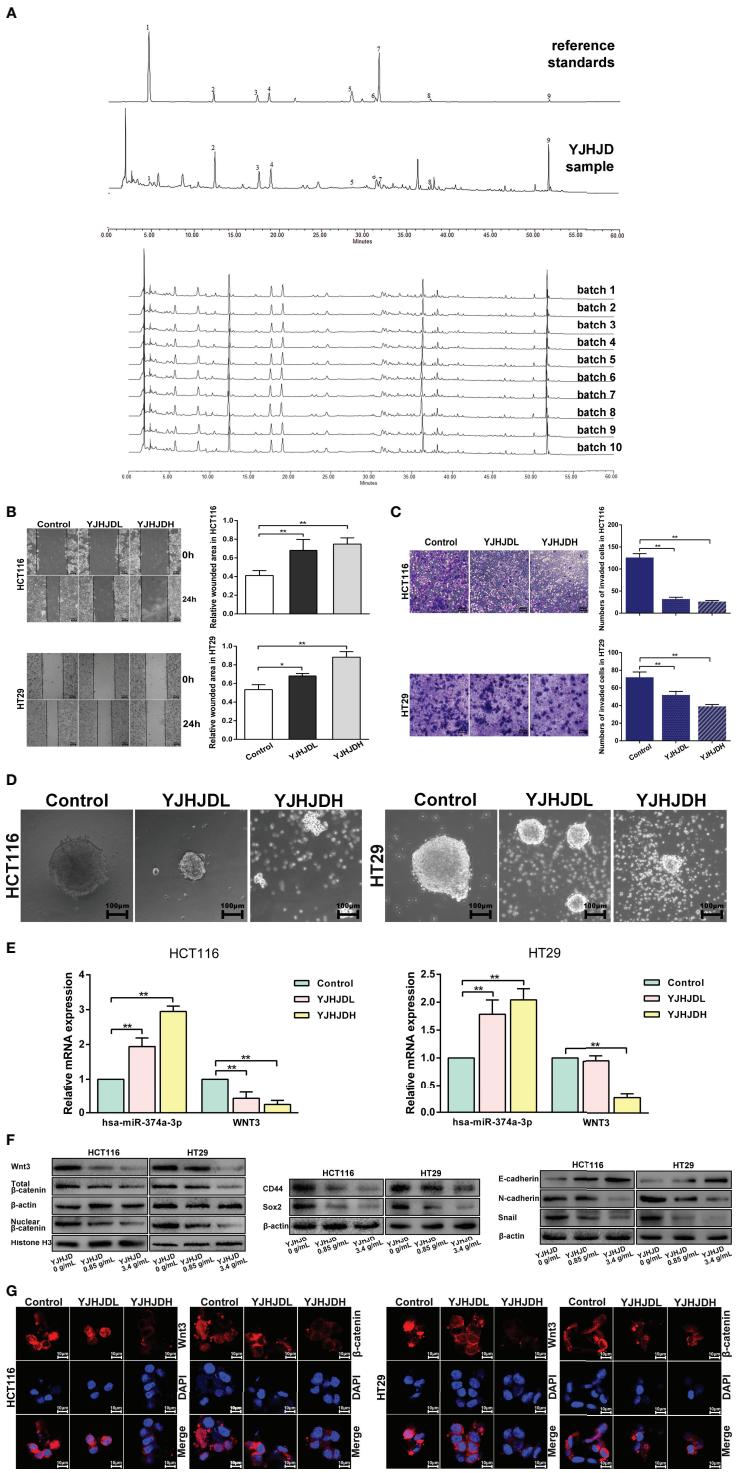

FIGURE 5 | YJHJD prohibits EMT, cellular plasticity, and hsa-miR-374a-3p/WNT3/β-catenin axis-related molecules in COAD cells. **(A)** The HPLC fingerprint of YJHJD was established and compared with the reference standards. **(B)** Migration ability was tested by wound-healing assay. **(C)** Cell invasion ability was measured through transwell assay. **(D)** Cellular plasticity was assessed by spheroid formation assay. **(E)** mRNA expression of hsa-miR-374a-3p and WNT3 in response to YJHJD was evaluated by PT-PCR assay. **(F)** WNT3/β-catenin, EMT, and cellular plasticity-associated markers at protein levels were estimated by Western blot assay. **(G)** Protein expression and location of Wnt3 and β-catenin in COAD cells were tested *via* immunofluorescence analysis. *P < 0.05, **P < 0.01 compared to control group.

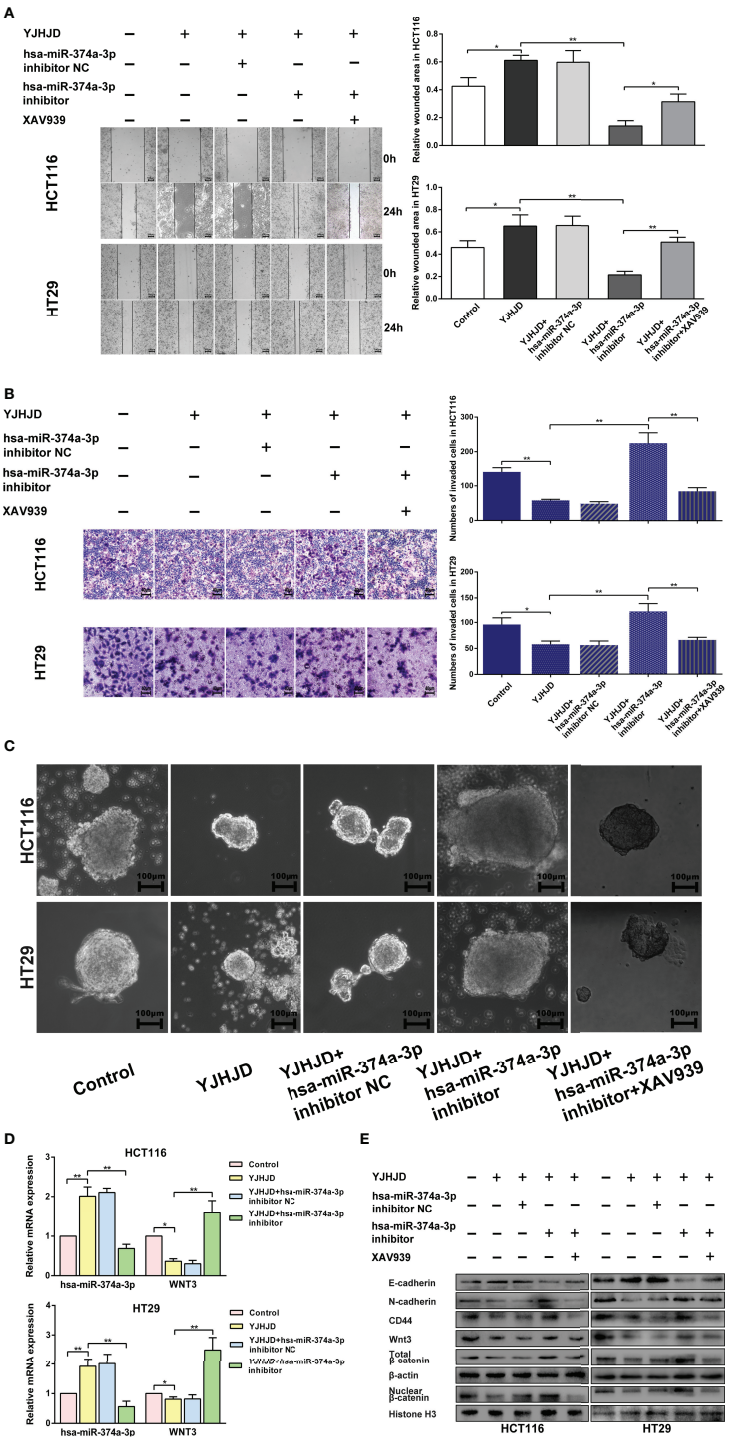

FIGURE 6 | The hsa-miR-374a-3p/WNT3/β-catenin axis plays a vital role in the suppressive effect of YJHJD. **(A)** A wound-healing experiment was performed to test cell migration ability. **(B)** Transwell assay was performed to explore cell invasion ability. **(C)** Spheroid formation assay was carried out to appraise cellular plasticity. **(D)** Hsa-miR-374a-3p and WNT3 mRNA expression was detected by PT-PCR experiment. **(E)** WNT3/β-catenin, EMT, and cellular plasticity-related protein expression was researched through Western blot assay. *P < 0.05, **P < 0.01 compared to control group. *P < 0.05, **P < 0.01 compared to control group.

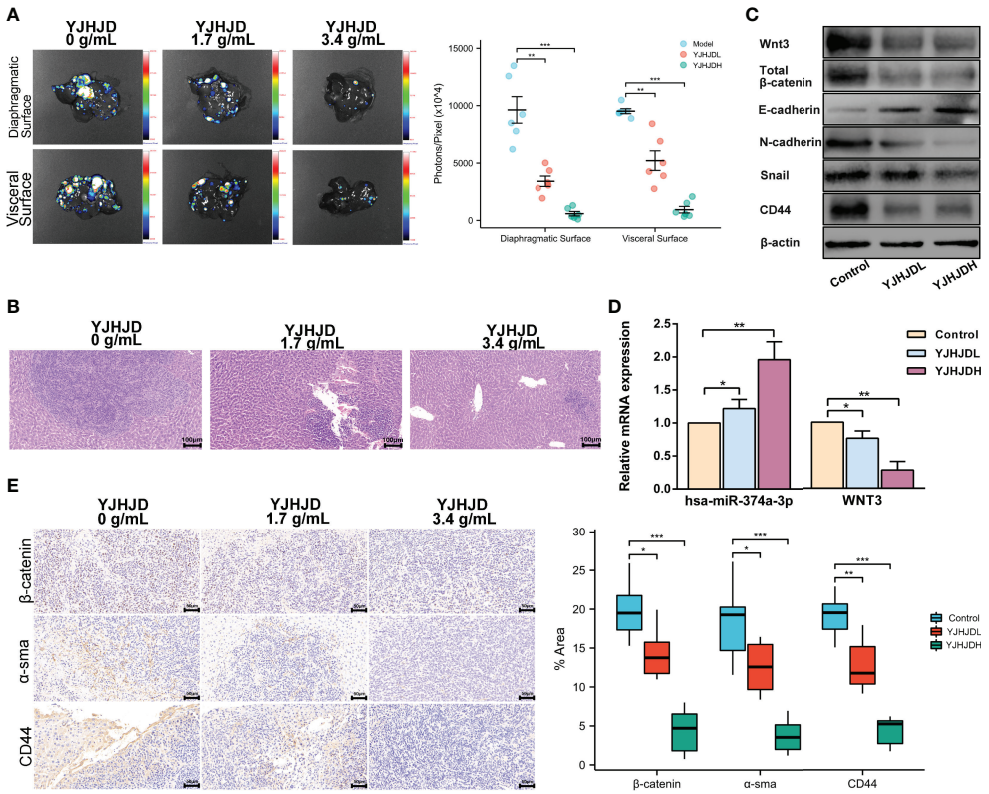

FIGURE 7 | YJHJD restrains liver metastasis of COAD *via* reversing hsa-miR-374a-3p/WNT3/β-catenin-mediated EMT and cellular plasticity. **(A)** Fluorescence intensity on behalf of liver metastases was assessed by the Live Animal Analysis System. **(B)** Liver metastatic lesions and tumor infiltration was evaluated by HE staining. **(C)** mRNA levels of hsa-miR-374a-3p, WNT3 was tested by PT-PCR assay. **(D)** Protein expression of WNT3/β-catenin, EMT, and cellular plasticity relevant molecules was studied through Western blot assay. **(E)** Expression of β-catenin and α-sma in the liver metastatic tumor tissues was examined *via* IHC analysis. *P <0.05, **P < 0.01, *** P < 0.001 compared to control group.

Moreover, the reciprocal action between microRNAs and the canonical Wnt pathway is a key regulator and prognostic factor in colon tumors (34). Our analysis of COAD data from TCGA revealed 1,078 upregulated genes, among which the expression of WNT3 was inversely connected with PFI. TargetScan Human 7.2. indicated that the binding domain of hsa-miR-374a-3p might be located at positions 531–538 and 1772–1778 of the WNT3 3'-UTR. The expression of hsa-miR-374a-3p decreased gradually in tumor-adjacent, COAD, and hepatic metastasis tissues, while WNT3 and β-catenin showed opposite trends. In addition, silencing of hsa-miR-374a-3p induced the EMT and cellular plasticity of COAD cells, as well as the expression of Wnt3 and β-catenin, while overexpression of hsa-miR-374a-3p resulted in a suppressive effect. Therefore, we concluded that hsa-miR-374a-3p regulated WNT3 expression and further mediated β-catenin signaling to inhibit EMT and cellular plasticity in COAD.

Traditional Chinese medicine is an ancient practice of medicine with a long-standing history that has been applied in clinics for thousands of years and has potential advantages in anti-tumor efficiency (35, 36). The YJHJD decoction is a traditional Chinese medicine compound based on the theory of "spleen deficiency and stasis toxin" that has been applied clinically for years. First, we demonstrated that YJHJD reduced COAD cell migration, invasion, and colony formation potential in a dose-dependent manner. Additionally, YJHJD reversed the EMT and the expression of cellular plasticity-related molecules, with increased hsa-miR-374a-3p and Wnt3 and β-catenin inhibition. Furthermore, the suppressive role of YJHJD was neutralized when hsa-miR-374a-3p was silenced by transfection, whereas the application of the β-catenin inhibitor XAV939 partially restored the effect of YJHJD. Further *in vivo* experiments confirmed that YJHJD inhibited liver metastasis in a dose-dependent manner by upregulating hsa-miR-374a-3p, downregulating the Wnt3/β-catenin axis, and inhibiting the EMT and cellular plasticity of COAD.

Therefore, hsa-miR-374a-3p is a potential tumor-inhibiting gene in COAD and is closely related to patient prognosis. Notably, hsa-miR-374a-3p/Wnt3/β-catenin signal transduction played a suppressive role by regulating the EMT and cellular plasticity in COAD. The YJHJD decoction established in the theory of "spleen deficiency and stasis toxin" can be applied for the treatment of liver metastasis of COAD. The underlying mechanism is that YJHJD inhibits the EMT and cellular

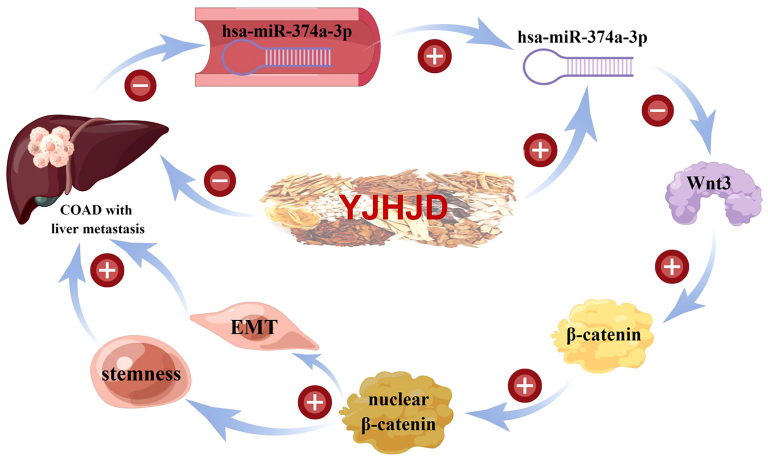

FIGURE 8 | Mechanism flowchart of the effect of YJHJD on COAD.

plasticity of COAD in an hsa-miR-374a-3p/Wnt3/β-catenin dependent manner (**Figure 8**). However, additional studies are needed to elucidate the specific mechanism by which YJHJD acts on hsa-miR-374a-3p and identify potential intermediate effector molecules between the hsa-miR-374a-3p/Wnt3/β-catenin axis and EMT or cellular plasticity.

DATA AVAILABILITY STATEMENT

The datasets presented in this study can be found in online repositories. The names of the repository/repositories and accession number(s) can be found at: https://www.ncbi.nlm.nih.gov/geo/query/acc.cgi?acc=GSE184669.

ETHICS STATEMENT

The studies involving human participants were reviewed and approved by the Ethics Committee of Nanjing University of Chinese Medicine. The patients/participants provided their written informed consent to participate in this study. The animal study was reviewed and approved by the Ethics Committee of Nanjing University of Chinese Medicine.

AUTHOR CONTRIBUTIONS

Conceptualization: YZ, JZ, SL, and CW. Data management: JZ and CW. Formal analysis: QW, JQ, XZ, and HP. Methodology: TX and ZJ. Resources: CW. Writing—original draft: YZ and CW. Writing—review and editing: JZ and SL. All authors contributed to the article and approved the submitted version.

FUNDING

This study was supported by the National Natural Science Foundation of China (82104950), the National Administration of Traditional Chinese Medicine: 2019 Project of building evidence based practice capacity for TCM (No.2019XZZX-ZL003), the National Traditional Chinese Medicine Inheritance and Innovation Platform Construction Project by National Administration of Traditional Chinese Medicine, Natural Science Foundation of Jiangsu Province (BK20191086, BK20201499), the Project of National Clinical Research Base of Traditional Chinese Medicine in Jiangsu Province, China (JD2019SZXYB01), the Medical Scientific Research Project of Jiangsu Health Commission (H2019094), and the College Project of Jiangsu Province Hospital of Chinese Medicine (Y2020CX57, Y2020CX67, and Y2021CX06).

REFERENCES

1. Sung H, Ferlay J, Siegel RL, Laversanne M, Soerjomataram I, Jemal A, et al. Global Cancer Statistics 2020: GLOBOCAN Estimates of Incidence and Mortality Worldwide for 36 Cancers in 185 Countries. *CA Cancer J Clin* (2021) 71(3):209–49. doi: 10.3322/caac.21660
2. Cao W, Chen HD, Yu YW, Li N, Chen WQ. Changing Profiles of Cancer Burden Worldwide and in China: A Secondary Analysis of the Global Cancer Statistics 2020. *Chin Med J (Engl)* (2021) 134(7):783–91. doi: 10.1097/CM9.0000000000001474
3. Siegel RL, Miller KD, Fedewa SA, Ahnen DJ, Meester R, Barzi A, et al. Colorectal Cancer Statistic. *CA Cancer J Clin* (2017) 67(3):177–93. doi: 10.3322/caac.21395
4. Zhu J, Lian P, Liu F, Xu Y, Xu J, Guan Z, et al. Phase II Trial of First-Line Chemoradiotherapy With Intensity-Modulated Radiation Therapy Followed by Chemotherapy for Synchronous Unresectable Distant Metastases Rectal Adenocarcinoma. *Radiat Oncol* (2013) 8:10. doi: 10.1186/1748-717X-8-10
5. Stemmler MP, Eccles RL, Brabletz S, Brabletz T. Non-Redundant Functions of EMT Transcription Factors. *Nat Cell Biol* (2019) 21(1):102–12. doi: 10.1038/s41556-018-0196-y

6. Bakir B, Chiarella AM, Pitarresi JR, Rustgi AK. EMT, MET, Plasticity, and Tumor Metastasis. *Trends. Cell Biol* (2020) 30(10):764–76. doi: 10.1016/j.tcb.2020.07.003
7. Soundararajan R, Paranjape AN, Maity S, Aparicio A, Mani SA. EMT, Stemness and Tumor Plasticity in Aggressive Variant Neuroendocrine Prostate Cancers. *Biochim Biophys Acta Rev Cancer* (2018) 1870(2):229–38. doi: 10.1016/j.bbcan.2018.06.006
8. Botchkina G. Colon Cancer Stem Cells–From Basic to Clinical Application. *Cancer Lett* (2013) 338(1):127–40. doi: 10.1016/j.canlet.2012.04.006
9. Lin S, Gregory RI. MicroRNA Biogenesis Pathways in Cancer. *Nat Rev Cancer* (2015) 15(6):321–33. doi: 10.1038/nrc3932
10. Zhen Y, Fang W, Zhao M, Luo R, Liu Y, Fu Q, et al. miR-374a-CCND1-Ppi3k/AKT-C-JUN Feedback Loop Modulated by PDCD4 Suppresses Cell Growth, Metastasis, and Sensitizes Nasopharyngeal Carcinoma to Cisplatin. *Oncogene* (2017) 36(2):275–85. doi: 10.1038/onc.2016.201
11. Pan Z, Shi Z, Wei H, Sun F, Song J, Huang Y, et al. Magnetofection Based on Superparamagnetic Iron Oxide Nanoparticles Weakens Glioma Stem Cell Proliferation and Invasion by Mediating High Expression of MicroRNA-374a. *J Cancer* (2016) 7(11):1487–96. doi: 10.7150/jca.15515
12. Cai J, Guan H, Fang L, Yang Y, Zhu X, Yuan J, et al. MicroRNA-374a Activates Wnt/β-Catenin Signaling to Promote Breast Cancer Metastasis. *J Clin Invest* (2013) 123(2):566–79. doi: 10.1172/JCI65871
13. Kim JG, Mahmud S, Min JK, Lee YB, Kim H, Kang DC, et al. RhoA GTPase Phosphorylated at Tyrosine 42 by Src Kinase Binds to β-Catenin and Contributes Transcriptional Regulation of Vimentin Upon Wnt3A. *Redox Biol* (2021) 40:101842. doi: 10.1016/j.redox.2020.101842
14. Kozomara A, Birgaoanu M, Griffiths-Jones S. Mirbase: From microRNA Sequences to Function. *Nucleic Acids Res* (2019) 47(D1):D155–62. doi: 10.1093/nar/gky1141
15. de Planell-Saguer M, Rodicio MC, Mourelatos Z. Rapid *in Situ* Codetection of Noncoding RNAs and Proteins in Cells and Formalin-Fixed Paraffin-Embedded Tissue Sections Without Protease Treatment. *Nat Protoc* (2010) 5(6):1061–73. doi: 10.1038/nprot.2010.62
16. Su D, Guo X, Huang L, Ye H, Li Z, Lin L, et al. Tumor-Neuroglia Interaction Promotes Pancreatic Cancer Metastasis. *Theranostics. 10* (2020) 11):5029–47. doi: 10.7150/thno.42440
17. Wang Z, Zhang Y, Liu Q, Sun L, Lv M, Yu P, et al. Investigation of the Mechanisms of Genkwa Flos Hepatotoxicity by a Cell Metabolomics Strategy Combined With Serum Pharmacology in HL-7702 Liver Cells. *Xenobiotica. 49* (2019) 2):216–26. doi: 10.1080/00498254.2018.1427905
18. Subramanian AP, Jaganathan SK, Mandal M, Supriyanto E, Muhamad II. Gallic Acid Induced Apoptotic Events in HCT-15 Colon Cancer Cells. *World. J Gastroenterol* (2016) 22(15):3952–61. doi: 10.3748/wjg.v22.i15.3952
19. Forester SC, Choy YY, Waterhouse AL, Oteiza PI. The Anthocyanin Metabolites Gallic Acid, 3-O-Methylgallic Acid, and 2,4,6-Trihydroxybenzaldehyde Decrease Human Colon Cancer Cell Viability by Regulating Pro-Oncogenic Signals. *Mol Carcinog* (2014) 53(6):432–9. doi: 10.1002/mc.21974
20. Hou N, Liu N, Han J, Yan Y, Li J. Chlorogenic Acid Induces Reactive Oxygen Species Generation and Inhibits the Viability of Human Colon Cancer Cells. *Anticancer Drugs* (2017) 28(1):59–65. doi: 10.1097/CAD.0000000000000430
21. Sadeghi ES, Li XQ, Ghorbani M, Azadi B, Kubow S. Chlorogenic Acid and Its Microbial Metabolites Exert Anti-Proliferative Effects, S-Phase Cell-Cycle Arrest and Apoptosis in Human Colon Cancer Caco-2 Cells. *Int J Mol Sci* (2018) 19(3):723. doi: 10.3390/ijms19030723
22. Senthil, Kumar C, Thangam R, Mary SA, Kannan PR, Arun G, Madhan B. Targeted Delivery and Apoptosis Induction of Trans-Resveratrol-Ferulic Acid Loaded Chitosan Coated Folic Acid Conjugate Solid Lipid Nanoparticles in Colon Cancer Cells. *Carbohydr Polym* (2020) 231:115682. doi: 10.1016/j.carbpol.2019.115682
23. Zuo Z, He L, Duan X, Peng Z, Han J. Glycyrrhizic Acid Exhibits Strong Anticancer Activity in Colorectal Cancer Cells *via* SIRT3 Inhibition. *Bioengineered* (2021) 13(2):2720–31. doi: 10.1080/21655979.2021.2001925
24. Shu P, Tang H, Zhou B, Wang R, Xu Y, Shao J, et al. Effect of Yiqi Huayu Jiedu Decoction on Stages II and III Gastric Cancer: A Multicenter, Prospective, Cohort Study. *Medicine (Baltimore) 98* (2019) (47):e17875. doi: 10.1097/MD.0000000000017875
25. Zhou JY, Chen M, Wu CE, Zhuang YW, Chen YG, Liu SL. The Modified Si-Jun-Zi Decoction Attenuates Colon Cancer Liver Metastasis by Increasing Macrophage Cells. *BMC Complement Altern Med* (2019) 19(1):86. doi: 10.1186/s12906-019-2498-4
26. Xi SY, Teng YH, Chen Y, Li JP, Zhang YY, Liu SL, et al. Jianpi Huayu Decoction Inhibits Proliferation in Human Colorectal Cancer Cells (SW480) by Inducing G0/G1-Phase Cell Cycle Arrest and Apoptosis. . *Evid Based Complement Alternat Med* (2015) 2015:236506. doi: 10.1155/2015/236506
27. Slattery ML, Herrick JS, Mullany LE, Valeri N, Stevens J, Caan BJ, et al. An Evaluation and Replication of miRNAs With Disease Stage and Colorectal Cancer-Specific Mortality. *Int J Cancer* (2015) 137(2):428–38. doi: 10.1002/ijc.29384
28. Slattery ML, Pellatt AJ, Lee FY, Herrick JS, Samowitz WS, Stevens JR, et al. Infrequently Expressed miRNAs Influence Survival After Diagnosis With Colorectal Cancer. *Oncotarget* (2017) 8(48):83845–59. doi: 10.18632/oncotarget.19863
29. O'Brien SJ, Netz U, Hallion J, Bishop C, Stephen V, Burton J, et al. Circulating Plasma microRNAs in Colorectal Neoplasia: A Pilot Study in Assessing Response to Therapy. *Transl Oncol* (2021) 14(1):100962. doi: 10.1016/j.tranon.2020.100962
30. Chizhikov VV, Iskusnykh IY, Steshina EY, Fattakhov N, Lindgren AG, Shetty AS, et al. Early Dorsomedial Tissue Interactions Regulate Gyrification of Distal Neocortex. *Nat Commun* (2019) 10(1):5192. doi: 10.1038/s41467-019-12913-z
31. Ji P, Zhou Y, Yang Y, Wu J, Zhou H, Quan W, et al. Myeloid Cell-Derived LL-37 Promotes Lung Cancer Growth by Activating Wnt/β-Catenin Signaling. *Theranostics* (2019) 9(8):2209–23. doi: 10.7150/thno.30726
32. Ahmad R, Kumar B, Chen Z, Chen X, Müller D, Lele SM, et al. Loss of Claudin-3 Expression Induces IL6/gp130/Stat3 Signaling to Promote Colon Cancer Malignancy by Hyperactivating Wnt/β-Catenin Signaling. *Oncogene* (2017) 36(47):6592–604. doi: 10.1038/onc.2017.259
33. Sacchetti A, Teeuwssen M, Verhagen M, Joosten R, Xu T, Stabile R, et al. Phenotypic Plasticity Underlies Local Invasion and Distant Metastasis in Colon Cancer. *eLife* (2021) 10:e61461. doi: 10.7554/eLife.61461
34. Uddin MN, Li M, Wang X. Identification of Transcriptional Markers and microRNA-mRNA Regulatory Networks in Colon Cancer by Integrative Analysis of mRNA and microRNA Expression Profiles in Colon Tumor Stroma. *Cells* (2019) 8(9):1054. doi: 10.3390/cells8091054
35. Qian Q, Chen W, Cao Y, Cao Q, Cui Y, Li Y, et al. Targeting Reactive Oxygen Species in Cancer *via* Chinese Herbal Medicine. *Oxid Med Cell Longev* (2019) 2019:9240426. doi: 10.1155/2019/9240426
36. Hao H. The Development of Online Doctor Reviews in China: An Analysis of the Largest Online Doctor Review Website in China. *J Med Internet Res* (2015) 17(6):e134. doi: 10.2196/jmir.4365

Conflict of Interest: The authors declare that the research was conducted in the absence of any commercial or financial relationships that could be construed as a potential conflict of interest.

Publisher's Note: All claims expressed in this article are solely those of the authors and do not necessarily represent those of their affiliated organizations, or those of the publisher, the editors and the reviewers. Any product that may be evaluated in this article, or claim that may be made by its manufacturer, is not guaranteed or endorsed by the publisher.

frontiers | Frontiers in Oncology

TYPE Review
PUBLISHED 11 August 2022
DOI 10.3389/fonc.2022.932608

OPEN ACCESS

EDITED BY
Jiannan Yao,
Beijing Chaoyang Hospital, Capital Medical University, China

REVIEWED BY
Bozena Kaminska,
Nencki Institute of Experimental Biology (PAS), Poland
Kshama Gupta,
Mayo Clinic, United States

*CORRESPONDENCE
Katherine T. Morris
Katherine-Morris@ouhsc.edu

SPECIALTY SECTION
This article was submitted to Gastrointestinal Cancers: Colorectal Cancer, a section of the journal Frontiers in Oncology

RECEIVED 30 April 2022
ACCEPTED 15 July 2022
PUBLISHED 11 August 2022

CITATION
Park SD, Saunders AS, Reidy MA, Bender DE, Clifton S and Morris KT (2022) A review of granulocyte colony-stimulating factor receptor signaling and regulation with implications for cancer. *Front. Oncol.* 12:932608. doi: 10.3389/fonc.2022.932608

A review of granulocyte colony-stimulating factor receptor signaling and regulation with implications for cancer

Sungjin David Park[1], Apryl S. Saunders[1], Megan A. Reidy[1], Dawn E. Bender[1], Shari Clifton[2] and Katherine T. Morris[1]*

[1]Department of Surgery, University of Oklahoma Health Science Center, Oklahoma City, OK, United States, [2]Department of Information Management, University of Oklahoma Health Science Center, Oklahoma City, OK, United States

Granulocyte colony-stimulating factor receptor (GCSFR) is a critical regulator of granulopoiesis. Studies have shown significant upregulation of GCSFR in a variety of cancers and cell types and have recognized GCSFR as a cytokine receptor capable of influencing both myeloid and non-myeloid immune cells, supporting pro-tumoral actions. This systematic review aims to summarize the available literature examining the mechanisms that control GCSFR signaling, regulation, and surface expression with emphasis on how these mechanisms may be dysregulated in cancer. Experiments with different cancer cell lines from breast cancer, bladder cancer, glioma, and neuroblastoma are used to review the biological function and underlying mechanisms of increased GCSFR expression with emphasis on actions related to tumor proliferation, migration, and metastasis, primarily acting through the JAK/STAT pathway. Evidence is also presented that demonstrates a differential physiological response to aberrant GCSFR signal transduction in different organs. The lifecycle of the receptor is also reviewed to support future work defining how this signaling axis becomes dysregulated in malignancies.

KEYWORDS

CSF3R, GCSFR, regulation, cancer, signaling/signaling pathways

Introduction

Granulocyte colony-stimulating factor (GCSF) is a pleiotropic cytokine expressed by the gene transcript *CSF3*. GCSF is a hematopoietic growth factor that regulates the viability, proliferation, and differentiation of granulocytic precursors and the function of neutrophils by signaling through its receptor granulocyte colony-stimulating factor receptor (GCSFR) encoded by *CSF3R*. Both GCSF and GCSFR play important roles as chemical mediators that regulate immune cell homeostasis and coordinators of signal-

dependent and non-specific immune responses upon microbial invasion. Cytokine signaling contributes to the effective first line of chemical defense against microbial invasion, resulting in chemotactic signaling to recruit neutrophils and natural killer cells to circulate in the blood and extravasate into interstitial spaces and epithelial surfaces. Because GCSF increases neutrophil mobilization and maturation, a recombinant human GCSF (rh-GCSF) has been used in clinical practice to prevent and treat neutropenia. In this capacity, it has proven highly effective in decreasing the frequency of febrile neutropenia among patients undergoing cytotoxic chemotherapy (1, 2). Consequently, the effects of GCSF on granulopoietic mobilization and differentiation have been evaluated extensively. However, investigators have also begun research into potentially unanticipated pro-tumor effects of GCSF in patients with malignancy, given the development of a broader understanding of the effects of this cytokine on non-immune cells. Recent studies have uncovered a potential oncogenic role for aberrant GCSFR expression and signaling in many hematologic malignancies and several solid cancers. Specifically, overexpression of GCSFR has been identified in nasopharyngeal, oral cavity, breast, colorectal, and ovarian cancer cells with data suggesting a potential role for GCSFR in cancer progression (3–6). Furthermore, an emerging body of evidence suggests that tumor microenvironments are regulated by increased GCSF signaling between tumor cells and adjacent immune cells in the development and progression of gastrointestinal (GI) cancers, which have also been noted to have increased GCSFR expression (7, 8).

Due to the evidence suggesting pro-tumor effects from dysregulated GCSFR signaling, here we seek to summarize what is known about GCSFR structure, signaling, and processing to inform future studies of the role played by GCSF in cancer. Studies performed in healthy cells are leveraged to further understand how the signal transduction pathways that GCSFR stimulates in normal tissues are co-opted in cancer cells. Increased understanding of the regulatory effect of GCSFR on cellular proliferation response patterns is important to guide additional studies into GCSFR's contribution to oncogenesis and progression of malignancies. This review will discuss recent advances in our understanding of the mechanisms behind the receptor-driven signal transduction in various organ systems and cancerous cell lines to further understand the link between the upregulation of GCSFR and cancer pathogenesis.

Structure

GCSFR is an 813-amino acid protein encoded by *CSF3R* gene and is a member of the class I cytokine receptor family (9). The receptor is a single transmembrane protein comprised of several functional extracellular and intracellular domains. As seen in Figure 1, the extracellular region contains an immunoglobulin (Ig)-like domain, a cytokine receptor homologous (CRH) domain, and three fibronectin type III (FNIII) domains (10). The intracellular region contains three distinct motifs called Box 1, Box 2, and Box 3 and four tyrosine residues (704, 729, 744, and 764) that are essential for mitogenic signal transduction. GCSF requires four highly conserved cysteine residues in the N-terminal half region and the WSXWS motif in the cytokine receptor-homologous (CRH) domain to bind GCSFR and initiate signal transduction (11). Additionally, these four cysteine residues in combination with an additional four cysteine residues at the N-terminal provide eight potential sites for N-linked glycosylation (12).

Isoforms

Seven messenger RNA (mRNA) isoforms (Class I through VII) can result from alternative splicing of *CSF3R*. While it is unclear which isoforms are expressed in non-hematopoietic cells, the only class I (the canonical type) and class IV (differentiation defective) GCSFR isoforms are detectable in hematopoietic cells (13). Functional mapping studies highlight the importance of the 87-amino acid residues of the carboxy-terminal region in the receptor that allow the signaling for cellular maturation and the 96-amino acid residues of the proximal membrane region that allow the signaling for cellular proliferation. Class IV GCSFR, which is expressed prominently in patients with acute myeloid leukemia (AML), contains a truncation of 87 amino acids at position 725 of the C-terminal along with dileucine residues required for normal receptor internalization, which are replaced by a unique 34-amino acid sequence (9, 14). These changes are thought to result in receptor overexpression due to a lack of normal internalization. Increased expression of Class IV GCSFR has also been linked to increased incidence of AML relapse (15).

Signal transduction

The immune response to pathogenic microbial invasions is triggered by the finely tuned cascading signal transductions of neighboring cells. GCSF and GCSFR play an integral role in an adaptive immune response through their immunomodulation effect. However, many investigators have also found that GCSFR signaling is increased in multiple cancers as compared to expression levels in healthy cells.

Activation of the receptor enhances the rate of cellular proliferation through the initiation of a cascade of intracellular signaling that is propagated by many factors, among which are Src and a tyrosine kinase protein, Janus Kinase (JAK). This results in the downstream activation of the transcription factors of signal transducers and activators of transcription (STAT) family. Suppressors of cytokine signaling proteins (SOCS) are

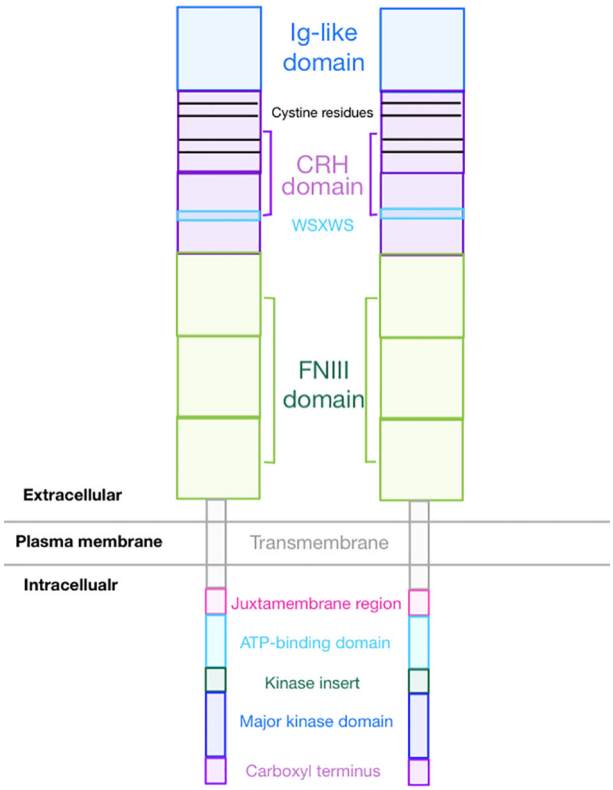

FIGURE 1
Overall GCSFR Structure.

critical negative regulators of GCSFR that inhibit the JAK/STAT pathway in a feedback loop. These proteins are primarily involved in the signal transduction pathways that GCSFR triggers, and stringent regulation of these proteins is integral for maintaining optimal expression of the receptor. Timely regulated initiation of the expression of GCSFR plays a central role in the sequence of events that lead to lineage divergence and in the establishment of malignancies (16). While the role played by GCSFR in neutrophil maturation and signaling is widely known, more recent work has shown considerable effects of GCSFR signaling in a wide variety of immune and non-immune cells. The results of signal transduction through GCSFR are also found to be dependent on both ligand concentration and cell location.

Like the interleukin-6 (IL-6) activation pathway, GCSF binding to GCSFR activates the signal transduction pathways by primarily inducing tyrosine phosphorylation of the receptor, which activates the JAK/STAT pathway (Figure 2). GCSFR has no intrinsic tyrosine kinase activity. However, upon GCSF binding, four conserved tyrosine residues in the cytoplasmic domain develop an increased affinity to STAT3, the adapter proteins Src homology and collagen homology (Shc), growth factor receptor bound protein 2, and suppressor of cytokine signaling 3 (SOCS3) after being phosphorylated by JAK1, JAK2, and Tyrosine kinase-2 Tyrosine kinase-2 (TYK2) (17). The cellular signal is propagated further when JAK2 recruits another tyrosine kinase, Lyn protein, a key inducing factor for the mitogenic behavior of GCSFR. Lyn, which directly binds to Casita B-lineage Lymphoma or Cbl, an E3 ubiquitin-protein ligase, couples Lyn to Phosphoinositide-3 kinase (PI3) (18, 19).

While JAKs are phosphorylated as a result of the GCSF ligation of GCSFR, STATs are simultaneously activated and traffic downstream signals. Like JAK proteins, STAT proteins have important tyrosine residue sites that need to be successfully phosphorylated to be activated. There is extensive evidence that the tyrosine residues in the membrane-proximal cytoplasmic region of GCSFR, Y704 and Y744, are integral for STAT activation *via* a direct docking mechanism at those sites (20). Three distinctive STAT proteins are involved in this activation step: STAT1, 3, and 5. While all three play roles in the activation of cellular proliferation, each of the three has a distinct mechanism of action. Phosphorylated STAT1 (pSTAT1) controls the dormant stem cell's entry into the cell cycle and stimulation of interferon (IFN) for an inflammatory response. Phosphorylated STAT3 (pSTAT3) acts as a mediator and a key regulator of pluripotent cell maintenance. Phosphorylated

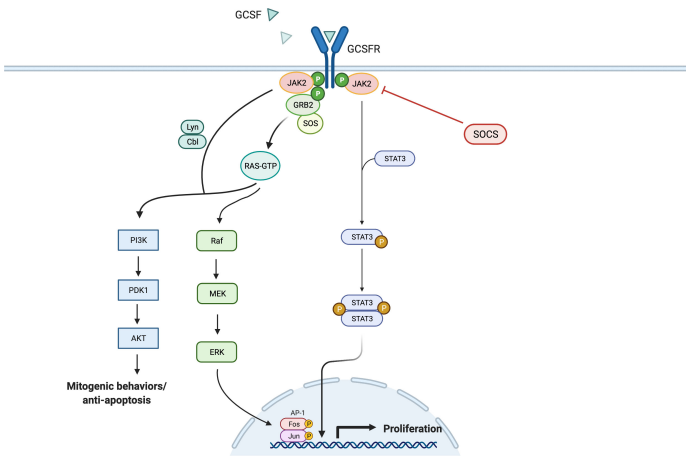

FIGURE 2
General Overview of GCSFR Signal Pathways. Adapted from "Hippo Pathway in Mammals", by BioRender.com (2022). Retrieved from https://app.biorender.com/biorender-templates.

STAT5 (pSTAT5) acts as a downstream messenger that induces the activation of the erythropoietin receptor (EPOR) in the setting of basal GCSFR activity (21, 22). STAT3 activation is required for GCSF-dependent granulocytic differentiation and regulation as the protein leads to sustained GCSF-induced proliferation in certain myeloid cell lines. This is demonstrated by the fact that reduced STAT3 signaling led to the loss of stem cell maintenance, while STAT5 and STAT1 largely affected cellular survival (23). STAT3 seems to hold greater importance in the signal transduction process, as it is expressed in greater amount than STAT5 and STAT1 in GCSF/GCSFR-dependent signaling (24, 25). Consistently, past findings differentiate STAT3 from STAT5 as the major proponent for oncogenesis in solid tumors. It has been detected in solid tumors at significantly increased levels, while STAT5 is found at higher levels in hematological malignancies. However, there is emerging evidence that shows STAT5 having a wider role in mediating solid tumorigenesis than previously thought. Although STAT5 has not been included in Figure 2, as it is not yet confirmed to be a potent oncogene in solid tumors, an increased expression level of STAT5 was notably found in lung cancer cells, promoting the survival of cancerous cells *via* the tyrosine-protein kinase ABL2 and transcriptional coactivator TAZ signaling axis (26, 27).

For STAT5 and STAT1, conserved Box 1 and Box 2 motifs in the cytoplasmic domain of GCSFR are required for activation (28, 29). Mutational analyses of the mouse GCSFR cytoplasmic domain elucidated the importance of conserved Box 1 and 2 sequence motifs in GCSF-mediated receptor growth signaling. These motifs are located at the carboxy-terminal end of the receptor close to the membrane-proximal 53 amino acids of the cytoplasmic domain and act as a latching site for tyrosine-specific phosphorylation of the transcriptional regulator $p75^{c\text{-}rel}$ in Ba/F3 transformants—a process integral for GCSFR growth signal transduction (30). However, STAT3 does not rely on the conserved motifs for activation. Instead, it acts through tyrosine-dependent and tyrosine-independent mechanisms for activation depending on the ligand concentration (Figure 3). Recently, a comparison of STAT3 activation between wild-type (WT) GCSFR with the deletion mutants d715 and Y704F suggests STAT3 activation has an alternate mechanism of activation at low GCSF concentrations. At low concentrations, STAT3 activation is mediated by the phosphorylation of the Y704 and 744 sites by receptor-associated JAK kinase family members, leading to dimerization mediated by reciprocal Src homology 2 (SH2)-pY705 motif interactions and then nuclear translocations and binding to specific DNA elements of *CSF3R* (31). Possible explanations for these two sites acting as the major docking sites may be that they allow more efficient phosphorylation or have higher affinity than the putative intermediate docking protein (32). In contrast, GCSFR is activated independently from intracellular tyrosine at the saturating concentrations of GCSF (100 ng/ml) (15). Under these high ligand concentration conditions, STAT3 activation is mediated by a mechanism involving the C-terminal region of the full-length GCSFR, removing the need for the tyrosine docking sites. The evidence suggests that emergency granulopoiesis in response to high levels of GCSF may be accomplished through an independent signaling pathway mediated by the distal region of GCSFR without the requirement of phosphotyrosine residues.

Unlike STAT3, STAT1 and STAT5 can be activated when a ligand binds to their receptors in the absence of receptor tyrosine phosphorylation. It is currently thought that JAK1 and JAK2 recruit and phosphorylate STAT1 and STAT5, respectively, in a direct manner. The expression of STAT5 is carefully regulated by Src homology phosphatase-1 (SHP1). A comparison of $SHP1^{WT}$ and

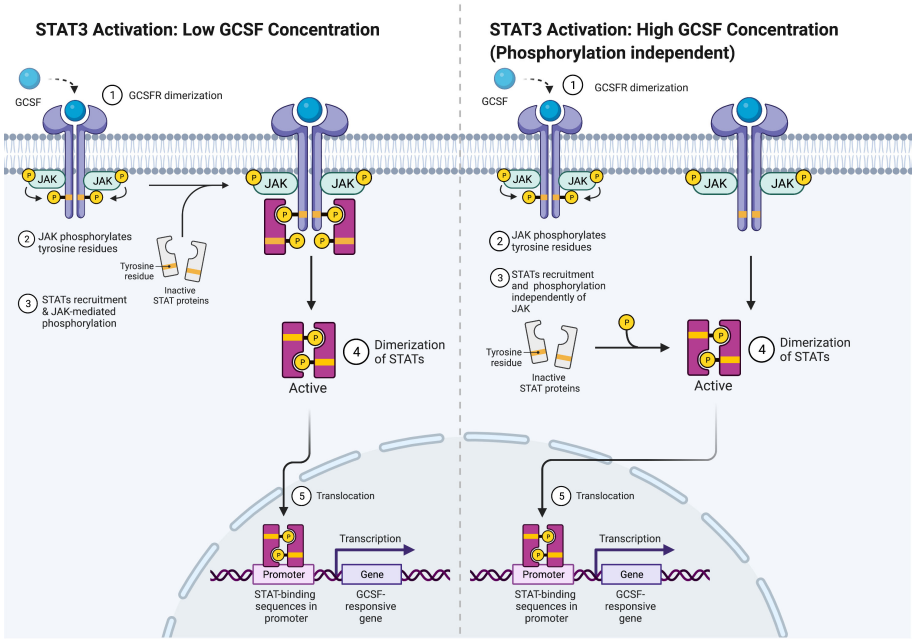

FIGURE 3
STAT3 Activation Mechanisms. Adapted from "Cytokine Signaling through the JAK-STAT Pathway", by BioRender.com (2022). Retrieved from https://app.biorender.com/biorender-templates.

SHP1^{mut} expression in 32D cells, which are murine pre-B cells that require the cytokine for growth and survival, led to the finding that SHP1 directly regulates the intensity of GCSF-mediated proliferation in a negative manner through direct association with Y729 and indirect interaction with phosphorylated Y729 of GCSFR carboxy terminus. Although the SH2 domain of SHP1 did not interact with phosphorylated tyrosine residues in an *in vitro* binding assay, Src homology phosphatase-2 (SHP2) still maintained its regulation on proliferation at the expense of GCSF-induced differentiation (31, 33). This could possibly be explained by the fact that STAT5 has three active isoforms: STAT5A, STAT5B, and STAT5p80. While STAT5A and STAT5B bind to the proliferation-specific domain of GCSFR, STAT5p80 binds to phosphorylated Y704 of GCSFR, which is essential for differentiation (28, 34). The activated STAT5 is now able to behave similarly as STAT3 in that it is able to cause STAT5 dimerization and attract transcription factors like lymphoid enhancer-binding factor-1 (LEF1) and C/EBPα to the nucleus (35, 36). Investigations using samples from congenital neutropenia (CN) patients with and without AML revealed that higher levels of phosphorylated STAT5 and LEF1 were found in CN patients who developed AML subsequently than in CN patients who did not develop AML. Furthermore, a recent study on breast cancer gene-1 (BRCA1) associated with ovarian cancers revealed a role for STAT5 in mediating solid tumorigenesis. Upregulated STAT5 inhibited the transcription factor p21, a cell-cycle inhibitor, leading to increased proliferation of ovarian carcinomas (37). Furthermore, studies on JAK2 V617F mutations, acquired somatic mutations often found in patients with myeloproliferative cancers, revealed that STAT5 over-activation can also cause increased cell proliferative behavior in non-myeloid cells such as mammary cells (38). A point mutation in JAK2 allowed constitutive activation of JAK2 in epithelial mammary cells, which led to hyperactivation of STAT5 that eventually enhanced the proliferation of epithelial memory cells. These findings highlight a greater role for STAT5 in the oncogenesis of both solid tumors and hematopoietic cancers.

Similar to STAT5, STAT1 activation is dependent on the successful formation of STAT1 homodimers by reciprocal phosphotyrosine–SH2 domain interactions, which allows for translocation of the homodimers to the nucleus, which is followed by binding to the promoters of the targeted genes (39). STAT1 is tightly regulated, as its response is rapid and transiently activated in response to ligand stimulation. It is also subjected to regulation by SHP1 and SHP2 in a negative regulatory manner. Both phosphatases reduce JAK/STAT1 signaling by inactivating the interferon receptors and JAKs through dephosphorylation (18, 23).

In earlier paragraphs, secondary GCSFR regulators specific to each protein were explored, but SOCS proteins are the primary regulators of GCSFR. While STAT signaling regulates the intensity of signal transduction induced by GCSF, members of the SOCS family control the duration of the signal. STAT activation induces the expression of SOCS, and in turn, SOCS inhibits the signaling cascade in a classic negative feedback loop.

While there are eight proteins in the SOCS family, SOCS1 and SOCS3 are currently at the center of interest, as they are unique in the SOCS family for their particularly short N-terminal domain, which allows direct interaction with JAKs to inhibit the catalytic activity. SOCS1 and SOCS3 have two described mechanisms of inhibition. First, the SH2 domain of SOCS3 directly binds to the phosphorylated activation loop of JAK and the killer-cell immunoglobulin-like receptor (KIR) domain, which then blocks the active site of JAK. Second, the elongin B/C heterodimer and ternary complex-bound SOCS box domain interact with Cullin 5 (CUL5) to form the scaffold of an E3 ubiquitin ligase that ubiquitinates both JAKs and GCSFR, marking them for degradation by proteasomes. (Figure 4) (40).

The complex signal transductions and physiological effects driven by the GCSF/GCSFR system were recently investigated using a global GCSF knockout mouse model by Zhang et al. to determine how GCSF signaling modulates the physiological effect of non-alcoholic fatty liver disease (NAFLD). Overall, GCSF deficiency in mice alleviated a high-fat diet (HFD) and palmitic acid (PA) induced obesity, hepatic steatosis, and insulin resistance. A comparison of isolated primary hepatocytes from both GCSF knockout (−/−) and WT (+/+) mice treated with either an HFD or a standard-chow diet (SCD) revealed that administration of exogenous GCSF significantly aggravated palmitic acid-induced lipid accumulation in both the GCSF knockout (−/−) and WT (+/+) mouse samples. The model also showed a physiological difference in GCSF−/− mice having significantly lower liver weight, a lower mass of epididymal white adipose tissue, and a lesser extent of hepatic steatosis than their control littermates after 13 weeks of HFD feeding before the introduction of exogenous GCSF (41). These findings were confirmed by intrahepatic triglyceride content from hepatic and cellular triglyceride assay, hematoxylin and eosin staining, and oil red O staining from the histological analysis. With the use of serine–threonine kinase (Akt) and glycogen synthase kinase-3 (GSK3) as markers for insulin sensitivity and glucose tolerance, Western blotting showed significantly increased phosphorylation of JAK1/2, STAT3, Akt, and GSK3 in the livers of HFD-fed GCSF−/− mice exposed to exogenous GCSF treatment. Consistently, decreased SOCS3 was detected in these mice, suggesting that GCSFR may be able to regulate lipid metabolism and insulin sensitivity *via* JAK/STAT3 signaling to modulate NAFLD. Immune cells in the liver through immunohistochemical staining and flow cytometry using myeloperoxidase as a marker for neutrophils and F4/80 for macrophages were also compared between GCSF−/− mice and WT prior to GCSF treatment.. Both neutrophils and macrophages were significantly decreased in the livers of HFD-fed GCSF−/− mice compared to WT, suggesting an alternate pathway in which GCSFR can indirectly affect the development of NAFLD by regulating the production and mobilization of neutrophils in the absence of GCSF (41). This study identifies the importance of GCSFR regulation in the presence of GCSF in response to diet-induced changes in hepatocyte metabolism. The study also suggests that increased GCSFR deregulates JAK/STAT/SOCS signal pathway, which can bring immunomodulation that may attenuate the hepatic metabolism process (41, 42).

Signal modulation

Whether GCSFR is susceptible to typical receptor translational modification remains investigated. However, emerging evidence suggests several mechanisms play functional roles in regulating the receptor. Specifically, C-mannosylation regulates the receptor by

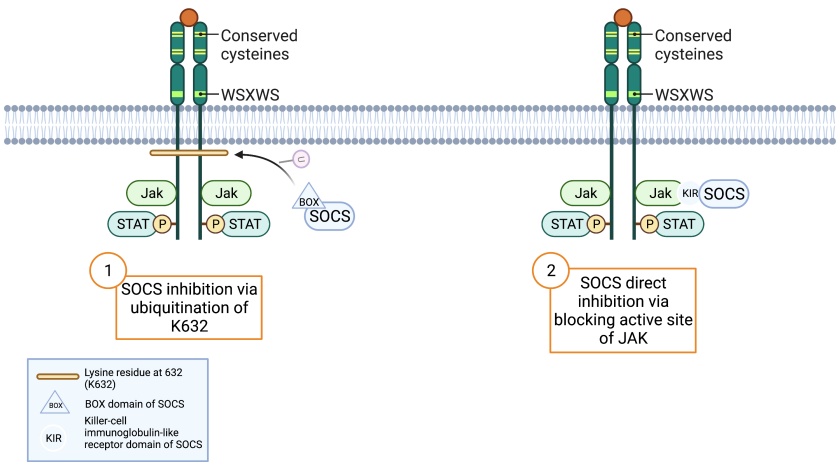

FIGURE 4
SOCS Inhibition Mechanisms. Adapted from "Cytokine Receptor Families", by BioRender.com (2022). Retrieved from https://app.biorender.com/biorender-templates.

modulating its signaling. A post-translational modification that occurs intracellularly in the endoplasmic reticulum before protein folding and secretion, C-mannosylation regulates protein folding, guidance of substrate of proteins, and cellular signaling. This mode of protein modification has been found to be functional in regulating the downstream signaling of GCSFR. In the receptor, C-mannosylation at W318 regulates granulocytic differentiation in myeloid 32D cells and affects GCSF-dependent downstream signaling by changing ligand binding capability. Investigators used transduction of myeloid 32D cells with WT or W318F GCSFR expressing lentivirus to show that the absence of this C-mannosylation site on GCSFR resulted in lower phosphorylation levels of STAT3 compared to WT-expressing cells as well as a lower number of differentiated cells (43). The *in vitro* experiment also confirmed that C-mannosylation regulates the JAK/STAT pathway by affecting the capability of ligand binding without any change in the cell surface localization of GCSFR, resulting in myeloid cell differentiation (44).

Regulation of granulocyte colony-stimulating factor receptor expression

Initially, it was thought that GCSFR was expressed only on myeloid and hematopoietic stem cells. However, GCSFR has been shown to be expressed on epithelial cells, endothelial cells, ganglion cells, neurons, cardiomyocytes, and numerous cancer cell lines (45–48). Furthermore, the expression of GCSF and GCSFR is increased in several types of solid tumors including breast cancer, bladder cancer, GI cancers, and gliomas (8, 49–51). While GCSFR regulation has primarily been studied in myeloid cells, here we will discuss what is also known about GCSFR regulation in both myeloid and non-myeloid cells. By understanding how GCSFR expression is regulated, we will have greater insight into why and how dysregulation occurs in tumor development.

Regulators of transcription

The first barrier to transcriptional activation is chromatin accessibility. Physical access to chromatin is regulated through the topological organization of DNA binding proteins like nucleosomes and other chromatin binding factors (52). Post-translational modifications of nucleosomes contribute to chromatin accessibility, which can restrict or promote transcription factor binding. Early investigations of the methylation status of GCSFR promotors suggest that hypermethylation of the HpaII restriction site inhibits GCSFR transcription.

Examination of methylation patterns in lymphocytes that lacked GCSFR expression revealed hypermethylation of the promoter region of *GCSFR* gene, while macrophages, known to have high levels of GCSFR expression, exhibited hypomethylation of the promoter region. Lastly, granulocytes and monocytes exhibited no methylation (53). Taken together, these data suggest that GCSFR promotor methylation is a critical regulator of GCSFR expression. While histone remodelers, like SWI/SNF-related, matrix-associated, actin-dependent regulator of chromatin, subfamily D, member 2 (SMARCD2), and STAT5, have been shown to contribute to the regulation of GCSF-induced differentiation of neutrophil granulocytes, the histone remodeler(s) involved in GCSFR specific modifications and whether they are conserved among cell types remain a mystery (54, 55).

Transcription factors also play a critical role in regulating gene expression. CCAAT/enhancer-binding proteins (C/EBPs) are a family of transcription factors that increase the transcription of numerous genes involved in proliferation, differentiation, and survival by binding the promotor regions of target genes (56). Currently, there are six known distinct C/EBPs (C/EBPα, C/EBPβ, C/EBPγ, C/EBP00190, C/EBPδ, and C/EBPζ). Several of these factors are critical for granulopoiesis including C/EBPα, which is also critical for the differentiation of several cell types including hepatocytes, adipocytes, lung cells, and ovarian cells (57). C/EBPα binds a GCAAT site found in the promotor region of *CSF3R* in myeloid nuclear extracts, and mutations in the site reduce promotor activity by 60% (58). C/EBPα (−/−) mice exhibited undetectable levels of GCSFR mRNA, supporting a critical role of this transcription factor (59). While one group found undetectable levels of GCSFR mRNA in C/EBPα KO mice, another group of investigators found that cell lines established in the fetal liver of C/EBPα (−/−) mice expressed GCSFR mRNA, which increased with the addition of granulocyte-macrophage colony-stimulating factor (GM-CSF), suggesting a mechanism of GCSFR expression independent of C/EBPα (60). Rat sarcoma virus (RAS) signaling enhances the ability of C/EBPα to transactivate the GCSFR promotor by phosphorylation of S248 of the C/EBPα transactivation domain in the U937 myeloid cell line and 293T embryonic kidney cells. Furthermore, PKC blocks this activation (61). C/EBP00190 can also regulate GCSFR when transiently transfected into HeLa cells, suggesting a potential additional level of regulation (57).

Two additional transcription factors have been identified that are involved in the regulation of GCSFR. PU.1, an ETS-family transcription factor encoded by the *Spi1* gene, is a key differentiation regulator that can alter the expression of thousands of genes involved in hematopoiesis including GCSFR (62, 63). PU.1 binds a purine-rich DNA sequence (5′-GAGGAA-3′) called the PU-box located at +36 and +43 in the 5′ untranslated region of the GCSFR promotor. Mutation of this region reduces promoter activity by 75%. Additionally, C/EBPα physically interacts with and activates PU.1 distal enhancer in myeloid differentiation, suggesting an additional level of transcriptional complexity (64). Interestingly, when promoter

activity was monitored by luciferase assay, activity increases were observed in NB4 and HL60 leukemic cell lines but not in the non-myeloid cell lines, Jurkat or BJAB (65–67). Later studies discovered an interaction between C/EBP00190 and activating transcription factor 4 (ATF4) at CEBP binding sites of the GCSFR promoter (Figure 5) (68). Investigators used a luciferase reporter construct in Jurkat cells to demonstrate that homodimers of C/EBP00190 and heterodimers of C/EBP00190 activate the GCSFR promotor equally well, whereas C/EBPα transcription is inhibited upon heterodimerization with ATF4 (68). These data suggest complicated and cell type-specific regulation of GCSFR expression. Many of these studies were done during the time when GCSFR was thought to be expressed explicitly in myeloid cells with later studies performed in lymphocytes. A more recent study found an additional step of GCSFR expression regulation in a neutrophilic granule protein (NGP) neuroblastoma subpopulation of $CD144^+$ cells (3). STAT3, which is activated through GCSF signaling, directly regulates GCSFR expression, suggesting a feed-forward loop. Whether these transcription factors are involved in GCSFR regulation in epithelial cells and fibroblasts within tumor microenvironments remains unknown.

Translational regulation

MicroRNAs (miRs), short non-coding RNA molecules, bind to target mRNAs and allow translational repression and gene silencing. miRs play regulatory roles in cellular processes from proliferation to apoptosis at the translation stage. In relation to GCSFR, miRs play a critical role in combatting truncated GCSFR variants, which is important, as defective receptors have been shown to confer resistance to apoptosis and contribute to oncologic transformation. Currently, several miRs have been shown to regulate GCSFR expression, and dysregulation of expression in miRs are linked to diseases.

The miR-155 is highly expressed in hematopoietic progenitor cells and several hematological malignancies. Patients with severe congenital neutropenia (SCN), who have higher levels of class IV GCSFR, are also found to have higher levels of miR-155. Itkin et al. demonstrated that miR-155 was aberrantly upregulated in a STAT5-dependent manner for individuals with a greater level of class IV GCSFR, suggesting that upregulated miR-155 can increase the risk of *de novo* leukemia or leukemia relapse for these individuals. The pro-tumor effects mediated by miR-155 upregulation include the suppression of growth factor independent-1 transcription repressor, which is crucial for myeloid differentiation and tumor suppression, and tumor protein p53 inducible nuclear protein-1, which has anti-proliferative and pro-apoptotic activities. Additionally, miR-155 indirectly promotes the secretion of C-C chemokine ligand-2 (CCL2), a strong chemotactic factor important for regulating macrophage recruitment and polarization during inflammation (69). The miR-155-mediated CCL2 upregulation was found to upregulate GCSF-induced mobilization *via* C-X-C motif chemokine-12/C-X-C motif chemokine receptor 4 (CXCL12-CXCR4) signaling axis and STAT5 activation when class IV GCSFR was present (70). This finding highlights the pro-tumorigenic implications of miR-155-mediated GCSF and GCSFR expression and increased leukemogenicity in SCN patients.

While miRNAs can regulate GCSFR expression, signaling through the GCSF axis can also increase the expression of pro-tumor miRNAs. Recent work by Zhang et al. demonstrated that GCSF treatment on the HCT-8 colon cancer cell line resulted in a gradual increase of miR-125b expression in a time-dependent manner (71). Previous studies suggest that miR-125b can act in a pro-metastasis manner by modulating the tumor microenvironment *via* promotion of apoptosis and epithelial to mesenchymal transition (72). A recent analysis of colorectal cancer (CRC) patient samples with or without node metastasis confirmed that samples from patients with metastasis had higher expression of miR-125b. Further work on the HCT-8 cell line by ectopically expressing miR-125b in the cell line revealed that ectopic miR-125b could significantly promote migration and invasion of CRC cells, indicated by the transwell migration array and Matrigel invasion array. The finding was consistent with tumors of mice injected with CRC cells with overexpressed miR-125b metastasizing in the liver and lung (71, 73). The migration speed of HCT-8 cells also increased in a dependently of in miR-125b overexpression, as the wound healing assay showed much faster wound healing than that of the control. Zhang et al. performed a dual-luciferase activity assay and identified myeloid cell leukemia-1 (MCL1), an inhibitor of apoptosis that contains 3′-UTR putative target sequences for miR-125b, to be the direct target of this translational modification. The result revealed miR-125b inhibiting the relative luciferase activity of WT MCL1 3′-UTR constructs with firefly luciferase vector when co-transfected with miR-125b mimics, suggesting that miR-125b directly binds to 3′-UTR of MCL1 to inhibit its expression (71). While the exact mechanism by which miR-125b acts in CRC initiation and progression is unclear, different studies have identified the increased presence of miR-125 in breast and liver cancers, suggesting that miR-125-induced inhibition of MCL1 protein may selectively promote apoptosis-resistant cancer cells, which then can have greater metastatic potential than the cancer cells susceptible to apoptosis, in various organs (73).

Trafficking and post-translational modifications

Localization

Protein localization requires the accumulation of a protein at a destined site to produce cellular signaling and is an important step for signal trafficking. Endocytosis is one method by which signal

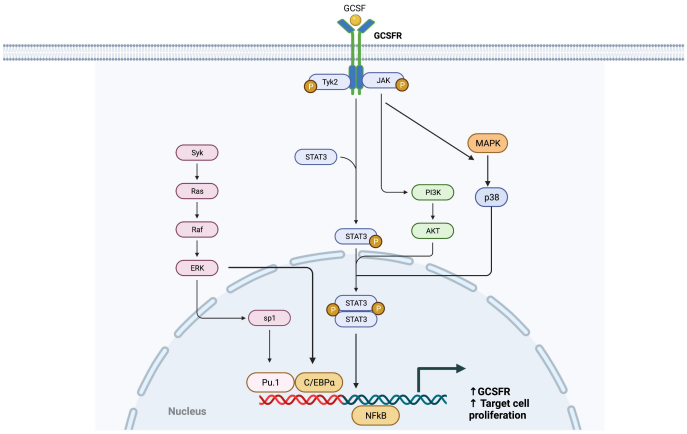

FIGURE 5
Transcription Factors of GCSFR (CSF3R). Adapted from "CREB Signaling Pathway", by BioRender.com (2022). Retrieved from https://app.biorender.com/biorender-templates.

transductions are modulated in terms of intensity and duration. In some disease processes, receptor trafficking can become altered, resulting in hampered receptor signaling pathways. Enhanced green fluorescent protein (EGFP)-tagged WT GCSFR demonstrated ligand-induced spontaneous receptor internalization with predominant localization in the Golgi apparatus, late endosomes, and lysosomes (74). Positions at 749–755 and 756–769 in the C-terminal region of GCSFR aid in the internalization of the receptor *via* their dileucine internalization motif, which is dependent on phosphorylation of a serine residue at position −4 to −5 upstream of the dileucine pair. The phosphorylation of this serine residue facilitates the interaction with activator protein-2 (AP2) (75). Internalization of the receptor has a synergizing effect on JAK activation. Additionally, the integrity of a crucial tryptophan residue (W650) in the juxta-membrane region of the receptor for JAK activation is found to further stabilize the internalization process.

Recycling

The fate of internalized receptors includes receptor degradation and recycling. Receptor recycling plays an important regulatory role in signal activation and overall signal trafficking. In WT GCSFR, GCSF binding of the receptor results in receptor internalization followed by endosome formation as presented in Figure 6. During this process, downstream signaling continues. The receptor inside the endosome now faces either degradation or recycling. If recycled, the early endosome undertakes a dynamic system for sorting and re-exporting membrane components *via* the endoplasmic reticulum and Golgi apparatus, respectively. Understanding the mechanism of recycling helps in determining the composition of the plasma membrane and the mechanisms of normal cellular homeostasis.

Damaged endosomal recycling is often linked to a variety of diseases, including cancer and neutropenia. Vacuolar protein sorting 45 homolog (VPS45) deficiency is often found in patients with serious infections and diseases including CN, bone marrow fibrosis, and extramedullary renal hematopoiesis. VPS45, a member of the secretory/mammalian uncoordinated 18 (SM) family, is a critical regulator that orchestrates trafficking through the endosomal system and promotes the recycling of cell surface receptors. Loss of VPS45 results in the trapping of GCSFR in endosomes and impaired lysosomal delivery (76). Linked to hypo-responsiveness to GCSF due to impaired trafficking of GCSFR, the absence of VPS45 reduced trafficking of colocalized GCSFR with lysosome-associated membrane glycoprotein-2 (LAMP2)-positive late endosomes, showing a sustained accumulation of receptor in early endosomes (77). The accumulation indicated that the absence of VPS45 arrests early endosomal activity in sorting receptors for recycling or degradation. Interestingly, past research draws a closer relationship between T224A mutation in *VPS45* gene that abolishes its gene expression in SCN patients who are often susceptible to dysregulated GCSFR (76).

In GCSFR, phosphorylation of the immediate upstream serine residue at 749 of carboxyl terminus (S749), positioned four residues downstream of the dileucine motif, is found to be a crucial determinant in the switch from slow constitutive endocytosis to fast, ligand-induced endocytosis (74). A mutation of the leucine in internalization motif-1 to alanine (L753754A) has been shown to elicit a significant reduction in GCSFR internalization, suggesting that the upstream leucine residue plays an integral role in both localization and internalization of the receptor (43). The internalization rate of WT GCSFR was compared to receptor mutants S749A and S749D that mimic an unphosphorylated lysine residue and a phosphorylated residue, respectively. Both WT and S749D GCSFR had internalized

10.3389/fonc.2022.932608

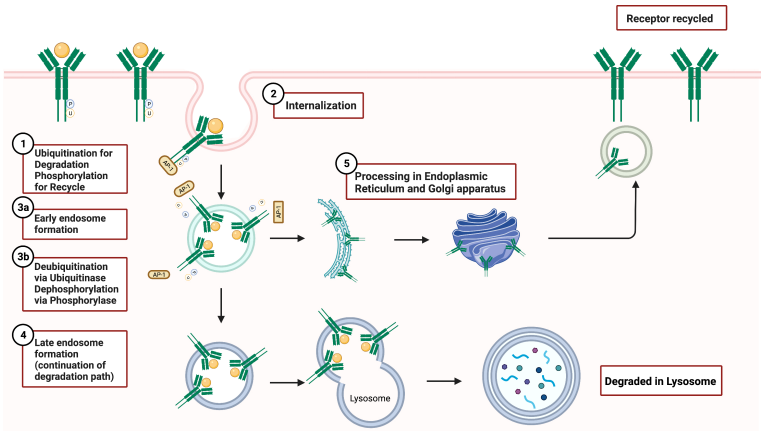

FIGURE 6
GCSFR Degradation and Recycle Mechanisms. Adapted from "Endocytosis and Exocytosis with Membrane Rupture (Layout)", by BioRender.com (2022). Retrieved from https://app.biorender.com/biorender-templates.

approximately 60% of the surface GCSFR within 5 min of incubation at 37°C, while only 20% of the cells expressing S749A were internalized at that timepoint. Both S749A S749D GCSFR mutant cells were not affected by spontaneous internalization of anti-GCSFR antibodies when compared with WT GCSFR cells, indicating that the phosphorylation of S749 is important in determining the rate of ligand-mediated GCSFR internalization but is not sufficient by itself to catalyze the internalization rate in the absence of GCSF (77, 78).

Degradation

The degradation mechanisms of GCSFR are similar to most cell surface protein processing and include glycosylation and targeted ubiquitination. Derangements in the degradation process of GCSFR are found in patients with SCN and AML, which increase in GCSFR induces hypersensitivity and enhanced growth response to GCSF. (79–81).

Degradation of GCSFR begins with ubiquitination modulated by *O*-glycosylation. The cluster of threonine residues proximal to amino acid position 618 is an important site for glycosylation. The glycosylated wild-type GCSFR is expressed at the cell surface and triggers ligand-dependent tyrosine phosphorylation (82). The phosphorylation then leads to ubiquitination for proteasomal degradation. At this step, JAK2 levels decrease to limit the signaling (83). Additionally, *O*-linked glycosylation decreases the dimerization of the receptor due to its bulky charged group, which sterically hinders the process. A recent finding elucidates a novel avenue of aberrant signaling of GCSFR when the degradation signal is compromised. Threonine residue at the 618 (T618) site of the proximal membrane region of the receptor, a part of the *O*-linked glycosylation cluster, is an important motif for endocytosis and degradation. Truncation in T618 directly prevents *O*-glycosylation of the receptor and increases receptor dimerization, highlighting the receptor's ability to be activated in a ligand-independent manner when T618 is compromised (84). Point mutation analysis of T618I mutant confirmed that this mutation prevented *O*-glycosylation of the receptor (82). Cells expressing the membrane-proximal *CSF3R* T618I mutation exhibited high rates of growth in the absence or presence of ligand without any change over the concentration gradient (85). This finding was consistent with previous reports that showed the T618I mutation causing rodent bone marrow colony formation in the absence of GCSF (86). The ligand-independent nature of T618 mutant underscores the relative potency of the truncation mutation and further highlights the importance of the threonine cluster in the function and regulation of GCSFR signaling.

The receptor is also susceptible to degradation through SOCS3-driven lysosomal degradation, in which ubiquitination of specific lysine residues in the conserved juxta-membrane motif plays a large role in regulating degradation. Unlike glycosylation, which partly inhibits JAK kinase activity, ubiquitination of the lysine residue at position 632 of juxta-membrane (K632) drives lysosomal degradation and targets STAT5 by downregulating and attenuating phosphorylation activity (Figure 4) (87). Covalent bonding of ubiquitin to a cytoplasmic lysine residue in GCSFR attracts lysosomal sorting effectors and proteins such as the hepatocyte growth factor regulated tyrosine kinase substrate, endocytic adaptor proteins (epsins), and the endosomal sorting complex required for transport machinery (ESCRT) complexes to create a binding site for membrane phosphoinositides. Subsequently, EAP45/Vps36 interacts with this complex to sort cargo proteins to the luminal vesicles of endosomes. SOCS's innate

ability to inhibit phosphorylation strengthens the effect of this downregulation pathway on GCSFR (39). Additionally, the lysine residue in the receptor holds importance in regulating the GCSFR-stimulated signal transduction. A lysine lacking GCSFR mutation is strongly associated with prolonged receptor expression, leading to unregulated cellular proliferation. Comparing the STAT phosphorylation activity between WT whole cell lysates and K762R/GCSFR transfectants, immunoblot analysis showed rapid diminishment of phosphorylation of both STAT3 and STAT5 in the WT compared to the mutated GCSFR counterpart 2 h post-GCSF stimulation. Akt signaling pathway, an important pathway for cell survival and proliferation, was also found to have prolonged activation in K762R mutants as compared to WT GCSFR transfectants in which Akt activity was undetected at 60 min (79).

Other biological inhibitors for degradation have been identified including methyl-β-cyclodextrin, hyperosmotic sucrose, severely reduced internalization-defective GCSFR mutants like D715, and GCSFR deletion mutations, which are often found in patients with neutropenia. Degradation inhibitors like MG132 and Bafilomycin-A take a more direct approach to restore GCSFR protein levels by preventing degradation. MG132, an effective reversible proteasome inhibitor, can readily permeate through the cell membrane and selectively inhibit proteosome machinery by attaching its peptide aldehydes to the lysosomal cysteine domain of proteases. Bafilomycin-A, a macrolide antibiotic, inhibits GCSFR degradation through acidification of either the extra cellular environment or intracellular organelles, denaturing lysosomes by specifically targeting vacuolar-type hydrogen ATPase (V-ATPase) (88).

Protein interactions

The GCSFR-driven signal transduction mechanism is complex. Its ability to contribute to proliferation and cellular differentiation signaling in different organs is a testament to the versatility of the receptor and highlights the potential for deleterious effects when GCSFR is upregulated. The *in vitro* investigation of GCSFR in hepatocytes discussed in the *Signal Transduction* section of this review reflects the organ specificity of GCSFR-stimulated signal transduction and highlights the vast presence of GCSFR in the human body. In the liver, GCSFR regulates hepatic lipid metabolism through downstream signaling activation of the JAK/STAT/SOCS pathway. GCSFR activation induced expression of SOCS3, which then inhibited JAK activation and limited STAT3 phosphorylation, negatively regulating GCSF response (41). This negative feedback pathway had a direct influence on instigating hepatic steatosis by inhibiting the expression of Akt and GSK3, which evoke insulin insensitivity, highlighting the intracellular interplay between organ-specific proteins and the GCSFR-mediated signaling proteins (89).

GCSFR is known to interact with transmembrane proteins involved in signal transduction pathways of cells to maintain healthy homeostasis. One of these interactions is with integrin α9β1. This transmembrane protein is often found in the epithelium and aids in the translation of extracellular signals that change cell behavior, specifically cell adhesion and migration (90). α9β1 is also prominently expressed on human neutrophils and mediates neutrophil migration through vascular cell adhesion molecule-1 (VCAM1) and tenascin-C (TNC). α9β1 improves the responsiveness of GCSFR to GCSF and promotes stimulation of the cascading signaling pathway by directly interacting with GCSFR. Comparing ltgα9 WT and ltgα9−/− bone marrow cells revealed that the STAT3 phosphorylation resulting from GCSF stimulation was significantly reduced in α9-deficient cells (91). While the specific mechanism remains unclear, the permissive role of α9β1 in the GCSFR-signaling pathway as indicated in the study suggests α9β1 is important for granulopoiesis, especially in enhancing the activation of STAT3.

Another important protein interaction of the receptor is with E6-associated protein (E6AP), a ligase protein best known for ubiquitinating the transcription factor p53. E6AP targets GCSFR for ubiquitin-mediated proteasome degradation, attenuating the receptor's function (88). GCSFR and E6AP are co-localized together in the cells, and the co-localization is enhanced in the presence of the proteasome inhibitor MG132 both *in vitro* and *in vivo* (88). E6AP is also found to promote early degradation of GCSFR, reducing the GCSFR signaling indicated by reduced STAT3 phosphorylation. Investigators determined the half-life of GCSFR in the presence and absence of E6AP by inhibition of *de novo* protein synthesis with cycloheximide. E6AP markedly reduced the half-life of GCSFR, while the half-life of T718 GCSFR mutant was modestly affected, highlighting the importance of the protein–protein interaction between E6AP and GCSFR (88, 92). The study further implicates the possibility of E6AP as an effective GCSFR inhibitor to treat GCSFR upregulated diseases.

Receptor expression and response to granulocyte colony-stimulating factor in non-myeloid cells

Previously established understanding of GCSFR implicates that the receptor can interact with non-immune cells in different organs. In recent years, the receptor and its substrate have been detected on the surface of other microvascular murine endothelial cells originating from the thymus, brain, heart, and skin, as well as other non-hematopoietic cells (3, 5, 78). In the endothelial cells of different organs, GCSFR is expressed at similar levels as in myeloid cells and acts similarly in aiding the cellular proliferation and migration of cells (93). The

signaling mechanism of rh-GCSF and the receptor (rh-GCSFR) in the ovarian adenocarcinoma cell line, HEY, allows a better understanding of GCSFR functioning beyond its typical role.

The *in vitro* model of rh-GCSFR in HEY constructed by Brandsetter et al. showed the active participation of the receptor in mediating mitogen-activated pathway (MAP). To demonstrate this, proliferative and differential signals were induced *via* GCSFR, and a similar signal transduction mechanism was shown in the model. Y646, 744, and 764 sites were important for activating JAK kinases and activating $p21^{Ras}$/MAP kinases. Upon exogenous GCSF stimulation of HEY cell lines, *AP-1-(c-Jun/c-Fos)* regulated gene accumulated and upregulated *CSF3R* expression by 40% (94). Three MAP kinase groups were involved in MAP: p38 kinases, the extracellularly regulated kinases (ERKs), and the c-Jun N-terminal kinases (JNKs) found in stress-activated pathways. Two methods by which these proteins are activated were identified: stress-associated and non-stress-associated pathways. Although these two pathways result in increased proliferation, the stress-associated pathway involves the JNKs and p38 kinases that are activated in response to inflammation. The non-stress-associated pathway involves cytokine activation of ERKs, which can phosphorylate c-jun, an integral component of AP-1 complexes that regulate transcriptional activity (95).

In addition to its proliferative role, the retinal ganglion cell (RGC) axotomy model used by Frank et al., highlights the receptor's neuroprotective nature in RGCs. Its constitutive expression in RGCs aids in the survival, differentiation, and proliferation of neutrophilic lineage cells. The investigators demonstrated that GCSF-mediated GCSFR expression protected RGCs from degeneration after transection of the optic nerve in a rat model (47). GCSFR-driven activation of RAS/RAF/ERK or PI3K/Akt kinases is understood to inhibit apoptosis through inhibition of caspase and by activating neurotrophins, potentially explaining this protective effect (96).

Regeneration of skeletal and cardiac muscle cells links proliferation of cells to cellular inflammatory response mediated by GCSFR upregulation. Examining rodent embryos using immunostaining, GCSFR expression was demonstrated to be increased at the period when early skeletal myocytes began differentiating and the expression of the receptor was affected by the autocrine GCSF signaling as myoblasts developed (97). A serial histological analysis up to 28 days after injury (inducing stress by injecting cardiotoxin directly into rodent femoral muscle cells) demonstrated the synchronous nature of inflammatory response and upregulation of GCSFR to protect cells and prevent apoptosis. GCSFR expression was observed *via* immunofluorescence on day 5 after cardiotoxin injection. Day 5 corresponded to the same day the skeletal muscle progenitor cells or satellite cells (SCs) began proliferating, confirming that increased expression of GCSFR coincides with the proliferation period of cells (97). Furthermore, in the isolated myofiber samples of day 5, 94.4% of activated SCs or migrating SCs into the injured site with syndecan-4 (SDC4) activation showed increased expression of GCSFR. This suggests that both activated SCs and inflammatory factors were present at the same time GCSFR expression increased during the first cellular proliferation (98). Upon the activation of GCSFR, the same important signal trafficking proteins seen in myeloid cells like ERK, JNK, p38MAPK, Akt, and STATs were activated. The level of expression of these proteins paralleled with the upregulation level of GCSFR, promoting the proliferation of myoblasts (97). A similar expression pattern of GCSFR was shown in post-myocardial infarction (MI) cardiomyocytes. Additionally, upregulation of the receptor in myocardial infarction cardiomyocytes and cardiac fibroblasts of cultured rodent cardiomyocytes evoked similar protective and anti-apoptotic roles for the damaged cells *via* the JAK/STAT pathway by producing angiogenic factors (99).

While these findings highlight the cell-protective characteristics of GCSFR signaling in cells, they also implicate the damning concern that GCSFR signaling can inhibit the cellular apoptosis mechanism to encourage cancer cells to grow (96).

Cancer

It is evident that unbridled expression of GCSFR causes unnecessary and possibly dangerous cellular proliferation and differentiation through complex downstream signal transduction. Its ability to induce proliferation pathways led investigators to look closely at GCSFR functioning in human tumor cells to better understand the relationship between upregulated GCSFR and different cancers. Wojtukiewicz et al. reported the detection of high GCSFR expression in 20 out of 28 assessed breast cancer tissue samples. Immunoblotting showed high GCSFR expression on the endothelial cells (ECs) of small blood vessels supplying breast cancers in those 20 samples, suggesting the possibility of GCSFR aiding in the proliferation and migration of ECs by supporting angiogenesis in breast cancers. Furthermore, co-expression of GCSFR with vascular endothelial growth factor (VEGF), VEGF receptor, and tissue factors were found in those samples, highlighting the interplay between the receptors for angiogenesis promotion and in providing mitogenic support for the progression of malignant cells. Similar to breast cancer, higher expression of GCSFR is found in nasopharyngeal, oral cavity, colorectal, gastric, and ovarian cancers, solidifying the relationship between increased levels of GCSFR expression and solid tumors (5, 8, 10, 84).

Many investigators have demonstrated a link between the overexpression of GCSFR and pro-tumor effects in numerous cancers such as neuroblastoma and CRC (3, 51, 99). In the central nervous system, endogenously expressed GCSFR was found to be upregulated in response to external stress-related stimulation such as nerve injuries or hypoxia, a common feature

of the tumor microenvironment (100). An *in vitro* mechanical scratch neuronal injury model showed upregulation of GCSFR in spinal cord capillaries compared to the control sample. The model also highlighted the functioning of nucleophosmin-1 (NPM1), a neuron-specific protein, that was increased alongside GCSFR to reduce apoptosis by inactivating caspase-activated DNase (48). Xenograft and allograft murine models of neuroblastoma showed increased GCSFR expression promoting the proliferation and metastasis of neuroblastoma through GCSF-dependent phosphorylation of STAT3 signaling in $CD114^+$ cells. Agarwel et al. reported a positive feedback loop between GCSFR and STAT3-mediated transcription of *CSF3R* (3).

Upregulation of GCSFR is also detected in glioma. While GCSF and GCSFR expressions were not detected in the normal brain cortex or primary cultured astrocytes, they were widely expressed in glioma samples (101). This finding suggests that GCSFR expression may facilitate both autocrine and paracrine modes of stimulation and maintenance of glioma. Using a bromodeoxyuridine incorporation assay, the investigators demonstrated a significant increase in proliferating glioma cells with exogenous GCSF treatment. Specifically, bromodeoxyuridine (BrdU)-positive cells were increased by 50% in GCSF-treated groups compared to groups without GCSF treatment (78). Treatment of primary cell cultures derived from glioblastoma patients and the glioma cell lines T98G, U251, and U87 with GCSFR antibody resulted in a significant decrease in the frequency of BrdU-positive cells and colony formation rate by an average of 15% compared to those without treatment (78).

The same behavior can be seen in bladder carcinomas in which tumor cells' continuous expression of GCSF and GCSFR allowed for a functional autocrine/paracrine signaling loop that promotes the survival and growth of bladder cancer cells. This upregulation bolstered poorly differentiated proliferation as observed in multiple epithelial cancers and was a significant defining factor of the invasiveness of cancer. Higher GCSFR expression was also associated with the presence of lymph node metastasis in gastric cancers. In cultured gastric cancer cells (SGC7901), GCSFR increased proliferating cell nuclear antigen levels and induced cell proliferation. Wound healing assays have confirmed that GCSFR also increases migration in gastric cancer (49). Transfection of TCC-SUP bladder cancer cells that innately lack expression of GCSF and the receptor with full-length GCSFR resulted in a twofold increase in the proliferation rate with a sustained increase of cell survival through abrogation of apoptosis in a GCSF dose-dependent manner (102). Both the GCSFR transfected TCC-SUP and 5637-GR bladder cancer cells had increased *survivin*, a STAT-regulated gene known to mediate pro-survival functions in cells.

GCSFR is also seen cross-interacting with components within tumor stromal cells to promote tumor migration. In breast and pancreatic cancer cells, cancer-associated fibroblasts (CAFs) are most frequently found in tumor stroma not only promoting tumor progression but also inducing therapeutic resistance (103). CXCL12 signaling, known to upregulate GCSF-induced mobilization, also induces activation of CAFs, resulting in increased breast cancer stem cells (104, 105). While the specific interplay between GCSFR and CAFs remains elusive, this finding suggests a close interaction between the two. Day et al. observed GCSFR interacting with mesenchymal-lineage stromal cells in the bone marrow, CXCL12-abundant reticular cells (CAR), and osteoblasts, decreasing their capacity to support B lymphopoiesis. GCSFR was also associated with CAR expansion and support of osteogenic lineage commitment (106). However, GCSFR suppressed the production of multiple B-cell trophic factors by CAR osteoblasts, along with other cytokine factors like interleukin-6, a pro-inflammatory cytokine, and interleukin-7, hematopoietic growth factor (106).

In addition to increased proliferation of tumor cells, recent findings suggest that GCSFR promotes a microenvironment favorable for solid tumor cells to metastasize *via* immunomodulation (107, 108). Karagiannidis et al. subcutaneously injected GCSFR−/− mice with the murine colon cancer cell line, MC38, to investigate the role of GCSF signaling. They found that the GCSFR−/− mice had slower tumor growth and hypothesized that this may be due to a lack of GCSF signaling in the immune cells. The authors also noted a decrease in T cell-associated cytokine production in these GCSFR−/− mice. Real-time quantitative reverse transcription polymerase chain reaction (qRT-PCR) with RNA extracted from $CD4^+$ T cells isolated from spleens of GCSFR−/− mice showed an increase in interferon-gamma (IFN*y*), which is associated with antitumor activity, and in interleukin-17 (IL-17A), which can be indicative of T-cell activation. These mice also showed a decrease in interleukin-10 (IL-10) at the mRNA level, which is indicative of regulatory T cells associated with poor anti-tumor response (108). The expression of IFN*y* and IL-17A, generally considered markers of cytotoxic $CD8^+$ responses and of Th17 helper cells, respectively, were found favorable as compared to the WT, while IL-10 level decreased in the absence of GCSFR. Conversely, GCSF treatment on WT $CD4^+$ cells significantly decreased IL-17A production but increased IL-10 production. These findings suggest that GCSFR directly affects T-cell phenotype and cytokine production in a GCSF-dependent manner. In *in vitro* studies, GCSFR−/− spleen-derived $CD4^+$ T cells had decreased levels of the gene forkhead box P3 (*FoxP3*), the transcription factor for T-regulatory cells. This was consistent with an increase of IL-10 and expression level of *FoxP3* in WT mice subjected to MC38 tumor injection, as compared to IL-10 and *FoxP3* levels in the GCSFR−/− mice (108). Multiplex cytokine analysis of conditioned media from cultures confirmed that IL-10 production was increased in WT mice as compared to cultures using tumor tissues from GCSFR −/− mice. This is consistent with previous studies that reported

an IL-10 serum level increase in human patients with progressing CRC (73, 108). These data suggest complicated regulation of GCSFR on the immune system. The pro-tumorigenic role of GCSFR in inhibiting CD4 and CD8 T-cell responses by promoting IL-10 is recognized to play an important role in shaping the tumor microenvironment.

Conclusion

Although GCSF has been widely used in clinics to successfully treat and prevent febrile neutropenia, a complete understanding of the complex results of GCSF signaling remains lacking. This review summarizes the available data regarding GCSFR structure, signaling, and regulation with emphasis on the role played by the receptor in diseases such as cancer. An emerging body of evidence reveals an adverse role played by GCSFR signaling in various cancers. Available evidence also shows that GCSFR activates the JAK/STAT pathway to drive the proliferation of both myeloid and non-myeloid cells. Because of this and the fact that recombinant GCSF is administered to patients with malignancy, there is an urgent need to increase our understanding of the multiple roles played by this pleiotropic cytokine beyond the well-known effects on neutrophil mobilization.

Author contributions

All authors listed have made a substantial, direct, and intellectual contribution to the work, and approved it for publication.

Funding

Research reported in this publication was supported by the National Institutes of General Medical Sciences of the National Institutes of Health under Award Number P20GM103639. The content is solely the responsibility of the authors and does not necessarily represent the official views of the National Institutes of Health.

Conflict of interest

The authors declare that the research was conducted in the absence of any commercial or financial relationships that could be construed as a potential conflict of interest.

Publisher's note

All claims expressed in this article are solely those of the authors and do not necessarily represent those of their affiliated organizations, or those of the publisher, the editors and the reviewers. Any product that may be evaluated in this article, or claim that may be made by its manufacturer, is not guaranteed or endorsed by the publisher.

Author disclaimer

The content is solely the responsibility of the authors and does not necessarily represent the official views of the National Institutes of Health.

References

1. Azoulay E, Delclaux C. Is there a place for granulocyte colony-stimulating factor in non-neutropenic critically ill patients? *Intensive Care Med* (2004) 30:10–7. doi: 10.1007/s00134-003-2049-8

2. Bennett CL, Djulbegovic B, Norris LB, Armitage JO. Colony-stimulating factors for febrile neutropenia during cancer therapy. *N. Engl J Med* (2013) 368:1131–9. doi: 10.1056/NEJMct1210890

3. Agarwal S, Lakoma A, Chen Z, Hicks J, Metelitsa LS, Kim ES, et al. G-CSF promotes neuroblastoma tumorigenicity and metastasis *via* STAT3-dependent cancer stem cell activation. *Cancer Res* (2015) 75:2566–79. doi: 10.1158/0008-5472.CAN-14-2946

4. Wang L, Arcasoy MO, Watowich SS, Forget BG. Cytokine signals through STAT3 promote expression of granulocyte secondary granule proteins in 32D cells. *Exp Hematol* (2005) 33:308–17. doi: 10.1016/j.exphem.2004.11.014

5. Wojtukiewicz MZ, Sierko E, Skalij P, Kaminska M, Zimnoch L, Brekken RA, et al. Granulocyte-colony stimulating factor receptor, tissue factor, and VEGF-r bound VEGF in human breast cancer in loco. *Adv Clin Exp Med* (2016) 25:505–11. doi: 10.17219/acem/62398

6. Touw IP, Van De Geijn GJ. Granulocyte colony-stimulating factor and its receptor in normal myeloid cell development, leukemia and related blood cell disorders. *Front Biosci* (2007) 12:800–15. doi: 10.2741/2103

7. Morris KT, Castillo EF, Ray AL, Weston LL, Nofchissey RA, Hanson JA, et al. Anti-G-CSF treatment induces protective tumor immunity in mouse colon cancer by promoting protective NK cell, macrophage and T cell responses. *Oncotarget* (2015) 6:22338–47. doi: 10.18632/oncotarget.4169

8. Morris KT, Khan H, Ahmad A, Weston LL, Nofchissey RA, Pinchuk IV, et al. G-CSF and G-CSFR are highly expressed in human gastric and colon cancers and promote carcinoma cell proliferation and migration. *Br J Cancer* (2014) 110:1211–20. doi: 10.1038/bjc.2013.822

9. Sloand EM, Yong AS, Ramkissoon S, Solomou E, Bruno TC, Kim S, et al. Granulocyte colony-stimulating factor preferentially stimulates proliferation of monosomy 7 cells bearing the isoform IV receptor. *Proc Natl Acad Sci United. States America* (2006) 103:14483–8. doi: 10.1073/pnas.0605245103

10. Dwivedi P, Greis KD. Granulocyte colony-stimulating factor receptor signaling in severe congenital neutropenia, chronic neutrophilic leukemia, and related malignancies. *Exp Hematol* (2017) 46:9–20. doi: 10.1016/j.exphem.2016.10.008

11. Shibata K, Maruyama-Takahashi K, Yamasaki M, Hirayama N. G-CSF receptor-binding cyclic peptides designed with artificial amino-acid linkers. *Biochem Biophys Res Commun* (2006) 341:483–8. doi: 10.1016/j.bbrc.2005.12.204

12. Layton JE, Hall NE. The interaction of G-CSF with its receptor. *Front Biosci* (2006) 11:3181–9. doi: 10.2741/2041

13. Mehta HM, Futami M, Glaubach T, Lee DW, Andolina JR, Yang Q, et al. Alternatively spliced, truncated GCSF receptor promotes leukemogenic properties and sensitivity to JAK inhibition. *Leukemia* (2014) 28:1041–51. doi: 10.1038/leu.2013.321

14. Dong F, Pouwels K, Hoefsloot LH, Rozemuller H, Lowenberg B, Touw IP. The c-terminal cytoplasmic region of the granulocyte colony-stimulating factor receptor mediates apoptosis in maturation-incompetent murine myeloid cells. *Exp Hematol* (1996) 24:214–20. Available at: https://www.exphem.org

15. Ehlers S, Herbst C, Zimmermann M, Scharn N, Germeshausen M, Von Neuhoff N, et al. Granulocyte colony-stimulating factor (G-CSF) treatment of childhood acute myeloid leukemias that overexpress the differentiation-defective G-CSF receptor isoform IV is associated with a higher incidence of relapse. *J Clin Oncol* (2010) 28:2591–7. doi: 10.1200/JCO.2009.25.9010

16. Billia F, Barbara M, Mcewen J, Trevisan M, Iscove NN. Resolution of pluripotential intermediates in murine hematopoietic differentiation by global complementary DNA amplification from single cells: confirmation of assignments by expression profiling of cytokine receptor transcripts. *Blood* (2001) 97:2257–68. doi: 10.1182/blood.V97.8.2257

17. Palande K, Meenhuis A, Jevdjovic T, Touw IP. Scratching the surface: signaling and routing dynamics of the CSF3 receptor. *Front Biosci (Landmark Ed)* (2013) 18:91–105. doi: 10.2741/4089

18. Wang L, Rudert WA, Loutaev I, Roginskaya V, Corey SJ. Repression of c-cbl leads to enhanced G-CSF jak-STAT signaling without increased cell proliferation. *Oncogene* (2002) 21:5346–55. doi: 10.1038/sj.onc.1205670

19. Corey SJ, Burkhardt AL, Bolen JB, Geahlen RL, Tkatch LS, Tweardy DJ. Granulocyte colony-stimulating factor receptor signaling involves the formation of a three-component complex with Lyn and syk protein-tyrosine kinases. *Proc Natl Acad Sci U S A* (1994) 91:4683–7. doi: 10.1073/pnas.91.11.4683

20. Marino VJ, Roguin LP. The granulocyte colony stimulating factor (G-CSF) activates Jak/STAT and MAPK pathways in a trophoblastic cell line. *J Cell Biochem* (2008) 103:1512–23. doi: 10.1002/jcb.21542

21. Fiévez L, Desmet C, Henry E, Pajak B, Hegenbarth S, Garzé V, et al. STAT5 is an ambivalent regulator of neutrophil homeostasis. *PLoS One* (2007) 2:e727. doi: 10.1371/journal.pone.0000727

22. Kimura A, Kinjyo I, Matsumura Y, Mori H, Mashima R, Harada M, et al. SOCS3 is a physiological negative regulator for granulopoiesis and granulocyte colony-stimulating factor receptor signaling. *J Biol Chem* (2004) 279:6905–10. doi: 10.1074/jbc.C300496200

23. Van De Geijn GJ, Gits J, Aarts LH, Heijmans-Antonissen C, Touw IP. G-CSF receptor truncations found in SCN/AML relieve SOCS3-controlled inhibition of STAT5 but leave suppression of STAT3 intact. *Blood* (2004) 104:667–74. doi: 10.1182/blood-2003-08-2913

24. Liu F, Kunter G, Krem MM, Eades WC, Cain JA, Tomasson MH, et al. Csf3r mutations in mice confer a strong clonal HSC advantage *via* activation of Stat5. *J Clin Invest* (2008) 118:946–55. doi: 10.1172/JCI32704

25. Tian SS, Tapley P, Sincich C, Stein RB, Rosen J, Lamb P. Multiple signaling pathways induced by granulocyte colony-stimulating factor involving activation of JAKs, STAT5, and/or STAT3 are required for regulation of three distinct classes of immediate early genes. *Blood* (1996) 88:4435–44. doi: 10.1182/blood.V88.12.4435.bloodjournal88124435

26. Luttman JH, Colemon A, Mayro B, Pendergast AM. Role of the ABL tyrosine kinases in the epithelial-mesenchymal transition and the metastatic cascade. *Cell Commun Signal* (2021) 19:59. doi: 10.1186/s12964-021-00739-6

27. Wang J, Pendergast AM. The emerging role of ABL kinases in solid tumors. *Trends Cancer* (2015) 1:110–23. doi: 10.1016/j.trecan.2015.07.004

28. Chakraborty A, Dyer KF, Tweardy DJ. Delineation and mapping of Stat5 isoforms activated by granulocyte colony-stimulating factor in myeloid cells. *Blood Cells Mol. Dis* (2000) 26:320–30. doi: 10.1006/bcmd.2000.0309

29. Dong F, Liu X, De Koning JP, Touw IP, Hennighausen L, Larner A, et al. Stimulation of Stat5 by granulocyte colony-stimulating factor (G-CSF) is modulated by two distinct cytoplasmic regions of the G-CSF receptor. *J Immunol* (1998) 161:6503–9.

30. Avalos BR, Hunter MG, Parker JM, Ceselski SK, Druker BJ, Corey SJ, et al. Point mutations in the conserved box 1 region inactivate the human granulocyte colony-stimulating factor receptor for growth signal transduction and tyrosine phosphorylation of p75c-rel. *Blood* (1995) 85:3117–26. doi: 10.1182/blood.V85.11.3117.bloodjournal85113117

31. Sampson M, Zhu QS, Corey SJ. Src kinases in G-CSF receptor signaling. *Front Biosci.* (2007) 12:1463–74. doi: 10.2741/2160

32. Shao H, Xu X, Jing N, Tweardy DJ. Unique structural determinants for Stat3 recruitment and activation by the granulocyte colony-stimulating factor receptor at phosphotyrosine ligands 704 and 744. *J Immunol* (2006) 176:2933–41. doi: 10.4049/jimmunol.176.5.2933

33. Ward AC, Oomen SP, Smith L, Gits J, Van Leeuwen D, Soede-Bobok AA, et al. The SH2 domain-containing protein tyrosine phosphatase SHP-1 is induced by granulocyte colony-stimulating factor (G-CSF) and modulates signaling from the G-CSF receptor. *Leukemia* (2000) 14:1284–91. doi: 10.1038/sj.leu.2401822

34. Recio C, Guerra B, Guerra-Rodríguez M, Aranda-Tavío H, Martín-Rodríguez P, De Mirecki-Garrido M, et al. Signal transducer and activator of transcription (STAT)-5: an opportunity for drug development in oncohematology. *Oncogene* (2019) 38:4657–68. doi: 10.1038/s41388-019-0752-3

35. Gupta K, Kuznetsova I, Klimenkova O, Klimiankou M, Meyer J, Moore MA, et al. Bortezomib inhibits STAT5-dependent degradation of LEF-1, inducing granulocytic differentiation in congenital neutropenia CD34(+) cells. *Blood* (2014) 123:2550–61. doi: 10.1182/blood-2012-09-456889

36. Skokowa J, Klimiankou M, Klimenkova O, Lan D, Gupta K, Hussein K, et al. Interactions among HCLS1, HAX1 and LEF-1 proteins are essential for G-CSF-triggered granulopoiesis. *Nat Med* (2012) 18:1550–9. doi: 10.1038/nm.2958

37. Wu CJ, Sundararajan V, Sheu BC, Huang RY, Wei LH. Activation of STAT3 and STAT5 signaling in epithelial ovarian cancer progression: Mechanism and therapeutic opportunity. *Cancers (Basel)* (2019) 12:2–15. doi: 10.3390/cancers12010024

38. Rah B, Rather RA, Bhat GR, Baba AB, Mushtaq I, Farooq M, et al. JAK/STAT signaling: Molecular targets, therapeutic opportunities, and limitations of targeted inhibitions in solid malignancies. *Front Pharmacol* (2022) 13:821344. doi: 10.3389/fphar.2022.821344

39. Wolfler A, Irandoust M, Meenhuis A, Gits J, Roovers O, Touw IP. Site-specific ubiquitination determines lysosomal sorting and signal attenuation of the granulocyte colony-stimulating factor receptor. *Traffic* (2009) 10:1168–79. doi: 10.1111/j.1600-0854.2009.00928.x

40. Babon JJ, Nicola NA. The biology and mechanism of action of suppressor of cytokine signaling 3. *Growth Factors.* (2012) 30:207–19. doi: 10.3109/08977194.2012.687375

41. Zhang Y, Zhou X, Liu P, Chen X, Zhang J, Zhang H, et al. GCSF deficiency attenuates non-alcoholic fatty liver disease through regulating GCSFR-SOCS3-JAK-STAT3 pathway and immune cells infiltration. *Am J Physiol Gastrointest. Liver. Physiol* (2021) 20:20. doi: 10.1152/ajpgi.00342.2020

42. Piscaglia AC, Shupe TD, Oh SH, Gasbarrini A, Petersen BE. Granulocyte-colony stimulating factor promotes liver repair and induces oval cell migration and proliferation in rats. *Gastroenterology* (2007) 133:619–31. doi: 10.1053/j.gastro.2007.05.018

43. Otani K, Niwa Y, Suzuki T, Sato N, Sasazawa Y, Dohmae N, et al. Regulation of granulocyte colony-stimulating factor receptor-mediated granulocytic differentiation by c-mannosylation. *Biochem Biophys Res Commun* (2018) 498:466–72. doi: 10.1016/j.bbrc.2018.02.210

44. Liongue C, Hall CJ, O'connell BA, Crosier P, Ward AC. Zebrafish granulocyte colony-stimulating factor receptor signaling promotes myelopoiesis and myeloid cell migration. *Blood* (2009) 113:2535–46. doi: 10.1182/blood-2008-07-171967

45. Bocchietto E, Guglielmetti A, Silvagno F, Taraboletti G, Pescarmona GP, Mantovani A, et al. Proliferative and migratory responses of murine microvascular endothelial cells to granulocyte-colony-stimulating factor. *J Cell Physiol* (1993) 155:89–95. doi: 10.1002/jcp.1041550112

46. Harada M, Qin Y, Takano H, Minamino T, Zou Y, Toko H, et al. G-CSF prevents cardiac remodeling after myocardial infarction by activating the jak-stat pathway in cardiomyocytes. *Nat Med* (2005) 11:305–11. doi: 10.1038/nm1199

47. Frank T, Schlachetzki JC, Goricke B, Meuer K, Rohde G, Dietz GP, et al. Both systemic and local application of granulocyte-colony stimulating factor (G-CSF) is neuroprotective after retinal ganglion cell axotomy. *BMC Neurosci* (2009) 10:49. doi: 10.1186/1471-2202-10-49

48. Guo Y, Liu S, Wang P, Zhang H, Wang F, Bing L, et al. Granulocyte colony-stimulating factor improves neuron survival in experimental spinal cord injury by regulating nucleophosmin-1 expression. *J Neurosci Res* (2014) 92:751–60. doi: 10.1002/jnr.23362

49. Fan Z, Li Y, Zhao Q, Fan L, Tan B, Zuo J, et al. Highly expressed granulocyte colony-stimulating factor (G-CSF) and granulocyte colony-stimulating factor receptor (G-CSFR) in human gastric cancer leads to poor survival. *Med Sci Monit.* (2018) 24:1701–11. doi: 10.12659/MSM.909128

50. Karagiannidis I, Salataj E, Said Abu Egal E, Beswick EJ. G-CSF in tumors: Aggressiveness, tumor microenvironment and immune cell regulation. *Cytokine* (2021) 142:155479. doi: 10.1016/j.cyto.2021.155479

51. Liu L, Liu Y, Yan X, Zhou C, Xiong X. The role of granulocyte colony-stimulating factor in breast cancer development: A review. *Mol Med Rep* (2020) 21:2019–29. doi: 10.3892/mmr.2020.11017

52. Klemm SL, Shipony Z, Greenleaf WJ. Chromatin accessibility and the regulatory epigenome. *Nat Rev Genet* (2019) 20:207–20. doi: 10.1038/s41576-018-0089-8

53. Felgner J, Heidorn K, Korbacher D, Frahm SO, Parwaresch R. Cell lineage specificity in G-CSF receptor gene methylation. *Leukemia* (1999) 13:530–4. doi: 10.1038/sj.leu.2401386

54. Rascle A, Lees E. Chromatin acetylation and remodeling at the cis promoter during STAT5-induced transcription. *Nucleic Acids Res* (2003) 31:6882–90. doi: 10.1093/nar/gkg907

55. Witzel M, Petersheim D, Fan Y, Bahrami E, Racek T, Rohlfs M, et al. Chromatin-remodeling factor SMARCD2 regulates transcriptional networks controlling differentiation of neutrophil granulocytes. *Nat Genet* (2017) 49:742–52. doi: 10.1038/ng.3833

56. Ramji DP, Foka P. CCAAT/enhancer-binding proteins: structure, function and regulation. *Biochem J* (2002) 365:561–75. doi: 10.1042/bj20020508

57. Yamanaka R, Kim GD, Radomska HS, Lekstrom-Himes J, Smith LT, Antonson P, et al. CCAAT/enhancer binding protein epsilon is preferentially up-regulated during granulocytic differentiation and its functional versatility is determined by alternative use of promoters and differential splicing. *Proc Natl Acad Sci United. States America* (1997) 94:6462–7. doi: 10.1073/pnas.94.12.6462

58. Cooper S, Guo H, Friedman AD. The +37 kb cebpa enhancer is critical for cebpa myeloid gene expression and contains functional sites that bind SCL, GATA2, C/EBPα, PU.1, and additional ets factors. *PLoS One* (2015) 10: e0126385. doi: 10.1371/journal.pone.0126385

59. Ma O, Hong S, Guo H, Ghiaur G, Friedman AD. Granulopoiesis requires increased C/EBPα compared to monopoiesis, correlated with elevated cebpa in immature G-CSF receptor versus m-CSF receptor expressing cells. *PLoS One* (2014) 9:e95784. doi: 10.1371/journal.pone.0095784

60. Collins SJ, Ulmer J, Purton LE, Darlington G. Multipotent hematopoietic cell lines derived from C/EBPalpha(-/-) knockout mice display granulocyte macrophage-colony-stimulating factor, granulocyte- colony-stimulating factor, and retinoic acid-induced granulocytic differentiation. *Blood* (2001) 98:2382–8. doi: 10.1182/blood.V98.8.2382

61. Behre G, Singh SM, Liu H, Bortolin LT, Christopeit M, Radomska HS, et al. Ras signaling enhances the activity of C/EBP alpha to induce granulocytic differentiation by phosphorylation of serine 248. *J Biol Chem* (2002) 277:26293–9. doi: 10.1074/jbc.M202301200

62. Burda P, Laslo P, Stopka T. The role of PU.1 and GATA-1 transcription factors during normal and leukemogenic hematopoiesis. *Leukemia* (2010) 24:1249–57. doi: 10.1038/leu.2010.104

63. Curik N, Burda P, Vargova K, Pospisil V, Belickova M, Vlckova P, et al. 5-azacitidine in aggressive myelodysplastic syndromes regulates chromatin structure at PU.1 gene and cell differentiation capacity. *Leukemia* (2012) 26:1804–11. doi: 10.1038/leu.2012.47

64. Mendoza H, Podoltsev NA, Siddon AJ. Laboratory evaluation and prognostication among adults and children with CEBPA-mutant acute myeloid leukemia. *Int J Lab Hematol* (2021) 43 Suppl 1:86–95. doi: 10.1111/ijlh.13517

65. Hohaus S, Petrovick MS, Voso MT, Sun Z, Zhang DE, Tenen DG. PU.1 (Spi-1) and C/EBP alpha regulate expression of the granulocyte-macrophage colony-stimulating factor receptor alpha gene. *Mol Cell Biol* (1995) 15:5830–45. doi: 10.1128/MCB.15.10.5830

66. Smith LT, Hohaus S, Gonzalez DA, Dziennis SE, Tenen DG. PU.1 (Spi-1) and C/EBP alpha regulate the granulocyte colony-stimulating factor receptor promoter in myeloid cells. *Blood* (1996) 88:1234–47. doi: 10.1182/blood.V88.4.1234.bloodjournal8841234

67. Cary LH, Noutai D, Salber RE, Williams MS, Ngudiankama BF, Whitnall MH. Interactions between endothelial cells and T cells modulate responses to mixed neutron/gamma radiation. *Radiat Res* (2014) 181:592–604. doi: 10.1667/RR13550.1

68. Gombart AF, Grewal J, Koeffler HP. ATF4 differentially regulates transcriptional activation of myeloid-specific genes by C/EBPepsilon and C/EBPalpha. *J Leukocyte. Biol* (2007) 81:1535–47. doi: 10.1189/jlb.0806516

69. Zhang H, Goudeva L, Immenschuh S, Schambach A, Skokowa J, Eiz-Vesper B, et al. miR-155 is associated with the leukemogenic potential of the class IV granulocyte colony-stimulating factor receptor in CD34+ progenitor cells. *Mol Med* (2015) 20:736–46. doi: 10.2119/molmed.2014.00146

70. Itkin T, Kumari A, Schneider E, Gur-Cohen S, Ludwig C, Brooks R, et al. MicroRNA-155 promotes G-CSF-induced mobilization of murine hematopoietic stem and progenitor cells *via* propagation of CXCL12 signaling. *Leukemia* (2017) 31:1247–50. doi: 10.1038/leu.2017.50

71. Zhang X, Xiao M, Huaying A, Changqing X, Wenjo C, Wei Y, et al. Upregulation of microRNA - 125b by G-CSF promotes metastasis in colorectal cancer. *Oncotarget* (2017) 8(31):50642–50654. doi: 10.18632/oncotarget.16892

72. Baffa R, Fassan M, Volinia S, O'hara B, Liu CG, Palazzo JP, et al. MicroRNA expression profiling of human metastatic cancers identifies cancer gene targets. *J Pathol* (2009) 219:214–21. doi: 10.1002/path.2586

73. Gong J, Zhang JP, Li B, Zeng C, You K, Chen MX, et al. MicroRNA-125b promotes apoptosis by regulating the expression of mcl-1, bcl-w and IL-6R. *Oncogene* (2013) 32:3071–9. doi: 10.1038/onc.2012.318

74. Aarts LH, Roovers O, Ward AC, Touw IP. Receptor activation and 2 distinct COOH-terminal motifs control G-CSF receptor distribution and internalization kinetics. *Blood* (2004) 103:571–9. doi: 10.1182/blood-2003-07-2250

75. Dietrich J, Hou X, Wegener AM, Geisler C. CD3 gamma contains a phosphoserine-dependent di-leucine motif involved in down-regulation of the T cell receptor. *EMBO J* (1994) 13:2156–66. doi: 10.1002/j.1460-2075.1994.tb06492.x

76. Frey L, Zietara N, Lyszkiewicz M, Marquardt B, Mizoguchi Y, Linder MI, et al. Mammalian VPS45 orchestrates trafficking through the endosomal system. *Blood* (2020) 21:21. doi: 10.1182/blood.2020006871

77. Stepensky P, Saada A, Cowan M, Tabib A, Fischer U, Berkun Y, et al. The Thr224Asn mutation in the VPS45 gene is associated with the congenital neutropenia and primary myelofibrosis of infancy. *Blood* (2013) 121:5078–87. doi: 10.1182/blood-2012-12-475566

78. Wang J, Yao L, Zhao S, Zhang X, Yin J, Zhang Y, et al. Granulocyte-colony stimulating factor promotes proliferation, migration and invasion in glioma cells. *Cancer Biol Ther* (2012) 13:389–400. doi: 10.4161/cbt.19237

79. Ai J, Druhan LJ, Loveland MJ, Avalos BR. G-CSFR ubiquitination critically regulates myeloid cell survival and proliferation. *PLoS One* (2008) 3:e3422. doi: 10.1371/journal.pone.0003422

80. Metcalf D. The colony-stimulating factors and cancer. *Nat Rev Cancer* (2010) 10:425–34. doi: 10.1038/nrc2843

81. Skokowa J, Germeshausen M, Zeidler C, Welte K. Severe congenital neutropenia: inheritance and pathophysiology. *Curr Opin Hematol* (2007) 14:22–8. doi: 10.1097/00062752-200701000-00006

82. Price A, Druhan LJ, Lance A, Clark G, Vestal CG, Zhang Q, et al. T618I CSF3R mutations in chronic neutrophilic leukemia induce oncogenic signals through aberrant trafficking and constitutive phosphorylation of the O-glycosylated receptor form. *Biochem Biophys Res Commun* (2020) 523:208–13. doi: 10.1016/j.bbrc.2019.12.030

83. Kindwall-Keller TL, Druhan LJ, Ai J, Hunter MG, Massullo P, Loveland M, et al. Role of the proteasome in modulating native G-CSFR expression. *Cytokine* (2008) 43:114–23. doi: 10.1016/j.cyto.2008.04.015

84. Beekman R, Valkhof MG, Sanders MA, Van Strien PM, Haanstra JR, Broeders L, et al. Sequential gain of mutations in severe congenital neutropenia progressing to acute myeloid leukemia. *Blood* (2012) 119:5071–7. doi: 10.1182/blood-2012-01-406116

85. Maxson JE, Luty SB, Macmaniman JD, Abel ML, Druker BJ, Tyner JW. Ligand independence of the T618I mutation in the colony-stimulating factor 3 receptor (CSF3R) protein results from loss of O-linked glycosylation and increased receptor dimerization. *J Biol Chem* (2014) 289:5820–7. doi: 10.1074/jbc.M113.508440

86. Mehta HM, Glaubach T, Long A, Lu H, Przychodzen B, Makishima H, et al. Granulocyte colony-stimulating factor receptor T595I (T618I) mutation confers ligand independence and enhanced signaling. *Leukemia* (2013) 27:2407–10. doi: 10.1038/leu.2013.164

87. Irandoust MI, Aarts LH, Roovers O, Gits J, Erkeland SJ, Touw IP. Suppressor of cytokine signaling 3 controls lysosomal routing of G-CSF receptor. *EMBO J* (2007) 26:1782–93. doi: 10.1038/sj.emboj.7601640

88. Chhabra S, Kumar Y, Thacker G, Kapoor I, Lochab S, Sanyal S, et al. E6AP inhibits G-CSFR turnover and functions by promoting its ubiquitin-dependent proteasome degradation. *Biochim Biophys Acta - Mol Cell Res* (2017) 1864:1545–53. doi: 10.1016/j.bbamcr.2017.05.026

89. Chen G, Wang T, Uttarwar L, Vankrieken R, Li R, Chen X, et al. SREBP-1 is a novel mediator of TGFβ1 signaling in mesangial cells. *J Mol Cell Biol* (2014) 6:516–30. doi: 10.1093/jmcb/mju041

90. Chakraborty A, White SM, Lerner SP. Granulocyte colony-stimulating factor receptor signals for beta1-integrin expression and adhesion in bladder cancer. *Urology* (2004) 63:177–83. doi: 10.1016/S0090-4295(03)00786-6

91. Chen C, Huang X, Atakilit A, Zhu QS, Corey SJ, Sheppard D. The integrin alpha9beta1 contributes to granulopoiesis by enhancing granulocyte colony-stimulating factor receptor signaling. *Immunity* (2006) 25:895–906. doi: 10.1016/j.immuni.2006.10.013

92. Pal P, Lochab S, Kanaujiya JK, Kapoor I, Sanyal S, Behre G, et al. E6AP, an E3 ubiquitin ligase negatively regulates granulopoiesis by targeting transcription factor C/EBPα for ubiquitin-mediated proteasome degradation. *Cell Death Dis* (2013) 4:e590. doi: 10.1038/cddis.2013.120

93. Li J, Zou Y, Ge J, Zhang D, Guan A, Wu J, et al. The effects of G-CSF on proliferation of mouse myocardial microvascular endothelial cells. *Int J Mol Sci* (2011) 12:1306–15. doi: 10.3390/ijms12021306

94. Katzenback BA, Belosevic M. Characterization of granulocyte colony stimulating factor receptor of the goldfish (Carassius auratus l.). *Dev Comp Immunol* (2012) 36:199–207. doi: 10.1016/j.dci.2011.07.005

95. Kamezaki K, Shimoda K, Numata A, Haro T, Kakumitsu H, Yoshie M, et al. Roles of Stat3 and ERK in G-CSF signaling. *Stem Cells* (2005) 23:252–63. doi: 10.1634/stemcells.2004-0173a

96. Van Raam BJ, Drewniak A, Groenewold V, Van Den Berg TK, Kuijpers TW. Granulocyte colony-stimulating factor delays neutrophil apoptosis by inhibition of

calpains upstream of caspase-3. *Blood* (2008) 112:2046–54. doi: 10.1182/blood-2008-04-149575

97. Hara M, Yuasa S, Shimoji K, Onizuka T, Hayashiji N, Ohno Y, et al. G-CSF influences mouse skeletal muscle development and regeneration by stimulating myoblast proliferation. *J Exp Med* (2011) 208:715–27. doi: 10.1084/jem.20101059

98. Hayashiji N, Yuasa S, Miyagoe-Suzuki Y, Hara M, Ito N, Hashimoto H, et al. G-CSF supports long-term muscle regeneration in mouse models of muscular dystrophy. *Nat Commun* (2015) 6:6745. doi: 10.1038/ncomms7745

99. Kohlstedt K, Trouvain C, Fromel T, Mudersbach T, Henschler R, Fleming I. Role of the angiotensin-converting enzyme in the G-CSF-induced mobilization of progenitor cells. *Basic. Res Cardiol* (2018) 113:18. doi: 10.1007/s00395-018-0677-y

100. Kirsch F, Kruger C, Schneider A. The receptor for granulocyte-colony stimulating factor (G-CSF) is expressed in radial glia during development of the nervous system. *BMC Dev Biol* (2008) 8:32. doi: 10.1186/1471-213X-8-32

101. Kast RE, Hill QA, Wion D, Mellstedt H, Focosi D, Karpel-Massler G, et al. Glioblastoma-synthesized G-CSF and GM-CSF contribute to growth and immunosuppression: Potential therapeutic benefit from dapsone, fenofibrate, and ribavirin. *Tumour. Biol* (2017) 39:1010428317699797. doi: 10.1177/1010428317699797

102. Chakraborty A, Guha S. Granulocyte colony-stimulating factor/granulocyte colony-stimulating factor receptor biological axis promotes survival and growth of bladder cancer cells. *Urology* (2007) 69:1210–5. doi: 10.1016/j.urology.2007.02.035

103. Mao Y, Keller ET, Garfield DH, Shen K, Wang J. Stromal cells in tumor microenvironment and breast cancer. *Cancer Metastasis. Rev* (2013) 32:303–15. doi: 10.1007/s10555-012-9415-3

104. Bendall LJ, Bradstock KF. G-CSF: From granulopoietic stimulant to bone marrow stem cell mobilizing agent. *Cytokine Growth Factor. Rev* (2014) 25:355–67. doi: 10.1016/j.cytogfr.2014.07.011

105. Christopher MJ, Rao M, Liu F, Woloszynek JR, Link DC. Expression of the G-CSF receptor in monocytic cells is sufficient to mediate hematopoietic progenitor mobilization by G-CSF in mice. *J Exp Med* (2011) 208:251–60. doi: 10.1084/jem.20101700

106. Day RB, Bhattacharya D, Nagasawa T, Link DC. Granulocyte colony-stimulating factor reprograms bone marrow stromal cells to actively suppress b lymphopoiesis in mice. *Blood* (2015) 125:3114–7. doi: 10.1182/blood-2015-02-629444

107. Martins A, Han J, Kim SO. The multifaceted effects of granulocyte colony-stimulating factor in immunomodulation and potential roles in intestinal immune homeostasis. *IUBMB Life* (2010) 62:611–7. doi: 10.1002/iub.361

108. Karagiannidis I, Jerman SJ, Jacenik D, Phinney BB, Yao R, Prossnitz ER, et al. G-CSF and G-CSFR modulate CD4 and CD8 T cell responses to promote colon tumor growth and are potential therapeutic targets. *Front Immunol* (2020) 11:1885. doi: 10.3389/fimmu.2020.01885

Advantages of publishing in Frontiers

OPEN ACCESS
Articles are free to read for greatest visibility and readership

FAST PUBLICATION
Around 90 days from submission to decision

HIGH QUALITY PEER-REVIEW
Rigorous, collaborative, and constructive peer-review

TRANSPARENT PEER-REVIEW
Editors and reviewers acknowledged by name on published articles

Frontiers
Avenue du Tribunal-Fédéral 34
1005 Lausanne | Switzerland

Visit us: www.frontiersin.org
Contact us: frontiersin.org/about/contact

REPRODUCIBILITY OF RESEARCH
Support open data and methods to enhance research reproducibility

DIGITAL PUBLISHING
Articles designed for optimal readership across devices

FOLLOW US
@frontiersin

IMPACT METRICS
Advanced article metrics track visibility across digital media

EXTENSIVE PROMOTION
Marketing and promotion of impactful research

LOOP RESEARCH NETWORK
Our network increases your article's readership